# The Retina as a Biomarker for Vascular and Neurodegenerative Brain Diseases

Ünal Mutlu

The work described in this thesis was conducted at the Department of Epidemiology in collaboration with the Department of Ophthalmology.
The Rotterdam Study is supported by the Erasmus MC and Erasmus University Rotterdam, the Netherlands Organization for Scientific Research (NWO), the Netherlands Organization for Health Research and Development (ZonMw), the Research Institute for Diseases in the Elderly (RIDE), the Ministry of Education, Culture and Science, the Ministry of Health, Welfare and Sports, and the Municipality of Rotterdam.

Financial support for publication of this thesis was kindly provided by Erasmus MC, Stichting Blindenhulp, Prof. Dr. Henkes Stichting, Bayer, Landelijke Stichting voor Blinden en Slechtzienden, Visus Oogkliniek, Alzheimer Nederland, and Hartstichting.

Cover design by Ünal Mutlu
Lay-out by Ünal Mutlu
Printed by Gildeprint

ISBN: 978-94-6233-891-3

# The Retina as a Biomarker for Vascular and Neurodegenerative Brain Diseases

## Het netvlies als biomarker voor vasculaire en neurodegeneratieve hersenaandoeningen

Proefschrift

ter verkrijging van de graad van doctor aan de
Erasmus Universiteit Rotterdam
op gezag van de
rector magnificus

Prof.dr. H.A.P. Pols
en volgens besluit van het College voor Promoties.

De openbare verdediging zal plaatsvinden op

woensdag 11 april 2018 om 15:30 uur

door

Ünal Mutlu

geboren te Rotterdam

Erasmus University Rotterdam

**Promotiecommissie**

| | |
|---|---|
| **Promotoren:** | Prof.dr. M.A. Ikram |
| | Prof.dr. C.C.W. Klaver |
| **Overige leden:** | Prof.dr. M.W. Vernooij |
| | Prof.dr. N.M. Jansonius |
| | Prof.dr. M.L. Bots |
| **Copromotor:** | Dr. M.K. Ikram |

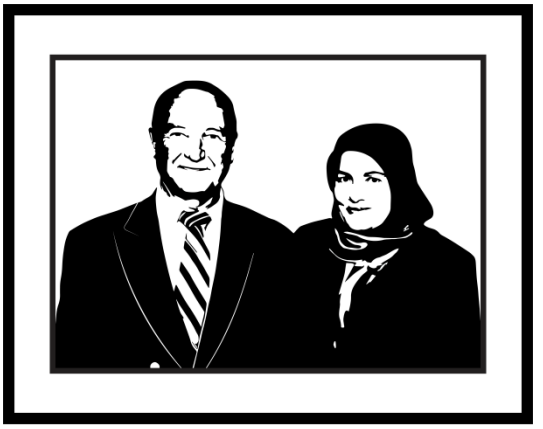

To my parents

# Table of contents

# Manuscripts based on this thesis

Chapter 2.1
MLP Portegies, **U Mutlu**, HI Zonneveld, MW Vernooij, MK Ikram, CCW Klaver, A Hofman, PJ Koudstaal, MA Ikram. The interaction between total brain perfusion and retinal vessels for the risk of stroke: the Rotterdam Study. Submitted.

Chapter 2.2
**U Mutlu**, SA Swanson, CCW Klaver, A Hofman, PJ Koudstaal, MA Ikram, MK Ikram. The mediating role of the venules between smoking and ischemic stroke. Submitted.

Chapter 2.3
**U Mutlu**, SA Swanson, MA Ikram, MK Ikram. Clinical interpretation of negative mediated interaction. Submitted.

Chapter 3.1
**U Mutlu**, MA Ikram, A Hofman, PTVM de Jong, AG Uitterlinden, CCW Klaver, MK Ikram. Vitamin D and retinal microvascular damage: the Rotterdam Study. Medicine (Baltimore). 2016;95:e5477.

Chapter 3.2
**U Mutlu**, MA Ikram, A Hofman, PTVM de Jong, CCW Klaver, MK Ikram. N-terminal pro-B-type natriuretic peptide is related to retinal microvascular damage: the Rotterdam Study. Arterioscler Thromb Vasc Biol. 2016;36:1698-1702.

Chapter 4.1
**U Mutlu**, LGM Cremers, M de Groot, A Hofman, WJ Niessen, A van der Lugt, CCW Klaver, MA Ikram, MW Vernooij, MK Ikram. Retinal microvasculature and white matter microstructure: the Rotterdam Study. Neurology. 2016;87:1003-1010.

Chapter 4.2
**U Mutlu**, HHH Adams, A Hofman, A van der Lugt, CCW Klaver, MW Vernooij, MK Ikram, MA Ikram. Retinal microvascular calibers are associated with enlarged perivascular spaces in the brain. Stroke. 2016;47:1374-1376.

Chapter 4.3
**U Mutlu**, PWM Bonnemaijer, MA Ikram, JM Colijn, LGM Cremers, GHS Buitendijk, JR Vingerling, WJ Niessen, MW Vernooij, CCW Klaver, MK Ikram.
Retinal neurodegeneration and brain MRI markers: the Rotterdam Study.
Neurobiol Aging. 2017;60:183-191.

Chapter 4.4
**U Mutlu**, MK Ikram, GV Roshchupkin, PWM Bonnemaijer, JM Colijn, JR Vingerling, WJ Niessen, MA Ikram, CCW Klaver, MW Vernooij. Retinal layer thickness and voxel-based morphometry of the brain: the Rotterdam Study. Submitted.

Chapter 5.1
KX Wen, **U Mutlu**, MK Ikram, M Kavousi, CCW Klaver, H Tiemeier, OH Franco, MA Ikram. The retinal microcirculation in migraine: the Rotterdam Study.
Cephalalgia. 2017:333102417708774.

Chapter 5.2
**U Mutlu**, JM Colijn, MA Ikram, PWM Bonnemaijer, S Licher, FJ Wolters, H Tiemeier, PJ Koudstaal, CCW Klaver, MK Ikram. Retinal neurodegeneration on optical coherence tomography and the risk of dementia. Submitted.

Chapter 5.3
**U Mutlu**, MK Ikram, FJ Wolters, A Hofman, CCW Klaver, MA Ikram.
Retinal microvasculature is associated with long-term survival in the general adult Dutch population. Hypertension. 2016;67:281-287.

# Chapter 1
# General Introduction

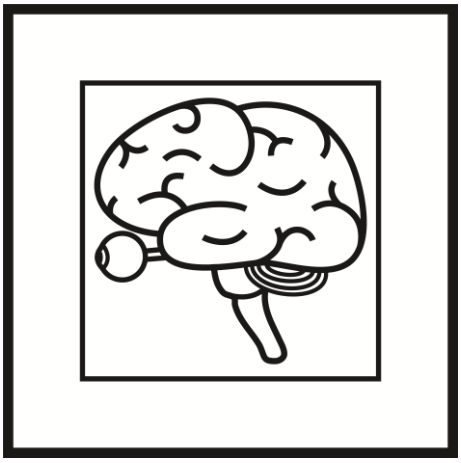

# General Introduction

*'Ut imago est animi voltus sic indices oculi'*

Thus said the roman politician and lawyer, Marcus Tullius Cicero (106-43 B.C.), which denotes that the face is a picture of the mind as the eyes are its interpreter. This quote is the earliest known reference to the more famous proverb '*the eyes are the mirror of the soul*'. Throughout history of mankind, the eyes have been the subject of our fascination and were of special interest in medicine and philosophy. At the 11th century, Alhazen (956-1040 A.D.) was the first to explain that vision occurs when light bounces on an object which is then directed to one's eyes.[1] He even considered that after the optic chiasm, the image goes to the '*ultimum sentiens*', which might be the brain, but he never tells where this last station is located. It was Leonardo da Vinci (1452-1519 A.D.) at the end of the 15th century who claimed that the eye generates spirits, going behind the eye to three cerebral rooms: the room of 'representation', the room of 'reasoning', and the room of 'memory'.[1] Since then, scientists tried to understand the visual system by linking the eye to the brain. As new discoveries were made contributing to our understanding of mechanisms underlying visual perception and eye movement, a strong link between the field of ophthalmology and neurology was established.

Over the years, the research field investigating the eye-brain connection has increased steeply, and researchers have begun to recognize the potential to use retinal structures as biomarkers for brain diseases. Given that retinal structures such as vessels and neurons share many similarities in anatomy and physiology to the brain, it has been thought that these structures provide a direct measure for the vascular and neuronal status of the brain.[2] Figures 1 and 2 show a schematic representation of retinal structures as biomarkers for vascular and neurodegenerative brain diseases. With advances in retinal imaging modalities, opportunities have been created to observe the living human microcirculation and neuronal tissue in a noninvasive way.[3-5] As for brain diseases, retinal imaging has mainly been used to study stroke and dementia.[6] Not only are stroke and dementia already highly prevalent in the elderly population, these diseases are also the leading causes of disability for elderly people worldwide.[7]

**Figure 1**. Schematic illustration of retinal microvascular damage as biomarker for vascular brain disease.

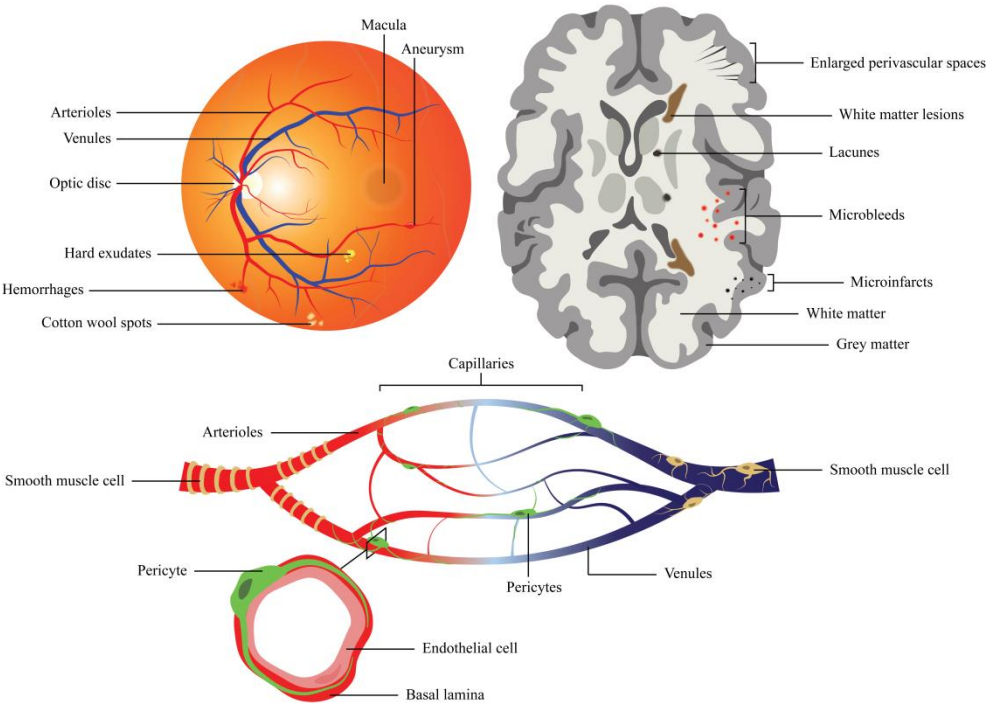


Microvascular damage of the retina (left corner) is often defined as the presence of hemorrhages, cotton wool spots, aneurysms, exudates, arteriolar narrowing, or venular widening. Certain lesions in the brain as detected by brain imaging (right corner) are thought to be caused by small vessel disease. Given that the small vessels in the brain are not easily visualized, the retinal vasculature has often been used as a non-invasive in vivo marker to study vascular brain diseases. In fact, blood vessels in the retina and the brain share many similarities in anatomy and physiology (lower image), and abnormalities of these blood vessels may occur concomitantly in the retina and the brain.

The physician Robert Marcus Gunn (1850-1909 A.D.) was the first to present a series of observations from stroke patients he made on the retinal microcirculation.[8] The retinopathy signs he described were generalized arteriolar narrowing, arteriovenous nicking, cotton wool spots, hemorrhages and papilledema.[8] However, these signs are qualitative measures of microvascular damage, and are prone to subjectivity.[9-12] Since the 1970s, methods have been developed to quantify retinopathy signs more objectively.[13-15] These methods enabled us to obtain quantitative measures of the retinal vasculature such as the average calibers of the retinal arterioles and venules. Existing evidence shows that persons with retinopathy signs and wider retinal venules are more likely to have white matter lesions in the brain,[16] and to develop stroke[17] and dementia.[18] Particularly, wider venules have shown to be related to white matter volume loss and the progression of white matter lesions.[19, 20]

Despite efforts in understanding the role of microvascular damage in vascular brain diseases, the underlying mechanisms are poorly understood, and more work needs to be done. To this end, the cerebral white matter is presumed to be already affected at early stages of vascular brain disease, but the link of microvascular damage with the white matter microstructure has not been investigated. Investigating the link of retinal microvascular damage with brain imaging markers may contribute to our knowledge on vascular brain diseases. Further, it remains unclear whether traditional and emerging cardiovascular risk factors are linked to cardiovascular disease through the presence of a microvascular component. More in-depth analyses such as interaction and mediation analysis – beyond one-on-one associations – can provide further insight in which way microvascular damage contributes to subclinical and clinical vascular brain diseases.

**Figure 2.** Schematic illustration of the retinal nerve tissue as biomarker for neurodegenerative brain disease.

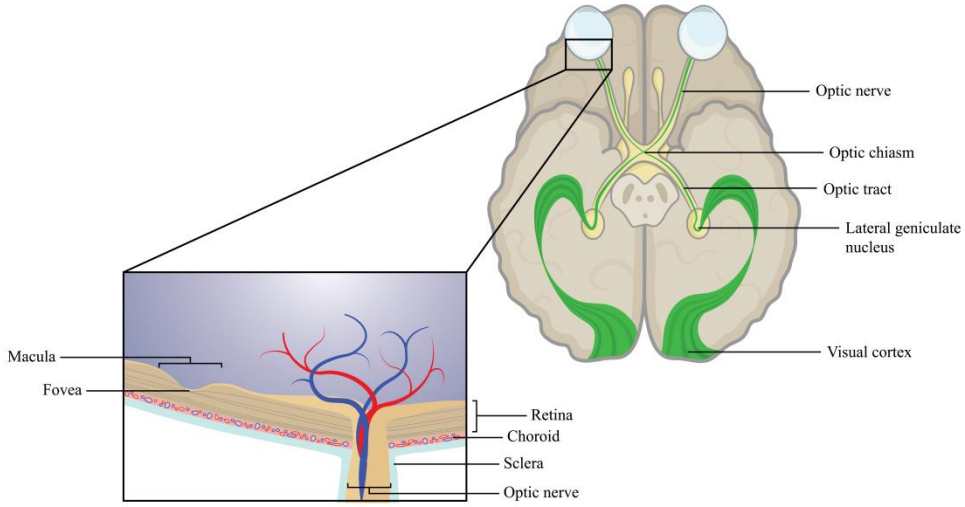


The retina is formed embryonically from the neural tissue and is connected to the brain by the optic nerve. The optic nerve consists of axons, and transmits visual signals to the lateral geniculate nucleus, a relay center for the visual pathway located in the thalamus. From there, signals are carried to the visual cortex where visual stimuli are processed. Given the structural connection of the retina with brain structures, global brain damage may manifest in the retina as thinning of the retinal layers.

Apart from retinal photography which enables us to visualize the retinal vasculature, a relatively new technique called ‘optical coherence tomography’ goes beyond capturing conventional images of the retina. Optical coherence tomography, first applied to the human eye in 1988,[21] uses low-coherence interferometry to produce cross-sectional images of retinal structures noninvasively. This technique is increasingly being used not only to study retinal abnormalities, but also to assess neurodegeneration in the brain. Optical

coherence tomography provides a great opportunity to visualize the retinal layers with biopsy-like precision and to detect subtle changes in the retina.[22] With advances in optical coherence tomography technology and image processing, it is possible to measure the average retinal layer thickness within a specified area. Initial histopathological studies conducted by Hinton[23] and Blanks[24] have shown that patients with Alzheimer's disease have extensive loss of retinal ganglion cells and reduced thickness of retinal nerve fiber layer compared to controls. Since then, clinical-based studies have confirmed those findings using optical coherence tomography, suggesting that thinning of those layers may be present before onset of clinical disease and might be related to subclinical disease.[25, 26] However, to test those hypotheses one should investigate such associations longitudinally. Moreover, to determine the association of retinal layer thickness with subclinical disease, data on brain imaging markers such as grey matter and white matter atrophy are needed.

The main objective of this thesis is to expand our current knowledge on retinal microvascular damage and retinal neurodegeneration as biomarker of vascular and neurodegenerative brain diseases. First, I aimed to apply novel epidemiologic methods to further elucidate processes underlying already observed associations. Furthermore, I aimed to understand whether traditional and emerging cardiovascular risk factors are linked to microvascular damage, and whether those factors affect vascular brain diseases through microvascular damage. Next, I aimed to determine whether retinal markers of microvascular damage and neurodegeneration are related to subclinical brain disease by investigating the relation of retinal markers with brain imaging markers. Finally, I aimed to determine whether retinal markers of microvascular damage and neurodegeneration yield clinical relevance by investigating their relation with clinical outcomes such as migraine, dementia, and mortality. The studies are embedded within the Rotterdam Study: a large prospective population-based cohort study.
In **chapter 2**, I elucidate mechanisms underlying stroke by focusing on interaction and mediation analysis. **Chapter 2.1** investigates whether the effect of small vessel disease on stroke depends in some way on the presence of large vessel disease, that is whether they interact. In **chapter 2.2**, I focus on the recently developed causal mediation analysis and apply this method to better understand the role of venules in the effect of smoking on ischemic stroke. In **chapter 2.3**, I discuss the clinical interpretation of this method with a special focus on negative mediated interaction. **Chapter 3** describes systemic blood markers including vitamin D (**chapter 3.1**) and NT-proBNP (**chapter 3.2**), and their association with retinopathy signs and retinal vascular calibers.
**Chapter 4** of this thesis is dedicated to the relation of retinal vascular calibers with white matter microstructure of the brain (**chapter 4.1**) and enlarged perivascular spaces in the brain (**chapter 4.2**). Chapter 4 continues by investigating the relation of retinal layer thickness with global structural brain measures (**chapter 4.3**), and with specific grey matter regions and white matter tracts (**chapter 4.4**).

In **chapter 5**, I focus on the role of retinal microvascular damage and retinal neurodegeneration in clinical outcomes. In this part, I investigate the association of the retinal vasculature with migraine (**chapter 5.1**) and the association of retinal layer thickness with prevalent and incident dementia (**chapter 5.2**). **Chapter 5.3** explores the relation of the retinal vasculature with cause-specific mortality. In **chapter 6**, I round up the main findings, discuss methodological issues, and reflect from a broader perspective regarding brain research.

## REFERENCES


1. A. N. Evolutionary history of neuro-ophthalmology. Neuro-Ophthalmology. 2000;23:95-126
2. Patton N, Aslam T, Macgillivray T, Pattie A, Deary IJ, Dhillon B. Retinal vascular image analysis as a potential screening tool for cerebrovascular disease: A rationale based on homology between cerebral and retinal microvasculatures. J Anat. 2005;206:319-348
3. Hart NJ, Koronyo Y, Black KL, Koronyo-Hamaoui M. Ocular indicators of alzheimer's: Exploring disease in the retina. Acta Neuropathol. 2016;132:767-787
4. Lim JK, Li QX, He Z, Vingrys AJ, Wong VH, Currier N, et al. The eye as a biomarker for alzheimer's disease. Front Neurosci. 2016;10:536
5. Liew G, Wang JJ, Mitchell P, Wong TY. Retinal vascular imaging: A new tool in microvascular disease research. Circ Cardiovasc Imaging. 2008;1:156-161
6. Cheung CY, Ikram MK, Chen C, Wong TY. Imaging retina to study dementia and stroke. Prog Retin Eye Res. 2017;57:89-107
7. Sousa RM, Ferri CP, Acosta D, Albanese E, Guerra M, Huang Y, et al. Contribution of chronic diseases to disability in elderly people in countries with low and middle incomes: A 10/66 dementia research group population-based survey. Lancet. 2009;374:1821-1830
8. Walsh JB. Hypertensive retinopathy. Description, classification, and prognosis. Ophthalmology. 1982;89:1127-1131
9. Keith NM, Wagener HP, Barker NW. Some different types of essential hypertension: Their course and prognosis. Am J Med Sci. 1974;268:336-345
10. Leishman R. The eye in general vascular disease: Hypertension and arteriosclerosis. Br J Ophthalmol. 1957;41:641-701
11. Tso MO, Jampol LM. Pathophysiology of hypertensive retinopathy. Ophthalmology. 1982;89:1132-1145
12. Scheie HG. Evaluation of ophthalmoscopic changes of hypertension and arteriolar sclerosis. AMA Arch Ophthalmol. 1953;49:117-138
13. Parr JC. Hypertensive generalised narrowing of retinal arteries. Trans Ophthalmol Soc N Z. 1974;26:55-60
14. Parr JC, Spears GF. General caliber of the retinal arteries expressed as the equivalent width of the central retinal artery. Am J Ophthalmol. 1974;77:472-477
15. Hubbard LD, Brothers RJ, King WN, Clegg LX, Klein R, Cooper LS, et al. Methods for evaluation of retinal microvascular abnormalities associated with hypertension/sclerosis in the atherosclerosis risk in communities study. Ophthalmology. 1999;106:2269-2280
16. Wong TY, Klein R, Sharrett AR, Couper DJ, Klein BE, Liao DP, et al. Cerebral white matter lesions, retinopathy, and incident clinical stroke. JAMA. 2002;288:67-74
17. Ikram MK, de Jong FJ, Bos MJ, Vingerling JR, Hofman A, Koudstaal PJ, et al. Retinal vessel diameters and risk of stroke: The rotterdam study. Neurology. 2006;66:1339-1343
18. de Jong FJ, Schrijvers EM, Ikram MK, Koudstaal PJ, de Jong PT, Hofman A, et al. Retinal vascular caliber and risk of dementia: The rotterdam study. Neurology. 2011;76:816-821
19. Ikram MK, De Jong FJ, Van Dijk EJ, Prins ND, Hofman A, Breteler MM, et al. Retinal vessel diameters and cerebral small vessel disease: The rotterdam scan study. Brain. 2006;129:182-188
20. Ikram MK, de Jong FJ, Vernooij MW, Hofman A, Niessen WJ, van der Lugt A, et al. Retinal vascular calibers associate differentially with cerebral gray matter and white matter atrophy. Alzheimer Dis Assoc Disord. 2013;27:351-355
21. Fercher AF, Mengedoht K, Werner W. Eye-length measurement by interferometry with partially coherent light. Opt Lett. 1988;13:186-188
22. London A, Benhar I, Schwartz M. The retina as a window to the brain-from eye research to cns disorders. Nat Rev Neurol. 2013;9:44-53

23. Hinton DR, Sadun AA, Blanks JC, Miller CA. Optic-nerve degeneration in alzheimer's disease. N Engl J Med. 1986;315:485-487
24. Blanks JC, Hinton DR, Sadun AA, Miller CA. Retinal ganglion cell degeneration in alzheimer's disease. Brain Res. 1989;501:364-372
25. Coppola G, Di Renzo A, Ziccardi L, Martelli F, Fadda A, Manni G, et al. Optical coherence tomography in alzheimer's disease: A meta-analysis. PLoS One. 2015;10:e0134750
26. Thomson KL, Yeo JM, Waddell B, Cameron JR, Pal S. A systematic review and meta-analysis of retinal nerve fiber layer change in dementia, using optical coherence tomography. Alzheimers Dement (Amst). 2015;1:136-143

# Chapter 2
# Mediation and Interaction

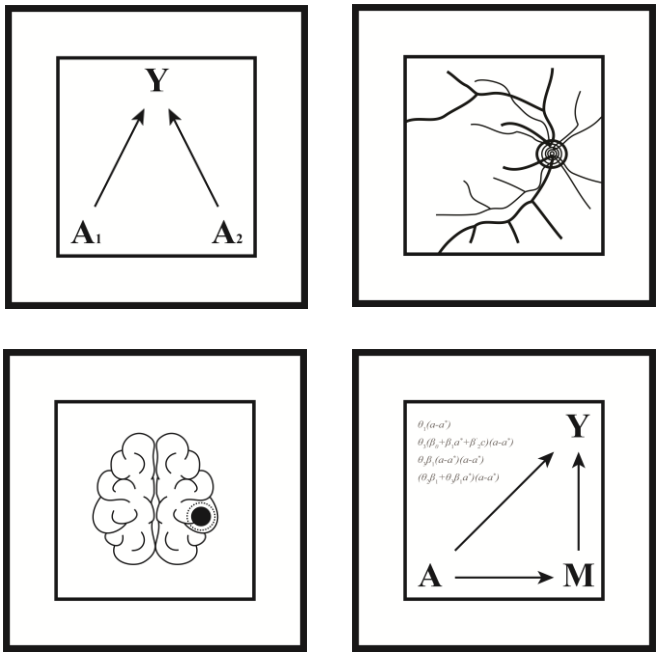

# Chapter 2.1
# The Interaction Between Total Brain Perfusion and Retinal Vessels for the Risk of Stroke: the Rotterdam Study

Marileen L.P. Portegies, Unal Mutlu, Hazel I. Zonneveld, Meike W. Vernooij, M. Kamran Ikram, Caroline C.W. Klaver, Albert Hofman, Peter J. Koudstaal, M. Arfan Ikram

**ABSTRACT**

**Background:** A stroke is often attributed to one causal mechanism. However, pathological mechanisms may interact. One hypothesis is that people with small vessel disease, which can be visualized using retinal diameters, may be more vulnerable to a decrease in brain perfusion. Within the Rotterdam Study, we examined whether total brain perfusion and retinal vessel interact for their risk of stroke or TIA.
**Methods:** Data on total brain perfusion and retinal vessel diameter was collected from 2004 to 2008 in 3000 participants (mean age 58.8 years, 56.4% women) without history of a stroke or TIA. Follow-up finished in 2014. Models were adjusted for age, sex, cardiovascular risk factors, and the other vessel diameter. Effect modification was tested using an interaction term of total brain perfusion and vessel diameter, and by stratification in tertiles.
**Results:** During 19,007 person-years, 29 persons suffered a stroke and 48 persons a TIA. We observed a significant interaction between retinal venular diameter and brain perfusion. Stratified analyses showed that venular diameter was only associated with stroke or TIA in people with the lowest tertile of total brain perfusion (hazard ratio (HR) 1.75, 95% confidence interval (CI) 1.17; 2.60). Total brain perfusion was only associated with stroke in people with the largest tertile of venular diameter (HR 1.70, 95% CI 1.12; 2.59) or arteriolar diameter (HR 1.71, 95% CI 1.10; 2.68).
**Conclusions:** Our results suggest that the risk of stroke and TIA is only increased in people with a combination of impaired brain perfusion and small vessel disease.

## INTRODUCTION

Annually, 17 million people suffer a first-ever stroke worldwide.[1] About 80% of these strokes is ischemic and the consequence of insufficient blood flow to the brain. Reasons for that may be hypoperfusion or an occlusion, which can have its origin anywhere in the vascular system, from the heart to the brain.[2, 3] For each stroke, usually one location is indicated as a cause.[2] Yet, people often have vascular disease at multiple locations, for instance in the small and large vessels.[4-6] Since people with vascular disease at multiple locations seem to have a higher risk of stroke,[5] it may be that assigning one cause is insufficient. Several pathological mechanisms may interact.

Two mechanisms that have the potential to interact are a diminished brain perfusion and small vessel disease. Individually, a low cerebral blood flow has been related to stroke in people with severe intracranial atherosclerotic disease.[7] Small vessel disease, as visualized through the retinal vessels, has been related to stroke in the general population.[8, 9] It has been hypothesized that if these markers are present together, their effect is amplified. Specifically, a previous study showed that a diminished cerebral blood flow had a stronger association with cognitive decline in combination with white matter lesions, suggesting that people with small vessel disease may be more vulnerable to changes in cerebral perfusion.[10] This could also mean that people with small vessel disease are more likely to get a stroke if cerebral perfusion is low compared to people without small vessel disease.

Against this background, our aim was to examine whether brain perfusion and retinal vessel diameter interact in their relation with stroke or TIA. First, we measured their individual effect in our general population. Then, we measured possible effect modification.

## METHODS

### Study setting and population

This study was conducted within the Rotterdam Study, a prospective population-based cohort study that aims to investigate causes and consequences of invalidating diseases in the elderly. Details regarding the objectives and design of the study have been reported previously.[11, 12] The study started in 1990 amongst 7983 participants (Rotterdam Study I (RS-I)) and was extended twice: in 2000 with 3011 persons (RS-II) and in 2006 with 3932 persons (RS-III). The study now consists of 14926 participants aged 45 years and older. Data on both cerebral perfusion and retinal vessels were collected in the second visit of RS-II (2004-2005) and the first visit of RS-III (2006-2008). In these periods, 6438 participants participated, of whom 4599 were invited for an MRI scan and 4161 actually underwent MRI scanning. Participants with an incomplete MRI (n = 429), no fundus color photography for the assessment of retinal vessels (n = 538), no informed consent for collection of follow-up data (n = 21), prevalent stroke or TIA (n = 132), silent cortical infarcts (n = 34), incomplete follow-up (n = 6), and an outlier (n = 1) were excluded (Figure 1). Eventually, 3000 participants were eligible for analysis.

The Rotterdam Study has been approved by the Medical Ethics Committee of the Erasmus MC and by the Ministry of Health, Welfare and Sport of the Netherlands, implementing the Wet Bevolkingsonderzoek: ERGO (Population Studies Act: Rotterdam Study). All participants provided written informed consent to participate in the study and to obtain information from their treating physicians.

**Figure 1.** Flow diagram of the study.

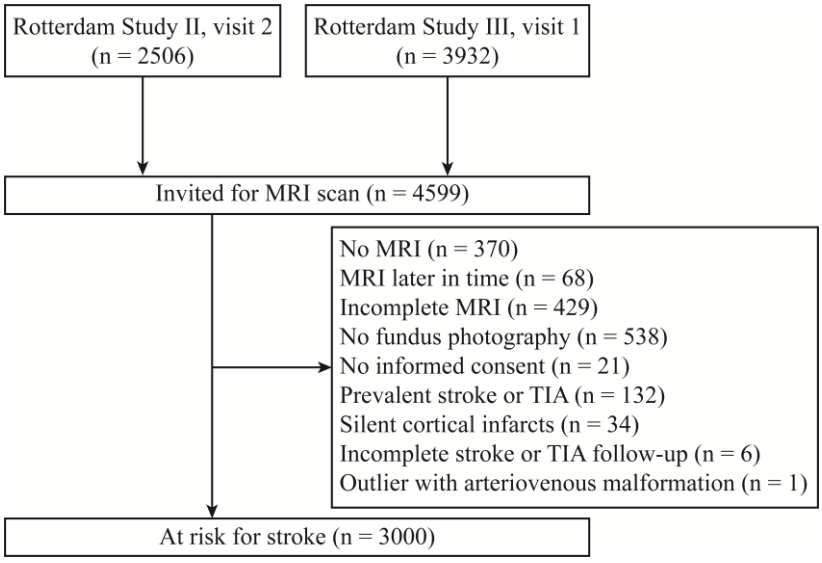

**Brain MRI and brain perfusion**

Magnetic resonance imaging was performed on a 1.5 Tesla MRI scanner (GE Healthcare, Milwaukee, Wisconsin), using an 8-channel head coil. Flow measurement was performed using 2D phase-contrast imaging, as described previously.[13] Additionally, three high-resolution axial MRI sequences were performed, namely a T1-weighted sequence, a proton-density-weighted sequence, and a fluid-attenuated inversion recovery sequence.[13]Cerebral blood flow was calculated from the phase-contrast images using interactive data language-based custom software (Cinetool version 4, GE Healthcare, Milwaukee, Wisconsin). Regions of interest were drawn manually around both carotids and the basilar artery at a level just under the skull base. Flow rates were calculated using the velocity and cross-sectional area of the vessels. To calculate total cerebral blood flow (tCBF), flow rates for the carotid arteries and the basilar artery were summed up and expressed in mL/min. Total brain perfusion (in mL/min per 100mL) was calculated by dividing tCBF by each individual's brain volume (mL) and multiplying the obtained result by 100.[13] Two independent experienced technicians drew all manual regions of interest and subsequently performed the flow measurements (interrater correlations ($n = 533$) > 0.94 for all vessels).[13]

**Retinal vessel measurements**

Details regarding retinal vessel measurements have been described previously.[8, 14] Participants underwent a full eye examination including fundus photography of the optic disc with a 35º visual field camera (TRV-50VT, Topcon Optical Company, Tokyo, Japan) after pharmacologic mydriasis. For each participant, the image with the best quality (left or right eye) was analyzed with a retinal vessel measurement system (IVAN, University of Wisconsin-Madison, Madison, Wisconsin).[15] For each participant, one summary measure was calculated for the arteriolar diameters (in µm) and one for the venular diameters, corrected for magnification changes attributable to refractive errors of the eye. In a random subsample of 100 participants in RS-I, we found no differences between the right and left eyes for the arteriolar and venular calibers. Measurements were performed by 2 trained raters, blinded to the clinical characteristics and outcomes of the participants. Pearson correlation coefficients for interrater agreement were 0.87 for arteriolar caliber and 0.91 for venular caliber in RS-II, and 0.85 for arteriolar caliber and 0.87 for venular caliber in RS-III. Intrarater agreement ranged from 0.65-0.87.[16, 17]

**Assessment of stroke and TIA**

History of stroke and TIA was assessed during the home interview at baseline and confirmed by reviewing medical records.[18, 19] Subsequently, participants were continuously followed for the occurrence of stroke and TIA through automatic linkage of general practitioners' medical records with the study database. Additionally, general practitioners' medical records of participants who moved out of the district and nursing home physicians' medical records were checked on a regular basis. For all potential strokes and TIAs,

information from general practitioners and hospital discharge letters were collected and reviewed by research physicians. An experienced vascular neurologist verified the diagnoses.[18, 19] Strokes were defined according to the World Health Organization Criteria[20] and classified into ischemic or hemorrhagic using neuroimaging reports. A stroke was classified as unspecified if neuroimaging was lacking.[18] Follow-up was complete until January 1, 2014, for 97.2% of potential person-years.

**Assessment of covariates**

Covariates were assessed during the same examination round as the fundus photography, with the use of structured interviews, physical examinations, and blood sampling.[21] Medication use and smoking status were assessed by interview. Smoking was categorized into current, former, or never smoking. Blood pressure was measured twice on the right arm with a random zero sphygmomanometer. The average of the two measurements was used. Total cholesterol and high-density lipoprotein cholesterol were acquired by an automated enzymatic procedure. Diabetes mellitus was defined as having a fasting glucose level of ≥ 7.0 mmol/L, a non-fasting glucose level of ≥ 11.1 mmol/L, or the use of antidiabetic medication. Body mass index was calculated as weight (kg) divided by length squared ($m^2$). Assessment of significant carotid stenosis (> 50%) was performed using 5-MHz pulsed Doppler ultrasonography through interpretation of velocity profiles according to standard criteria.[22]

**Statistical analysis**

We analyzed the association of total brain perfusion and retinal vessel diameter with ischemic stroke and TIA using Cox proportional hazards models. We combined ischemic stroke and TIA to increase power, which is reasonable since they have a similar pathophysiology.[23] Follow-up started at the date of MRI scan. We censored participants at date of stroke, date of TIA, date of death, end of follow-up, or January 1$^{st}$ 2014, whichever came first. Hazard ratios (HRs) with 95% confidence intervals (CIs) were calculated adding total brain perfusion and retinal vessel diameters per standard deviation (SD) increase or decrease into the models. All models were adjusted for age and sex. In all models with vessel diameter as exposure, we adjusted for the other vessel diameter (i.e. venular diameter was adjusted for arteriolar diameter and arteriolar diameter for venular diameter). In the multivariable model, we additionally adjusted for study cohort, systolic blood pressure, diastolic blood pressure, blood pressure lowering medication, total cholesterol, high-density lipoprotein cholesterol, lipid-lowering medication, smoking, diabetes mellitus, body mass index, and carotid stenosis. Effect modification between total brain perfusion and retinal vessel diameter was tested using an interaction term.

In order to further explore possible effect modification, we additionally performed a stratified analysis. Within tertiles of retinal diameter (venular and arteriolar), we examined the association between total brain perfusion and stroke or TIA, and within tertiles of total

brain perfusion, we examined the association between retinal vessel diameter and stroke or TIA. Finally, we categorized the participants based on both tertiles of retinal diameter and tertiles of cerebral perfusion and related these categories to the risk of stroke or TIA. All analyses were done using SPSS version 21.0 (IBM Corporation, Armonk, New York).

## RESULTS

The baseline characteristics of the study population are presented in Table 1. Participants had a mean age (± SD) of 58.8 (± 7.1) years and 56.4% was women. After an average follow-up of 6.3 (± 1.2) years, 29 participants had a stroke, and 48 a TIA.
Table 2 describes the association between total brain perfusion, retinal venular diameter, and retinal arteriolar diameter with stroke or TIA. We only observed an association of retinal venular diameter with stroke or TIA (adjusted HR per SD increase in venular diameter 1.39, 95% CI 1.07; 1.81). Total brain perfusion was not associated with stroke or TIA in the total population (HR 1.17 (0.91; 1.49)). However, stratified for age at median, we did find an association in people younger than 58.7 years (HR 1.61 (1.01; 2.56)). In the total population, we observed interactions between total brain perfusion and both the venular (p-value = 0.006) and arteriolar diameter (p-value = 0.020).
In Table 3, the results of the stratified analyses are shown. Total brain perfusion was only associated with stroke or TIA in people with the largest tertile of venular diameter (HR 1.70 (1.12; 2.59)) or the largest tertile of arteriolar diameter (HR 1.71 (1.10; 2.68)). Venular diameter was only associated with stroke or TIA in people with the lowest tertile of total brain perfusion (HR 1.75 (1.17; 2.60)). Arteriolar diameter was not associated with stroke in any tertile of brain perfusion. Combining all this information in one graph (Figure 2), it appeared that the risk of stroke or TIA was mainly large in people with both the lowest tertile of cerebral perfusion and the highest tertile of venular diameter. The HR of being in tertile 1 of cerebral perfusion and tertile 3 of venular diameter, compared to the reference category (tertile 3 of cerebral perfusion and tertile 1 of venular diameter) was 2.11 (0.77; 5.79). Since the group with tertile 1 of cerebral perfusion and tertile 3 of venular diameter stood out of the rest, we also compared this category with all other categories, which gave a HR of 1.93 (1.07; 3.47). The pattern with arteriolar diameter was less clear.

**Table 1. Baseline characteristics.**

| | At risk for stroke or TIA |
|---|---|
| N | 3000 |
| Age, years | 58.8 (7.1) |
| Women | 1691 (56.4%) |
| Systolic blood pressure, mmHg | 134 (19) |
| Diastolic blood pressure, mmHg | 82 (11) |
| Blood pressure lowering medication | 674 (22.6%) |
| Total cholesterol, mmol/L | 5.6 (1.0) |
| High-density lipoprotein cholesterol, mmol/L | 1.4 (0.4) |
| Lipid-lowering medication | 614 (20.6%) |
| Diabetes mellitus | 243 (8.2%) |
| Smoking | |
| Never | 878 (29.4%) |
| Former | 1400 (46.9%) |
| Current | 708 (23.7%) |
| Body mass index, kg/m$^2$ | 27.5 (4.3) |
| Carotid stenosis > 50% on ultrasound | 55 (1.8%) |
| Total brain perfusion, mL/min per 100 mL | 57.3 (9.4) |
| Venular diameter, µm | 238.3 (22.8) |
| Arteriolar diameter, µm | 156.8 (15.9) |

Data are presented as means (standard deviations) or as numbers (percentages).
Percentages are calculated without missing data.

**Table 2. Total brain perfusion and retinal vessel diameter and the risk of ischemic stroke or TIA.**

| | Ischemic stroke or TIA, n = 77 | | |
|---|---|---|---|
| | **Model 1** | **Model 2** | **Model 3** |
| | **HR (95% CI)** | **HR (95% CI)** | **HR (95% CI)** |
| Total brain perfusion, per SD decrease | 1.16 (0.91; 1.49) | 1.16 (0.91; 1.49) | 1.17 (0.91; 1.49) |
| Retinal venular diameter, per SD increase | 1.40 (1.08; 1.81) | 1.39 (1.07; 1.81) | 1.39 (1.07; 1.81) |
| Retinal arteriolar diameter, per SD decrease | 1.07 (0.82; 1.41) | 1.06 (0.80; 1.42) | 1.06 (0.80; 1.41) |

Abbreviations: TIA, transient ischemic attack; n, number of cases; HR, hazard ratio; CI, confidence interval; SD, standard deviation.
Model 1: adjusted for age, sex, study cohort, and other retinal vessel if applicable.
Model 2: as Model 1, additionally adjusted for systolic blood pressure, diastolic blood pressure, blood pressure lowering medication, total cholesterol, high-density lipoprotein cholesterol, lipid-lowering medication, smoking, diabetes mellitus, body mass index, and carotid stenosis.
Model 3: as Model 2, additionally adjusted for brain perfusion in analyses with vessel diameters, and for vessel diameters in analyses with brain perfusion.

**Table 3. Total brain perfusion and retinal vessel diameter and the risk of ischemic stroke or TIA, within tertiles of retinal vessel diameter or brain perfusion.**

| | | | Ischemic stroke or TIA HR (95% CI) | |
|---|---|---|---|---|
| | | n/N | Model 1 | Model 2 |
| Venular diameter | Total brain perfusion | | | |
| Tertile 1 | per SD decrease | 26/1000 | 0.89 (0.59; 1.36) | 0.88 (0.57; 1.35) |
| Tertile 2 | per SD decrease | 21/1000 | 0.97 (0.61; 1.53) | 0.96 (0.60; 1.52) |
| Tertile 3 | per SD decrease | 30/1000 | 1.69 (1.11; 2.58) | 1.70 (1.12; 2.59) |
| Total brain perfusion | Venular diameter | | | |
| Tertile 3 | per SD increase | 16/1000 | 0.89 (0.49; 1.62) | 0.95 (0.51; 1.76) |
| Tertile 2 | per SD increase | 28/1000 | 1.36 (0.90; 2.05) | 1.29 (0.84; 1.99) |
| Tertile 1 | per SD increase | 33/1000 | 1.70 (1.16; 2.51) | 1.75 (1.17; 2.60) |
| Total brain perfusion | Arteriolar diameter | | | |
| Tertile 3 | per SD decrease | 16/1000 | 0.97 (0.52; 1.80) | 0.97 (0.50; 1.87) |
| Tertile 2 | per SD decrease | 28/1000 | 1.12 (0.71; 1.76) | 1.14 (0.72; 1.81) |
| Tertile 1 | per SD decrease | 33/1000 | 1.01 (0.66; 1.54) | 1.05 (0.67; 1.63) |
| Arteriolar diameter | Total brain perfusion | | | |
| Tertile 3 | per SD decrease | 27/1000 | 1.74 (1.12; 2.69) | 1.71 (1.10; 2.68) |
| Tertile 2 | per SD decrease | 20/1000 | 1.14 (0.70; 1.87) | 1.14 (0.70; 1.86) |
| Tertile 1 | per SD decrease | 30/1000 | 0.89 (0.63; 1.28) | 0.93 (0.64; 1.33) |

Abbreviations: TIA, transient ischemic attack; n, number of cases; N, number of persons included in study; HR, hazard ratio; CI, confidence interval; SD, standard deviation.
Model 1: adjusted for age, sex, study cohort, and other retinal vessel.
Model 2: adjusted for age, sex, study cohort, systolic blood pressure, diastolic blood pressure, blood pressure lowering medication, total cholesterol, high-density lipoprotein cholesterol, lipid-lowering medication, smoking, diabetes mellitus, body mass index, carotid stenosis, and other retinal vessel.

**Figure 2.** Interaction between brain perfusion and venular diameter for the risk of ischemic stroke or TIA. Values are fully adjusted hazard ratios compared to the reference category: tertile 3 of cerebral perfusion and tertile 1 of venular diameter.

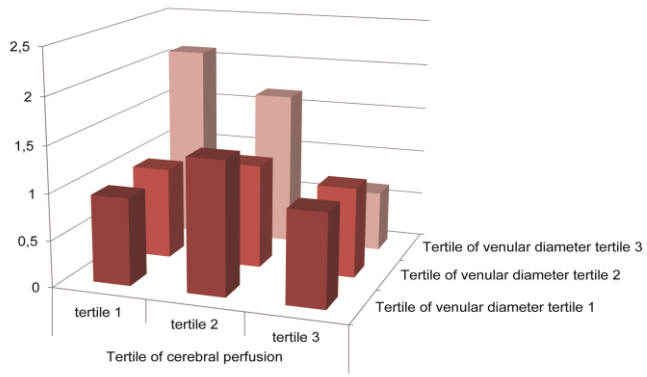


*Hazard ratio 2.11 (95% CI 0.77; 5.79) compared to reference category. Hazard ratio 1.93 (95% CI 1.07; 3.47) compared to all other categories combined.

## DISCUSSION

In this population-based study, we observed that wider retinal venules were associated with an increased risk of stroke or TIA. Total cerebral perfusion was not associated with the risk of stroke in the total population. Interestingly, we observed an interaction between cerebral perfusion and both retinal venules and retinal arterioles for their risk of stroke or TIA. Total cerebral perfusion was associated with stroke or TIA in the highest tertile of venular diameter and in the highest tertile of arteriolar diameter. Correspondingly, venular diameter was only associated with stroke or TIA in the lowest tertile of cerebral perfusion.
A low cerebral blood flow[7] and a wide venular diameter[8, 24, 25] were separately related to stroke in previous studies. The reason why we did not find an association of low cerebral perfusion and stroke in our total population may be explained by our different study population. We included a general population and the previous study included patients with severe stenosis in the intracranial vessels.[7] People in the previous study therefore had a larger impairment of the blood flow than people in our general population. The brain has compensatory mechanisms to keep the local blood perfusion intact for a long time, i.e. cerebral autoregulation, which may be sufficient if people do not have a severe stenosis.[26] In people with cerebral small vessel disease, cerebral autoregulation can be impaired.[27] Although a diminished autoregulation by itself seemed not sufficient to increase the risk of stroke in a previous study,[28] it may increase the risk of stroke or TIA in combination with a low perfusion.[29] A high perfusion may compensate for a diminished autoregulation and a good autoregulation for a diminished perfusion. If both fail, however, this may lead to an increased risk of stroke and TIA. This is a possible explanation for our finding that a lower cerebral perfusion was associated with an increased risk of stroke or TIA in people with wide retinal venules, reflecting small vessel disease, and that wider retinal venules were only associated with an increased risk of stroke in people with a low perfusion. It implies that in people with a stroke or TIA based on small vessel disease, also a source of diminished perfusion should be sought e.g. large artery atherosclerosis.[7] Similarly, in people with a low cerebral perfusion, the amount of small vessel disease should be examined. Another possible explanation is the risk factor load that may be higher in people with both a low perfusion and small vessel disease. However, the associations remained after adjustment for many possible confounders. Furthermore, a diminished perfusion may relate to stroke mediated by small vessel disease,[6, 17] although it is uncertain whether a diminished perfusion leads to small vessel disease or whether this association is inverse.[30] A final explanation therefore is that small vessel disease gives rise to white matter lesions[31] and that these can reduce the blood flow due to a diminished metabolic demand.[30] It may be that small vessel disease only relates to stroke if it is severe enough to demand a lower perfusion.
The finding that a low brain perfusion was also associated with stroke in people with wider arterioles is actually the opposite of what we expected, since arteriolar narrowing is

associated with atherosclerosis.[9, 32] An explanation may be that arteriolar and venular diameter are highly correlated and people with wide venules therefore have wide arterioles.[32] However, we adjusted the analyses with arteriolar diameter for venular diameter and the associations remained. Another explanation may be that arterioles keep the ability to dilate in response to a poor blood flow.[8, 33] This may reflect an exhausted autoregulation or vasomotor reactivity.[33] If arterioles are fully widened in response to the usual blood flow in a person, they may not be able to widen any further in response to extra stimuli, which could lead to a stroke or TIA.[29, 33]

Strengths of our study are the population-based setting and the thorough follow-up for stroke and TIA. A limitation is that pathophysiological subtypes were unavailable for many ischemic strokes. Therefore, we could not define whether the increased risk was the consequence of strokes based on large or small vessel disease. We even had a limited amount of stroke cases, so we had to pool the results of ischemic stroke and TIA. This seems reliable since stroke and TIA have the same etiology.[23] However, these findings should be replicated in a study with more power.

In conclusion, total brain perfusion and retinal vessel diameter interact in their risk of stroke or TIA. This suggests that a combination of a low brain perfusion and small vessel disease is necessary to increase the risk of stroke or TIA. If people have a stroke or TIA based on one of both, it may be useful to also search for the other. Future studies should examine the pathophysiological pathway of this effect and whether prediction of stroke can be improved taking both markers into account.

## REFERENCES


1. Feigin VL, Forouzanfar MH, Krishnamurthi R, Mensah GA, Connor M, Bennett DA, et al. Global and regional burden of stroke during 1990-2010: Findings from the global burden of disease study 2010. Lancet. 2014;383:245-254
2. Adams HP, Jr., Bendixen BH, Kappelle LJ, Biller J, Love BB, Gordon DL, et al. Classification of subtype of acute ischemic stroke. Definitions for use in a multicenter clinical trial. Toast. Trial of org 10172 in acute stroke treatment. Stroke. 1993;24:35-41
3. Jauch EC, Saver JL, Adams HP, Jr., Bruno A, Connors JJ, Demaerschalk BM, et al. Guidelines for the early management of patients with acute ischemic stroke: A guideline for healthcare professionals from the american heart association/american stroke association. Stroke. 2013;44:870-947
4. Bos D, Ikram MA, Elias-Smale SE, Krestin GP, Hofman A, Witteman JC, et al. Calcification in major vessel beds relates to vascular brain disease. Arterioscler Thromb Vasc Biol. 2011;31:2331-2337
5. Kwon HM, Lynn MJ, Turan TN, Derdeyn CP, Fiorella D, Lane BF, et al. Frequency, risk factors, and outcome of coexistent small vessel disease and intracranial arterial stenosis: Results from the stenting and aggressive medical management for preventing recurrent stroke in intracranial stenosis (sammpris) trial. JAMA Neurol. 2016;73:36-42
6. De Silva DA, Liew G, Wong MC, Chang HM, Chen C, Wang JJ, et al. Retinal vascular caliber and extracranial carotid disease in patients with acute ischemic stroke: The multi-centre retinal stroke (mcrs) study. Stroke. 2009;40:3695-3699
7. Dubow JS, Salamon E, Greenberg E, Patsalides A. Mechanism of acute ischemic stroke in patients with severe middle cerebral artery atherosclerotic disease. J Stroke Cerebrovasc Dis. 2014;23:1191-1194
8. Ikram MK, de Jong FJ, Bos MJ, Vingerling JR, Hofman A, Koudstaal PJ, et al. Retinal vessel diameters and risk of stroke: The rotterdam study. Neurology. 2006;66:1339-1343
9. Wong TY. Is retinal photography useful in the measurement of stroke risk? Lancet Neurol. 2004;3:179-183
10. Appelman AP, van der Graaf Y, Vincken KL, Mali WP, Geerlings MI. Combined effect of cerebral hypoperfusion and white matter lesions on executive functioning - the smart-mr study. Dement Geriatr Cogn Disord. 2010;29:240-247
11. Hofman A, Brusselle GG, Darwish Murad S, van Duijn CM, Franco OH, Goedegebure A, et al. The rotterdam study: 2016 objectives and design update. Eur J Epidemiol. 2015;30:661-708
12. Ikram MA, van der Lugt A, Niessen WJ, Koudstaal PJ, Krestin GP, Hofman A, et al. The rotterdam scan study: Design update 2016 and main findings. Eur J Epidemiol. 2015;30:1299-1315
13. Vernooij MW, van der Lugt A, Ikram MA, Wielopolski PA, Vrooman HA, Hofman A, et al. Total cerebral blood flow and total brain perfusion in the general population: The rotterdam scan study. J Cereb Blood Flow Metab. 2008;28:412-419
14. Ikram MK, de Jong FJ, Vingerling JR, Witteman JC, Hofman A, Breteler MM, et al. Are retinal arteriolar or venular diameters associated with markers for cardiovascular disorders? The rotterdam study. Invest Ophthalmol Vis Sci. 2004;45:2129-2134
15. Hubbard LD, Brothers RJ, King WN, Clegg LX, Klein R, Cooper LS, et al. Methods for evaluation of retinal microvascular abnormalities associated with hypertension/sclerosis in the atherosclerosis risk in communities study. Ophthalmology. 1999;106:2269-2280
16. Mutlu U, Ikram MK, Wolters FJ, Hofman A, Klaver CC, Ikram MA. Retinal microvasculature is associated with long-term survival in the general adult dutch population. Hypertension. 2016;67:281-287
17. de Jong FJ, Vernooij MW, Ikram MK, Ikram MA, Hofman A, Krestin GP, et al. Arteriolar oxygen saturation, cerebral blood flow, and retinal vessel diameters. The rotterdam study. Ophthalmology. 2008;115:887-892
18. Wieberdink RG, Ikram MA, Hofman A, Koudstaal PJ, Breteler MM. Trends in stroke incidence rates and stroke risk factors in rotterdam, the netherlands from 1990 to 2008. Eur J Epidemiol. 2012;27:287-295

19. Bos MJ, van Rijn MJ, Witteman JC, Hofman A, Koudstaal PJ, Breteler MM. Incidence and prognosis of transient neurological attacks. JAMA. 2007;298:2877-2885
20. Hatano S. Experience from a multicentre stroke register: A preliminary report. Bull World Health Organ. 1976;54:541-553
21. Kavousi M, Elias-Smale S, Rutten JH, Leening MJ, Vliegenthart R, Verwoert GC, et al. Evaluation of newer risk markers for coronary heart disease risk classification: A cohort study. Ann Intern Med. 2012;156:438-444
22. Taylor DC, Strandness DE, Jr. Carotid artery duplex scanning. J Clin Ultrasound. 1987;15:635-644
23. Easton JD, Saver JL, Albers GW, Alberts MJ, Chaturvedi S, Feldmann E, et al. Definition and evaluation of transient ischemic attack: A scientific statement for healthcare professionals from the american heart association/american stroke association stroke council; council on cardiovascular surgery and anesthesia; council on cardiovascular radiology and intervention; council on cardiovascular nursing; and the interdisciplinary council on peripheral vascular disease. The american academy of neurology affirms the value of this statement as an educational tool for neurologists. Stroke. 2009;40:2276-2293
24. Cheung CY, Tay WT, Ikram MK, Ong YT, De Silva DA, Chow KY, et al. Retinal microvascular changes and risk of stroke: The singapore malay eye study. Stroke. 2013;44:2402-2408
25. Wieberdink RG, Ikram MK, Koudstaal PJ, Hofman A, Vingerling JR, Breteler MM. Retinal vascular calibers and the risk of intracerebral hemorrhage and cerebral infarction: The rotterdam study. Stroke. 2010;41:2757-2761
26. van Beek AH, Claassen JA, Rikkert MG, Jansen RW. Cerebral autoregulation: An overview of current concepts and methodology with special focus on the elderly. J Cereb Blood Flow Metab. 2008;28:1071-1085
27. Markus HS. Genes, endothelial function and cerebral small vessel disease in man. Exp Physiol. 2008;93:121-127
28. Portegies ML, de Bruijn RF, Hofman A, Koudstaal PJ, Ikram MA. Cerebral vasomotor reactivity and risk of mortality: The rotterdam study. Stroke. 2014;45:42-47
29. Gupta A, Chazen JL, Hartman M, Delgado D, Anumula N, Shao H, et al. Cerebrovascular reserve and stroke risk in patients with carotid stenosis or occlusion: A systematic review and meta-analysis. Stroke. 2012;43:2884-2891
30. van der Veen PH, Muller M, Vincken KL, Hendrikse J, Mali WP, van der Graaf Y, et al. Longitudinal relationship between cerebral small-vessel disease and cerebral blood flow: The second manifestations of arterial disease-magnetic resonance study. Stroke. 2015;46:1233-1238
31. Pantoni L. Cerebral small vessel disease: From pathogenesis and clinical characteristics to therapeutic challenges. Lancet Neurol. 2010;9:689-701
32. Sun C, Wang JJ, Mackey DA, Wong TY. Retinal vascular caliber: Systemic, environmental, and genetic associations. Surv Ophthalmol. 2009;54:74-95
33. Reinhard M, Gerds TA, Grabiak D, Zimmermann PR, Roth M, Guschlbauer B, et al. Cerebral dysautoregulation and the risk of ischemic events in occlusive carotid artery disease. J Neurol. 2008;255:1182-1189

# Chapter 2.2
# The Mediating Role of the Venules Between Smoking and Ischemic Stroke

Unal Mutlu, Sonja A. Swanson, Caroline C.W. Klaver, Albert Hofman, Peter J. Koudstaal, M. Arfan Ikram, M. Kamran Ikram

**ABSTRACT**

**Background:** Smoking is a well-established risk factor for ischemic stroke. A potential mechanism by which smoking affects ischemic stroke is through wider venules, but this mediating role of wider venules has never been quantified. In this study, we aimed to estimate to what extent the effect of smoking on ischemic stroke is possibly mediated by the venules via the recently developed four-way effect decomposition.
**Methods:** This study was part of the prospective population-based Rotterdam Study including 9109 stroke-free persons participated in the study in 1990, 2004, or 2006 (mean age: 63.7 years; 58% women). Smoking behavior (smoking versus non-smoking) was identified by interview at participants' first visit. Retinal venular calibers were measured semi-automatically on retinal photographs at the same visit. Incident strokes were assessed between participants' first visit and 1 January 2016. A regression-based approach was used with venular calibers as mediator to decompose the total effect of smoking compared to non-smoking into four components: controlled direct effect (neither mediation nor interaction), pure indirect effect (mediation only), reference interaction effect (interaction only) and mediated interaction effect (both mediation and interaction).
**Results:** During a mean follow-up of 12.5 years, 665 persons suffered an ischemic stroke. Smoking increased the risk of developing ischemic stroke compared to non-smoking with an excess risk of 0.41 (95% confidence interval: 0.10; 0.67). With retinal venules as a potential mediator, the excess relative risk could be decomposed into 77% controlled direct effect, 4% mediation only, 4% interaction only, and 15% mediated interaction.
**Conclusions:** In the pathophysiology of ischemic stroke, the effect of smoking on ischemic stroke may be partly explained by changes in the venules, where there is both pure mediation and mediated interaction.

## INTRODUCTION

As it is well-established that smoking increases the risk of ischemic stroke, mechanisms by which this occurs have been broadly investigated in recent decades. One possible mechanism by which smoking may lead to ischemic stroke is through changes in the cerebral venules.[1] Existing evidence shows that damage to the venules plays an important role in the development of ischemic stroke.[2] At the same time, it has been shown that smoking is associated with wider venules, implicating that changes in cerebral venules mediate the effect of smoking on ischemic stroke.[1] However, it remains unclear whether the effects of smoking on ischemic stroke are mediated through wider venules, whether there is interaction between smoking and wider venules, or whether a combination of mediation and interaction could be occurring. In epidemiologic studies, questions pertaining to mediation have been traditionally tackled with methods that assume no exposure-mediator interaction. Recent advances in the conceptual framework of causal mediation allow estimating the direct and indirect effect even in the presence of an exposure-mediator interaction.[3] Moreover, these advances allow further effect decomposition to explore both mediation and interaction simultaneously i.e. to decompose the exposure's effect on the outcome into components related to mediation only, interaction only, both, or neither (formal definitions are provided below).[4] When free of bias, this approach provides insight into relevant processes in the pathways under study, and enables researchers to better understand biological mechanisms. Thus far, the four-way decomposition method has not been extensively used in clinical research. Application of this counterfactual approach of causal mediation analysis in clinical research may provide insight into the pathophysiology of clinical outcomes. Moreover, in terms of future interventions, this approach may aid the clinician in identifying the best target for treatment, or even show why certain treatments do not work.

In this study, we aimed to understand the role of the venules in the effect of smoking on ischemic stroke by applying the four-way decomposition method.

## METHODS

### Study setting and population

This study is based on the Rotterdam Study (RS), a large prospective population-based cohort study in the Netherlands that investigates causes and consequences of chronic diseases in the general population.[5] All inhabitants of the Ommoord district in the city Rotterdam, aged 55 years or older, were invited to the study in 1990 (RS-I). In 2000 those who had become 55 years of age or moved into the study district were invited (RS-II). In 2006 a further extension of the cohort was initiated and inhabitants aged 45 years or older were invited (RS-III). Home interviews including assessment of smoking, and physical examinations take place every three to four years. Retinal vascular calibers were measured at the baseline visit of RS-I (RS-I-1), in a random sample of the second visit of RS-II (RS-II-2), and at the baseline visit of RS-III (RS-III-1), see Figure 1. We considered the date at which smoking assessment was done in RS-I-1, RS-II-2 and RS-III-1 as our baseline. We excluded persons without data on smoking, without gradable retinal photographs, persons with a history of stroke at baseline, and persons who did not give permission to monitor for future disease event. The Rotterdam Study has been approved by the Medical Ethics Committee of the Erasmus MC and by the Ministry of Health, Welfare and Sport of the Netherlands, implementing the "Population Studies Act: Rotterdam Study" (Wet Bevolkingsonderzoek: ERGO). All participants provided written informed consent to participate in the study and to obtain information from their treating physicians.

**Figure 1.** Flow diagram of the study.

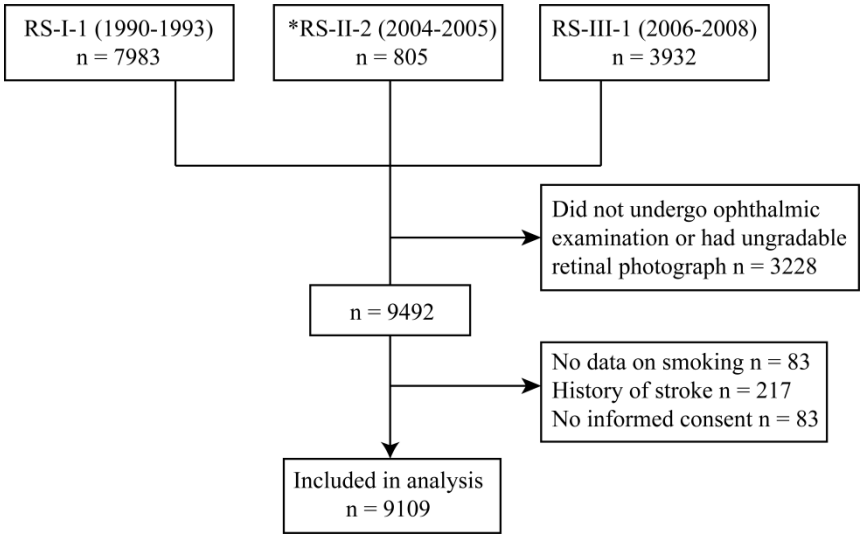


*Retinal images of 805 persons from 2506 participants were randomly selected for retinal caliber measurement.

**Assessment of smoking**

Information on smoking behavior was obtained using a computerized questionnaire during the home visits. Participants were classified as current smokers, or non-smokers (including both former or never smokers). Current smokers were participants who answered yes to the question: "are you currently smoking?" Former smokers were participants who answered no to this question and answered positively to the question: "are you a former smoker?"

**Assessment of the venules**

Participants underwent a full eye examination at each subcohort's baseline (1990, 2004, and 2006) including retinal photography of the optic disc of both eyes after pharmacological mydriasis. For visit RS-I-1 a 20° visual field camera (TRC-SS2, Topcon, Tokyo, Japan) was used, and for visits RS-II-2 and RS-III-1 a 35° visual field camera (TRC-50EX, Topcon Optical Company, Tokyo, Japan) was used. For each participant, the image of one eye with the best quality was analyzed with a retinal vessel measurement system (IVAN, University of Wisconsin-Madison, Madison, Wisconsin). For each participant one summary value was calculated for the arteriolar diameters (in μm) and one for the venular diameters (in μm) of the blood column after correction for differences in magnification due to refractive status of the eye, enabling us to use the separate arteriolar and venular diameter sum values.[6, 7] We verified in a random subsample of 100 participants in RS-I that individual measurements in the left and right eye were similar. Measurements were performed by total four trained raters, masked for participant characteristics. Pearson correlation coefficient for interrater agreement were for arteriolar diameters 0.67-0.87, and for venular diameters 0.91-0.94. For intrarater agreement the correlation coefficients were 0.65-0.88 for arteriolar diameters, and 0.82-0.95 for venular diameters.

**Assessment of stroke**

History of stroke was assessed using home interviews and confirmed by reviewing medical records. Participants were continuously followed up for stroke through digital linkage of general practitioners' files with the study database.[8] Furthermore, nursing home physicians' files and files from general practitioners of participants who moved out of the district were checked on a regular basis. Hospital discharge letters and information from general practitioners was collected for all potential strokes. Research physicians reviewed the information and an experienced neurologist verified the strokes. Strokes were further classified into ischemic or hemorrhagic based on neuroimaging reports. Subarachnoid hemorrhages were excluded. Infarcts that turned hemorrhagic were classified as ischemic stroke. If neuroimaging was lacking, a stroke was classified as unspecified. Follow-up was complete until 1 January 2016. Participants suffering stroke at any point in follow-up were dichotomized as yes/no.

**Assessment of covariates**

We considered the "smoking/ischemic stroke" relation, and "wider venules/ischemic stroke" relation to be confounded by the same set of measured persons characteristics. All confounders were assessed at the same visit period when smoking was assessed and when retinal photographs were obtained. Blood pressure was measured twice in sitting position at the right brachial artery with a random-zero sphygmomanometer, and the average of two readings was used for analysis. Body mass index was computed as weight (kg) divided by height squared ($m^2$). Serum total and high-density lipoprotein cholesterol concentrations were determined by means of an automated enzymatic procedure. White blood cell count was assessed in citrate plasma using a Coulter counter T540 (Coulter electronics, Luton, England). Diabetes mellitus was considered present if participants reported use of antidiabetic medication or when non-fasting serum glucose level was equal to or greater than 11.1 mmol/L, or when fasting serum glucose level was equal to or greater than 7.0 mmol/L. Alcohol consumption was calculated as amount of alcohol in g/day. Carotid plaques were assessed by ultrasound at the carotid artery bifurcation, common carotid artery, and internal carotid artery on both sides. Plaques were defined as focal thickening of the vessel wall of at least 1.5 times the average intima-media thickness relative to adjacent segments with or without calcified components. The carotid artery plaque score (range: 0 to 6) reflected the number of these locations with plaques. Information on blood pressure lowering medication use and education level (low: primary education, intermediate: secondary general or vocational education, or high: higher vocational education or university) was obtained during the home interview by a questionnaire. Definitions of a history of myocardial infarction, coronary artery bypass graft, and percutaneous coronary intervention has been described extensively previously.[9]

**Four-way decomposition method**

In causal mediation analysis, the total causal effect of the exposure on the outcome can be decomposed into four components in the presence of an exposure-mediator interaction[4]: the controlled direct effect due to neither mediation nor interaction (in the current study: the effect of smoking on ischemic stroke which does not go through wider venules), reference interaction effect due to interaction alone (in the current study: the interaction of smoking with the observed level of wider venules), mediated interaction effect due to both mediation and interaction (in the current study: the interaction of smoking with wider venules that has been explicitly caused by smoking), and the pure indirect effect due to mediation alone (in the current study: the effect of smoking on ischemic stroke which purely goes through wider venules). Of note, for mediated interaction it is defined by the mediator having an effect on the outcome only in the presence of the exposure, but not in the absence of exposure, i.e. the exposure is necessarily present for the mediator to affect the outcome. Pure mediation is defined by the mediator having an effect on the outcome even in the absence of the exposure. Moreover, the controlled direct effect and reference interaction

effect can be combined into the natural direct effect. Similarly, the mediated interaction effect and pure indirect effect can be combined into the natural indirect effect.[10-12] Figure 2 shows a causal diagram representing the association of smoking with risk of ischemic stroke mediated by wider venules. Several conditions need to be met in order to identify each of the four components, including the following assumptions concerning confounding: (1) the effect of smoking on ischemic stroke should be unconfounded conditional on the baseline covariates; (2) the effect of wider venules on incident ischemic stroke should be unconfounded conditional on smoking and baseline covariates; (3) the effect of smoking on wider venules should be unconfounded conditional on baseline covariates; (4) the mediator-outcome confounders should not be affected by smoking. Of note, for the total effect only the first of these assumptions is required; the controlled direct effect only requires the first and second assumptions.[4]

**Figure 2.** A causal diagram in which *C* confounds the smoking/ischemic stroke, wider venules/ischemic stroke, and smoking/wider venules relation. We assume that there is no unmeasured confounding, and that smoking does not affect *C*. Here *C* and *U* refer to the following list of measured person characteristics: age, sex, subcohort, education, systolic blood pressure, diastolic blood pressure, blood pressure lowering medication use, body mass index, total cholesterol, high-density lipoprotein cholesterol, white blood cell count, diabetes mellitus, alcohol intake, carotid plaques, history of cardiovascular disease, and retinal arteriolar caliber.

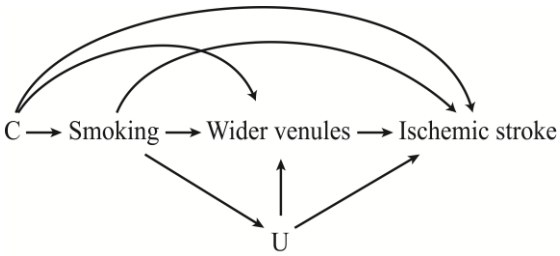


**Statistical analyses**

To obtain estimates of the four components from the data, a regression-based approach was used. First, we used a logistic regression model of incident ischemic stroke by smoking, retinal venular caliber, a product term denoting the interaction between smoking and the retinal venular caliber, and the covariates. Next, we used a linear regression model of retinal venular caliber on smoking and the covariates. We adjusted both regressions for the following covariates: age, sex, subcohort, education, systolic blood pressure, diastolic blood pressure, blood pressure lowering medication use, body mass index, total cholesterol, high-density lipoprotein cholesterol, white blood cell count, diabetes mellitus, alcohol intake, carotid plaque, history of cardiovascular disease, and the retinal arteriolar caliber. We obtained estimates of the four components by combining parameters from these two models according to the analytic expressions provided by VanderWeele.[4] Confidence intervals for the effect estimates were obtained via case resampling bootstrapping with 1000 iterations.

We defined the proportion of the effect that was attributable to each component by dividing the estimate of a component by the excess relative risk. The overall proportion mediated was defined as the pure indirect effect plus mediated interaction divided by the excess relative risk; the overall proportion attributable to interaction was defined as the reference interaction plus mediated interaction divided by the excess relative risk; the overall proportion eliminated was defined as the excess relative risk minus the controlled direct effect divided by the excess relative risk.

In additional analyses, we aimed to address whether it is the smoking at the moment of the venular caliber assessment or the history of smoking that mattered most. Therefore, we redid the analyses by comparing ever smoking (i.e. past smoking and current smoking) to never smoking.

Finally, we performed sensitivity analyses to determine how much the estimates of the natural direct and indirect effect would change under different degrees of confounding by a hypothetical unmeasured binary confounder. Although we have adjusted for several potential confounders, the estimates will of course be biased if there remains important unmeasured or residual confounding of the relation between wider venules and ischemic stroke; here, for example, we may be concerned that there is residual confounding by unhealthy lifestyle (e.g. unhealthy diets or physical inactivity). For this analysis, we used bias formulas for odds ratios for natural direct and indirect effects as described in VanderWeele.[13] Briefly, bias-corrected-effect estimates for the natural direct and indirect effect were calculated by specifying a range of plausible values for the effect of the unmeasured confounder on ischemic stroke, and specifying a range of plausible values for the prevalence of unmeasured confounder among non-smokers and smokers. Next, these bias-corrected-effect estimates were subtracted from the crude natural direct and indirect effect (i.e. adjusted for age, sex, and subcohort) to address change in effect estimate if we had been able to adjust for this unmeasured confounder. Hence, a positive difference could be interpreted as an underestimation of the observed natural direct or indirect effect estimate failing to adjust for the unmeasured confounder, whereas a negative difference could be interpreted as an overestimation. All analyses were performed in R version 3.2.3.

## RESULTS

Table 1 shows the baseline characteristics of the study population by persons included and excluded from analysis. Compared to persons included in the analysis, persons excluded from the analysis were older, were lower educated, were more users of blood pressure lowering medication, had a higher diastolic blood pressure, a higher serum total cholesterol, a lower serum high-density lipoprotein cholesterol, a higher white blood cell count, a higher daily alcohol intake, and had more often carotid plaques, diabetes mellitus, and a history of cardiovascular disease.

Table 2 shows the baseline characteristics of the study population by smoking status. While some characteristics were similar across the groups, others were notably different. For example, comparing the groups to each other, never smokers were more often women and had a higher systolic blood pressure; past smokers had more often diabetes mellitus and a history of cardiovascular disease; current smokers had wider venular calibers and had more incident stroke cases.

During a mean follow-up of 12.5 years (113,885.0 person-years), 665 persons had an ischemic stroke. Without adjustment for retinal vascular calibers, smoking increases the risk of ischemic stroke, odds ratio (OR): 1.38 (95% CI: 1.13; 1.67), but this risk decreases to 1.34 (1.09; 1.63) after adjusting for the retinal vascular calibers.

Table 3 shows the results of the four-way decomposition. In the model accounting for the presence of an interaction between smoking and venules (P-value for interaction = 0.029), smoking increases the risk of ischemic stroke: 1.41 (1.10; 1.67), whereas in the model accounting for the presence of an interaction between smoking and arterioles (P-value for interaction = 0.737), the risk of smoking on ischemic stroke is 1.34 (1.06; 1.59). With venules as being the mediator, 77% of the excess relative risk of smoking on ischemic stroke compared to non-smoking is attributable to the controlled direct effect, 4% to only interaction, 15% to both interaction and mediation, and 4% is only attributable to mediation. Hence, the overall proportion of the effect of smoking on ischemic stroke that is mediated by wider venules is 19%. Redoing this causal mediation analysis but now comparing ever smoking to never smoking showed that 93% of the excess relative risk of ever smoking on ischemic stroke compared to never smoking is attributable to the controlled direct effect, whereas 11% to both interaction and mediation (P-value for interaction = 0.004).

Figure 3 shows the results of the sensitivity analysis. Assuming that the unmeasured confounder (e.g. unhealthy lifestyle) increases the risk of ischemic stroke, and that this confounder is more prevalent among smokers compared to non-smokers, the crude natural direct effect of 1.48 seems to overestimate the bias-corrected effect; the crude natural indirect effect of 1.05 seems to underestimate the bias-corrected effect. In these scenarios, the degree of mediation of smoking by venules would be underestimated without adjustment. In contrast, if the unmeasured confounder is more prevalent among non-smokers compared to smokers, the observed natural direct effect underestimates the true effect, whereas the natural indirect effect overestimates the true effect.

**Table 1. Characteristics of the study population by persons included and excluded from analysis.**

| Characteristic | Included | Excluded |
|---|---|---|
| N | 9109 | 3611 |
| Age, years | 63.7 (9.0) | 71.7 (12.7) |
| Female sex | 5286 (58) | 2251 (62) |
| Education | | |
| Low | 3869 (43) | 2019 (56) |
| Intermediate | 3839 (42) | 1190 (33) |
| High | 1401 (15) | 402 (11) |
| Systolic blood pressure, mmHg | 136.7 (21.0) | 140.8 (22.5) |
| Diastolic blood pressure, mmHg | 77.2 (11.9) | 76.4 (12.8) |
| Blood pressure lowering medication | 2638 (29) | 1377 (38) |
| Body mass index, $kg/m^2$ | 26.9 (4.1) | 26.7 (4.2) |
| Total cholesterol, mmol/L | 6.2 (1.3) | 6.2 (1.3) |
| High-density lipoprotein cholesterol, mmol/L | 1.4 (0.4) | 1.3 (0.4) |
| White blood cell, $count/mm^3$ | 6.7 (1.9) | 6.9 (2.3) |
| Diabetes mellitus type 2 | 663 (7) | 331 (9) |
| Daily alcohol intake | | |
| Non-drinker | 2626 (29) | 635 (18) |
| ≤ 15 g | 4251 (47) | 1898 (53) |
| > 15 g | 2232 (25) | 1078 (30) |
| Carotid plaque score ≥ 4 | 1338 (15) | 702 (19) |
| History of cardiovascular disease | 575 (6) | 230 (6) |
| Smoking status | | |
| Non-smoker | 2921 (32) | 1339 (37) |
| Past smoker | 4012 (44) | 1525 (42) |
| Current smoker | 2176 (24) | 747 (21) |
| Venular caliber, µm | 228.6 (23.1) | NA |
| Arteriolar caliber, µm | 150.8 (15.7) | NA |

Values are presented as means (standard deviation) or as numbers (percentage).
Abbreviation: NA, not applicable.

**Table 2. Characteristics of the study population by smoking status.**

| Characteristic | Never smoking | Past smoking | Current smoking |
|---|---|---|---|
| N | 2921 | 4012 | 2176 |
| Age, years | 65.0 (10.0) | 63.9 (8.5) | 61.9 (8.2) |
| Female sex | 2397 (82) | 1824 (46) | 1065 (49) |
| Education | | | |
| Low | 1422 (49) | 1494 (37) | 953 (44) |
| Intermediate | 1094 (38) | 1823 (45) | 922 (42) |
| High | 405 (14) | 695 (17) | 301 (14) |
| Systolic blood pressure, mmHg | 138.3 (21.2) | 136.9 (20.5) | 134.2 (21.2) |
| Diastolic blood pressure, mmHg | 77.1 (11.8) | 77.6 (11.8) | 76.3 (12.2) |
| Blood pressure lowering medication | 886 (30) | 1256 (31) | 496 (23) |
| Body mass index, $kg/m^2$ | 27.1 (4.1) | 27.1 (4.0) | 26.1 (4.1) |
| Total cholesterol, mmol/L | 6.3 (1.3) | 6.2 (1.2) | 6.2 (1.3) |
| High-density lipoprotein cholesterol, mmol/L | 1.5 (0.4) | 1.4 (0.4) | 1.3 (0.4) |
| White blood cell, $count/mm^3$ | 6.3 (1.6) | 6.5 (1.7) | 7.8 (2.1) |
| Diabetes mellitus type 2 | 202 (7) | 304 (8) | 157 (7) |
| Daily alcohol intake | | | |
| Non-drinker | 1198 (41) | 918 (23) | 510 (23) |
| ≤ 15 g | 1412 (48) | 1944 (49) | 895 (41) |
| > 15 g | 311 (11) | 1150 (29) | 771 (35) |
| Carotid plaque score ≥ 4 | 285 (10) | 615 (15) | 438 (20) |
| History of cardiovascular disease | 104 (4) | 359 (9) | 112 (5) |
| Venular caliber, µm | 223.8 (22.7) | 227.7 (22.0) | 236.8 (23.4) |
| Arteriolar caliber, µm | 149.4 (15.7) | 149.9 (15.5) | 154.7 (15.8) |
| Incident stroke cases | 188 (6) | 287 (7) | 190 (9) |

Values are presented as means (standard deviation) or as numbers (percentage).

| **Table 3. Four-way decomposition of the effect of smoking on stroke by venules.** | |
|---|---|
| | **Current smokers compared to non-smokers Effect estimate (95% confidence interval)** |
| Total Effect | 1.41 (1.10; 1.67) |
| Excess relative risk due to each component | |
| Controlled Direct Effect | 0.32 (0.03; 0.58) |
| Reference Interaction | 0.02 (-0.03; 0.03) |
| Mediated Interaction | 0.06 (-0.00; 0.11) |
| Pure Indirect Effect | 0.02 (-0.01; 0.04) |
| Proportion of effect due to each component | |
| Controlled Direct Effect | 77% (60%; 120%) |
| Reference Interaction | 4% (-10%; 8%) |
| Mediated Interaction | 15% (-10%; 28%) |
| Pure Indirect Effect | 4% (-8%; 11%) |
| Overall proportion | |
| Mediated | 19% (-12%; 31%) |
| Attributable to interaction | 19% (-18%; 35%) |
| Eliminated | 22% (-20%; 39%) |

Values are adjusted for age, sex, subcohort, education, systolic blood pressure, diastolic blood pressure, blood pressure lowering medication use, body mass index, total cholesterol, high-density lipoprotein cholesterol, white blood cell count, diabetes mellitus, alcohol intake, carotid plaques, history of cardiovascular disease, and retinal arteriolar caliber.

**Figure 3.** Illustrates how a crude natural direct effect estimate of 1.48 and a crude natural indirect effect estimate of 1.05 (the intercept on y-axis) would change under different magnitudes of confounding by a binary unmeasured variable *U*. The difference between the observed effect and bias-corrected-effect is depicted on the Y-axis, and the difference in prevalence of *U* between non-smokers and smokers is depicted on the X-axis. The colored lines are a range of plausible values for the effect of *U* on ischemic stroke.

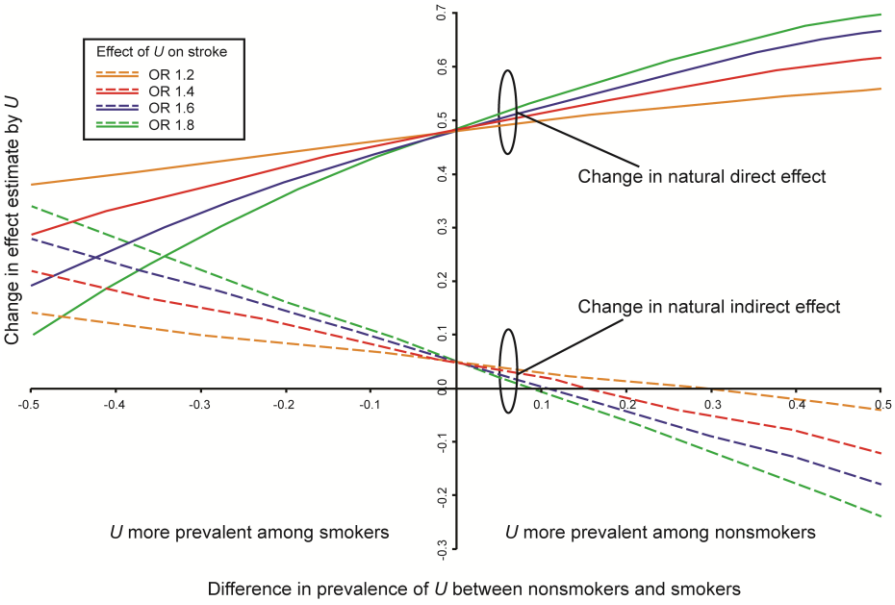


## DISCUSSION

In this population-based cohort study, we found that the effect of smoking on incident ischemic stroke is partly explained through changes in the venules, where there is both mediation and mediated interaction between smoking and the venules.

Thus far, studies focusing on the relation of microvascular damage with the risk of ischemic stroke found that wider venules, but not narrower arterioles were related to incident ischemic stroke.[14, 15] Given that smoking is related to wider venules and not to narrower arterioles, these findings suggest that the effect of smoking on ischemic stroke might be mediated by wider venules. Indeed, our indirect effect estimate (1.08, 95% CI: 1.01; 1.14) supports this hypothesis. Importantly, we have further decomposed the direct effect into the controlled direct effect and reference interaction effect, and the indirect effect into the mediated interaction effect and the pure indirect effect, and indeed found evidence that the mediated component reflects in part mediation only and in part a mediated interaction between smoking and wider venules.

It is well-established that the components of the total effect decomposition we estimated here (with the exception of the controlled direct effect) do not directly address questions pertaining clinical or public health decision-making.[16, 17] Rather, this total effect

decomposition can be seen as a means of exploring *why* certain total effects are present (in our study: why smoking affects ischemic stroke), and therefore can possibly inspire further research directions that lend themselves to more directly clinical implications. For example, a recent study has conceptualized mediated interaction and illustrated the concept of reversible and irreversible damage.[17] This conceptualization of our mediated interaction effect estimate could be viewed as the effect of smoking on ischemic stroke by wider venules that is reversible. Similarly, the conceptualization of our pure indirect effect would be the effect of smoking on ischemic stroke by wider venules that is irreversible.[17] With this particular interpretation, our findings suggest that smoking cessation might not lower the risk of ischemic stroke completely by changing venules. Practically, this could mean that once the venules have become wider due to smoking, even if you stop smoking, wider venules will affect the risk of ischemic stroke. Note, however, that explicitly assessing this hypothesis is feasible with longitudinal data on smoking behaviors and the venules. In other words, our findings inspire and support this as a topic for future research. Interestingly, one Japanese study has investigated the effect of smoking cessation on the retinal vascular calibers, and showed that the effect of smoking on wider venules is reversible in women, following 10 or more years of smoking cessation.[18]

Some limitations merit attention. Within the causal inference literature on mediation and interaction, it remains unclear to what extent each of the four components are susceptible to different forms of bias.[4] Recent evidence suggests that interaction may be more robust to confounding, but may be more sensitive to measurement error when the two exposures are correlated.[19] Here, we reflect separately on confounding, selection bias, and information bias. First, it should be noted that the mediation analyses are subject to strong 'no unmeasured confounding' conditions.[20] As the Rotterdam Study is conducted in an ethnically homogenous Dutch population, it is unlikely that ethnicity related genes will result in major confounding of the smoking/wider venules, or smoking/ischemic stroke relation. Although we adjusted for many measured demographic and health-related person characteristics, residual or unmeasured confounding from socioeconomic status, sedentary lifestyle, physical inactivity, and unhealthy diets may affect our estimates. Currently, there are no bias formulas for each of the four components, and therefore, we performed a sensitivity analysis developed for the natural direct and indirect effects.[13] Given the expected direction of residual confounding (i.e. unmeasured confounders like unhealthy lifestyle increases the risk of ischemic stroke, and that smokers have more often an unhealthy lifestyle than non-smokers), our sensitivity analysis suggests that the indirect effect reported here underestimates the true mediated effect whereas the observed direct effect overestimates the true direct effect.

Concerning selection bias, persons excluded from our analyses had a worse cardiovascular risk profile, suggesting a possible but likely limited role for bias due to selecting on mediator assessments. Likely, these persons did not participate in our study due to their poor health condition which implicates the inclusion of relatively healthy persons in our

study.
Ignoring measurement error have been suggested to overestimate the direct effect of an exposure, and thus, underestimate the indirect effect.[21] In our study, we did not use a dynamic measure of the venules, synchronized on the cardiac cycle, but a static measure. As such, this may have caused independent non-differential misclassification leading to an underestimation of the indirect effects. Another independent non-differential misclassification that may have occurred is due to the fact that we have used the retinal microvasculature as a proxy for the condition of the cerebral microvasculature. Given that the retinal and cerebral microvasculature have similarities in anatomy, physiology and embryology, the retinal microvasculature has been widely used to study vascular brain diseases.[22] However, it is conceivable that such proxy measures may have caused some independent non-differential misclassification of the effect estimates.
In conclusion, we found that in the pathophysiology of ischemic stroke, the effect of smoking on the risk of ischemic stroke may partly be explained by changes in the venules, where there is both pure mediation and mediated interaction between smoking status and the venules. Our study shows that causal mediation analysis in clinical research may provide insights into the pathophysiology of clinical outcomes.

## REFERENCES


1. Ikram MK, de Jong FJ, Vingerling JR, Witteman JC, Hofman A, Breteler MM, et al. Are retinal arteriolar or venular diameters associated with markers for cardiovascular disorders? The rotterdam study. Invest Ophthalmol Vis Sci. 2004;45:2129-2134
2. McGeechan K, Liew G, Macaskill P, Irwig L, Klein R, Klein BE, et al. Prediction of incident stroke events based on retinal vessel caliber: A systematic review and individual-participant meta-analysis. Am J Epidemiol. 2009;170:1323-1332
3. Valeri L, Vanderweele TJ. Mediation analysis allowing for exposure-mediator interactions and causal interpretation: Theoretical assumptions and implementation with sas and spss macros. Psychol Methods. 2013;18:137-150
4. VanderWeele TJ. A unification of mediation and interaction: A 4-way decomposition. Epidemiology. 2014;25:749-761
5. Hofman A, Brusselle GG, Darwish Murad S, van Duijn CM, Franco OH, Goedegebure A, et al. The rotterdam study: 2016 objectives and design update. Eur J Epidemiol. 2015;30:661-708
6. Knudtson MD, Lee KE, Hubbard LD, Wong TY, Klein R, Klein BE. Revised formulas for summarizing retinal vessel diameters. Curr Eye Res. 2003;27:143-149
7. Littmann H. [determining the true size of an object on the fundus of the living eye] zur bestimmung der wahren grosse eines objektes auf dem hintergrund eines lebenden auges. Klin Monbl Augenheilkd. 1988;192:66-67
8. Wieberdink RG, Ikram MA, Hofman A, Koudstaal PJ, Breteler MM. Trends in stroke incidence rates and stroke risk factors in rotterdam, the netherlands from 1990 to 2008. Eur J Epidemiol. 2012;27:287-295
9. Leening MJ, Kavousi M, Heeringa J, van Rooij FJ, Verkroost-van Heemst J, Deckers JW, et al. Methods of data collection and definitions of cardiac outcomes in the rotterdam study. Eur J Epidemiol. 2012;27:173-185
10. Robins JM, Greenland S. Identifiability and exchangeability for direct and indirect effects. Epidemiology. 1992;3:143-155
11. Pearl J. Direct and indirect effects. Proceedings of the Seventeenth Conference on Uncertainty and Artificial Intelligence. 2001;411-420
12. VanderWeele TJ. A three-way decomposition of a total effect into direct, indirect, and interactive effects. Epidemiology. 2013;24:224-232
13. VanderWeele TJ. Bias formulas for sensitivity analysis for direct and indirect effects. Epidemiology. 2010;21:540-551
14. Ikram MK, de Jong FJ, Bos MJ, Vingerling JR, Hofman A, Koudstaal PJ, et al. Retinal vessel diameters and risk of stroke: The rotterdam study. Neurology. 2006;66:1339-1343
15. Wong TY, Kamineni A, Klein R, Sharrett AR, Klein BE, Siscovick DS, et al. Quantitative retinal venular caliber and risk of cardiovascular disease in older persons: The cardiovascular health study. Arch Intern Med. 2006;166:2388-2394
16. Naimi AI, Kaufman JS, MacLehose RF. Mediation misgivings: Ambiguous clinical and public health interpretations of natural direct and indirect effects. Int J Epidemiol. 2014;43:1656-1661
17. Richardson T, Robins JM. Single world intervention graphs (swigs): A unification of the counterfactual and graphical approaches to causality.Working paper number 128, Center for Statistics and the Social Sciences, University of Washington
18. Yanagi M, Misumi M, Kawasaki R, Takahashi I, Itakura K, Fujiwara S, et al. Is the association between smoking and the retinal venular diameter reversible following smoking cessation? Invest Ophthalmol Vis Sci. 2014;55:405-411
19. Valeri L, Lin X, VanderWeele TJ. Mediation analysis when a continuous mediator is measured with error and the outcome follows a generalized linear model. Stat Med. 2014;33:4875-4890

20. Ding P, VanderWeele TJ. Sensitivity analysis without assumptions. Epidemiology. 2016;27:368-377
21. VanderWeele TJ, Valeri L, Ogburn EL. The role of measurement error and misclassification in mediation analysis: Mediation and measurement error. Epidemiology. 2012;23:561-564
22. Liew G, Wang JJ, Mitchell P, Wong TY. Retinal vascular imaging: A new tool in microvascular disease research. Circ Cardiovasc Imaging. 2008;1:156-161

# Chapter 2.3
# Clinical Interpretation of Negative Mediated Interaction

Unal Mutlu, Sonja A. Swanson, M. Arfan Ikram, M. Kamran Ikram

**ABSTRACT**

Recently, using a counterfactual framework, a causal mediation analysis has been formalized to decompose the total effect of a time-fixed exposure on an outcome into four components, that can be loosely defined as being components due to mediation only, interaction only, mediated interaction, and neither. The interpretation of the estimated effect sizes of each component will be hard when some components are of opposite sign. Particularly, a negative mediated interaction might be intuitively difficult to conceptualize, and so far, lacks an easy-to-understand biological or mechanical interpretation. In this paper, we focus on negative mediated interaction, and propose an interpretation using biological examples. We aim to make researchers realize that negative effect estimates might reflect relevant biological process in the mechanism under study.

## BACKGROUND

Advances in causal inference on the topic of mediation have provided new opportunities to better understand causal pathways in epidemiology. Recently, the causal mediation analysis has been formalized to decompose the total effect *(TE)* of a time-fixed exposure or treatment on an outcome into four components, that can be loosely defined as being components due to mediation only, interaction only, mediated interaction, and neither (formal definitions are provided below).[1] These components are typically presented as either estimated effect sizes, which can be positive or negative, or as estimated proportions of the total effect attributable to each component. When all effects in the pathway under study are thought to operate in the same direction, the estimated effect sizes of each component will be in the same direction. However, the interpretation of these components will be hard when some components are of opposite sign. In some scenarios, this may indicate violations of the core assumptions for mediation analysis. For instance, when the no-unmeasured confounding assumption does not satisfy for the mediator–outcome relation, this might give an estimated effect in the opposite direction for the component due to mediation only. In other scenarios, components with estimated effects with opposite sign may be an artefact of sampling variability around a small or null component. In the absence of these two scenarios, it remains unclear whether components with estimated effects in opposite sign may be indicative of underlying biology.

Negative interaction or negative mediation have already been discussed extensively with appropriate biological or mechanical interpretations.[2, 3] Briefly, negative interaction on the additive scale implies that the effect of the combined action of two exposures is less than the sum of their individual effects. Negative mediation implies that the effect of the exposure on the outcome, that goes through the mediator, is opposite to the direct effect of the exposure on the outcome. Within the causal mediation analysis, negative mediated interaction might be seen as the component that is intuitively more difficult to understand, and so far, lacks an easy-to-understand interpretation. An interpretation of positive mediated interaction is already quite difficult, but was recently provided.[4] Negative mediated interaction would be even harder to conceptualize and therefore we focus on that here.

In this paper, we provide biological examples of negative mediated interaction with their possible interpretation. First, we describe the notation of the methods, and the assumptions we made that our examples rely on. Second, we briefly discuss the four-way decomposition approach. Finally, we describe four biological examples and highlight the phenomenon that reflects negative mediated interaction.

## NOTATION AND ASSUMPTIONS

Let *A* denote an exposure of interest for each individual, *M* a potential mediator of interest for each individual, *Y* an outcome of interest for each individual, *C* a set of baseline covariates for each individual, and *U* a set of unknown covariates for each individual. We define $Y_a$ and $M_a$ as the potential or counterfactual outcome and mediator, respectively, if *A* had been set to *a*. We define $Y_{am}$ as the potential counterfactual outcome for each individual if *A* had been set to *a* and *M* to *m.* The reference level to which '*a*' and '*m*' are being compared to are given as '*a**' and '*m**'. For binary variables, these could be '1' and '0'; for continuous variables, these could be any value of interest, but often the mean value is used as reference level. We assume that for all individuals in a particular population, the exposure affects the mediator and the outcome in the same direction, and that the mediator affects the outcome in the same direction (i.e. 'monotonicity'). Throughout our examples, we assume that the conditions for causal inference are met, the assumptions for mediation analysis are fulfilled (see section 'a four-way decomposition'), and that there is negligible effect of sampling variability. Hence, the no-unmeasured confounding assumptions satisfy. Let us also assume that a person's outcome does not depend on other persons' exposure values. Furthermore, we are not focusing on time-varying mediators, or failure-time outcomes.

## A FOUR-WAY DECOMPOSITION

The total effect of *A* on *Y* is given by $Y_1 - Y_0$, whereas the total effect of *A* on *M* is given by $M_1 - M_0$. In general, we will not know what the effects are at an individual level, but we aim to estimate these on average for a study population. The four-way decomposition of the total effect of an exposure on the outcome can be written as:
Counterfactual definition at an individual level:

$$TE = (Y_{10} - Y_{00}) + (Y_{11} - Y_{10} - Y_{01} + Y_{00})(M_0) + (Y_{11} - Y_{10} - Y_{01} + Y_{00})(M_1 - M_0) + (Y_{01} - Y_{00})(M_1 - M_0) \quad (1)$$

Counterfactual definition at a population level:

$$TE = E[Y_{am*} - Y_{a*m*}] + E[Y_{am} - Y_{am*} - Y_{a*m} + Y_{a*m*}]\, E[M_{a*}] + E[Y_{am} - Y_{am*} - Y_{a*m} + Y_{a*m*}]\, E[M_a - M_{a*}] + E[Y_{a*m} - Y_{a*m*}]\, E[M_a - M_{a*}] \quad (2)$$

The letter E represents the population mean and is also referred to as 'Expectation'. The first component is given by $(Y_{10} - Y_{00})$, and is referred to as the controlled direct effect (*CDE*). That is the effect of the exposure in the absence of the mediator (neither mediation, nor interaction). The second component is given by $(Y_{11} - Y_{10} - Y_{01} + Y_{00})(M_0)$, and is referred to as the reference interaction $(INT_{ref})$. This component consists of the additive interaction and $M_0$, which means that the additive interaction operates only if the mediator

is present in the absence of the exposure i.e. $M_0 \neq 0$. In other words, the reference interaction is the effect due to interaction but not mediation. The third component is given by $(Y_{11} - Y_{10} - Y_{01} + Y_{00})(M_1 - M_0)$, and is referred to as the mediated interaction *($INT_{med}$).* This component consists of the additive interaction and $(M_1 - M_0)$, which means that the additive interaction operates only if the exposure has an effect on the mediator i.e. $(M_1 - M_0) \neq 0$. Hence, the exposure is necessarily present for the mediator to affect the outcome. In other words, the mediated interaction is the effect due to both mediation and interaction. The fourth component is given by $(Y_{01} - Y_{00})(M_1 - M_0)$, and is referred as the pure indirect effect *(PIE).* That is the effect of the mediator on the outcome in the absence of the exposure multiplied by the effect of the exposure on the mediator. In other words, the pure indirect effect is the effect just due to mediation but not interaction.
This mathematical formalization of the four-way decomposition can also be written as:

$$TE = CDE + INT_{ref} + INT_{med} + PIE$$

## CONCEPT OF NEGATIVE MEDIATED INTERACTION

For negative mediated interaction to be present one of the following conditions should be met:

Condition 1: $(Y_{11} - Y_{10} - Y_{01} + Y_{00}) < 0$ and $(M_1 - M_0) > 0$.
Condition 2: $(Y_{11} - Y_{10} - Y_{01} + Y_{00}) > 0$ and $(M_1 - M_0) < 0$.

The examples discussed in this paper will satisfy Condition 1. In fact, Condition 2 can be conceived as Condition 1, but with the outcome, the mediator, or the exposure recoded.[5] For instance, if we denote $Y = 1$ to be the presence of a disease in Condition 1, we can also say that $Y = 1$ is the absence of a disease in Condition 2. We refer the reader to VanderWeele and Knol[5] for extensive remarks concerning these forms of interaction (i.e. synergism and antagonism).
We speak of negative or subadditive interaction when the joint effect of the exposure and mediator is lower than the sum of their individual effect, that is, $(Y_{11} - Y_{00}) < (Y_{10} - Y_{00}) + (Y_{01} - Y_{00})$. This can also be rewritten as $(Y_{11} - Y_{10} - Y_{01} + Y_{00}) < 0$ or as $(Y_{11} - Y_{10}) - (Y_{01} - Y_{00}) < 0$, which is an additive interaction often referred to as the relative excess risk due to interaction (RERI).[6] In contrast, when $(Y_{11} - Y_{10} - Y_{01} + Y_{00}) > 0$, we speak of positive or superadditive interaction, that is, the joint effect of the exposure and mediator is higher than the sum of their individual effect. For negative $INT_{med}$ it is required that, when there is negative interaction, $(M_1 - M_0)$ should be higher than zero, meaning that the effect of *A* on *M* should be positive.

## EXAMPLE 1: ATTENTION DEFICIT HYPERACTIVITIY DISORDER (ADHD), AMPHETAMINE AND HYPERACTIVITY

The first example originates from clinical practice in which children with ADHD are treated with amphetamine. Children with ADHD are recognized by their inability to concentrate and excessive activity compared to a child's age. While the pathogenesis of ADHD is unknown, existing evidence suggest that dysfunction of the neurotransmitter system may be a crucial underlying cause. Amphetamine is often prescribed to children with ADHD to help relieve their symptoms including hyperactivity.[7] At the same time, use of amphetamine among healthy persons will induce hyperactivity by stimulating noradrenalin and adrenalin. Although the mechanisms by which amphetamine reduces hyperactivity in ADHD are not completely clear, amphetamine may modulate dopamine and noradrenalin signaling in the prefrontal cortex. Amphetamine blocks the presynaptic dopamine and noradrenalin transporters, leading to an increased availability of these hormones at the synaptic space.[8] Let $A = a$ denote the presence of the disease underlying ADHD in a child, and $A = a^*$ the absence of the disease; let $M = m$ denote amphetamine use, and $M = m^*$ not using amphetamine; let $Y = 1$ denote the presence of hyperactivity after a certain period of treatment, and $Y = 0$ the absence of hyperactivity. In this example, $Y_{11} = 0$, because a child with ADHD treated with amphetamine and who responds to the treatment will not be hyperactive anymore; $Y_{10} = 1$ and $Y_{01} = 1$, because in the presence of either ADHD only or amphetamine use only, a child will be hyperactive; $Y_{00} = 0$, because in the absence of both ADHD and amphetamine use (i.e. a healthy child), a child will not be hyperactive. Hence, the joint effect of $A$ and $M$ together on $Y$ is lower than the sum of their individual effects i.e. $(Y_{11} - Y_{10} - Y_{01} + Y_{00}) = -2$, indicating the presence of negative interaction. Given that amphetamine will only be used in the presence of ADHD and not in the absence, that is $(M_1 - M_0) = 1$, $INT_{med}$ will be negative. This negative $INT_{med}$ shows us that ADHD must be present for amphetamine use in order to affect hyperactivity. In other words, without ADHD, amphetamine would not have been used, and thus, not affected hyperactivity. Moreover, the negative $INT_{med}$ shows us that there is antagonism between the joint effect of the exposure and the mediator on the outcome, and the effect of the exposure on the mediator. Of the total effect of ADHD on hyperactivity, $INT_{med}$ is the only component with an opposite sign and shows the absence of hyperactivity. While the controlled direct effect and the pure indirect effect shows the presence of hyperactivity, the reference interaction effect shows no effect at all, because amphetamine will – under normal clinical circumstances – not be used in the absence of ADHD i.e. $M_0 = 0$ (see Figure).

**Figure.** A causal diagram showing the effect of ADHD on hyperactivity with amphetamine use as an intermediate. Arrow 1 can be seen as the controlled direct effect i.e. the effect of ADHD on hyperactivity in the absence of amphetamine use ($Y_{10} - Y_{00}$). Arrow 2 is the effect of ADHD on amphetamine use ($M_1 - M_0$). Arrows 2 and 3 together can be seen as the pure indirect effect i.e. once ADHD caused amphetamine use ($M_1 - M_0$), amphetamine will affect hyperactivity in the absence of ADHD ($Y_{01} - Y_{00}$). Arrows 1 and 3 can be seen as the reference interaction effect i.e. the joint effect of ADHD and amphetamine use ($Y_{11} - Y_{10} - Y_{01} + Y_{00}$) where ADHD does not cause amphetamine use ($M_0$). Arrows 1, 2 and 3 together can be seen as the mediated interaction effect i.e. ADHD causes amphetamine use ($M_1 - M_0$), and subsequently both ADHD and amphetamine interacts with each other ($Y_{11} - Y_{10} - Y_{01} + Y_{00}$).

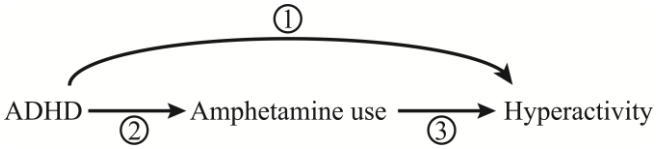


## EXAMPLE 2: INCOMPLETE COMBUSTION AND OXYGEN SATURATION

The second example originates from the field of biochemistry and involves the concept of allosteric regulation. Allosteric regulation occurs when the binding of a ligand to a protein induces a conformational change in the protein such that another ligand is able to bind at another site of the protein. A well-known example of such a regulation is the binding of oxygen to hemoglobin. This physiological phenomenon is called the Bohr effect, and was first described in 1904 by the Danish physiologist Christian Bohr. Hemoglobin, a protein contained in red blood cells, is the primary vehicle for transporting oxygen in the blood. Although oxygen is also carried in blood plasma, most of it is carried via hemoglobin. Hemoglobin contains four components/sites called 'heme', each capable of carrying one oxygen molecule. When an oxygen molecule binds to any of these sites, it causes a conformational change in hemoglobin facilitating the binding of oxygen to the other sites. How much of the oxygen is bound to hemoglobin is called the oxygen saturation (in percentage), which can be measured using pulse oximetry. The oxygen saturation is calculated as the concentration of oxygen that is bound to hemoglobin as a proportion of the maximal concentration that can be potentially bound to hemoglobin. Apart from oxygen, carbon monoxide also binds to hemoglobin at the same sites as oxygen, but approximately 200 times more tightly. The binding of oxygen or carbon monoxide induces a conformational change (i.e. allosteric regulation) in hemoglobin facilitating the binding of these molecules to the other sites. As such, oxygen and carbon monoxide compete with each other to bind to hemoglobin. While oxygen is easily released from hemoglobin, carbon monoxide is not. This strong affinity can cause an accumulation of carbon monoxide bound hemoglobin, and thus, reducing the number of hemoglobin available to bind to oxygen. Now, consider a scenario of incomplete combustion, for where oxygen is needed and carbon monoxide is formed. In such a scenario, as one inhales carbon monoxide, there will be some competition between oxygen and carbon monoxide to bind to hemoglobin. Let *A*

denote the oxygen concentration level in a room; let *M* denote the carbon monoxide concentration level in that room; let *Y* denote the oxygen saturation measured in a healthy person in that room. While the oxygen concentration in the room affects the oxygen saturation, the oxygen is also needed for incomplete combustion in order to form carbon monoxide (the oxygen can be seen as an essential cause). In turn, both oxygen and carbon monoxide will compete to bind to hemoglobin. Obviously, when both molecules are present in the same concentrations, carbon monoxide will bind more tightly to hemoglobin ($Y_{11}$), leading to a decrease in oxygen saturation. In other words, carbon monoxide competes with oxygen and thereby prevents the binding of oxygen to hemoglobin. When neither molecule is present ($Y_{00}$), or when merely carbon monoxide is present ($Y_{01}$), there will be no oxygen saturation. Oxygen saturation will only be high in the presence of oxygen alone ($Y_{10}$). Looking at the joint effect of *A* and *M* on *Y*, this joint effect will be lower than the sum of their individual effects i.e. $(Y_{11} - Y_{10} - Y_{01} + Y_{00}) < 0$, indicating the presence of negative interaction. Given that oxygen is needed to form carbon monoxide i.e. $(M_1 - M_0) > 0$, $INT_{med}$ will be negative.

## EXAMPLE 3: HYPERTENSION, INTRACRANIAL ARTERIAL STIFNESS AND COGNITIVE DECLINE

This example originates from clinical practice and illustrates how arterial stiffness of intracranial vessels mediates the effect of hypertension on cognitive decline. Hypertension is a medical condition in which the pressure in the blood vessels throughout the body is raised. Typically, hypertension is defined as a systolic blood pressure ≥ 140 mmHg or a diastolic blood pressure ≥ 90 mmHg, and has been considered a crucial risk factor for coronary heart disease and stroke. Apart from these cardiovascular diseases, it is well-established that high blood pressure is also associated with cognitive decline and dementia.[9] One possible mechanism how hypertension may cause cognitive decline, or dementia is through arterial stiffness of intracranial vessels. Studies have firmly established a relation between hypertension and arterial stiffness,[10] and between arterial stiffness and cognitive decline.[11] Interestingly, it has been thought that in particularly elderly people who have developed arterial stiffness, the body is maintaining a high blood pressure to provide sufficient perfusion to the brain, and thereby preventing cognitive decline.[12, 13] In other words, the effect of hypertension on cognitive decline is opposite in strata with and without arterial stiffness.

Let $A = a$ denote the presence of hypertension, and $A = a^*$ the absence of hypertension; let *M* denote the presence of arterial stiffness, and $M = m^*$ the absence of arterial stiffness; let $Y = 1$ denote the presence of cognitive decline, and $Y = 0$ the absence of cognitive decline. In this (simplistic) example, $Y_{11} = 0$, because cognitive decline will be prevented when both hypertension and arterial stiffness are present; $Y_{10} = 1$ and $Y_{01} = 1$, because in the presence of either hypertension only or arterial stiffness only, cognitive decline will occur; $Y_{00} = 0$,

because in the absence of both hypertension and arterial stiffness, there will be no cognitive decline. Hence, the joint effect of *A* and *M* together on *Y* is lower than the sum of their individual effects i.e. $(Y_{11} - Y_{10} - Y_{01} + Y_{00}) = -2$, indicating the presence of negative interaction. Given that arterial stiffness will be caused in the presence of hypertension i.e. $(M_1 - M_0) = 1$, $INT_{med}$ will be negative. In line with previous examples, also here, the negative $INT_{med}$ shows us that there is antagonism between the joint effect of the exposure and the mediator on the outcome, and the effect of the exposure on the mediator.

## EXAMPLE 4: ANTIBIOTIC THERAPY FOR ESCHERICHIA COLI

The fourth example originates from microbiology and pharmacology, and illustrates the concept of drug combinations. In this example, the outcome can be seen as a time-varying variable. Combining drugs are increasingly important in medicine for combating antibiotic resistance, for increasing treatment efficacy, and for probing biological systems. It is common clinical practice to start with a second drug to create a synergistic effect in case the initial drug does not have a sufficient effect (e.g. due to resistance). Note that in clinical practice, although doxycycline cannot directly cause the use of ciprofloxacin, the use of ciprofloxacin might be initiated after an insufficient effect of doxycycline is observed. By combining two drugs it is assumed that the drug combination will have either an additive effect or ideally more than additive effect (i.e. synergy). However, studies have shown that this might not always be the case. In fact, combining drugs may lead to antagonistic or even suppressive effects (i.e. hyper-antagonistic), which may be understood in terms of negative mediation interaction. For instance, in combating E. coli, studies have investigated the growth rate of E. coli with various combinations of antibiotics.[14, 15] It has been shown that the combination of doxycycline and ciprofloxacin rather than giving a synergistic effect in reducing the growth rate of E. Coli, in fact, demonstrates a strong suppressive effect, whereby doxycycline relieves the inhibitory effect of ciprofloxacin on the growth rate of E. coli. Within the sufficient-cause framework, an insufficient effect of doxycycline may be conceived as a component cause for initiating ciprofloxacin. Given that ciprofloxacin treatment will only be initiated after an insufficient effect of doxycycline was observed, and that there is negative interaction between the two drugs, $INT_{med}$ will be negative. This means that the joint effect of the exposure and the mediator on the outcome, and the effect of the exposure on the mediator are in opposite direction i.e. Condition 1 is met.

We will now demonstrate this example with scenarios of additive, synergistic, antagonistic, and suppressive effects using causal mediation terminology. Consider now a thought experiment in which we have several plates of glass with 100 E. coli cells on each plate, which we can count microscopically. We aim to quantify the number of these cells that die after exposing them to concentrations of doxycycline alone, ciprofloxacin alone, both, and neither.

Let $A = a$ denote the use of a high concentration of doxycycline, and $A = a^*$ no doxycycline use; let $M = m$ denote the use of a high concentration of ciprofloxacin after an insufficient effect of doxycycline was observed, and $M = m^*$ no ciprofloxacin use after an insufficient effect of doxycycline was observed; let $Y$ denote the number of E. coli cells that die after one day. When neither drug is included, $Y_{00} = 0$, because there will be no bacterial cell death. Now assume that doxycycline is insufficiently effective and only kills 25 bacteria i.e. $Y_{10} = 25$. When only ciprofloxacin is used, which is more effective, this drug kills 50 bacteria i.e. $Y_{01} = 50$. In a scenario of additive effect, $Y_{11}$ will be 75, resulting in $(Y_{11} - Y_{10} - Y_{01} + Y_{00}) = 0$. In a scenario of synergism, $Y_{11}$ should be larger than $(Y_{10} + Y_{01})$, and thus might be e.g. 80, resulting in $(Y_{11} - Y_{10} - Y_{01} + Y_{00}) > 0$, which is a positive (mediated) interaction. In a scenario of antagonism, or suppression, $Y_{11}$ should be smaller than $(Y_{10} + Y_{01})$, and thus might be $Y_{11} = 70$ (for antagonism) and $Y_{11} = 0$ (for suppression), resulting in $(Y_{11} - Y_{10} - Y_{01} + Y_{00}) < 0$.
Apart from the combination of doxycycline and ciprofloxacin that demonstrated a strong suppressive effect, there are many other examples of drug combination showing an antagonistic effect when combined, and possibly resulting in a negative $INT_{med}$.[14]

## CONCLUSION

The conceptual framework of causal mediation has been formalized to estimate the direct and indirect effects even in the presence of an exposure-mediator interaction. Moreover, in the presence of an exposure-mediator interaction, the direct and indirect effects can be further decomposed into four components. We see that the causal mediation analysis is increasingly being used in biomedical research, but that it is difficult to interpret the estimates of the components when these are in opposite direction. While there is abundant literature on negative interaction or negative mediation, the interpretation of negative mediated interaction so far lacks an easy-to-understand interpretation. In this paper, we have now shown that negative mediated interaction might actually reflect relevant biological processes. We suggest investigators using causal mediation analysis to interpret components with opposite sign carefully.

## REFERENCES


1. VanderWeele TJ. A unification of mediation and interaction: A 4-way decomposition. Epidemiology. 2014;25:749-761
2. VanderWeele TJ, Knol MJ. A tutorial on interaction. Epidemiologic Methods. 2014;3:33-72
3. MacKinnon DP, Fairchild AJ, Fritz MS. Mediation analysis. Annu Rev Psychol. 2007;58:593-614
4. Ikram MA, VanderWeele TJ. A proposed clinical and biological interpretation of mediated interaction. Eur J Epidemiol. 2015;30:1115-1118
5. VanderWeele TJ, Knol MJ. Remarks on antagonism. Am J Epidemiol. 2011;173:1140-1147
6. Knol MJ, VanderWeele TJ, Groenwold RH, Klungel OH, Rovers MM, Grobbee DE. Estimating measures of interaction on an additive scale for preventive exposures. Eur J Epidemiol. 2011;26:433-438
7. Punja S, Shamseer L, Hartling L, Urichuk L, Vandermeer B, Nikles J, et al. Amphetamines for attention deficit hyperactivity disorder (adhd) in children and adolescents. Cochrane Database Syst Rev. 2016;2:CD009996
8. Sulzer D, Sonders MS, Poulsen NW, Galli A. Mechanisms of neurotransmitter release by amphetamines: A review. Prog Neurobiol. 2005;75:406-433
9. Iadecola C. Hypertension and dementia. Hypertension. 2014;64:3-5
10. Mitchell GF. Arterial stiffness and hypertension: Chicken or egg? Hypertension. 2014;64:210-214
11. Zeki Al Hazzouri A, Yaffe K. Arterial stiffness and cognitive function in the elderly. J Alzheimers Dis. 2014;42 Suppl 4:S503-514
12. Euser SM, van Bemmel T, Schram MT, Gussekloo J, Hofman A, Westendorp RG, et al. The effect of age on the association between blood pressure and cognitive function later in life. J Am Geriatr Soc. 2009;57:1232-1237
13. Corrada MM, Hayden KM, Paganini-Hill A, Bullain SS, DeMoss J, Aguirre C, et al. Age of onset of hypertension and risk of dementia in the oldest-old: The 90+ study. Alzheimers Dement. 2017;13:103-110
14. Yeh P, Tschumi AI, Kishony R. Functional classification of drugs by properties of their pairwise interactions. Nat Genet. 2006;38:489-494
15. Chait R, Craney A, Kishony R. Antibiotic interactions that select against resistance. Nature. 2007;446:668-671

# Chapter 3
## Blood Markers

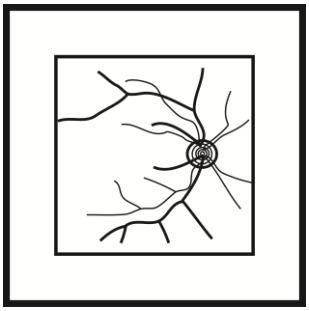

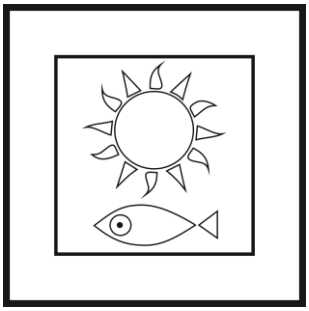

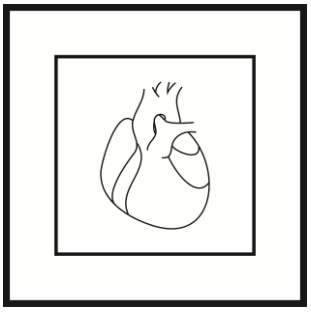

# Chapter 3.1
# Vitamin D and Retinal Microvascular Damage: the Rotterdam Study

Unal Mutlu, M. Arfan Ikram, Albert Hofman, Paulus T.V.M. de Jong, Andre G. Uitterlinden, Caroline C.W. Klaver, M. Kamran Ikram

**ABSTRACT**

**Background:** Vitamin D has been linked to various cardiovascular risk factors including indices of large vessel disease. However, it remains unclear whether vitamin D is also associated with indices of microvascular disease. In a community-dwelling population, we studied associations between vitamin D serum levels and retinal microvascular damage defined as retinopathy signs, narrower arterioles, and wider venules.
**Methods:** From the population-based Rotterdam Study, we included 5,675 participants aged ≥ 45 years with vitamin D data and gradable retinal photographs. Serum levels of vitamin D were measured using an antibody-based assay. Retinal exudates, microaneurysms, cotton wool spots and dot/blot hemorrhages were graded on fundus photographs by experienced graders in the whole sample; retinal vascular calibers i.e. arteriolar and venular diameters, were semi-automatically measured in a subsample (n = 2,973). We examined the cross-sectional association between vitamin D and retinal microvascular damage using logistic, and linear regression models, adjusting for age, sex, and cardiovascular risk factors.
**Results:** We found that persons with lower vitamin D levels were more likely to have retinopathy (adjusted odds ratio per standard deviation (SD) decrease of vitamin D: 1.30; 95% confidence interval (CI): 1.12-1.49). Furthermore, lower vitamin D levels were associated with wider venular calibers (adjusted mean difference per SD decrease in vitamin D: 1.35; 95% CI: 0.64; 2.06). This association was strongest among men (p-value for interaction = 0.023).
**Conclusions:** Lower levels of vitamin D are associated with retinal microvascular damage, suggesting that the link of vitamin D with cardiovascular risk may partly run through changes in the microvasculature.

## INTRODUCTION

Over the past decades, vitamin D deficiency has emerged as a potentially modifiable risk factor for cardiovascular disease.[1] The exact mechanisms for how vitamin D relates to cardiovascular disease are uncertain, but existing data show a strong link between vitamin D and cardiovascular risk factors, which themselves contribute to the development of cardiovascular disease. In particular, population-based studies have primarily focused on the relation of vitamin D with various indices of large vessel disease such as atherosclerosis,[2] arterial stiffness,[3] and arterial stenosis.[4] Together with traditional cardiovascular risk factors, large vessel disease explains about 60% of the variance of incident cardiovascular disease.[5]

Yet, a growing body of evidence shows that microvascular disease is also an important contributor to the development of cardiovascular disease.[6] Retinal imaging provides a great opportunity to study the microvasculature in vivo, and retinal microvascular damage – assessed as retinopathy signs, arteriolar narrowing, and venular widening – has been widely used as markers of microvascular disease.[7] As such, studies have related these markers to incident hypertension,[8] stroke,[9] and coronary heart disease,[10] supporting the notion of a microvascular component in cardiovascular disease. In view of these observations, we hypothesize that vitamin D could be linked to cardiovascular disease through the presence of a microvascular component.[11] Studies investigating the link between vitamin D and indices of microvascular disease have shown that vitamin D deficiency was associated with poor coronary microcirculation,[12] endothelial dysfunction,[13] nephropathy[14], and with markers of cerebral small vessel disease.[15] Although these studies suggest a microvascular component in the link of vitamin D with cardiovascular disease, no study has investigated the direct relation of vitamin D with markers of microvascular damage in humans.

In this study, we investigated associations between vitamin D and direct visualization of microvascular damage using retinal imaging in a community-dwelling population.

## METHODS

### Study setting and population

This study was performed as part of the Rotterdam Study (RS), a prospective population-based cohort study.[16] All inhabitants of the Ommoord district in the city Rotterdam, the Netherlands, aged 55 years or older were invited to the study in 1990 (RS-I, n = 7,932) and 2000 (RS-II, n = 3,011). In 2006 a further extension of the cohort was initiated and participants aged 45 years or older were invited (RS-III, n = 3,932). Vitamin D was measured in RS-II and RS-III. Signs of retinopathy were graded on fundus photographs in both cohorts, and retinal vascular calibers were measured only in RS-III. In total, data on vitamin D were available in 5,918 persons. Of these 5,918 persons, 243 persons had no (gradable) fundus photographs centered on the macula, or did not undergo ophthalmic examinations. Thus, data on both vitamin D and retinopathy were available in 5,675 persons. In RS-III, data on vitamin D were available in 3,445 persons. Of these, 472 had no (gradable) fundus photographs centered on the optic disc, or did not undergo ophthalmic examinations, resulting in 2,973 persons with complete data on vitamin D and retinal vascular calibers. Baseline home interviews and examinations were performed in each cohort. The Rotterdam Study has been approved by the medical ethics committee according to the Population Study Act: Rotterdam Study, executed by the Ministry of Health, Welfare and Sports of the Netherlands. A written informed consent was obtained from all participants.

### Assessment of 25-hydroxyvitamin D

Plasma levels of 25-hydroxyvitamin D were measured using an electrochemiluminescence-based assay (Elecsys Vitamin D Total, Roche Diagnostics, Mannheim, Germany). This assay has a functional sensitivity of 10 nmol/L with 18.5% coefficient of variation for intra-analyses. The repeatability is given by the within-run precision of $\leq 6.5\%$ and the reproducibility by the intermediate precision of $\leq 11.5\%$. Vitamin D deficiency was considered as a level lower than 50 nmol/L.[1]

### Assessment of retinopathy signs

Participants underwent a full eye examination of both eyes including fundus photography centered on the macula and optic disc with a 35º visual field camera (TRV-50VT (in RS-II) and TRC-50EX (in RS-III), Topcon Optical Company, Tokyo, Japan) after pharmacological mydriasis on both eyes. Fundus photographs were checked for quality and the presence of age-related maculopathy by two experienced graders. These graders, each having 20 years of experience, divided their work and graded all fundus photographs particularly focusing on fundus signs of age-related maculopathy. Consensus sessions and between-grader comparisons were performed regularly, and weighted $\kappa$ coefficients ranged from 0.58 to 0.80 for various fundus lesions. Retinopathy was defined as the presence of

one or more dot/blot hemorrhages, microaneurysms, hard exudates, cotton wool spots, or evidence of laser treatment for retinopathy in one eye (Figure 1A). Retinopathy was also considered to be present in participants with central retinal artery or vein occlusion.

**Assessment of retinal vascular calibers**

Retinal vascular calibers were measured in RS-III on fundus photographs centered on the optic disc (Figure 1B). For each participant the image of one eye with the best quality was analyzed with a semi-automated system (IVAN, University of Wisconsin-Madison, Madison, Wisconsin), and one summary value was calculated for the arteriolar calibers (in μm) and one for the venular calibers (in μm).[17] As eyes may have different magnification due to refractive changes, we adjusted vessel measurements for possible magnification variations with Littmann formula to approximate absolute measures.[18] We verified in a random subsample of 100 participants that individual measurements in the left and right eye were similar. Measurements were performed by one rater, masked for participant characteristics. Pearson correlation coefficients for interrater and intrarater agreement (n = 100) were 0.85 and 0.86 for arteriolar calibers, and 0.87 and 0.87 for venular calibers, respectively.

**Figure 1.** Fundus photographs showing (A) signs of retinopathy and (B) measurements of retinal vascular calibers. In (A), white arrow: small hemorrhages; black arrow: hard exudates. In (B), red lines: arteriolar calibers; blue lines: venular calibers.

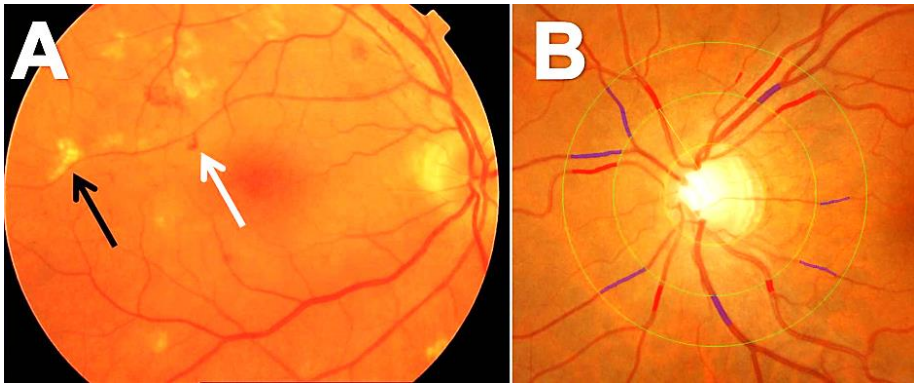


**Assessment of other measurements**

Blood pressure was measured twice in sitting position at the right brachial artery with a random-zero sphygmomanometer. We used the average of two readings for analysis. We defined hypertension as a systolic blood pressure of 140 mmHg or more, a diastolic blood pressure of 90 mmHg or more, use of antihypertensive medication, or any combination of these 3 factors. Body mass index was computed as weight (kg) divided by height squared ($m^2$). Fasting serum total and high-density lipoprotein cholesterol concentrations were determined by an automated enzymatic procedure.[19] Diabetes mellitus was considered to be

present if participants reported use of antidiabetic medication or when fasting serum glucose level was equal to or greater than 7.0 mmol/L. Serum levels of C-reactive protein were determined by a near-infrared particle immunoassay method (Immage, Beckman Coulter, Fullerton, California). Carotid plaques were assessed by ultrasound at the carotid artery bifurcation, common carotid artery, and internal carotid artery on both sides. Presence of plaques were defined as focal thickening of the vessel wall of at least 2 mm relative to adjacent segments with or without calcified components at any site. Information on smoking (never, former or current), antihypertensive and lipid-lowering medication use, and vitamin D supplement use was obtained during the home interview by a computerized questionnaire. In RS-III, dietary intake data were collected using a semi-quantitative 289-item food-frequency questionnaire. Vitamin D intake from foods was calculated using the Dutch Food Composition Table of 2006. Prevalent cardiovascular disease was assessed as a history of myocardial infarction, coronary artery bypass graft, percutaneous coronary intervention, or stroke. An extensive description on definitions of cardiovascular outcomes has been described previously.[20, 21] Kidney function was assessed by calculating an estimated glomerular filtration rate for serum creatinine and cystatin combined, according to the Chronic Kidney Disease Epidemiology Collaboration formula.[22] An estimated glomerular filtration rate lower than 60 mL/min/1.73 $m^2$ was considered as having kidney disease.

**Statistical analyses**

We standardized vitamin D values by creating z-scores (individual value minus study mean, divided by the standard deviation (SD)). In addition, we categorized participants into quartiles on the basis of vitamin D levels. We assessed associations of vitamin D with retinopathy using logistic regression models and with retinal vascular calibers using linear regression models. In Model 1, we adjusted for age, sex, season when the blood was drawn, the other vascular caliber (if applicable), and subcohort (if applicable). In Model 2, we additionally adjusted for the following cardiovascular risk factors: systolic blood pressure, diastolic blood pressure, use of antihypertensive and lipid-lowering medication, body mass index, total cholesterol, high-density lipoprotein cholesterol, C-reactive protein, and smoking. As the use of vitamin D supplements could influence these associations, we repeated our analyses after adjusting for use of any vitamin supplements, and again after excluding these persons. Also, in RS-III, we adjusted for vitamin D from food intake. We explored effect modification by stratifying for sex, history of cardiovascular disease, hypertension, diabetes mellitus, and kidney disease. We also created interaction terms with corresponding p-values in the statistical models. Missing values for covariates, if present, occurred in less than 3% of the cases, and were dealt with using fivefold multiple imputations based on determinant, outcome, and covariates. We explored the possibility of collinearity, given the Pearson correlation coefficient between arteriolar and venular diameter (r = 0.53), by calculating the variance inflation factor, but no indication of high

collinearity was identified (variance inflation factor < 1.2). Statistical tests were performed at the 0.05 level of significance (two-tailed) using SPSS version 21.0 (IBM Corporation, Armonk, New York) for Windows.

## RESULTS

The characteristics of the study population are reported in Table 1. Of the total 5,675 participants, 56% were women and the average age was 60.1 years (SD: 8.1). The average vitamin D level was 60.8 nmol/L (range: 8 to 175 nmol/L), and 40% of the participants had vitamin D deficiency. Persons with retinopathy had an average vitamin D level of 52.3 nmol/L (SD: 27.7), and persons without retinopathy had an average vitamin D level of 61.2 nmol/L (SD: 28.1).

Table 2 shows the associations between vitamin D and the presence of retinopathy. Lower levels of vitamin D were significantly associated with the presence of retinopathy: odds ratio (OR) per SD decrease of vitamin D 1.42 (1.21-1.66). This association attenuated after adjusting for cardiovascular risk factors, but remained statistically significant (OR: 1.28 (1.09-1.50)). Adjusted OR for the presence of retinopathy was 1.62 (1.05-2.49) for persons in the first quartile of vitamin D compared to persons in the fourth quartile.

Table 3 shows associations of vitamin D with retinal vascular calibers. We found that lower levels of vitamin D were significantly associated with larger venular calibers, irrespective of cardiovascular risk factors: adjusted mean difference per SD decrease of vitamin D 1.37 (0.65; 2.09). On the other hand, lower vitamin D levels were weakly associated with narrower arteriolar calibers: adjusted mean difference 0.15 (-0.32; 0.61).

Furthermore, the associations between vitamin D and microvascular damage remained similar after adjusting for vitamin supplement use, or excluding supplement users (n = 1,343).

Also, in RS-III, adjusting for vitamin D from food intake attenuated the associations, but it remained statistically significant: adjusted OR for the presence of retinopathy was 1.58 (1.18-2.13), and adjusted mean difference for venular calibers was 0.99 (0.14; 1.83). In stratified analyses (Table 4), we found that sex modified the associations of vitamin D with venules with a significant p-value for formal interaction term (p-value for interaction = 0.023).

**Table 1. Characteristics of the study population.**

| Characteristic | Retinopathy signs (RS-II and RS-III) | Retinal vascular calibers (RS-III) |
|---|---|---|
| Sample size, n | 5,675 | 2,973 |
| Age, years | 60.1 (8.1) | 56.8 (6.5) |
| Female sex | 3,157 (56) | 1,784 (57) |
| Systolic blood pressure, mmHg | 137.2 (20.8) | 132.4 (18.8) |
| Diastolic blood pressure, mmHg | 81.2 (11.1) | 82.5 (10.9) |
| Antihypertensive medication | 1,558 (28) | 787 (27) |
| Lipid-lowering medication | 1,059 (19) | 670 (23) |
| Body mass index, kg/m$^2$ | 27.5 (4.4) | 27.7 (4.6) |
| Total cholesterol, mmol/L | 5.6 (1.0) | 5.6 (1.1) |
| HDL cholesterol, mmol/L | 1.4 (0.4) | 1.4 (0.4) |
| Diabetes mellitus type 2 | 555 (10) | 247 (8) |
| C-reactive protein, mg/L | 2.5 (4.6) | 2.6 (4.5) |
| Carotid plaque | 2,936 (52) | 1,046 (35) |
| Current smoker | 1,223 (22) | 679 (23) |
| eGFR, mL/min/1.73 m$^2$ | 84.0 (14.7) | 86.2 (13.7) |
| Vitamin D, nmol/L | 60.8 (28.1) | 60.2 (27.6) |
| Retinopathy signs | 264 (5) | 87 (3) |
| Arteriolar caliber, µm | NA | 158.4 (15.5) |
| Venular caliber, µm | NA | 239.6 (22.8) |

Values are presented as means (standard deviation) or as numbers (percentage).
Abbreviations: RS, Rotterdam Study; HDL, high-density lipoprotein; eGFR, estimated glomerular filtration rate; NA, not applicable.

**Table 2. Associations between vitamin D and retinopathy.**

| | | Presence of retinopathy Odds ratio (95% CI) | |
|---|---|---|---|
| **Vitamin D** | **n/N** | **Model 1** | **Model 2** |
| Per SD decrease | 264/5,675 | 1.42 (1.21-1.66) | 1.28 (1.09-1.50) |
| Quartiles (range) | | | |
| 4$^{th}$ quartile (79.2-175.0) | 97/1,414 | 1.00 (reference) | 1.00 (reference) |
| 3$^{rd}$ quartile (57.7-79.2) | 72/1,413 | 1.26 (0.87-1.81) | 1.14 (0.78-1.65) |
| 2$^{nd}$ quartile (38.8-57.6) | 49/1,431 | 2.13 (1.40-3.22) | 1.79 (1.17-2.74) |
| 1$^{st}$ quartile (7.5-38.8) | 46/1,417 | 2.07 (1.37-3.13) | 1.62 (1.05-2.49) |
| P-value for trend | | <0.001 | 0.006 |
| Vitamin D deficiency (≤ 50 nmol/L) | | | |
| Absent | 119/3,396 | 1.00 (reference) | 1.00 (reference) |
| Present | 145/2,279 | 1.86 (1.39-2.48) | 1.54 (1.14-2.08) |

Abbreviations: CI, confidence interval; n/N, number of persons with retinopathy among total number of persons; SD, standard deviation.
Model 1: adjusted for age, sex, season, and subcohort.
Model 2: as Model 1, additionally adjusted for systolic blood pressure, diastolic blood pressure, antihypertensive medication, lipid-lowering medication, body mass index, total cholesterol, high-density lipoprotein cholesterol, diabetes mellitus, C-reactive protein, carotid plaque, estimated glomerular filtration rate, and smoking.

**Table 3. Associations between vitamin D and retinal vascular calibers.**

| | Arteriolar caliber Mean difference (95% CI) | | Venular caliber Mean difference (95% CI) | |
|---|---|---|---|---|
| **Vitamin D** | **Model 1** | **Model 2** | **Model 1** | **Model 2** |
| Per SD decrease | -0.27 (-0.75; 0.21) | 0.15 (-0.32; 0.61) | 2.07 (1.36; 2.77) | 1.37 (0.65; 2.09) |
| Quartiles (range) | | | | |
| 4th quartile (79.2-175.0) | 0 (reference) | 0 (reference) | 0 (reference) | 0 (reference) |
| 3rd quartile (57.7-79.2) | 0.47 (-0.85; 1.77) | 0.71 (-0.54; 1.95) | 0.74 (-1.21; 2.69) | 0.50 (-1.45; 2.41) |
| 2nd quartile (38.8-57.6) | 0.35 (-0.98; 1.67) | 1.06 (-0.21; 2.34) | 2.77 (0.79; 4.74) | 1.67 (-0.28; 3.62) |
| 1st quartile (7.5-38.8) | -0.68 (-2.00; 0.64) | 0.44 (-0.85; 1.73) | 5.42 (3.46; 7.38) | 3.58 (1.61; 5.55) |
| P-value for trend | 0.300 | 0.433 | <0.001 | <0.001 |

Abbreviations: CI, confidence interval; SD, standard deviation.
Model 1: adjusted for age, sex, season, and the other vascular caliber.
Model 2: as Model 1, additionally adjusted for systolic blood pressure, diastolic blood pressure, antihypertensive medication, lipid-lowering medication, body mass index, total cholesterol, high-density lipoprotein cholesterol, diabetes mellitus, C-reactive protein, carotid plaque, estimated glomerular filtration rate, and smoking.

**Table 4. Stratified analyses for associations between vitamin D levels and retinal microvascular damage.**

| | Presence of retinopathy | | Venular caliber | |
|---|---|---|---|---|
| | **n/N** | **Odds ratio (95% CI)** | **N** | **Mean difference (95% CI)** |
| Men | 145/2,518 | 1.34 (1.08-1.66) | 1,275 | 2.38 (1.32; 3.45) |
| Women | 119/3,157 | 1.21 (0.94-1.57) | 1,698 | 0.75 (-0.22; 1.71) |
| | | | | |
| Cardiovascular disease, yes | 40/409 | 1.53 (0.88-2.65) | 184 | 0.80 (-2.67; 4.27) |
| Cardiovascular disease, no | 223/5,241 | 1.25 (1.06-1.49) | 2,771 | 1.33 (0.60; 2.07) |
| | | | | |
| Hypertension, yes | 187/3,196 | 1.20 (0.98-1.46) | 1,491 | 1.79 (0.74; 2.83) |
| Hypertension, no | 77/2,479 | 1.43 (1.07-1.91) | 1,482 | 1.01 (0.02; 2.00) |
| | | | | |
| Diabetes mellitus, yes | 82/555 | 1.67 (1.16-2.42) | 247 | 2.72 (-0.33; 5.78) |
| Diabetes mellitus, no | 182/5,120 | 1.18 (0.99-1.42) | 2,726 | 1.24 (0.50; 1.98) |
| | | | | |
| Kidney disease, yes | 44/357 | 1.32 (0.93-4.13) | 102 | 1.73 (-2.80; 6.26) |
| Kidney disease, no | 220/5,318 | 1.25 (1.05-1.48) | 2,871 | 1.37 (0.64; 2.10) |

Abbreviations: n/N, number of persons with retinopathy among total number of persons; CI, confidence interval; SD, standard deviation.
Adjusted for age, sex, season, subcohort, the other vascular caliber, systolic blood pressure, diastolic blood pressure, antihypertensive medication, lipid-lowering medication, body mass index, total cholesterol, high-density lipoprotein cholesterol, diabetes mellitus, C-reactive protein, carotid plaque, estimated glomerular filtration rate, and smoking.

## DISCUSSION

In this population-based study, we found that lower vitamin D serum levels were associated with the presence of microvascular damage, independent of cardiovascular risk factors. Vitamin D has been widely recognized to play an important role in the development of cardiovascular disease, and investigators have repeatedly shown that patients deficient in vitamin D are more likely to develop coronary heart disease[23], stroke,[24] and cardiovascular mortality.[25] Despite robust evidence of vitamin D to be a risk factor for cardiovascular disease, exact mechanisms through which vitamin D leads to the development of cardiovascular disease remain unclear. Thus far, studies have suggested that vitamin D affects cardiovascular health through its association with cardiovascular risk factors such as diabetes mellitus,[26] an unfavorable lipid profile,[27] inflammation,[28] and indices of large vessel disease.[29] Apart from these factors, it has been suggested that vitamin D may act on cardiovascular health through changes in the microvasculature. Given the increasing importance of microvascular disease in the development of cardiovascular disease,[30] it is possible that the link between vitamin D and cardiovascular disease may be explained by a microvascular component. Indeed, recent studies have shown that vitamin D is associated with nephropathy and with structural MRI markers of microvascular disease in the brain i.e. white matter lesions and lacunar infarcts.[15] Extending these previous findings, the main novelty of our study is that we show a link between vitamin D and direct visualization of microvascular damage, as reflected by qualitative and quantitative retinal parameters. Several explanations can be proposed for the association of vitamin D with microvascular damage. First, vitamin D may alter the structure and arrangement of microvasculature by endothelium activation. Both in large vessel disease, and in microvascular disease, endothelium is the key component that initiates pathological vascular processes. As such, vitamin D receptors (i.e. DNA-binding transcription factors) expressed on endothelial cells modulate endothelial cell function by binding to these receptors. Subsequently, the activated endothelium promotes endothelial cell proliferation and migration by stimulating the production of nitric oxide, and reducing the production of reactive oxygen species.[31] It also inhibits innate inflammatory process by modulating specific signaling pathways and reduces vascular tone via the production of endothelium-derived contracting factors.[32] Against this background, it is conceivable that these antioxidative and vasodilatory processes may not be initiated in case of low vitamin D levels, and therefore damage to the blood vessels may occur. It is noteworthy to mention that in recent years, apart from arterioles, the role of venules in cardiovascular disease has gained attention, and converging evidence shows wider venules to be an important marker for cardiovascular disease. Also in our study, vitamin D was particularly related to venules and not arterioles, which further points towards the importance of venules in cardiovascular disease. Given that both lower vitamin D levels and wider venules are related to ischemia, it is likely that vitamin D and venules are connected in the pathways of ischemia.[33]

How exactly these two factors are connected should be investigated in further research. Other potential mechanisms through which vitamin D could lead to microvascular damage include inflammation, lipid metabolism, and renin-angiotensin-aldosterone system, which are all processes involved in the pathogenesis of arteriosclerosis.[29] In our study, adjusting for markers of these processes (e.g. C-reactive protein, cholesterol and blood pressure) showed that the associations between vitamin D and retinal microvascular damage greatly attenuated, pointing further towards some effects of these processes. However, the associations remained statistically significant, indicating that other processes likely also play a role or that measurement error in covariates led to insufficient adjustment.
Several limitations need to be discussed. First, the cross-sectional design of our study limits our ability to infer a temporal link between vitamin D and retinal microvascular damage. Another limitation is that retinal fundus photographs were taken at a single point in time, and thus, we were unable to measure dynamic measures synchronized on the cardiac cycle. This may have caused random misclassification, leading to an underestimation of our associations. Third, we were not able to measure important confounding factors such as (lifetime) sun-exposure, and food intake. These factors could confound the effect of vitamin D on microvascular damage. Finally, participants in the Rotterdam Study are mainly middle-class white persons, which limits the generalizability of our findings. Strengths of our study are the population-based setting, large study size and the extensive information on covariates.
In conclusion, lower vitamin D serum levels are associated with the presence of retinal microvascular damage, suggesting that the link of vitamin D with cardiovascular risk may partly run through changes in the microvasculature.

## REFERENCES


1. Holick MF. Vitamin d deficiency. N Engl J Med. 2007;357:266-281
2. de Boer IH, Kestenbaum B, Shoben AB, Michos ED, Sarnak MJ, Siscovick DS. 25-hydroxyvitamin d levels inversely associate with risk for developing coronary artery calcification. J Am Soc Nephrol. 2009;20:1805-1812
3. Dong Y, Stallmann-Jorgensen IS, Pollock NK, Harris RA, Keeton D, Huang Y, et al. A 16-week randomized clinical trial of 2000 international units daily vitamin d3 supplementation in black youth: 25-hydroxyvitamin d, adiposity, and arterial stiffness. J Clin Endocrinol Metab. 2010;95:4584-4591
4. Lim S, Shin H, Kim MJ, Ahn HY, Kang SM, Yoon JW, et al. Vitamin d inadequacy is associated with significant coronary artery stenosis in a community-based elderly cohort: The korean longitudinal study on health and aging. J Clin Endocrinol Metab. 2012;97:169-178
5. Global Burden of Metabolic Risk Factors for Chronic Diseases C. Cardiovascular disease, chronic kidney disease, and diabetes mortality burden of cardiometabolic risk factors from 1980 to 2010: A comparative risk assessment. Lancet Diabetes Endocrinol. 2014;2:634-647
6. Lanza GA, Crea F. Primary coronary microvascular dysfunction: Clinical presentation, pathophysiology, and management. Circulation. 2010;121:2317-2325
7. Liew G, Wang JJ, Mitchell P, Wong TY. Retinal vascular imaging: A new tool in microvascular disease research. Circ Cardiovasc Imaging. 2008;1:156-161
8. Ikram MK, Witteman JC, Vingerling JR, Breteler MM, Hofman A, de Jong PT. Retinal vessel diameters and risk of hypertension: The rotterdam study. Hypertension. 2006;47:189-194
9. Ikram MK, de Jong FJ, Bos MJ, Vingerling JR, Hofman A, Koudstaal PJ, et al. Retinal vessel diameters and risk of stroke: The rotterdam study. Neurology. 2006;66:1339-1343
10. Wong TY, Klein R, Sharrett AR, Duncan BB, Couper DJ, Tielsch JM, et al. Retinal arteriolar narrowing and risk of coronary heart disease in men and women. The atherosclerosis risk in communities study. JAMA. 2002;287:1153-1159
11. Grunwald JE, Ying GS, Maguire M, Pistilli M, Daniel E, Alexander J, et al. Association between retinopathy and cardiovascular disease in patients with chronic kidney disease (from the chronic renal insufficiency cohort [cric] study). Am J Cardiol. 2012;110:246-253
12. Capitanio S, Sambuceti G, Giusti M, Morbelli S, Murialdo G, Garibotto G, et al. 1,25-dihydroxy vitamin d and coronary microvascular function. Eur J Nucl Med Mol Imaging. 2013;40:280-289
13. Al Mheid I, Patel R, Murrow J, Morris A, Rahman A, Fike L, et al. Vitamin d status is associated with arterial stiffness and vascular dysfunction in healthy humans. J Am Coll Cardiol. 2011;58:186-192
14. Usluogullari CA, Balkan F, Caner S, Ucler R, Kaya C, Ersoy R, et al. The relationship between microvascular complications and vitamin d deficiency in type 2 diabetes mellitus. BMC Endocr Disord. 2015;15:33
15. Chung PW, Park KY, Kim JM, Shin DW, Park MS, Chung YJ, et al. 25-hydroxyvitamin d status is associated with chronic cerebral small vessel disease. Stroke. 2015;46:248-251
16. Hofman A, Brusselle GG, Darwish Murad S, van Duijn CM, Franco OH, Goedegebure A, et al. The rotterdam study: 2016 objectives and design update. Eur J Epidemiol. 2015;30:661-708
17. Knudtson MD, Lee KE, Hubbard LD, Wong TY, Klein R, Klein BE. Revised formulas for summarizing retinal vessel diameters. Curr Eye Res. 2003;27:143-149
18. Littmann H. [determining the true size of an object on the fundus of the living eye] zur bestimmung der wahren grosse eines objektes auf dem hintergrund eines lebenden auges. Klin Monbl Augenheilkd. 1988;192:66-67
19. van Gent CM, van der Voort HA, de Bruyn AM, Klein F. Cholesterol determinations. A comparative study of methods with special reference to enzymatic procedures. Clin Chim Acta. 1977;75:243-251

20. Leening MJ, Kavousi M, Heeringa J, van Rooij FJ, Verkroost-van Heemst J, Deckers JW, et al. Methods of data collection and definitions of cardiac outcomes in the rotterdam study. Eur J Epidemiol. 2012;27:173-185
21. Bos MJ, Koudstaal PJ, Hofman A, Ikram MA. Modifiable etiological factors and the burden of stroke from the rotterdam study: A population-based cohort study. PLoS Med. 2014;11:e1001634
22. Inker LA, Schmid CH, Tighiouart H, Eckfeldt JH, Feldman HI, Greene T, et al. Estimating glomerular filtration rate from serum creatinine and cystatin c. N Engl J Med. 2012;367:20-29
23. Giovannucci E, Liu Y, Hollis BW, Rimm EB. 25-hydroxyvitamin d and risk of myocardial infarction in men: A prospective study. Arch Intern Med. 2008;168:1174-1180
24. Poole KE, Loveridge N, Barker PJ, Halsall DJ, Rose C, Reeve J, et al. Reduced vitamin d in acute stroke. Stroke. 2006;37:243-245
25. Autier P, Gandini S. Vitamin d supplementation and total mortality: A meta-analysis of randomized controlled trials. Arch Intern Med. 2007;167:1730-1737
26. Pittas AG, Lau J, Hu FB, Dawson-Hughes B. The role of vitamin d and calcium in type 2 diabetes. A systematic review and meta-analysis. J Clin Endocrinol Metab. 2007;92:2017-2029
27. Ponda MP, Huang X, Odeh MA, Breslow JL, Kaufman HW. Vitamin d may not improve lipid levels: A serial clinical laboratory data study. Circulation. 2012;126:270-277
28. Jablonski KL, Chonchol M, Pierce GL, Walker AE, Seals DR. 25-hydroxyvitamin d deficiency is associated with inflammation-linked vascular endothelial dysfunction in middle-aged and older adults. Hypertension. 2011;57:63-69
29. Kassi E, Adamopoulos C, Basdra EK, Papavassiliou AG. Role of vitamin d in atherosclerosis. Circulation. 2013;128:2517-2531
30. Grunwald JE, Pistilli M, Ying GS, Maguire M, Daniel E, Whittock-Martin R, et al. Retinopathy and the risk of cardiovascular disease in patients with chronic kidney disease (from the chronic renal insufficiency cohort study). Am J Cardiol. 2015;116:1527-1533
31. Molinari C, Rizzi M, Squarzanti DF, Pittarella P, Vacca G, Reno F. 1alpha,25-dihydroxycholecalciferol (vitamin d3) induces no-dependent endothelial cell proliferation and migration in a three-dimensional matrix. Cell Physiol Biochem. 2013;31:815-822
32. Wong MS, Man RY, Vanhoutte PM. Calcium-independent phospholipase a(2) plays a key role in the endothelium-dependent contractions to acetylcholine in the aorta of the spontaneously hypertensive rat. Am J Physiol Heart Circ Physiol. 2010;298:H1260-1266
33. Ikram MK, De Jong FJ, Van Dijk EJ, Prins ND, Hofman A, Breteler MM, et al. Retinal vessel diameters and cerebral small vessel disease: The rotterdam scan study. Brain. 2006;129:182-188

# Chapter 3.2
# N-terminal Pro-B-Type Natriuretic Peptide is Related to Retinal Microvascular Damage: the Rotterdam Study

Unal Mutlu, M. Arfan Ikram, Albert Hofman, Paulus T.V.M. de Jong, Caroline C.W. Klaver, M. Kamran Ikram

**ABSTRACT**

**Background:** N-terminal pro-B-type natriuretic peptide (NT-proBNP) is a marker of cardiac dysfunction and has been linked to various indices of large vessel disease. However, it remains unclear whether NT-proBNP also relates to indices of microvascular disease. In a community-dwelling population, we studied the association between NT-proBNP and retinal microvascular damage.
**Methods:** From the population-based Rotterdam Study, we included 8,437 participants (mean age 64.1 years and 59% women) without a history of cardiovascular disease, with NT-proBNP data and gradable retinal images. NT-proBNP serum levels were measured using an immunoassay. Retinopathy signs i.e. exudates, microaneurysms, cotton wool spots and dot/blot hemorrhages, present on fundus photographs were graded in the total study population; retinal vascular calibers i.e. arteriolar and venular calibers, were semi-automatically measured in a subsample (n = 2,763) of the study population. We conducted cross-sectional analyses on the association between NT-proBNP and retinal microvascular damage using logistic and linear regression models, adjusting for age, sex, and cardiovascular risk factors.
**Results:** We found that NT-proBNP was associated with the presence of retinopathy (adjusted odds ratio (95% confidence interval) per standard deviation (SD) increase in natural log-transformed NT-proBNP: 1.14 (1.03-1.27)). We also found that higher NT-proBNP was associated with narrower arteriolar calibers (adjusted mean difference in arteriolar caliber per SD increase in natural log-transformed NT-proBNP: -0.89 µm (-1.54; -0.24)). This association remained unchanged after excluding persons with retinopathy signs.
**Conclusions:** In persons free of clinical cardiovascular disease, higher levels of NT-proBNP are associated with retinal microvascular damage, suggesting a potential role for NT-proBNP as marker for microvascular disease.

## INTRODUCTION

An important cornerstone in cardiovascular research has been the identification of markers that not only relate to clinical disease, but are also indicative of subclinical disease. In recent years, N-Terminal pro-B-type Natriuretic Peptide (NT-proBNP) has emerged as such a marker, associated in particular with heart failure.[1, 2] NT-proBNP is a biologically inactive metabolite secreted together with its biologically active counterpart BNP from cardiac myocytes in response to cardiac stress.[3] Typically, studies have measured NT-proBNP instead of BNP, given its lower cost and easier availability of assays. Importantly, NT-proBNP is not only informative about clinically overt heart failure but is also increased in persons with subclinical cardiac dysfunction.[3] Given the strong link between cardiac disease and large vessel disease, studies have also shown NT-proBNP to be related to various indices of large vessel disease such as coronary atherosclerosis,[4] carotid-pulse wave velocity,[5] aortic valve disease,[6] and aortic stenosis.[7] Although cardiac disease has a substantial component due to large vessel disease, nevertheless, up to 40% of patients with symptoms of cardiac ischemia have normal arteries on coronary angiography.[8]
Observations primarily from cardiac imaging studies have indeed demonstrated that these patients have impaired myocardial blood flow and coronary flow reserve despite normal arteries, pointing towards other mechanisms of cardiac ischemia.[9] Currently, such patient populations are being recognized as a distinct entity representing a wide spectrum of coronary microvascular dysfunction.[10]
Against this background, it is conceivable that NT-proBNP – as marker of subclinical cardiac dysfunction – may also be related to indices of small vessel disease. As such, studies have repeatedly shown the usefulness of NT-proBNP as biomarker for clinical endpoints in patients with renal disease.[11, 12] Thus, the link between NT-proBNP and renal function may reflect cardiac stress and signifies the presence of microvascular pathology. However, the link of NT-proBNP with direct visualization of microvascular damage has not been studied, primarily because of a lack of noninvasive markers of small vessel disease. The retina provides an opportunity to visualize the microvasculature in vivo. Microvascular damage in the retina often manifests itself as exudates, microaneurysms, cotton wool spots, dot/blot hemorrhages and narrower arterioles, which can be quantified on retinal imaging. These measures of microvascular damage have been widely used in large-population based studies, and findings from these studies have often shown that retinal microvascular damage is related to subclinical and clinical cardiovascular disease.[13, 14] In view of these observations, we hypothesize that, besides large vessel disease, cardiac stress due to microvascular dysfunction may also lead to higher levels of NT-proBNP.
Therefore, in a community-dwelling population free of clinical cardiovascular disease, we investigated the association of NT-proBNP with the presence of retinopathy and retinal vascular calibers.

## METHODS

### Study setting

This study is based on the Rotterdam Study (RS), a large prospective population-based cohort study in the Netherlands that investigates the etiology of chronic diseases in the general population.[15] All inhabitants of the Ommoord district in the city Rotterdam, aged 55 years or older, were invited to the study in 1990 and 2000. In 2006 a further extension of the cohort was initiated and participants aged 45 years or older were invited. Follow-up examinations for participants take place every three to four years. NT-proBNP was measured in the third visit of the first cohort (RS-I-3), and at the beginning of the second (RS-II-1) and third (RS-III-1) cohort. Retinopathy signs were graded in all cohorts, whereas retinal vascular calibers were only measured in RS-III-1. The Rotterdam Study has been approved by the medical ethics committee according to the Population Study Act Rotterdam Study, executed by the Ministry of Health, Welfare and Sports of the Netherlands. A written informed consent was obtained from all participants.

### Study population

Out of 11,740 participants, NT-proBNP levels were measured in 9,946 participants (84.7%). Of these 9,946, we excluded 1,048 participants with a history of myocardial infarction, coronary artery bypass graft, percutaneous coronary intervention, heart failure, and stroke. An extensive description on definitions of cardiovascular outcomes has been described previously.[16, 17] We excluded persons with a history of cardiovascular disease because it is a clinically detectable condition in which NT-proBNP levels are known to be high. Also, participants with NT-proBNP values above the age-specific heart failure cut-points (n = 135) were excluded from further analyses. Age-specific heart failure cut-points were defined as NT-proBNP levels above 54 pmol/L for participants aged < 50 years, 108 pmol/L for participants aged 50-75 years, and 216 pmol/L for participants aged > 75 years.[18] Furthermore, participants without (gradable) fundus photographs (n = 265), and end-stage age-related macular degeneration (n = 61) were excluded from analyses, because end-stage age-related macular degeneration has mostly a different pathogenesis than hypertensive or diabetic retinopathy, and thus could affect our estimates if included. A total of 8,437 participants with both NT-proBNP and retinopathy data were thus eligible for analysis. As retinal vascular calibers were only measured in RS-III-1, complete data in 2,763 participants were available for this analysis. A flow diagram of the study population is depicted in Figure 1.

**Figure 1.** Flow diagram of the study population.

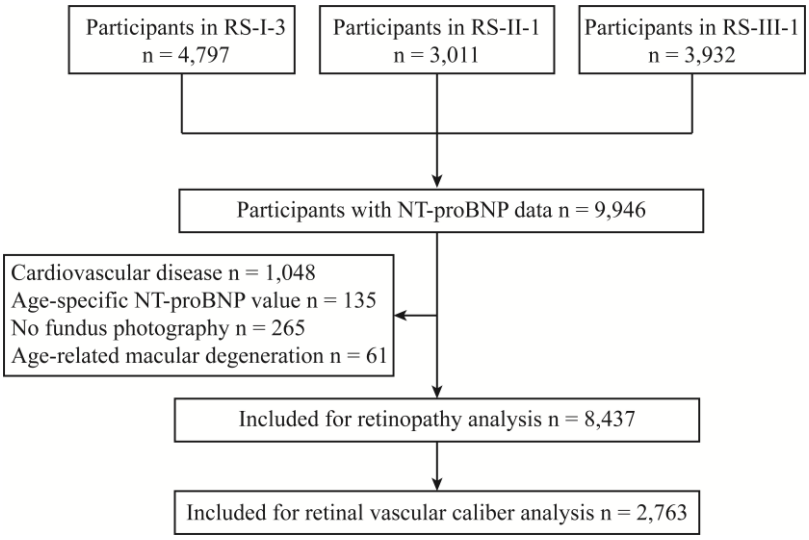


**Assessment of NT-proBNP**

Blood samples for NT-proBNP measurements were collected in glass tubes containing clot activator and gel for serum separation. After collection, samples were allowed to stand for 30 min for clotting and then centrifuged for 20 min at 3000 rpm at 4°C. Subsequently, serum was stored at −80°C. NT-proBNP was measured using commercially available electrochemiluminescence immunoassay (Elecsys proBNP, F. Hoffman-La Roche Limited, Basel, Switzerland) on an Elecsys 2010 analyzer. The precision, analytic sensitivity and stability features of the system have been described previously.[19]

**Assessment of retinopathy signs**

Participants underwent a full eye examination of both eyes including fundus photography centered on the macula and optic disc with a 35º visual field camera (TRV-50VT (in RS-I-3 and RS-II-1) and TRC-50EX (in RS-III-1), Topcon Optical Company, Tokyo, Japan) after pharmacological mydriasis. Fundus photographs centered on the macula, were checked for quality and presence of retinal pathology. The presence of exudates, microaneurysms, cotton wool spots and the presence of dot/blot hemorrhages were graded by two trained graders. An example of retinopathy signs is shown in Figure 2A. In addition, the presence of laser coagulation scars was graded and the indication for laser therapy was categorized into either retinopathy or other diseases, using available clinical data. Retinopathy was defined as the presence of one or more dot/blot hemorrhages, microaneurysms, exudates, cotton wool spots or evidence of laser treatment for retinopathy. Retinopathy was also considered present in participants with central or branch retinal artery or vein occlusion.

**Assessment of retinal vascular calibers**

Retinal vascular calibers were measured in RS-III-1 with fundus photographs centered on the optic disc. For each participant the image of one eye with the best quality was analyzed with a semi-automated system (IVAN, University of Wisconsin-Madison, Madison, Wisconsin). An example of retinal vascular caliber measurements is shown in Figure 2B. For each participant one summary value was calculated for the arteriolar calibers (in μm) and one for the venular calibers (in μm) enabling us to use the separate arteriolar and venular caliber sum values.[20] Because eyes may have different magnification due to refractive changes, we adjusted vessel measurements for possible magnification variations with Littmann formula to approximate absolute measures.[21] We verified in a random subsample of 100 participants that individual measurements in the left and right eye were similar. Measurements were performed by one rater, masked for participant characteristics. Pearson correlation coefficients for interrater and intrarater agreement (n = 100) were 0.85 and 0.86 for arteriolar calibers, and 0.87 and 0.87 for venular calibers, respectively.

**Figure 2.** Fundus photographs showing (A) signs of retinopathy and (B) measurement of retinal vascular calibers. In (A), white arrow: small hemorrhages; black arrow: hard exudates. In (B), red lines: arteriolar calibers; blue lines: venular calibers.

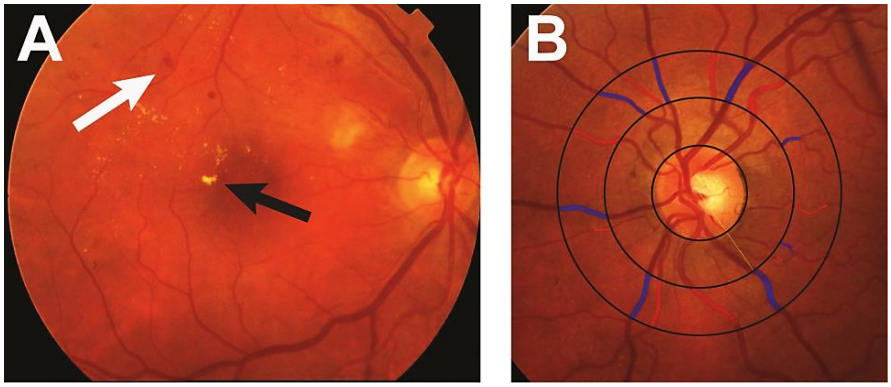


**Other measurements**

Blood pressure was measured twice in sitting position at the right brachial artery with a random-zero sphygmomanometer. We used the average of two readings for analysis. Antihypertensive medication use was obtained during the home interview by a computerized questionnaire. We defined hypertension as a systolic blood pressure of 140 mmHg or more, a diastolic blood pressure of 90 mmHg or more, use of antihypertensive medication, or any combination of these 3 factors. Body mass index was computed as weight (kg) divided by height squared ($m^2$). Fasting serum total and high-density lipoprotein cholesterol concentrations were determined by an automated enzymatic procedure (Hitachi Analyzer, Roche Diagnostics, Indianapolis, Indiana). Diabetes mellitus was considered present if participants reported use of antidiabetic medication or when

fasting serum glucose level was equal to or greater than 7.0 mmol/L. Serum levels of C-reactive protein were determined by a near-infrared particle immunoassay method (Immage, Beckman Coulter, Fullerton, California). Carotid plaques were assessed by ultrasound at the carotid artery bifurcation, common carotid artery, and internal carotid artery on both sides. Presence of plaques were defined as focal thickening of the vessel wall of > 50% (in RS-I-3 and RS-II-1) or at least 2 mm thickening (in RS-III-1) relative to adjacent segments with or without calcified components. Information on smoking (never, former or current) was obtained during the home interview.

**Statistical analysis**

We performed our analysis on two datasets: one dataset including data on retinopathy, and one dataset including data on retinal vascular calibers. NT-proBNP levels were transformed using natural logarithm to achieve a normal distribution. We standardized NT-proBNP values by calculating z-scores (log-transformed NT-proBNP minus mean of log-transformed NT-proBNP, divided by standard deviation of log-transformed NT-proBNP). We assessed the association of NT-proBNP with the presence of retinopathy and retinal vascular calibers using logistic and linear regression models, respectively. NT-proBNP was treated as a continuous variable (per standard deviation increase in natural log-transformed) as well as categorized into quartiles. In Model 1, we adjusted for age, sex, subcohort and the other retinal vascular caliber (if applicable), and additionally in Model 2 for the following cardiovascular risk factors: systolic blood pressure, diastolic blood pressure, antihypertensive medication, body mass index, total cholesterol, high-density lipoprotein cholesterol, diabetes mellitus, C-reactive protein, carotid plaque and smoking status. The test of trend was determined by treating quartiles of NT-proBNP as a continuous variable in the models. We explored effect modification by stratifying for sex, because it has been hypothesized that small vessel disease may play a prominent role in the development of cardiac disease in women.[22] We redid the analyses with retinal vascular calibers after excluding persons with retinopathy. Missing values for all variables, if present, were less than 3% of the study population (except for carotid plaque which was 7%), which we dealt with using fivefold multiple imputations based on determinant, outcome, and covariates. We explored the possibility of collinearity, given the Pearson correlation coefficient between arteriolar and venular diameter ($r = 0.59$), by calculating the variance inflation factor, but no indication of high collinearity was present (variance inflation factor < 1.2). Statistical tests were performed at the 0.05 level of significance (two-tailed) using SPSS version 21.0 (IBM Corporation, Armonk, New York). for Windows

## RESULTS

Table 1 shows the characteristics of the study population. Of the total 8,437 participants, the average age was 64.1 years (standard deviation (SD): 9.4) and 59% were women. Persons with retinopathy had a mean NT-proBNP level of 10.7 pmol/L (interquartile range: 5.5-21.1), whereas persons without retinopathy had a mean NT-proBNP level of 7.3 pmol/L (interquartile range: 4.0-13.6).

Table 2 shows the association between NT-proBNP and the presence of retinopathy. We found that higher levels of NT-proBNP were significantly associated with the presence of retinopathy: odds ratio per SD increase of natural log-transformed NT-proBNP 1.22 (95% confidence interval (CI): 1.10-1.35). The association attenuated after adjusting for cardiovascular risk factors, but it remained statistically significant. Furthermore, when categorizing NT-proBNP levels into quartiles, we found a graded increase in the likelihood of having retinopathy, although these effects attenuated slightly in Model 2.

Table 3 shows the association between NT-proBNP and retinal vascular calibers. Higher levels of NT-proBNP (both continuously and in quartiles) were significantly associated with narrower arteriolar calibers: mean difference in arteriolar caliber per SD increase of natural log-transformed NT-proBNP: -1.36 (95% CI: -2.03; -0.70). Adjusting for cardiovascular risk factors attenuated the association, but it remained statistically significant. In contrast, NT-proBNP levels were not associated with venular calibers. Stratification on sex did not reveal any interaction with NT-proBNP (p-value for interaction > 0.05). After excluding persons with retinopathy (n = 71) we found, if anything, stronger associations with retinal vascular calibers: mean difference in arteriolar caliber per SD increase of natural log-transformed NT-proBNP: -1.51 (-2.19; -0.83) in Model 1, and -1.01 (-1.64; -0.35) in Model 2.

**Table 1. Characteristics of the study population.**

| Characteristic | Total | Subsample (RS-III-1) |
|---|---|---|
| N | 8,437 | 2,763 |
| Age, years | 64.1 (9.4) | 56.4 (6.2) |
| Females | 5,006 (59) | 1,623 (59) |
| Systolic blood pressure, mmHg | 139.3 (21.0) | 132.3 (18.6) |
| Diastolic blood pressure, mmHg | 79.2 (11.3) | 82.7 (10.9) |
| Antihypertensive medication | 2,340 (28) | 633 (23) |
| Body mass index, $kg/m^2$ | 27.3 (4.2) | 27.6 (4.6) |
| Total cholesterol, mmol/L | 5.8 (1.0) | 5.6 (1.1) |
| High-density lipoprotein cholesterol, mmol/L | 1.4 (0.4) | 1.4 (0.4) |
| Diabetes Mellitus type 2 | 811 (10) | 191 (7) |
| C-reactive protein, mg/L | 3.0 (5.4) | 2.5 (4.4) |
| Carotid plaque | 4,758 (56) | 907 (33) |
| Current smoker | 1,668 (20) | 625 (23) |
| NT-proBNP*, pmol/L | 7.6 (4.1-14.2) | 5.5 (3.1-9.7) |
| Arteriolar caliber, µm | NA | 158.5 (15.5) |
| Venular caliber, µm | NA | 239.7 (22.7) |
| Retinopathy | 729 (9) | 71 (3) |

Values are presented as means (standard deviation) or as numbers (percentage).
Abbreviations: NT-proBNP, N-terminal pro-B-type natriuretic peptide; NA, not applicable.
*Presented as medians (interquartile range) because of skewed distribution.

**Table 2. The association of NT-proBNP with the presence of retinopathy.**

| Natural log-transformed NT-proBNP | n/N | Presence of retinopathy Odds Ratio (95% CI) Model 1 | Model 2 |
|---|---|---|---|
| Per SD increase | 729/8,437 | 1.22 (1.10-1.35) | 1.14 (1.03-1.27) |
| Quartiles | | | |
| 1st quartile (0.59-4.08) | 112/2,111 | 1 (reference) | 1 (reference) |
| 2nd quartile (4.09-7.54) | 147/2,106 | 1.03 (0.79-1.34) | 1.04 (0.79-1.35) |
| 3rd quartile (7.55-14.20) | 186/2,111 | 1.13 (0.87-1.47) | 1.11 (0.85-1.44) |
| 4th quartile (14.21-216.20) | 284/2,109 | 1.39 (1.07-1.80) | 1.25 (0.95-1.63) |
| P-value for trend | | 0.005 | 0.079 |

Abbreviations: NT-proBNP, N-terminal pro-B-type natriuretic peptide CI, confidence interval; n/N, number of persons with retinopathy among persons at risk; SD, standard deviation.
Model 1: adjusted for subcohort, age, and sex.
Model 2: as Model 1, additionally adjusted for systolic blood pressure, diastolic blood pressure, use of antihypertensive medication, body mass index, total cholesterol, high-density lipoprotein cholesterol, diabetes mellitus, C-reactive protein, carotid plaque, and smoking.

**Table 3. The association of NT-proBNP with retinal vascular calibers.**

| Natural log-transformed NT-proBNP | Arteriolar caliber Mean difference (95% CI) | | Venular caliber Mean difference (95% CI) | |
|---|---|---|---|---|
| | Model 1 | Model 2 | Model 1 | Model 2 |
| Per SD increase | -1.36 (-2.03; -0.70) | -0.89 (-1.54; -0.24) | 0.61 (-0.39; 1.60) | 0.19 (-0.81; 1.19) |
| Quartiles (range) | | | | |
| 1st quartile (0.59-3.33) | 0 (reference) | 0 (reference) | 0 (reference) | 0 (reference) |
| 2nd quartile (3.34-6.02) | -1.18 (-2.55; 0.19) | -1.38 (-2.69; -0.08) | -0.46 (-2.52; 1.59) | -0.06 (-2.07; 1.95) |
| 3rd quartile (6.03-11.24) | -1.94 (-3.36; -0.51) | -1.72 (-3.09; -0.36) | -1.57 (-3.70; 0.56) | -1.25 (-3.35; 0.85) |
| 4th quartile (11.25-178.50) | -2.87 (-4.34; -1.40) | -2.03 (-3.46; -0.59) | 1.18 (-1.02; 3.39) | 0.53 (-1.67; 2.73) |
| P-value for trend | <0.001 | 0.01 | 0.46 | 0.90 |

Abbreviations: NT-proBNP, N-terminal pro-B-type natriuretic peptide; CI, confidence interval; SD, standard deviation.
Model 1: adjusted for age, sex, and the other vascular caliber.
Model 2: as Model 1, additionally adjusted for systolic blood pressure, diastolic blood pressure, use of antihypertensive medication, body mass index, total cholesterol, high-density lipoprotein cholesterol, diabetes mellitus, C-reactive protein, carotid plaque, and smoking.

## DISCUSSION

We found that in persons without cardiovascular disease, higher levels of NT-proBNP were associated with microvascular damage as reflected by the presence of retinopathy and narrower retinal arterioles. These associations were independent of cardiovascular risk factors.

Thus far, evidence of a role of NT-proBNP in cardiovascular disease comes primarily from research focused on coronary heart disease[23] and heart failure.[24] In addition, it is increasingly being suggested that NT-proBNP might be a general marker of vascular disease beyond specific heart disease. For instance, previous studies have shown that higher NT-proBNP levels were associated with indices of large vessel disease,[25] stroke,[26] and mortality.[27] In this sense, the strong link of NT-proBNP with various cardiovascular diseases may be explained by the strong link of cardiac dysfunction with vascular damage (i.e. atherosclerosis, arteriosclerosis, and endothelial dysfunction), which is a substantial component of cardiovascular diseases. Although most studies investigating the association of NT-proBNP with vascular damage revolved around large vessel disease, there are now indications that NT-proBNP also relates to small vessel disease. Indeed, recent studies have shown NT-proBNP to be associated with kidney disease,[28] and cerebral small vessel disease[29] such as white matter lesions and silent brain infarcts. However, no study has investigated the association of NT-proBNP with direct visualization of microvascular damage.

Our findings showed an independent link between higher NT-proBNP levels and markers of retinal microvascular damage. Several mechanisms may explain this association. NT-proBNP is a biologically inactive metabolite, whereas BNP is the physiologically active

hormone, which both are in 1:1 ratio the product of the precursor proBNP. Physiologically, BNP leads to vasodilatation through inhibition of the renin and aldosterone production, inhibition of the sympathetic nervous system activity, and induction of diuresis.[30, 31] Beside these indirect effects on the vessels, BNP may exert its effect also directly. In vitro studies have demonstrated that BNP activates the guanylate cyclase receptors on both endothelial and vascular smooth muscle cells, which subsequently activate potassium and calcium channels promoting arterial vasodilatation.[32] Another important feature of BNP is that it stimulates the production of nitric oxide which also leads to vasodilatation.[33]

Given that BNP leads to vasodilatation of the arteries, and our findings demonstrate an association with narrower arterioles, we hypothesize that most likely high levels of NT-proBNP may occur in response to systemic microvascular damage. Previous studies have shown narrower arterioles to be associated with the risk of hypertension, and coronary heart disease.[22, 34] Also, a recent study has shown that higher NT-proBNP levels were related to incident hypertension.[35] Altogether, those findings support the hypothesis that narrower arterioles may lead to higher cardiac output or hypoxia, and thus, initiate NT-proBNP release in cardiac myocytes due to myocardial stress or ischemia.[36] Nevertheless, higher NT-proBNP levels may reflect a substantial component in cardiac dysfunction that is due to microvascular damage.

Another explanation linking NT-proBNP to microvascular damage is shared cardiovascular risk factors i.e. residual confounding. After adjusting for these factors, the associations attenuated greatly, indeed showing some effect of these mechanisms. However, the associations remained statistically significant, indicating that other processes likely also play a role. Future studies should further elucidate what mechanisms underlie the interplay of these (sub)clinical markers of cardiovascular disease.

Several methodological issues need to be discussed. A limitation of our study is the cross-sectional design that prevents us inferring causality of the outcomes. Another limitation might be that we used a static measure of the microcirculation instead of dynamic functional measures synchronized on the cardiac cycle. A variation of 2-17% in retinal vascular caliber has been reported.[37] This may have caused random misclassification, leading to an underestimation of our associations.

Furthermore, in our study, besides retinopathy signs, we did not have data on AV-nicking and focal arteriolar narrowing. Despite presumed differences in etiology of specific retinal signs (e.g. AV-nicking and focal arteriolar narrowing are driven by hypertensive damage), both retinopathy signs, and AV-nicking and focal arteriolar narrowing, are considered markers of microvascular pathology. As such, previous studies have shown the most consistent and strongest association of these retinal signs with subclinical and clinical cardiovascular diseases.[38] Although a positive association of NT-proBNP with AV-nicking and focal arteriolar narrowing would have further supported our findings, we think that our current findings with retinopathy signs and NT-proBNP are in themselves in line with previous findings on retinopathy signs and cerebrovascular diseases.

Strengths of our study are the population-based setting, large study size and extensive available data on cardiovascular risk factors, and clinical outcomes.
In conclusion, we found that higher NT-proBNP levels were associated with retinal microvascular damage, independent of cardiovascular risk factors. Our findings add important corroboration to a growing body of evidence implicating NT-proBNP as a general marker of vascular disease, representing damage to not only large vessels, but also small vessels.

## REFERENCES


1. Kim HN, Januzzi JL, Jr. Natriuretic peptide testing in heart failure. Circulation. 2011;123:2015-2019
2. de Lemos JA, McGuire DK, Drazner MH. B-type natriuretic peptide in cardiovascular disease. Lancet. 2003;362:316-322
3. Weber M, Hamm C. Role of b-type natriuretic peptide (bnp) and nt-probnp in clinical routine. Heart. 2006;92:843-849
4. Ashley KE, Galla JM, Nicholls SJ. Brain natriuretic peptides as biomarkers for atherosclerosis. Prev Cardiol. 2008;11:172-176
5. Schnabel RB, Wild PS, Schulz A, Zeller T, Sinning CR, Wilde S, et al. Multiple endothelial biomarkers and noninvasive vascular function in the general population: The gutenberg health study. Hypertension. 2012;60:288-295
6. Weber M, Arnold R, Rau M, Elsaesser A, Brandt R, Mitrovic V, et al. Relation of n-terminal pro b-type natriuretic peptide to progression of aortic valve disease. Eur Heart J. 2005;26:1023-1030
7. Gerber IL, Stewart RA, Legget ME, West TM, French RL, Sutton TM, et al. Increased plasma natriuretic peptide levels reflect symptom onset in aortic stenosis. Circulation. 2003;107:1884-1890
8. Patel MR, Peterson ED, Dai D, Brennan JM, Redberg RF, Anderson HV, et al. Low diagnostic yield of elective coronary angiography. N Engl J Med. 2010;362:886-895
9. Camici PG, Rimoldi OE. The clinical value of myocardial blood flow measurement. J Nucl Med. 2009;50:1076-1087
10. Crea F, Camici PG, Bairey Merz CN. Coronary microvascular dysfunction: An update. Eur Heart J. 2014;35:1101-1111
11. Wang AY, Lai KN. Use of cardiac biomarkers in end-stage renal disease. J Am Soc Nephrol. 2008;19:1643-1652
12. Vickery S, Price CP, John RI, Abbas NA, Webb MC, Kempson ME, et al. B-type natriuretic peptide (bnp) and amino-terminal probnp in patients with ckd: Relationship to renal function and left ventricular hypertrophy. Am J Kidney Dis. 2005;46:610-620
13. Mutlu U, Ikram MK, Wolters FJ, Hofman A, Klaver CC, Ikram MA. Retinal microvasculature is associated with long-term survival in the general adult dutch population. Hypertension. 2016;67:281-287
14. Liew G, Wang JJ, Mitchell P, Wong TY. Retinal vascular imaging: A new tool in microvascular disease research. Circ Cardiovasc Imaging. 2008;1:156-161
15. Hofman A, Brusselle GG, Darwish Murad S, van Duijn CM, Franco OH, Goedegebure A, et al. The rotterdam study: 2016 objectives and design update. Eur J Epidemiol. 2015;30:661-708
16. Leening MJ, Kavousi M, Heeringa J, van Rooij FJ, Verkroost-van Heemst J, Deckers JW, et al. Methods of data collection and definitions of cardiac outcomes in the rotterdam study. Eur J Epidemiol. 2012;27:173-185
17. Bos MJ, Koudstaal PJ, Hofman A, Ikram MA. Modifiable etiological factors and the burden of stroke from the rotterdam study: A population-based cohort study. PLoS Med. 2014;11:e1001634
18. Januzzi JL, van Kimmenade R, Lainchbury J, Bayes-Genis A, Ordonez-Llanos J, Santalo-Bel M, et al. Nt-probnp testing for diagnosis and short-term prognosis in acute destabilized heart failure: An international pooled analysis of 1256 patients: The international collaborative of nt-probnp study. Eur Heart J. 2006;27:330-337
19. Yeo KT, Wu AH, Apple FS, Kroll MH, Christenson RH, Lewandrowski KB, et al. Multicenter evaluation of the roche nt-probnp assay and comparison to the biosite triage bnp assay. Clin Chim Acta. 2003;338:107-115
20. Knudtson MD, Lee KE, Hubbard LD, Wong TY, Klein R, Klein BE. Revised formulas for summarizing retinal vessel diameters. Curr Eye Res. 2003;27:143-149

21. Littmann H. [determining the true size of an object on the fundus of the living eye] zur bestimmung der wahren grosse eines objektes auf dem hintergrund eines lebenden auges. Klin Monbl Augenheilkd. 1988;192:66-67
22. Wong TY, Klein R, Sharrett AR, Duncan BB, Couper DJ, Tielsch JM, et al. Retinal arteriolar narrowing and risk of coronary heart disease in men and women. The atherosclerosis risk in communities study. JAMA. 2002;287:1153-1159
23. Bibbins-Domingo K, Ansari M, Schiller NB, Massie B, Whooley MA. B-type natriuretic peptide and ischemia in patients with stable coronary disease: Data from the heart and soul study. Circulation. 2003;108:2987-2992
24. Januzzi JL, Jr., Camargo CA, Anwaruddin S, Baggish AL, Chen AA, Krauser DG, et al. The n-terminal pro-bnp investigation of dyspnea in the emergency department (pride) study. Am J Cardiol. 2005;95:948-954
25. Kragelund C, Gronning B, Omland T, Kober L, Strande S, Steffensen R, et al. Is n-terminal pro b-type natriuretic peptide (nt-probnp) a useful screening test for angiographic findings in patients with stable coronary disease? Am Heart J. 2006;151:712 e711-712 e717
26. Portegies ML, Kavousi M, Leening MJ, Bos MJ, van den Meiracker AH, Hofman A, et al. N-terminal pro-b-type natriuretic peptide and the risk of stroke and transient ischaemic attack: The rotterdam study. Eur J Neurol. 2015;22:695-701
27. Kragelund C, Gronning B, Kober L, Hildebrandt P, Steffensen R. N-terminal pro-b-type natriuretic peptide and long-term mortality in stable coronary heart disease. N Engl J Med. 2005;352:666-675
28. Luchner A, Hengstenberg C, Lowel H, Riegger GA, Schunkert H, Holmer S. Effect of compensated renal dysfunction on approved heart failure markers: Direct comparison of brain natriuretic peptide (bnp) and n-terminal pro-bnp. Hypertension. 2005;46:118-123
29. Dadu RT, Fornage M, Virani SS, Nambi V, Hoogeveen RC, Boerwinkle E, et al. Cardiovascular biomarkers and subclinical brain disease in the atherosclerosis risk in communities study. Stroke. 2013;44:1803-1808
30. Hall C. Essential biochemistry and physiology of (nt-pro)bnp. Eur J Heart Fail. 2004;6:257-260
31. Levin ER, Gardner DG, Samson WK. Natriuretic peptides. N Engl J Med. 1998;339:321-328
32. Schirger JA, Grantham JA, Kullo IJ, Jougasaki M, Wennberg PW, Chen HH, et al. Vascular actions of brain natriuretic peptide: Modulation by atherosclerosis and neutral endopeptidase inhibition. J Am Coll Cardiol. 2000;35:796-801
33. van der Zander K, Houben AJ, Kroon AA, De Mey JG, Smits PA, de Leeuw PW. Nitric oxide and potassium channels are involved in brain natriuretic peptide induced vasodilatation in man. J Hypertens. 2002;20:493-499
34. McGeechan K, Liew G, Macaskill P, Irwig L, Klein R, Klein BE, et al. Meta-analysis: Retinal vessel caliber and risk for coronary heart disease. Ann Intern Med. 2009;151:404-413
35. Bower JK, Lazo M, Matsushita K, Rubin J, Hoogeveen RC, Ballantyne CM, et al. N-terminal pro-brain natriuretic peptide (nt-probnp) and risk of hypertension in the atherosclerosis risk in communities (aric) study. Am J Hypertens. 2015;28:1262-1266
36. Hopkins WE, Chen Z, Fukagawa NK, Hall C, Knot HJ, LeWinter MM. Increased atrial and brain natriuretic peptides in adults with cyanotic congenital heart disease: Enhanced understanding of the relationship between hypoxia and natriuretic peptide secretion. Circulation. 2004;109:2872-2877
37. Knudtson MD, Klein BE, Klein R, Wong TY, Hubbard LD, Lee KE, et al. Variation associated with measurement of retinal vessel diameters at different points in the pulse cycle. Br J Ophthalmol. 2004;88:57-61
38. Wong TY, McIntosh R. Hypertensive retinopathy signs as risk indicators of cardiovascular morbidity and mortality. Br Med Bull. 2005;73-74:57-70

# Chapter 4
# Subclinical Brain Damage

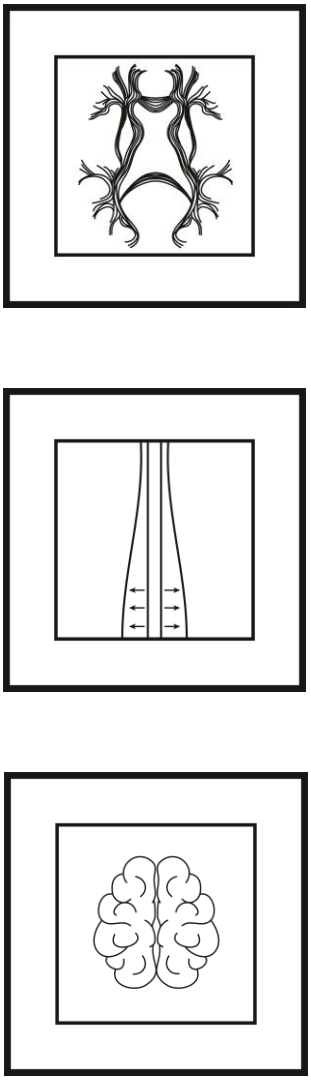

# Chapter 4.1
# Retinal Microvasculature and White Matter Microstructure: the Rotterdam Study

Unal Mutlu, Lotte G.M. Cremers, Marius de Groot, Albert Hofman, Wiro J. Niessen, Aad van der Lugt, Caroline C.W. Klaver, M. Arfan Ikram, Meike W. Vernooij, M. Kamran Ikram

**ABSTRACT**

**Background:** Microvascular pathology on retinal imaging has been linked to structural MRI markers of microvascular brain damage, including white matter lesions. However, damage to the white matter is often more widespread than is visible as structural MRI markers, and can be detected as microstructural damage. We studied whether retinal vascular calibers are related to normal-appearing white matter microstructure.
**Methods:** We included 2,436 participants (aged ≥ 45 years) from the population-based Rotterdam Study (2005-2009) who had gradable retinal images and brain MRI scans. Retinal arteriolar and venular calibers were measured semi-automatically on fundus photographs. White matter microstructure was assessed using diffusion tensor MRI. We used linear regression models to investigate the associations of retinal vascular calibers with markers of normal-appearing white matter microstructure, adjusting for age, sex, the fellow vascular caliber, and additionally for structural MRI markers and cardiovascular risk factors.
**Results:** Narrower arterioles and wider venules were associated with poor white matter microstructure: adjusted mean difference in fractional anisotropy per standard deviation decrease in arteriolar caliber -0.061 (95% confidence interval (CI): -0.106; -0.016) and increase in venular caliber -0.054 (-0.096; -0.011), adjusted mean difference in mean diffusivity per standard deviation decrease in arteriolar caliber 0.048 (0.007; 0.088), and increase in venular caliber 0.047 (0.008; 0.085). The associations for venules were more prominent in women.
**Conclusions:** Retinal vascular calibers are related to normal-appearing white matter microstructure. This suggests that microvascular damage in the white matter is more widespread than visually detectable on MRI.

## INTRODUCTION

With aging populations, the number of persons with age-related neurologic disorders such as stroke and dementia will rise substantially.[1] Vascular brain pathology has been recognized as an important contributor to the development of both these disorders.[2-4] Besides large vessel disease, pathology of the cerebral small vessels (< 200 μm) has also been implicated as a crucial substrate in stroke and dementia.[5] However, the direct examination of cerebral small vessels is difficult with current neuroimaging modalities. Alternatively, the retinal microvasculature is thought to reflect the condition of the cerebral microvasculature, and is therefore increasingly being used to study vascular brain pathology.[6, 7] Indeed, several studies have shown a link of retinal vascular calibers with stroke and dementia.[8, 9] By extension, these retinal markers have also been associated with brain MRI markers such as white matter lesions, lacunar infarcts, and cerebral microbleeds.[10, 11]

However, these structural MRI markers of microvascular damage are considered the tip of the iceberg of a more widespread vascular brain pathology.[12] In the last decade, advanced MRI techniques such as diffusion tensor MRI (DT-MRI) have enabled us to visualize and quantify the microstructure of normal-appearing white matter, which is presumed to be affected already at early stages of vascular brain disease.[13] However, the exact link of microvascular damage with such microstructural MRI markers has never been investigated. Therefore, our primary aim was to investigate the relation between retinal vascular calibers and microstructure of normal-appearing white matter. As a secondary aim, we examined the association of retinal vascular calibers with structural MRI markers of cerebral microvascular damage.

## METHODS

### Study population

This study is embedded within the second extension of the Rotterdam Study (2005-2009), a prospective population-based cohort study in the Ommoord district in the city Rotterdam, the Netherlands, including 3,932 participants aged ≥ 45 years.[14] A total of 976 participants did not undergo a MRI for the following reasons: did not visited the research center (n = 410), refused or physically/mentally unable to attend (n = 277), non-respondent (n = 108), had MRI contraindications (n = 154), or could not complete MRI (n = 27). From the remaining 2,956 participants who underwent a multi-sequence MRI, we excluded persons with cortical infarcts (n = 76) and those who had scans with artifacts that hampered automated analysis (n = 55). This left 2,825 persons with available DT-MRI data, of whom a further 389 had no (gradable) fundus photographs. For the current study, 2,436 persons were included with available DT-MRI and retinal data. The Rotterdam Study has been approved by the medical ethics committee according to the Population Study Act Rotterdam Study, executed by the Ministry of Health, Welfare and Sports of the Netherlands. All participants gave written informed consent. Baseline home interviews and examinations were performed between 2005 and 2009.

### Grading of retinal vascular calibers

A full ophthalmic examination was done including fundus color photography of the optic disc with a 35º visual field camera (TRC-50EX, Topcon Optical Company, Tokyo, Japan) after pharmacological mydriasis. We analyzed for each participant the fundus photograph of one eye with the best quality with a semi-automated system (IVAN, University of Wisconsin-Madison, Madison, Wisconsin). Then we calculated one summary value for the arteriolar calibers (in μm) and one for the venular calibers (in μm) for each participant.[15] Subsequently, we adjusted these summary measures for refractive errors to approximate absolute measures.[11] We verified in a random subsample (n = 100) that individual measurements in both eyes were similar. Measurements were performed by two trained raters masked for participant characteristics. Pearson correlation coefficients for interrater and intrarater reliability (n = 100) were 0.85 and 0.86 for arteriolar calibers, and 0.87 and 0.87 for venular calibers, respectively.

### Assessment of DT-MRI parameters

All brain MRI scanning was performed on a single 1.5 Tesla MRI scanner (GE Healthcare, Milwaukee, Wisconsin). Scan protocol details are described extensively elsewhere.[16] For DT-MRI, we performed a single shot, diffusion-weighted spin echoplanar imaging sequence with maximum b value of 1,000 s/mm$^2$ in 25 non-collinear directions. A standardized pipeline was used to preprocess all diffusion data, including correction for motion and eddy currents, and registration to tissue segmentation to obtain global mean

DT-MRI measures of the normal-appearing white matter. The normal-appearing white matter is being considered as the white matter volume without white matter lesion volumes. The global DT-MRI measures included fractional anisotropy (FA), mean diffusivity (MD), axial diffusivity (AxD), and radial diffusivity (RD). In general, lower values of FA and higher values of MD are indicative of poorer white matter microstructure. Also, changes in AxD and RD values may give extra information about the underlying cause of poor white matter microstructure. In 1,338 participants, the diffusion acquisition scheme was rotated with the phase and frequency encoding directions swapped, which led to a mild ghost artifact in the phase encoding direction. Therefore, we treated the phase encoding direction as a covariate in the analyses.[17]

**Other MRI markers**

Volumetric measures of normal-appearing white matter volume, intracranial volume, and white matter lesion volume (in milliliters) were obtained supratentorially using a validated tissue segmentation approach that included conventional k-nearest-neighbor brain tissue classification and white matter lesion segmentation.[18, 19] The presence of cerebral microbleeds and lacunar infarcts was rated by 1 of 5 trained research physicians, blinded to the participants' data, on a 3D T2-weighted gradient-recalled echo MRI. The presence of lacunes of presumed ischemic origin was rated on fluid-attenuated inversion recovery, proton density-weighted and T1-weighted sequences.[20] We defined lacunes as focal lesions $\geq 3$ and $< 15$ mm in size with the same signal intensity as cerebrospinal fluid on all sequences and a hyperintense rim on fluid-attenuated inversion recovery.

**Assessment of cardiovascular risk factors**

We measured the systolic and diastolic blood pressure twice in sitting position at the right upper arm with a random-zero sphygmomanometer. The mean of these two readings was used for further analysis. We calculated the body mass index as weight (kg) divided by height squared ($m^2$). An automated enzymatic procedure measured fasting serum concentrations of total and high-density lipoprotein cholesterol.[21] We defined diabetes mellitus as present if fasting serum glucose concentration was $\geq 7.0$ mmol/L, or if participants reported antidiabetic medication use. C-reactive protein serum concentration was measured by a near-infrared particle immunoassay method (Immage, Beckman Coulter, Fullerton, California ). We determined the presence of carotid plaques at the carotid artery bifurcation, common carotid artery, and internal carotid artery on both sides by ultrasound. Presence of these plaques was defined as focal thickening of the vessel wall $\geq 2$ mm with or without calcified components relative to adjacent segments. We retrieved data on smoking (non, former, or current) and antihypertensive medication use by a computerized questionnaire.

**Statistical analysis**

We used analysis of covariance, adjusted for age and sex, to assess difference in population characteristics between participants and non-participants. White matter lesion volumes were transformed using natural logarithm to account for a skewed distribution. We calculated z-scores for retinal vascular calibers, log-transformed white matter lesion volumes, and DT-MRI parameters to better compare the arteriolar and venular effects on imaging parameters. Associations of retinal vascular calibers with DT-MRI parameters were evaluated using linear regression models. Mean differences and corresponding 95% confidence intervals (CI) in DT-MRI parameters were estimated per standard deviation (SD) decrease in arteriolar caliber or increase in venular caliber, and in tertiles of retinal vascular calibers. We adjusted for age, sex, and the other vascular caliber (Model 1), and additionally for white matter volume, intracranial volume, white matter lesion volume, lacunar infarcts, and cerebral microbleeds (Model 2). We further adjusted for systolic and diastolic blood pressure, antihypertensive medication, body mass index, total and high-density lipoprotein cholesterol, diabetes mellitus, C-reactive protein, carotid plaque and smoking (Model 3). We explored effect modification by stratifying for age (median: 56 years), sex, hypertension, diabetes mellitus, and smoking, and by adding interaction terms to the statistical models. In all analyses, we treated the phase encoding direction for the diffusion acquisition as a confounder. We compared the effect estimates of arterioles and venules with age – an established risk factor for poor white matter microstructure – to have an impression about the magnitude of these associations. First, we calculated the effect estimates for the association of age with FA and MD. Then, we divided the betas (per SD) of retinal vascular calibers by the betas of age in relation to DT-MRI measures and reported the corresponding ratios. Furthermore, to assess the relation of retinal vascular calibers with white matter lesion volumes, cerebral microbleeds and lacunar infarcts, we used linear and logistic regression models. Missing values, if present, were less than in 4% of the cases, which we dealt with using fivefold multiple imputations based on determinant, outcome, and covariates. Given the Pearson correlation coefficient between systolic and diastolic blood pressure ($r = 0.77$), we examined the possibility of collinearity by calculating the variance inflation factor, but no indication of high collinearity was identified (variance inflation factor < 2.9). Statistical tests were performed at the 0.05 significance level (two-tailed) using SPSS 21.0 for Windows (IBM Corporation, Armonk, New York).

## RESULTS

Table 1 shows the characteristics of the study population. Of the total 3,932 participants, 1,496 (38%) did not participate in this study. After adjusting for age and sex (if applicable), non-participants were on average older, had higher blood pressure, had higher body mass index, had higher C-reactive protein levels, and were more smokers compared to participants. Of the 2,436 (62%) participants, 56% were women and the average age was 56.5 years (SD: 6.2).

Table 2 shows the associations between retinal vascular calibers and white matter microstructure. Both narrower arterioles and wider venules were associated with lower FA, higher MD, higher AxD, and higher RD. After adjusting for other MRI markers, the associations between retinal vascular calibers and DT-MRI parameters attenuated, but remained statistically significant. Additional adjustments for cardiovascular risk factors marginally changed the results.

Figure 1 shows absolute mean differences in FA and MD by tertiles of arteriolar and venular calibers (adjusted for age and sex). In stratified analyses (Figure 2), adjusted for variables in Model 3, we found that the association of arterioles with MD was modified by hypertension (P-value for interaction = 0.021), whereas for venules, the associations with FA and MD were in both cases modified by sex (P-value for interaction = 0.006, and 0.034, respectively). With respect to diabetes mellitus, we observed that the effects of arterioles and venules on DT-MRI parameters were more pronounced in persons with diabetes mellitus. However, p-values for the formal interaction terms were not significant: for arterioles these were 0.180 for FA and 0.172 for MD, whereas for venules these were 0.091 for FA and 0.097 for MD.

In an additional analysis to compare the magnitude of the associations with age, we observed that each year increase in age was associated with lower FA (-0.009 (-0.016; -0.002)) and higher MD (0.023 (0.016; 0.029)). We found that each SD narrower arterioles and wider venules in relation to FA had the magnitude equal to 6.8 years and 6.0 years of increase in age, respectively. Similarly, each SD narrower arterioles and wider venules in relation to MD had the magnitude equal to 2.1 and 2.0 years increase in age, respectively.

Table 3 shows the associations between retinal vascular calibers and structural MRI markers of cerebral microvascular damage. Both narrower arterioles and wider venules were significantly associated with larger white matter lesion volumes. Additional adjustment for cardiovascular risk factors (Model 3) attenuated these associations. Narrower arterioles and wider venules were also associated with the presence of cerebral microbleeds and lacunar infarcts in Model 1. Statistical significance of these associations disappeared after adjusting for other MRI markers and cardiovascular risk factors.

**Table 1. Characteristics of the eligible study cohort.**

| Characteristic | Participants (n = 2,436) | Non-participants (n = 1,496) |
|---|---|---|
| Age, years | 56.5 (6.2) | 58.2 (8.6)* |
| Female | 1374 (56) | 878 (59) |
| Systolic blood pressure, mmHg | 131.9 (18.5) | 134.1 (20.3)* |
| Diastolic blood pressure, mmHg | 82.3 (10.8) | 83.2 (11.4)* |
| Antihypertensive medication | 406 (28) | 523 (22)* |
| Hypertension | 1,117 (46) | 726 (56)* |
| Body mass index, $kg/m^2$ | 27.5 (4.3) | 28.4 (5.2)* |
| Total cholesterol, mmol/L | 5.6 (1.1) | 5.5 (1.1) |
| High-density lipoprotein cholesterol, mmol/L | 1.4 (0.4) | 1.4 (0.4) |
| Diabetes mellitus type 2 | 190 (8) | 131 (9) |
| C-reactive protein, mg/L | 2.5 (4.4) | 3.0 (5.3)* |
| Carotid plaque | 604 (25) | 476 (32) |
| Smoking status | | |
| Non-smoker | 786 (32) | 459 (31) |
| Former smoker | 1,116 (46) | 608 (41)* |
| Current smoker | 534 (22) | 417 (28)* |
| Arteriolar caliber, µm | 158.7 (15.4) | - |
| Venular caliber, µm | 239.8 (22.7) | - |
| White matter volume, ml | 418.7 (57.3) | - |
| Intracranial volume, ml | 1,129.0 (119.2) | - |
| White matter lesion volume†, ml | 2.0 (1.3-3.5) | - |
| Cerebral microbleeds | 302 (12) | - |
| Lacunar infarcts | 87 (4) | - |
| Fractional anisotropy | 0.34 (0.01) | - |
| Mean diffusivity, $10^{-3}$ $mm^2/s$ | 0.73 (0.02) | - |
| Axial diffusivity, $10^{-3}$ $mm^2/s$ | 1.01 (0.02) | - |
| Radial diffusivity, $10^{-3}$ $mm^2/s$ | 0.59 (0.02) | - |

Values are presented as means (standard deviation) or as numbers (percentage).
*Significantly different from included persons (age and sex adjusted p-value < 0.05).
†Presented as median (interquartile range) because of skewed distribution.
The following variables had missing values: systolic and diastolic blood pressure (n = 7), use of antihypertensive medication (n = 18), body mass index (n = 2), total cholesterol (n = 27), high-density lipoprotein cholesterol (n = 29), diabetes mellitus (n = 18), C-reactive protein (n = 92), carotid plaque (n = 6), smoking (n = 5).

| Table 2. The association between retinal vascular calibers and white matter microstructure. | | | | |
|---|---|---|---|---|
| | **Fractional anisotropy** | **Mean diffusivity** | **Axial diffusivity** | **Radial diffusivity** |
| Arteriolar caliber, per SD decrease | | | | |
| Model 1 | -0.121 (-0.166; -0.077) | 0.108 (0.065; 0.150) | 0.065 (0.022; 0.108) | 0.119 (0.075; 0.162) |
| Model 2 | -0.061 (-0.104; -0.018) | 0.054 (0.015; 0.092) | 0.032 (-0.006; 0.070) | 0.059 (0.019; 0.099) |
| Model 3 | -0.061 (-0.106; -0.016) | 0.048 (0.007; 0.088) | 0.025 (-0.016; 0.065) | 0.055 (0.013; 0.097) |
| Venular caliber, per SD increase | | | | |
| Model 1 | -0.086 (-0.130; -0.043) | 0.080 (0.038; 0.123) | 0.045 (0.003; 0.087) | 0.090 (0.048; 0.133) |
| Model 2 | -0.060 (-0.101; -0.019) | 0.054 (0.016; 0.091) | 0.027 (-0.010; 0.064) | 0.062 (0.023; 0.101) |
| Model 3 | -0.054 (-0.096; -0.011) | 0.047 (0.008; 0.085) | 0.023 (-0.016; 0.061) | 0.054 (0.015; 0.094) |

Values represent difference in z-scores of DT-MRI parameters with 95% confidence interval.
Abbreviation: SD, standard deviation.
Model 1: adjusted for age, sex and the other vascular caliber.
Model 2: as Model 1, additionally adjusted for white matter volume, intracranial volume, white matter lesion volume, lacunar infarcts and cerebral microbleeds.
Model 3: as Model 2, additionally adjusted for systolic blood pressure, diastolic blood pressure, antihypertensive medication, body mass index, total cholesterol, high-density lipoprotein cholesterol, diabetes mellitus, C-reactive protein, carotid plaque and smoking

**Figure 1.** Absolute mean difference in (A) fractional anisotropy and (B) mean diffusivity by tertiles of retinal vascular calibers.

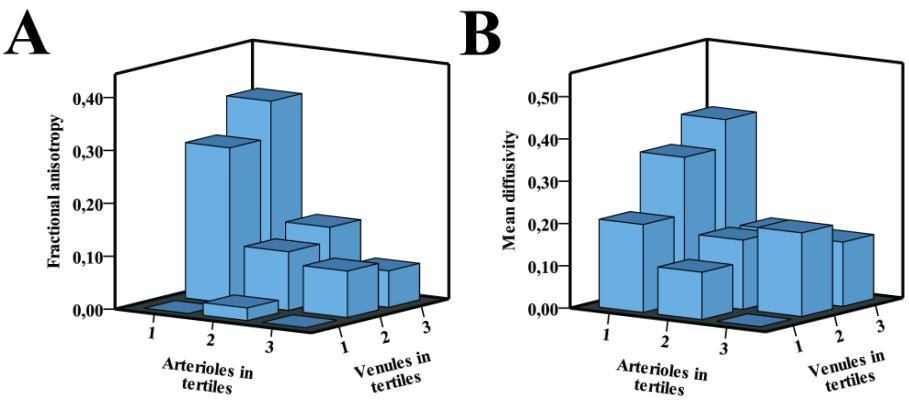

**Figure 2.** Stratified analyses on the association of (A) arteriolar and (B) venular calibers with white matter microstructure measures.

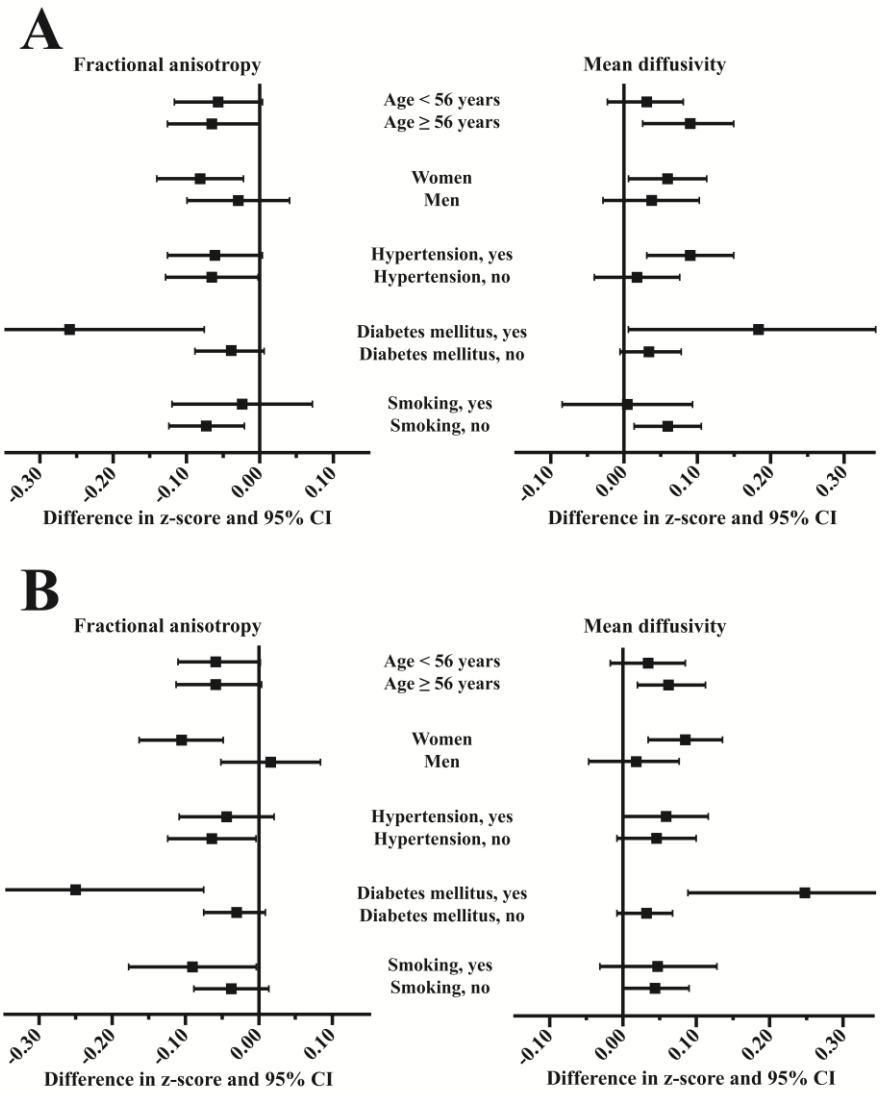

**Table 3. The association between retinal vascular calibers and markers of cerebral small vessel disease.**

| | White matter lesion volume | Presence of cerebral microbleeds | Presence of lacunar infarcts |
|---|---|---|---|
| | Difference in z-score (95% CI) | Odds ratio (95% CI) | Odds ratio (95% CI) |
| Arteriolar caliber, per SD decrease | | | |
| Model 1 | 0.145 (0.100; 0.189) | 1.20 (1.04; 1.40) | 1.34 (1.03; 1.75) |
| Model 2 | 0.146 (0.104; 0.188) | 1.15 (0.99; 1.34) | 1.10 (0.84; 1.43) |
| Model 3 | 0.101 (0.057; 0.145) | 1.14 (0.97; 1.33) | 1.10 (0.83; 1.45) |
| Venular caliber, per SD increase | | | |
| Model 1 | 0.061 (0.018; 0.104) | 1.09 (0.95; 1.26) | 1.31 (1.02; 1.68) |
| Model 2 | 0.059 (0.018; 0.100) | 1.07 (0.92; 1.24) | 1.17 (0.90; 1.52) |
| Model 3 | 0.030 (-0.012; 0.071) | 1.09 (0.94; 1.27) | 1.15 (0.88; 1.51) |

White matter lesion volumes are natural log-transformed.
Abbreviations: CI, confidence interval; SD, standard deviation.
Model 1: adjusted for age, sex and the other vascular caliber.
Model 2: as Model 1, additionally adjusted for intracranial volume, white matter lesion volume, lacunar infarcts and cerebral microbleeds (if applicable).
Model 3: as Model 2, additionally adjusted for systolic blood pressure, diastolic blood pressure, antihypertensive medication, body mass index, total cholesterol, high-density lipoprotein cholesterol, diabetes mellitus, C-reactive protein, carotid plaque and smoking.

## DISCUSSION

In this study, we found that retinal microvascular pathology is related to poorer microstructure of normal-appearing cerebral white matter.
With respect to retinal vascular imaging as a tool in assessing vascular brain pathology, several large population-based studies have shown that retinal microvascular damage is related to subclinical and clinical vascular brain diseases. Community-based cohorts of predominantly healthy people have shown that retinopathy signs were associated with incident stroke, cognitive decline and dementia.[22, 23] Apart from clinical outcomes, these studies also showed that persons with retinopathy signs had more often subclinical microvascular brain damage such as white matter lesions, cerebral infarcts and cerebral microbleeds.[22-26] Overall these findings suggest that both retinal and cerebral microvascular damage may appear simultaneously as part of systemic microvascular disease with common pathogenesis.[26] However, signs of retinopathy are relatively late manifestations of organ damage and presumably reflect advanced stages of microvascular damage including blood-retina barrier disruption.[27] There are ongoing efforts to unravel earlier retinal markers (e.g. narrower arterioles and wider venules), as they likely represent a point in the pathophysiologic cascade that is potentially reversible, offering great potential for the

development of preventive strategies or surrogate markers for trials.

Interestingly, cross-sectional data from the Rotterdam Study showed that the association of retinal vascular calibers with markers of cerebral small vessel disease was not significant.[28] In contrast, longitudinal data from the same study showed that wider venular caliber was associated with progression of white matter lesions in both periventricular and subcortical regions, and with incident lacunar infarcts on MRI.[28] Overall, these findings indicate that changes in retinal vascular calibers may precede the development of white matter lesions and lacunar infarcts. Findings from our current study are in line with these observations. We found that retinal vascular calibers were strongly related to markers of normal-appearing white matter on DT-MRI, independently of structural MRI markers of cerebral small vessel disease. Moreover, the joint effect of narrower arterioles and wider venules on white matter microstructure appears to be much stronger than their individual effect.

Pathophysiologically, a narrow retinal arteriolar caliber may reflect not only active vasoconstriction, but also systemic structural changes such as arteriolosclerosis.[29] These processes may concomitantly occur in the brain, where they affect the ability of cerebral arterioles to maintain control of local blood flow. Thus, predisposed areas as served by these vessels may lead to ischemic damage, and eventually to a state of chronic hypoperfusion of the white matter with subsequent demyelination and axonal damage.[12] It has been shown that subtle changes in the white matter due to demyelination and axonal damage can be detected using DT-MRI.[30] With respect to the venous system, several histopathological studies have reported venular abnormalities such as venous collagenosis in areas affected by white matter lesions.[31] In line with these observations, our findings show that subtle changes in retinal venular calibers are associated with DT-MRI markers of normal-appearing white matter.

A growing body of evidence now suggests that microvascular damage primarily affects women.[32] Indeed, narrower arterioles were found to increase the risk of coronary heart disease in women, but not in men.[33] In addition, cardiovascular risk factors typically associated with female sex such as an unfavorable lipid profile and inflammatory markers were also found to be associated with wider venules.[7] Our findings provide further evidence suggesting that the pathogenesis of vascular brain diseases is different between men and women. Furthermore, we found that the relation of retinal microvasculature with white matter microstructure is more pronounced in persons with diabetes mellitus. It is well-known that diabetes mellitus primarily affects small vessels due to chronic exposure to hyperglycemia, which can lead to impaired function of endothelium as well as pericytes.[34] It is conceivable that such more severe damage to the microcirculation might translate into stronger associations among diabetics compared to non-diabetics. At the same time, persons with diabetes mellitus very often have other cardiometabolic comorbidities, such as dyslipidemia and subclinical inflammation, all of which can further aggravate the small vessel damage.[35] Although we did adjust for covariates that are considered proxies for these processes, a substantial residual effect remains likely and may explain the stronger

associations among diabetics compared to non-diabetics.

DT-MRI is highly sensitive to changes in water diffusion in the white matter microstructure and thus a robust method to detect microstructural changes.[30] Experimental studies have suggested that perpendicular diffusivity may reflect myelin loss, whereas axial diffusivity may point towards axonal degeneration.[36] Although it is not completely clear which pathophysiological processes underlie alterations in white matter DT-MRI measures, possible mechanisms besides microvascular lesions include inflammation, demyelination and blood-brain barrier disruption. Nevertheless, DT-MRI is a useful research tool to probe not only cerebrovascular pathology, but also other brain diseases such as multiple sclerosis and other inflammatory demyelinating diseases. With respect to our study, given the rarity of these other diseases, it is unlikely that our findings may have been affected by these conditions.

Several methodological issues need to be discussed. First, the cross-sectional design of our study prevented us from assessing the temporal link between the retinal microvasculature and white matter microstructure. Second, persons excluded from these analyses had a slightly worse cardiovascular risk profile, suggesting a limited role for selection bias. Third, retinal caliber measurements were assessed at a single point in time and were not synchronized to the cardiac cycle. Hence, we were not able to assess dynamic changes in the microcirculation. This random misclassification suggests that the true effect sizes may have been larger. Fourth, we were unable to measure some confounding factors such as previous blood pressure or cholesterol levels, which could have influenced our associations by introducing residual confounding. Furthermore, participants in the Rotterdam Study are mainly middle-class white persons, which limits the generalizability of our findings. Also, due to the low number of incident clinical endpoints (stroke/dementia) in this extended cohort, we were not able to examine the association between retinal vascular calibers and DT-MRI markers with these endpoints. Finally, we acknowledge that the sensitivity of DT-MRI to a broad spectrum of other factors (e.g. noise, artifacts, and crossing white matter tracts) makes interpretation difficult, thus inferences should be drawn carefully.

Strengths of our study are the population-based setting including relatively young and healthy individuals, the large study size and available data on macrostructural and microstructural brain imaging markers, enabling us to assess independent associations.

In this study, we have shown that retinal vascular calibers are associated with poorer white matter microstructure in normal-appearing white matter. These findings suggest that microvascular damage in the white matter is more widespread than visually detectable on MRI. Future studies with longitudinal data on incident clinical cerebrovascular diseases are needed to examine the clinical implications of these retinal and DT-MRI markers.

## REFERENCES


1. World Health Organization. Neurological disorders: Public health challenges. 2006
2. Akoudad S, Portegies ML, Koudstaal PJ, Hofman A, van der Lugt A, Ikram MA, et al. Cerebral microbleeds are associated with an increased risk of stroke: The rotterdam study. Circulation. 2015;132:509-516
3. Kester MI, Goos JD, Teunissen CE, Benedictus MR, Bouwman FH, Wattjes MP, et al. Associations between cerebral small-vessel disease and alzheimer disease pathology as measured by cerebrospinal fluid biomarkers. JAMA Neurol. 2014;71:855-862
4. Vermeer SE, Longstreth WT, Jr., Koudstaal PJ. Silent brain infarcts: A systematic review. Lancet Neurol. 2007;6:611-619
5. Thompson CS, Hakim AM. Living beyond our physiological means: Small vessel disease of the brain is an expression of a systemic failure in arteriolar function: A unifying hypothesis. Stroke. 2009;40:e322-330
6. Wong TY, Klein R, Klein BE, Tielsch JM, Hubbard L, Nieto FJ. Retinal microvascular abnormalities and their relationship with hypertension, cardiovascular disease, and mortality. Surv Ophthalmol. 2001;46:59-80
7. Ikram MK, de Jong FJ, Vingerling JR, Witteman JC, Hofman A, Breteler MM, et al. Are retinal arteriolar or venular diameters associated with markers for cardiovascular disorders? The rotterdam study. Invest Ophthalmol Vis Sci. 2004;45:2129-2134
8. Ikram MK, de Jong FJ, Bos MJ, Vingerling JR, Hofman A, Koudstaal PJ, et al. Retinal vessel diameters and risk of stroke: The rotterdam study. Neurology. 2006;66:1339-1343
9. de Jong FJ, Schrijvers EM, Ikram MK, Koudstaal PJ, de Jong PT, Hofman A, et al. Retinal vascular caliber and risk of dementia: The rotterdam study. Neurology. 2011;76:816-821
10. Hilal S, Ong YT, Cheung CY, Tan CS, Venketasubramanian N, Niessen WJ, et al. Microvascular network alterations in retina of subjects with cerebral small vessel disease. Neurosci Lett. 2014;577:95-100
11. Littmann H. [determining the true size of an object on the fundus of the living eye] zur bestimmung der wahren grosse eines objektes auf dem hintergrund eines lebenden auges. Klin Monbl Augenheilkd. 1988;192:66-67
12. Pantoni L. Cerebral small vessel disease: From pathogenesis and clinical characteristics to therapeutic challenges. Lancet Neurol. 2010;9:689-701
13. de Groot M, Verhaaren BF, de Boer R, Klein S, Hofman A, van der Lugt A, et al. Changes in normal-appearing white matter precede development of white matter lesions. Stroke. 2013;44:1037-1042
14. Hofman A, Brusselle GG, Darwish Murad S, van Duijn CM, Franco OH, Goedegebure A, et al. The rotterdam study: 2016 objectives and design update. Eur J Epidemiol. 2015;30:661-708
15. Knudtson MD, Lee KE, Hubbard LD, Wong TY, Klein R, Klein BE. Revised formulas for summarizing retinal vessel diameters. Curr Eye Res. 2003;27:143-149
16. Ikram MA, van der Lugt A, Niessen WJ, Koudstaal PJ, Krestin GP, Hofman A, et al. The rotterdam scan study: Design update 2016 and main findings. Eur J Epidemiol. 2015;30:1299-1315
17. de Groot M, Ikram MA, Akoudad S, Krestin GP, Hofman A, van der Lugt A, et al. Tract-specific white matter degeneration in aging: The rotterdam study. Alzheimers Dement. 2015;11:321-330
18. Vrooman HA, Cocosco CA, van der Lijn F, Stokking R, Ikram MA, Vernooij MW, et al. Multi-spectral brain tissue segmentation using automatically trained k-nearest-neighbor classification. Neuroimage. 2007;37:71-81
19. de Boer R, Vrooman HA, van der Lijn F, Vernooij MW, Ikram MA, van der Lugt A, et al. White matter lesion extension to automatic brain tissue segmentation on mri. Neuroimage. 2009;45:1151-1161

20. Vernooij MW, Ikram MA, Wielopolski PA, Krestin GP, Breteler MM, van der Lugt A. Cerebral microbleeds: Accelerated 3d t2*-weighted gre mr imaging versus conventional 2d t2*-weighted gre mr imaging for detection. Radiology. 2008;248:272-277
21. Hofman A, van Duijn CM, Franco OH, Ikram MA, Janssen HL, Klaver CC, et al. The rotterdam study: 2012 objectives and design update. Eur J Epidemiol. 2011;26:657-686
22. Wong TY, Klein R, Sharrett AR, Couper DJ, Klein BE, Liao DP, et al. Cerebral white matter lesions, retinopathy, and incident clinical stroke. JAMA. 2002;288:67-74
23. Qiu C, Cotch MF, Sigurdsson S, Jonsson PV, Jonsdottir MK, Sveinbjrnsdottir S, et al. Cerebral microbleeds, retinopathy, and dementia: The ages-reykjavik study. Neurology. 2010;75:2221-2228
24. Qiu C, Cotch MF, Sigurdsson S, Klein R, Jonasson F, Klein BE, et al. Microvascular lesions in the brain and retina: The age, gene/environment susceptibility-reykjavik study. Ann Neurol. 2009;65:569-576
25. Cheung N, Mosley T, Islam A, Kawasaki R, Sharrett AR, Klein R, et al. Retinal microvascular abnormalities and subclinical magnetic resonance imaging brain infarct: A prospective study. Brain. 2010;133:1987-1993
26. Cooper LS, Wong TY, Klein R, Sharrett AR, Bryan RN, Hubbard LD, et al. Retinal microvascular abnormalities and mri-defined subclinical cerebral infarction: The atherosclerosis risk in communities study. Stroke. 2006;37:82-86
27. Bergers G, Song S. The role of pericytes in blood-vessel formation and maintenance. Neuro Oncol. 2005;7:452-464
28. Ikram MK, De Jong FJ, Van Dijk EJ, Prins ND, Hofman A, Breteler MM, et al. Retinal vessel diameters and cerebral small vessel disease: The rotterdam scan study. Brain. 2006;129:182-188
29. Liew G, Wang JJ, Mitchell P, Wong TY. Retinal vascular imaging: A new tool in microvascular disease research. Circ Cardiovasc Imaging. 2008;1:156-161
30. Alexander AL, Lee JE, Lazar M, Field AS. Diffusion tensor imaging of the brain. Neurotherapeutics. 2007;4:316-329
31. Brown WR, Moody DM, Challa VR, Thore CR, Anstrom JA. Venous collagenosis and arteriolar tortuosity in leukoaraiosis. J Neurol Sci. 2002;203-204:159-163
32. Shaw LJ, Bugiardini R, Merz CN. Women and ischemic heart disease: Evolving knowledge. J Am Coll Cardiol. 2009;54:1561-1575
33. Wong TY, Klein R, Sharrett AR, Duncan BB, Couper DJ, Tielsch JM, et al. Retinal arteriolar narrowing and risk of coronary heart disease in men and women. The atherosclerosis risk in communities study. JAMA. 2002;287:1153-1159
34. Armulik A, Genove G, Betsholtz C. Pericytes: Developmental, physiological, and pathological perspectives, problems, and promises. Dev Cell. 2011;21:193-215
35. Fox CS, Coady S, Sorlie PD, Levy D, Meigs JB, D'Agostino RB, Sr., et al. Trends in cardiovascular complications of diabetes. JAMA. 2004;292:2495-2499
36. Song SK, Sun SW, Ramsbottom MJ, Chang C, Russell J, Cross AH. Dysmyelination revealed through mri as increased radial (but unchanged axial) diffusion of water. Neuroimage. 2002;17:1429-1436

# Chapter 4.2
# Retinal Microvascular Calibers are Associated with Enlarged Perivascular Spaces in the Brain

Unal Mutlu, Hieab H.H. Adams, Albert Hofman, Aad van der Lugt, Caroline C.W. Klaver, Meike W. Vernooij, M. Kamran Ikram, M. Arfan Ikram

**ABSTRACT**

**Background:** Perivascular enlargement in the brain is a putative imaging marker for microvascular brain damage, but this link has not yet been confirmed using direct in vivo visualization of small vessels. We investigated the relation between microvascular calibers on retinal imaging, and enlarged perivascular spaces on brain magnetic resonance imaging (MRI).
**Methods:** We included 704 participants from the Rotterdam Study. Retinal arteriolar and venular calibers were measured semi-automatically on fundus photographs. Enlarged perivascular spaces were counted in the centrum semiovale, basal ganglia, hippocampus, and mesencephalon, using a standardized rating method. We determined the association between retinal microvascular calibers and enlarged perivascular spaces using negative binomial regression models, adjusting for age, sex, the other vascular caliber, structural brain MRI markers, and cardiovascular risk factors.
**Results:** Both narrower arteriolar and wider venular calibers were associated with more enlarged perivascular spaces in the centrum semiovale and hippocampal region. Rate ratios (95% confidence interval) for arterioles in the centrum semiovale and hippocampus were 1.07 (1.01-1.14) and 1.13 (1.04-1.22), respectively, and for venules 1.08 (1.01-1.16) and 1.09 (1.00-1.18), respectively. These associations were independent from other brain MRI markers, and cardiovascular risk factors.
**Conclusions:** Retinal microvascular calibers are related to enlarged perivascular spaces, confirming the putative link between microvascular damage and enlarged perivascular spaces.

## INTRODUCTION

Enlarged perivascular spaces in the brain, also known as Virchow-Robin spaces, have emerged as a promising imaging biomarker for vascular brain pathology.[1] These are spaces filled with interstitial fluid that surround the blood vessels as they extend into the brain. Increasing evidence suggests that enlarged perivascular spaces are affected by vascular risk factors, including high blood pressure and inflammation.[2] Additionally, enlarged perivascular spaces are strongly associated with other structural brain imaging markers, such as white matter lesions and lacunes, both hallmarks of cerebral small vessel disease.[3] In histopathology, enlarged perivascular spaces and characteristics of small vessel disease are often found concomitantly, further indicating that enlarged perivascular spaces might reflect damage to cerebral microvessels.[4] However, the link between microvascular damage and enlarged perivascular spaces has not yet been shown in vivo. The main difficulty is to directly assess the cerebral microvessels (< 200 μm) in vivo with current brain imaging techniques. A robust alternative is visualization of the retinal microvasculature, as the retinal and cerebral microvasculature share similarities in anatomy, physiology and embryology.[5] Indeed, there is convincing evidence showing links between retinal microvascular damage and (sub)clinical vascular brain disease.[6] Here, we investigated the association of retinal microvasculature with enlarged perivascular spaces in the general population.

## METHODS

### Study setting and population

This study was performed as part of the Rotterdam Study, a prospective population-based cohort study, details of which have been described previously.[7] In brief, the original cohort started in 1990 and from 2000 to 2002 the cohort was extended with 3,011 persons (aged ≥ 55 years). Home interviews and physical examinations, including eye examinations, were performed during both the baseline (2000-2002) and a follow-up examination (2004-2006) of this extended cohort.

Between August 2005 and May 2006, we randomly invited 1,073 of the 3,011 persons to undergo brain magnetic resonance imaging (MRI) as part of the Rotterdam Scan Study.[8] The institutional review board approved the study. After exclusion of individuals who were demented or had MRI contraindications, 977 persons were eligible, of whom 905 participated and gave written informed consent (response 93%). Due to physical inabilities, imaging could not be performed or completed in 8 individuals. Therefore, a total of 897 individuals had complete scans. Of these 897, 193 persons were excluded because they did not undergo ophthalmic examinations or had ungradable fundus transparencies on both eyes, leaving a total of 704 persons in the present study. The Rotterdam Study has been approved by the medical ethics committee according to the Population Study Act Rotterdam Study, executed by the Ministry of Health, Welfare and Sports of the Netherlands. A written informed consent was obtained from all participants.

### Retinal vascular calibers

Fundus photographs were taken centered on the optic disc with a 35° visual field camera (TRC-50EX, Topcon Optical Company, Tokyo, Japan) after pharmacological mydriasis, and digitized with a high resolution scanner (LS-4000, Nikon, Tokyo, Japan). For each participant the image of one eye with the best quality was analyzed with a semi-automated system (IVAN, University of Wisconsin-Madison, Madison, Wisconsin). For each participant one summary value was calculated for the arteriolar calibers (in μm) and one for the venular calibers (in μm) enabling us to use the separate arteriolar and venular caliber sum values.[9] Because eyes may have different magnification due to refractive changes, we adjusted vessel measurements for possible magnification variations with Littmann formula to approximate absolute measures.[10] We verified in a random subsample of 100 participants that individual measurements in the left and right eye were similar. Two trained graders performed the assessments masked to participant characteristics. Pearson correlation coefficients for intergrader agreement were 0.87 for arteriolar and 0.91 for venular diameters. Intragrader agreement was 0.65-0.85 for arteriolar and 0.82-0.86 for venular diameters.

**Perivascular spaces**

Brain scans were performed on a 1.5 Tesla MRI unit (GE Healthcare, Milwaukee, Wisconsin). The protocol has been extensively described and includes axial T1-, T2-weighted, and fluid-attenuated inversion recovery sequences (FLAIR).[8] Perivascular enlargements were counted in 4 brain regions: the centrum semiovale, basal ganglia, hippocampus, and mesencephalon. This choice was based on the pronounced presence of perivascular enlargements in these regions, which was reported earlier, and is known from our own experience.[11, 12] For differential diagnosis with lacunar infarcts, symmetry of the lesions, sharp demarcation, and absence of a hyperintense rim on the FLAIR sequence supported rating them as enlarged perivascular spaces. White matter lesions are mostly confluent and were differentiated from enlarged perivascular spaces by signal intensity not equivalent to cerebrospinal fluid on T2. Perivascular spaces were identified by their linear, ovoid, or round shape depending on the slice direction and considered enlarged when their diameter was ≥ 1 mm. Scans were counted and graded by one investigator, blinded to clinical data, according to a recent developed rating protocol with excellent intraclass correlation coefficients (ICC) for intrarater variability (ICC > 0.8) and good interrater variability (ICC: 0.6-0.8).[13]

**Other MRI markers**

Image preprocessing and the tissue classification algorithm have been described elsewhere. Briefly, preprocessing included co-registration, non-uniformity correction and intensity normalization. Afterwards, we used the k-nearest-neighbor classifier to classify voxels into cerebrospinal fluid, grey matter, white matter, and white matter lesions.[14] Intracranial volume was defined as the sum of these volumes. To remove non-cerebral tissue, we used non-rigid transformation to register to each brain a template scan, in which all non-cerebral tissue was manually masked.[15] Validation methods and results showed very good to excellent agreement between automated classification and manual classification as reference.[16] All scans were rated by 1 of 5 trained research physicians to determine the presence and location of infarcts and microbleeds. The raters were blinded to clinical data. The presence of lacunes and cortical infarcts was rated on FLAIR, proton density-weighted and T1-weighted sequences, and were defined as focal lesions ≥ 3 and < 15 mm in size, with the same signal intensity as cerebrospinal fluid on all sequences and a hyperintense rim on FLAIR (when located supratentorially). Infarcts showing involvement of grey matter were classified as cortical infarcts. The presence of cerebral microbleeds was rated as small, focal, round to ovoid areas of signal loss on 3D T2-weighted gradient-recalled echo MRI.[17]

**Covariates**

Blood pressure was measured twice in sitting position at the right brachial artery with a random-zero sphygmomanometer. We used the average of two readings for analysis. Body mass index was computed as weight (kg) divided by height squared ($m^2$). Serum total and high-density lipoprotein cholesterol concentrations were determined by an automated enzymatic procedure. Diabetes mellitus was considered present if participants reported use of antidiabetic medication or when fasting serum glucose level was equal to or greater than 7.0 mmol/L. Serum levels of C-reactive protein were determined by a near-infrared particle immunoassay method (Immage, Beckman Coulter, Fullerton, California). Participants underwent ultrasonography of both carotid arteries to assess the presence of plaques in the common carotid artery, bifurcation, and internal carotid artery. Carotid plaques were defined as focal thickening of the vessel wall of more than 50% relative to adjacent segments, composed of calcified or non-calcified components. The plaque score reflected the total number of sites with plaques and ranged from 0 to 6 (left- and right sided common carotid artery, bifurcation, and internal carotid artery).[18] Information on smoking (categorized as non or current) and antihypertensive medication use was obtained during the home interview by a computerized questionnaire. We defined hypertension as a systolic blood pressure of 140 mmHg or more, a diastolic blood pressure of 90 mmHg or more, use of antihypertensive medication, or any combination of these 3 factors. Assessment of stroke events has been described previously.[19]

**Statistical analysis**

We calculated z-scores for retinal vascular calibers (individual vascular caliber minus mean vascular caliber, divided by the standard deviation (SD)) to enable better comparison between the effects of arterioles and venules on perivascular enlargements. Initially, we used Poisson regression models to determine the association between retinal vascular calibers and perivascular enlargements count. However, the variances of the estimates were larger than the mean estimate (i.e. overdispersion), thus violating the assumption of Poisson regression. Therefore, we applied the negative binomial distribution, which gave a better fit to the data. Rate ratios with corresponding 95% confidence intervals (CIs) were estimated per SD decrease in arterioles, or increase in venules. We adjusted for age, sex, and the other vascular caliber (Model 1). We further constructed two models in addition to Model 1. In Model 2 we adjusted for intracranial volume, white matter lesion volume, presence of infarcts, and presence of cerebral microbleeds. In Model 3, we adjusted for systolic blood pressure, diastolic blood pressure, antihypertensive medication, body mass index, total cholesterol, high-density lipoprotein cholesterol, diabetes mellitus, C-reactive protein, carotid plaque score and smoking (Model 3). We explored effect modification by stratifying for sex, hypertension, diabetes mellitus, and smoking. We stratified for these variables because sex differences might influence microvascular function,[20] and hypertension typically affects the small perforating end-arteries of the deep grey nuclei and deep white

matter.[21] We also considered diabetes mellitus and smoking as potential effect modifiers, because differential contribution of these factors in cerebral small vessel disease has already been demonstrated.[22, 23] Statistical tests were performed at the 0.05 level of significance (two-tailed) using SPSS version 21.0 (IBM Corporation, Armonk, New York) for Windows.

## RESULTS

Study population characteristics are reported in Table 1. Average age was 66.0 years, and 52% were females. We found that narrower arteriolar calibers and, to a lesser extent, wider venular calibers were significantly associated with more enlarged perivascular spaces in the hippocampus and centrum semiovale. Adjusting for structural brain MRI markers and cardiovascular risk factors slightly attenuated these associations, but these remained statistically significant (Table 2). Figure 1 shows the difference in count of enlarged perivascular spaces for tertiles of arterioles and venules compared to the reference tertile. Excluding participants with a history of stroke (n = 11) did not change the associations. Stratified analyses revealed no interactions (p-value for interaction > 0.05).

**Table 1. Characteristics of the study population, n = 704.**

| Characteristic | Descriptive |
|---|---|
| Age, years | 66.0 (5.1) |
| Female | 365 (52%) |
| Systolic blood pressure, mmHg | 143.1 (17.8) |
| Diastolic blood pressure, mmHg | 81.0 (10.3) |
| Antihypertensive medication | 249 (35%) |
| Body mass index, kg/m$^2$ | 27.5 (3.9) |
| Total cholesterol, mmol/L | 5.7 (0.9) |
| High-density lipoprotein cholesterol, mmol/L | 1.4 (0.4) |
| Diabetes mellitus | 65 (9%) |
| C-reactive protein, mg/L | 2.1 (3.7) |
| Carotid plaque score ≥ 4 | 173 (25%) |
| Current smoker | 89 (13%) |
| Intracranial volume, ml | 1138.4 (115.5) |
| White matter lesion volume*, ml | 3.5 (2.1-7.0) |
| Infarcts | 58 (8%) |
| Cerebral microbleeds | 111 (16) |
| Central retinal artery equivalent, µm | 149.3 (15.3) |
| Central retinal vein equivalent, µm | 232.4 (22.1) |
| Regions of enlarged perivavascular spaces* | |
| Centrum semiovale | 6.0 (3.0-11.0) |
| Basal ganglia | 3.0 (1.0-5.0) |
| Hippocampus | 3.0 (1.0-5.0) |
| Mesencephalon | 2.0 (0.0-3.0) |

Values are presented as means (standard deviation) or as numbers (percentage).
*Values are presented as median (interquartile range).

**Table 2. The association between retinal vascular calibers and enlarged perivascular spaces.**

| Retinal vascular caliber | Centrum semiovale | Basal ganglia | Hippocampus | Mesencephalon |
|---|---|---|---|---|
| Arteriolar caliber, per SD decrease | | | | |
| Model 1* | 1.07 (1.01-1.14) | 1.06 (0.99-1.13) | 1.14 (1.05-1.24) | 1.07 (0.99-1.16) |
| Model 2† | 1.07 (1.01-1.14) | 1.03 (0.97-1.10) | 1.12 (1.04-1.22) | 1.07 (0.99-1.15) |
| Model 3‡ | 1.07 (1.01-1.14) | 1.05 (0.98-1.13) | 1.13 (1.04-1.22) | 1.06 (0.98-1.14) |
| Venular caliber, per SD increase | | | | |
| Model 1 | 1.07 (1.00-1.15) | 1.05 (0.97-1.12) | 1.08 (1.00-1.17) | 1.05 (0.97-1.15) |
| Model 2 | 1.07 (1.00-1.14) | 1.03 (0.96-1.10) | 1.06 (0.98-1.15) | 1.05 (0.97-1.14) |
| Model 3 | 1.08 (1.01-1.16) | 1.05 (0.98-1.13) | 1.09 (1.00-1.18) | 1.06 (0.98-1.16) |

Values are rate ratios for count of enlarged perivascular spaces (95% confidence interval).
Abbreviation: SD, standard deviation.
*adjusted for age, sex, and the other vascular caliber.
†as Model 1, additionally adjusted for intracranial volume, white matter lesion volume, infarcts, and cerebral microbleeds.
‡as Model 1, additionally adjusted for systolic blood pressure, diastolic blood pressure, antihypertensive medication, body mass index, total cholesterol, high-density lipoprotein cholesterol, diabetes mellitus, C-reactive protein, carotid plaque score, smoking.

**Figure 1.** Number of enlarged perivascular spaces in tertiles of retinal vascular calibers in centrum semiovale (A) and hippocampus (B), after adjusting for age, sex, and cardiovascular risk factors. Asterisk indicates significant difference ($p < 0.05$) compared to the reference tertile.

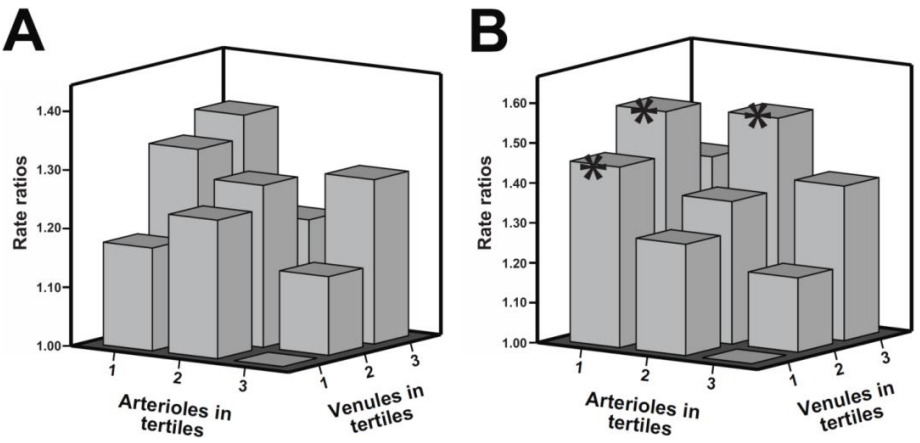

## DISCUSSION

We found that narrower arteriolar and wider venular calibers were associated with more enlarged perivascular spaces, independently of structural brain MRI markers, and cardiovascular risk factors.

Previous studies showed that enlarged perivascular spaces are related to subclinical and clinical vascular brain disease,[1, 2] supporting the notion that perivascular enlargements reflect microvascular damage. However, no study has directly investigated in vivo the association of enlarged perivascular spaces with microvasculature. We provide the first in vivo evidence that microvascular calibers are related to enlarged perivascular spaces, but the mechanism remains undetermined.

First, perivascular spaces drain interstitial and cerebrospinal fluid to the subarachnoid space, and eventually into cervical lymph nodes. Hence, a failure in this transmission may result in hemodynamic pressure differences that might manifest themselves in changed vascular calibers. Future studies are warranted to show how that would specifically lead to narrower arterioles. Second, narrower arterioles may lead to a state of cerebral hypoperfusion, eventually resulting in atrophy, and thus to perivascular enlargement. This ischemic mechanism is further supported by findings showing wider venular calibers to be associated with cerebral hypoxia.[24] Finally, it is also possible that shared risk factors explain the relation between retinal microvascular calibers and enlarged perivascular spaces. Structural MRI markers of cerebral small vessel disease, or cardiovascular risk factors, are likely candidates as confounders, but these factors did not fully explain the association in our study, indicating that other processes also play a role. These include arteriolosclerosis, inflammation, venous collagenosis, and cerebral amyloid angiopathy. Interestingly, enlarged perivascular spaces in the brain regions most associated with the retinal microvessels, namely the centrum semiovale and hippocampus, are related to cerebral amyloid angiopathy.[25] The perivascular drainage system in the basal ganglia is thought to process amyloid more efficiently and enlarged perivascular spaces there are associated more to vascular pathology. However, we did not find a significant association of retinal vascular calibers and enlarged perivascular spaces in the basal ganglia.

Strengths of our study are the population-based setting, the standardized rating protocol, and the extensive available data on brain MRI markers and cardiovascular risk factors.

A limitation is the cross-sectional design of our study, which precludes inferences on the temporal link between microvascular damage and enlarged perivascular spaces. Also, it is difficult to completely rule out misclassification of small infarcts as perivascular enlargements. This potential differential misclassification may have led to overestimation of our associations. However, because we used count data on perivascular spaces as outcome, a single or even a few misclassified infarcts are unlikely to have majorly influenced our results. Finally, we used a static measure of the microcirculation instead of dynamic functional measures synchronized on the cardiac cycle. This may have caused

random misclassification, leading to an underestimation of our associations.
In conclusion, our study shows that microvascular calibers are related to enlarged perivascular spaces, independent of structural MRI markers of cerebral small vessel disease, and cardiovascular risk factors.

## REFERENCE


1. Groeschel S, Chong WK, Surtees R, Hanefeld F. Virchow-robin spaces on magnetic resonance images: Normative data, their dilatation, and a review of the literature. Neuroradiology. 2006;48:745-754
2. Zhu YC, Tzourio C, Soumare A, Mazoyer B, Dufouil C, Chabriat H. Severity of dilated virchow-robin spaces is associated with age, blood pressure, and mri markers of small vessel disease: A population-based study. Stroke. 2010;41:2483-2490
3. Doubal FN, MacLullich AM, Ferguson KJ, Dennis MS, Wardlaw JM. Enlarged perivascular spaces on mri are a feature of cerebral small vessel disease. Stroke. 2010;41:450-454
4. Adachi M, Hosoya T, Haku T, Yamaguchi K. Dilated virchow-robin spaces: Mri pathological study. Neuroradiology. 1998;40:27-31
5. Liew G, Wang JJ, Mitchell P, Wong TY. Retinal vascular imaging: A new tool in microvascular disease research. Circ Cardiovasc Imaging. 2008;1:156-161
6. Heringa SM, Bouvy WH, van den Berg E, Moll AC, Kappelle LJ, Biessels GJ. Associations between retinal microvascular changes and dementia, cognitive functioning, and brain imaging abnormalities: A systematic review. J Cereb Blood Flow Metab. 2013;33:983-995
7. Hofman A, Brusselle GG, Darwish Murad S, van Duijn CM, Franco OH, Goedegebure A, et al. The rotterdam study: 2016 objectives and design update. Eur J Epidemiol. 2015;30:661-708
8. Ikram MA, van der Lugt A, Niessen WJ, Krestin GP, Koudstaal PJ, Hofman A, et al. The rotterdam scan study: Design and update up to 2012. Eur J Epidemiol. 2011;26:811-824
9. Knudtson MD, Lee KE, Hubbard LD, Wong TY, Klein R, Klein BE. Revised formulas for summarizing retinal vessel diameters. Curr Eye Res.2003;27:143-149
10. Littmann H. [determining the true size of an object on the fundus of the living eye] zur bestimmung der wahren grosse eines objektes auf dem hintergrund eines lebenden auges. Klin Monbl Augenheilkd. 1988;192:66-67
11. Chen W, Song X, Zhang Y, Alzheimer's Disease Neuroimaging I. Assessment of the virchow-robin spaces in alzheimer disease, mild cognitive impairment, and normal aging, using high-field mr imaging. AJNR Am J Neuroradiol. 2011;32:1490-1495
12. Zhu YC, Dufouil C, Mazoyer B, Soumare A, Ricolfi F, Tzourio C, et al. Frequency and location of dilated virchow-robin spaces in elderly people: A population-based 3d mr imaging study. AJNR Am J Neuroradiol. 2011;32:709-713
13. Adams HH, Cavalieri M, Verhaaren BF, Bos D, van der Lugt A, Enzinger C, et al. Rating method for dilated virchow-robin spaces on magnetic resonance imaging. Stroke. 2013;44:1732-1735
14. de Boer R, Vrooman HA, van der Lijn F, Vernooij MW, Ikram MA, van der Lugt A, et al. White matter lesion extension to automatic brain tissue segmentation on mri. Neuroimage. 2009;45:1151-1161
15. Klein S, Staring M, Andersson P, Pluim JP. Preconditioned stochastic gradient descent optimisation for monomodal image registration. Med Image Comput Comput Assist Interv. 2011;14:549-556
16. Vrooman HA, Cocosco CA, van der Lijn F, Stokking R, Ikram MA, Vernooij MW, et al. Multi-spectral brain tissue segmentation using automatically trained k-nearest-neighbor classification. Neuroimage. 2007;37:71-81
17. Vernooij MW, Ikram MA, Wielopolski PA, Krestin GP, Breteler MM, van der Lugt A. Cerebral microbleeds: Accelerated 3d t2*-weighted gre mr imaging versus conventional 2d t2*-weighted gre mr imaging for detection. Radiology. 2008;248:272-277
18. Hollander M, Bots ML, Del Sol AI, Koudstaal PJ, Witteman JC, Grobbee DE, et al. Carotid plaques increase the risk of stroke and subtypes of cerebral infarction in asymptomatic elderly: The rotterdam study. Circulation. 2002;105:2872-2877
19. Portegies ML, Kavousi M, Leening MJ, Bos MJ, van den Meiracker AH, Hofman A, et al. N-terminal pro-b-type natriuretic peptide and the risk of stroke and transient ischaemic attack: The rotterdam study. Eur J Neurol. 2015;22:695-701

20. Wong TY, Klein R, Sharrett AR, Duncan BB, Couper DJ, Tielsch JM, et al. Retinal arteriolar narrowing and risk of coronary heart disease in men and women. The atherosclerosis risk in communities study. JAMA. 2002;287:1153-1159
21. Charidimou A, Meegahage R, Fox Z, Peeters A, Vandermeeren Y, Laloux P, et al. Enlarged perivascular spaces as a marker of underlying arteriopathy in intracerebral haemorrhage: A multicentre mri cohort study. J Neurol Neurosurg Psychiatry. 2013;84:624-629
22. Khan U, Porteous L, Hassan A, Markus HS. Risk factor profile of cerebral small vessel disease and its subtypes. J Neurol Neurosurg Psychiatry. 2007;78:702-706
23. Staals J, Makin SD, Doubal FN, Dennis MS, Wardlaw JM. Stroke subtype, vascular risk factors, and total mri brain small-vessel disease burden. Neurology. 2014;83:1228-1234
24. de Jong FJ, Vernooij MW, Ikram MK, Ikram MA, Hofman A, Krestin GP, et al. Arteriolar oxygen saturation, cerebral blood flow, and retinal vessel diameters. The rotterdam study. Ophthalmology. 2008;115:887-892
25. Charidimou A, Jaunmuktane Z, Baron JC, Burnell M, Varlet P, Peeters A, et al. White matter perivascular spaces: An mri marker in pathology-proven cerebral amyloid angiopathy? Neurology. 2014;82:57-62

# Chapter 4.3
# Retinal Neurodegeneration and Brain MRI Markers: the Rotterdam Study

Unal Mutlu, Pieter W.M. Bonnemaijer, M. Arfan Ikram, Johanna M. Colijn, Lotte G.M. Cremers, Gabriëlle H.S. Buitendijk, Johannes R. Vingerling, Wiro J. Niessen, Meike W. Vernooij, Caroline C.W. Klaver, M. Kamran Ikram

**ABSTRACT**

**Background:** A relation between retinal neurodegeneration, quantified on optical coherence tomography (OCT), and cerebral atrophy and small vessel disease has been suggested, but evidence is lacking. We investigated the association of specific retinal layer thickness on OCT with markers of cerebral atrophy and small vessel disease on MRI.
**Methods:** We included 2124 persons (mean age 67.0 years; 56% women) from the Rotterdam Study who had gradable retinal OCT images and brain MRI scans. Thickness of retinal nerve fiber layer (RNFL), ganglion cell layer (GCL), and inner plexiform layer (IPL) were measured on OCT images. Volumetric, microstructural, and focal markers of brain tissue were assessed on MRI.
**Results:** We found that thinner RNFL, GCL and IPL were associated with smaller grey matter and white matter volume. Furthermore, we found that thinner RNFL and GCL were associated with worse white matter microstructure. No association was found between retinal layer thickness and white matter lesion volumes, cerebral microbleeds or lacunar infarcts.
**Conclusions:** Markers of retinal neurodegeneration are associated with markers of cerebral atrophy, suggesting that retinal OCT may provide information on neurodegeneration in the brain.

## INTRODUCTION

With an increase in life expectancy, the prevalence of common neurodegenerative disorders such as Alzheimer's disease is likely to rise accordingly.[1] Typically, these disorders are clinically recognized at the stage of dementia, or even mild cognitive impairment, when extensive neurodegeneration or vascular damage in the brain is already present, and modification of disease progression is ineffective.[2] Currently, magnetic resonance imaging (MRI) markers of diffuse brain atrophy such as grey matter and white matter loss, and markers of small vessel disease such as white matter lesions, cerebral microbleeds and lacunar infarcts, are implicated as pathologic substrates in dementia.[3-6] In addition, white matter abnormalities, assessed on diffusion tensor (DT-MRI), are presumed to be more widespread than visually detectable on MRI, and have been associated with cognitive deficits.[7] Although these brain MRI markers are widely used in the assessment of brain diseases, undergoing MRI scanning is time-consuming, costly, and some patients may have contraindications for undergoing MRI.

Advances in noninvasive optical imaging techniques enable us to assess neurodegeneration in the retina.[8] Particularly, optical coherence tomography (OCT) provides the opportunity to visualize retinal structures in vivo with biopsy-like precision (spatial resolution < 10 μm). Given that the retina is formed embryonically from neuronal tissue, and connected to the brain by the optic nerve, it is possible that certain abnormalities in the brain may be reflected in the retina.[9] Indeed, previous histopathological and clinical studies have shown that patients with Alzheimer's disease have extensive loss of retinal ganglion cells and reduced thickness of retinal nerve fiber layer (RNFL) compared to controls.[10-13] Findings from those studies implicate that thinner RNFL may be present before onset of clinical disease, and thus may be a manifestation of subclinical brain disease. However, whether retinal degeneration may be a marker of subclinical brain disease needs to be studied in large samples of relatively healthy persons.

Apart from the RNFL, with improvements in OCT devices and segmentation algorithms, we are now able to segment other retinal layers including the ganglion cell layer (GCL) and inner plexiform layer (IPL). These three layers form together the ganglion cell complex, in which the RNFL is composed of axons, the GCL is composed of cell bodies and the IPL is composed of the dendrites. Hence, it is possible that the GCL may reflect more the condition of the cerebral grey matter, whereas the RNFL and IPL may reflect more the condition of the cerebral white matter. This hypothesis is further supported by a previous study examining the link between OCT measurements and cerebral atrophy on MRI.[14]

In this population-based study, we aimed to investigate the association of retinal layer thicknesses on OCT with volumetric, microstructural and focal markers of brain tissue on MRI in a community-dwelling elderly population free of dementia and mild cognitive impairment.

## METHODS

### Study population

This study was part of the Rotterdam Study (RS): a prospective population-based cohort study that investigates causes and consequences of chronic diseases in residents of the Ommoord district in the city Rotterdam, the Netherlands, aged 45 years or older.[15] The original cohort started in 1990 (n = 7,983), and was extended in 2000 (n = 3,011) and 2006 (n = 3,932). Follow-up examinations take place every three to four years. In brief, participants were interviewed at home and examined at the research center. In 2007, spectral-domain OCT scanning was added to the protocol, and thus was performed in the fifth visit of the first cohort (RS-I-5), the third visit of the second cohort (RS-II-3), and at the baseline visit in about half of the third cohort (RS-III-1), see Figure 1. Since the introduction of OCT in the Rotterdam Study, a total of 5,065 persons were eligible for OCT-scanning, but 664 persons did not undergo OCT-scanning due to logistic reasons (e.g. lack of personnel, device maintenance or replacement) or personal reasons (e.g. sickness or unable to attend). A further 803 persons were excluded because OCT scans had motion artefacts, segmentation failures, missing data, or poor signal strength. We also excluded persons with dementia (n = 43) or history of clinical stroke (n = 115), persons that did not undergo dementia screening (n = 21), and persons with mild cognitive impairment (n = 198). History of clinical stroke was assessed and verified as described previously.[16] From the remaining 3,221 persons, 855 persons had no brain MRI scans or the scans were unusable for the following reasons: non-respondent or not visited the research center, refused or physical/mentally unable to attend, had MRI contra-indications, could not complete MRI scan, or poorly segmented scans. Subsequently, we only included persons if they had data on GCL and IPL thicknesses measured at the macular region, and RNFL thickness measured at the peripapillary region on the same eye. Finally, we excluded persons with age-related macular degeneration (n = 9), glaucoma (n = 42), and hypertensive or diabetic retinopathy that could affect retinal thickness measurement (n = 56). This resulted in 2,124 persons from which primarily the right eye (94%) was chosen for further analysis. At the beginning of the study, only the right eyes were scanned in the interest of time. This was the case for 883 persons. To maintain consistency, we chose primarily the right eye.

The Rotterdam Study has been approved by the Medical Ethics Committee of the Erasmus MC and by the Ministry of Health, Welfare and Sport of the Netherlands, implementing the Wet Bevolkingsonderzoek: ERGO (Population Studies Act: Rotterdam Study). All participants provided written informed consent to participate in the study and to obtain information from their treating physicians

**Figure 1.** Flow diagram of the study population.

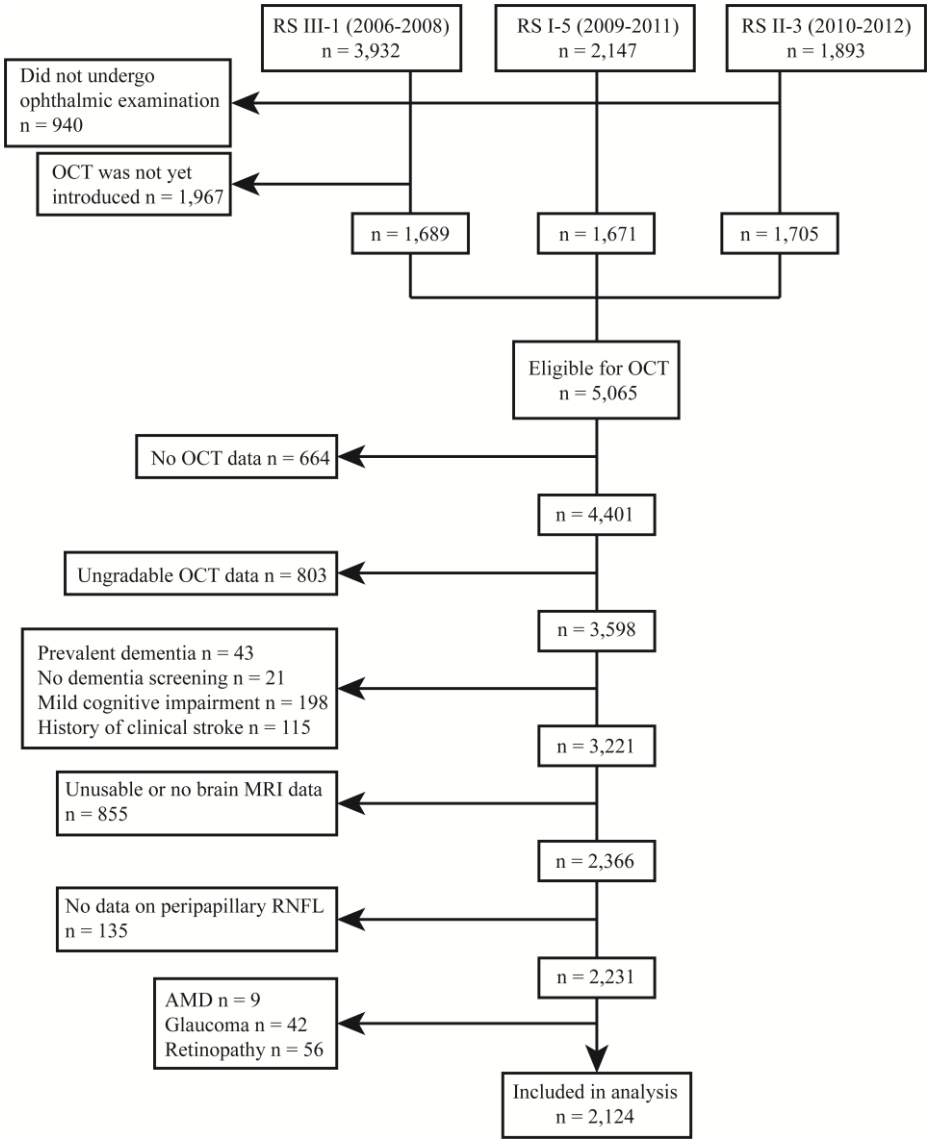


Abbreviations: RS, Rotterdam Study; OCT, optical coherence tomography; MRI, magnetic resonance imaging; RNFL, retinal nerve fiber layer; AMD, age-related macular degeneration.

**Spectral domain optical coherence tomography**

From September 2007 to June 2011 participants underwent a standard ophthalmic examination after pharmacological mydriasis, including fundus photography of the macula and optic nerve, and OCT scanning. Initially, participants' eyes were scanned with the Topcon 3D OCT-1000 (n = 1,730; Topcon Optical Company, Tokyo, Japan). From August 2011 onwards, due to an update during the study, this device was replaced with the Topcon 3D OCT-2000 (n = 394). The macula and optic nerve head were scanned in the horizontal direction in an area of 6 × 6 × 1.68 mm with 512 × 512 × 480 voxels for OCT-1000 and in an area of 6 × 6 × 2.30 mm with 512 × 512 × 885 voxels for OCT-2000, enabling us to detect structures with a resolution of 5 µm (Figure 2). Thickness of the peripapillary RNFL was measured automatically by Topcon's built-in segmentation algorithm. This was done in twelve peripapillary segments of $30^{o}$ each, and the average RNFL thickness was derived from the calculation circle. For the macula, volumes were segmented using Iowa Reference Algorithms 3.6, which has been validated for most widely available commercial OCT scanners (available from https://www.iibi.uiowa.edu/content/shared-software-download).[17] Thicknesses of the GCL and IPL were measured in nine regions of the Early Treatment Diabetic Retinopathy Study Grid. The average retinal layer thicknesses were calculated and used in further statistical analyses. Scans in our study had a segmentation index of more than 30%, an undefined region of less than 20%, and a quality factor of more than 30, which is considered acceptable quality.[18] Because the retinal layer thicknesses varies with the axial length of eyes, we treated the axial length, measured using Lenstar LS900 (Haag-Streit AG, Köniz, Switzerland), as a covariate in the statistical analyses.

**Brain imaging markers**

Brain MRI scanning was performed on a 1.5 Tesla MRI-scanner (GE Healthcare, Milwaukee, Wisconsin).[19] The scan protocol included four high-resolution axial sequences: a 3D T1-weighted (slice thickness 1.6 mm, zero-padded to 0.8), a proton-density-weighted (slice thickness 1.6 mm), a fluid-attenuated inversion recovery (FLAIR, slice thickness 2.5 mm) and a 3D T2*-weighted gradient-recalled echo scan (slice thickness 1.6 mm, zero-padded to 0.8). After preprocessing, we used k-nearest-neighbor classifier to segment voxels into grey matter, white matter, white matter lesion and cerebrospinal fluid. Summing all voxels of a certain tissue across the whole brain and multiplying by the voxel volume (1 voxel = 1.25 $mm^3$) yielded volumes in cubic milliliters. Supratentorial intracranial volume was defined as the sum of total grey matter volume, white matter volume, white matter lesion volume, and cerebrospinal fluid.[20, 21] Total brain volume was defined as the sum of grey matter and white matter volume. Individual lobes have been segmented by non-rigidly registering a template image in which the lobes have been outlined manually.[22] For the hippocampus, left and right hippocampal volumes were segmented separately on a 3D T-weighted sequence using an automated method as described previously.[23]

We used the average of the left and right hippocampus volume for further analysis.
For diffusion tensor-MRI (DT-MRI), we performed a single-shot, diffusion-weighted, spin-echo, echo-planar imaging sequence with maximum b-value of 1,000 s/mm2 in 25 non-collinear directions (slice thickness 3.5 mm). To obtain global mean DT-MRI measures in the normal-appearing white matter, all diffusion data were preprocessed using a standardized pipeline, including correction for motion and eddy currents, estimation of the diffusion tensor, and registration to tissue segmentation. DT-MRI maps were combined with the tissue segmentation results, from which the mean global DT-MRI measures were derived including fractional anisotropy (FA) and mean diffusivity (MD).[24] In general, FA is lower and MD is higher in older and damaged brains, which is thought to reflect worse white matter microstructure. In 513 persons, the diffusion acquisition scheme was rotated with the phase and frequency encoding directions swapped, which led to a mild ghost artifact in the phase encoding direction. Therefore, we treated the phase encoding direction as a covariate in the statistical analyses.
The presence of cerebral microbleeds, lacunar infarcts and cortical infarcts was counted visually by one of five trained research physicians. These focal measures were found incidentally on brain MRI. The raters were blinded to the clinical data. The presence of cerebral microbleeds was rated on 3D T2*-weighted gradient-recalled echo MRI.[25] The presence of lacunar and cortical infarcts were rated on FLAIR, proton density-weighted and 3D T1-weighted sequences. Lacunar infarcts were defined as focal lesions $\geq 3$ and $< 15$ mm in size with the same signal intensity as cerebrospinal fluid on all sequences and a hyperintense rim on FLAIR (when located supratentorially). Infarcts showing involvement of cortical grey matter were classified as cortical infarcts. Volumetric measures comprised total brain, grey matter, white matter, white matter lesion and hippocampal volume. Microstructural measures comprised fractional anisotropy and mean diffusivity. Focal measures comprised cerebral microbleeds and lacunar infarcts.

**Figure 2.** Output of the Topcon OCT-2000 device focusing on the macula (A) and optic nerve (B) with corresponding cross-sectional view of the retina (C and D, respectively).

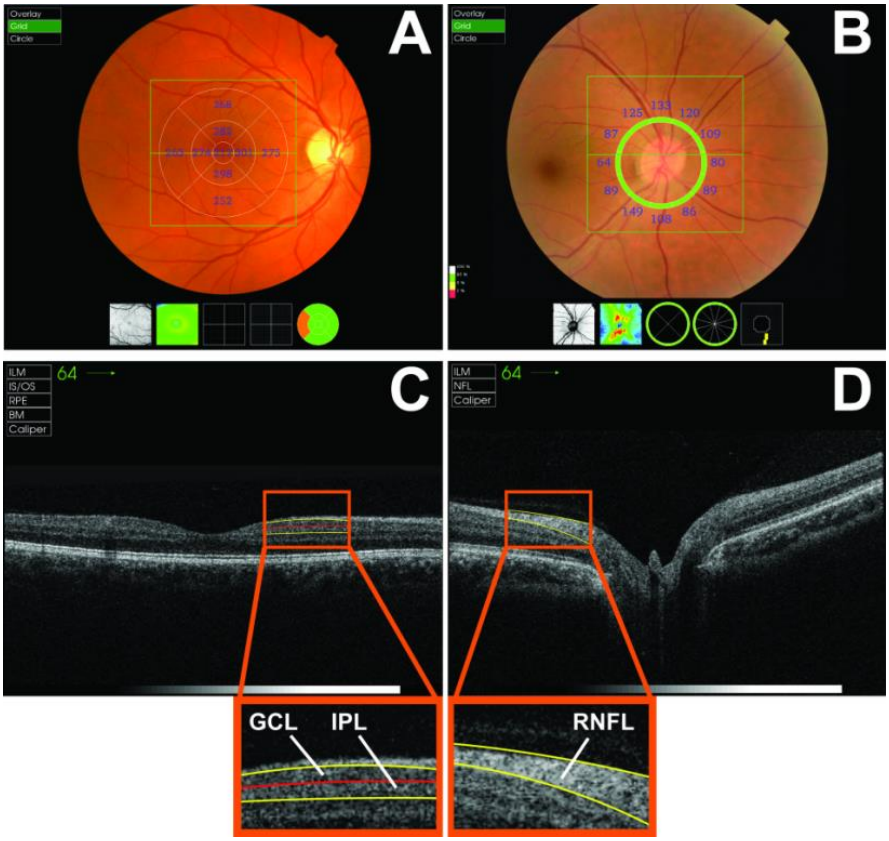


## Cognitive screening

During center visits, participants underwent a cognitive test battery, and dementia-screening was done using the Mini-Mental State Examination (MMSE) and the Geriatric Mental State Schedule (GMS) organic level.[26] Those with MMSE < 26 or GMS > 0 underwent examination and informant interview using the Cambridge Examination for Mental Disorders of the Elderly. In addition, continuous monitoring of the cohort for incident dementia took place through electronic linkage of the study database with medical records from general practitioners and the regional institute for outpatient mental health care. Available information on clinical neuroimaging was used when required for diagnosis of dementia (subtype). A consensus panel led by a consultant neurologist established the final diagnosis according to standard criteria for dementia (DSM-III-R). In our study, mild cognitive impairment was assessed using the following criteria: 1) presence of subjective memory complaints, 2) presence of objective cognitive impairment, and 3) absence of

dementia.[27] Subjective complaints were assessed by interview, and objective cognitive impairment was assessed using a cognitive test battery including letter-digit substitution task, Stroop test, verbal fluency test, and 15-word verbal learning test. For objective cognitive impairment, compound scores for various cognitive domains including memory function, information processing speed, and executive function were calculated, and those with < 1.5 standard deviation of the age-and education adjusted means were classified as cognitively impaired.[27] Educational level was measured based on degree of literacy as this measures educational attainment more directly and might therefore be a good marker of cognitive reserve. Participants were classified having low (primary, unfinished secondary and lower vocational), intermediate (secondary or intermediate vocational) or high education (higher vocational or university).

**Cardiovascular risk factors**

Blood pressure was measured twice in sitting position at the right brachial artery with a random-zero sphygmomanometer, and the average of two readings was used for analysis. Body mass index was computed as weight (kg) divided by height squared ($m^2$). Fasting serum total cholesterol concentration was determined by an automated enzymatic procedure. Diabetes mellitus was considered present if fasting serum glucose level was equal to or greater than 7.0 mmol/L, or when persons reported use of antidiabetic medication. Information on smoking (never, former or current), and blood pressure lowering medication use was obtained during the home interview by a computerized questionnaire.

**Statistical analysis**

As eyes were scanned with two different devices and in order to standardize the measurements, we calculated z-scores for the OCT measurements of each device. White matter lesion volumes were transformed using natural logarithm due to a skewed distribution. We also calculated z-scores for grey matter and white matter volumes, log-transformed white matter lesion volume, and DT-MRI measures to enable better comparison between the effects of RNFL, GCL and IPL on these different imaging parameters. Z-scores were calculated by subtracting individual value from the mean value, and dividing by the standard deviation. We used linear regression models to investigate the association of retinal layer thickness with volumetric, and microstructural measures. We used logistic regression models to investigate the association of retinal layer thickness with the presence of cerebral microbleeds and lacunar infarcts. Mean differences in z-score and odds ratios with corresponding 95% confidence intervals (CIs) were estimated per standard deviation decrease (SD) of retinal layer thickness. We adjusted for age, sex, education, subcohort, axial length of the eyes, intracranial volume, and for the following cardiovascular risk factors: mean arterial blood pressure, use of blood pressure lowering medication, body mass index, total cholesterol, diabetes mellitus, and smoking.

Missing values for covariates were dealt with using fivefold multiple imputations based on determinant, outcome, and covariates. In our analyses with DT-MRI measures, we excluded persons with cortical infarcts (n = 63) as tissue loss and gliosis surrounding cortical infarct may cause unreliable white matter lesion segmentations. In these analyses, we additionally adjusted for white matter volume and the phase encoding direction for the diffusion acquisition. Furthermore, in our analyses with white matter lesion volumes, cerebral microbleeds and lacunar infarcts, in persons free of cortical infarcts, we adjusted these measures for each other. For instance, in our analyses with white matter lesion volume as an outcome, we adjusted for cerebral microbleeds and lacunar infarcts. In sensitivity analyses, we assessed the effect of aging on the retinal layer thicknesses by using linear regression models. Also, we explored the effect of aging on the association of retinal layer thickness with volumetric and microstructural measures by stratifying for age in tertiles and by constructing interaction terms in the linear regression models.
Finally, in our analysis of retinal layer thickness with brain MRI markers, we have additionally adjusted for the two OCT devices to check whether our results were affected by the measurements of these two OCT devices. All analyses were performed at the 0.05 level of significance (two-tailed) using R version 3.2.3.

## RESULTS

Table 1 shows the characteristics of the study population. Mean age was 67.0 years (SD: 9.8), and 1,180 (56%) of the participants were women.
Figure 3 shows the association of retinal layer thickness with volumetric and microstructural measures. Thinner RNFL, GCL and IPL were all three significantly associated with smaller brain volume, mean difference in z-score (95% CI) per SD decrease in retinal layer thickness, respectively: -0.025 (-0.040; -0.011, $p < 0.001$), -0.036 (-0.050; -0.022, $p < 0.001$) and -0.023 (-0.037; -0.009, $p = 0.001$). These associations were driven by the association of thinner retinal layers with both grey matter and white matter volume. We did not find strong evidence for an association between retinal layer thickness and white matter lesion volumes. For the association of retinal layer thicknesses with white matter microstructural measures, we found that both thinner RNFL and GCL were significantly associated with a lower FA, mean difference in z-score of FA per SD decrease in RNFL and GCL, respectively: -0.067 (-0.111; -0.024, $p = 0.002$) and -0.078 (-0.121; -0.035, $p < 0.001$). Moreover, thinner GCL was associated with a higher MD: 0.040 (0.007; 0.073, $p = 0.018$). In our analysis with hippocampal volume, we found that thinner RNFL, GCL and IPL were associated with smaller hippocampal volume, mean difference in z-score (95% CI) per SD decrease in retinal layer thickness, respectively: -0.045 (-0.081; -0.010, $p = 0.013$), -0.043 (-0.078; -0.008, $p = 0.016$) and -0.031 (-0.065; 0.004, $p = 0.083$).

Table 2 shows the association of retinal layer thickness with grey matter and white matter volume in different lobes. In general, among associations between retinal layer thickness and lobe-specific volumes, we found the strongest associations within the occipital lobes. Table 3 shows the association of retinal layer thicknesses with cerebral microbleeds and lacunar infarcts. We did not find an association of retinal layer thicknesses with cerebral microbleeds or lacunar infarcts.
Furthermore, we found that an increased age was associated with thinner RNFL, GCL and IPL, mean difference in z-score per SD increase in age, respectively: -0.128 (-0.202; -0.054, $p < 0.001$), -0.228 (-0.302; -0.153, $p < 0.001$), and -0.165 (-0.240; -0.089, $p < 0.001$). In stratified analysis (Supplemental Table 1), we found that the associations of retinal layer thickness with volumetric and microstructural measures were slightly modified by age. In general, the associations were stronger in elderly people, but the interaction terms were not significant. Finally, we found that our associations were not affected by the two OCT devices as the results remained similar after adjusting for these devices.

**Table 1. Characteristics of the study population.**

| Characteristic | Descriptive |
|---|---|
| N | 2,124 |
| Age, years | 67.0 (9.8) |
| Female sex | 1,180 (56) |
| Systolic blood pressure, mmHg | 143.9 (21.8) |
| Diastolic blood pressure, mmHg | 84.7 (10.8) |
| Mean arterial blood pressure, mmHg | 104.4 (13.4) |
| Blood pressure lowering medication | 824 (39) |
| Body mass index, $kg/m^2$ | 27.3 (4.0) |
| Diabetes mellitus | 211 (10) |
| Total cholesterol, mmol/L | 5.5 (1.1) |
| Smoking status | |
| Never smoker | 686 (32) |
| Past smoker | 1109 (52) |
| Current smoker | 329 (16) |
| Education | |
| Lower education | 594 (28) |
| Intermediate education | 1040 (49) |
| Higher education | 490 (23) |
| Mini-mental state examination | 28.0 (1.7) |
| Axial length, mm | 23.5 (1.2) |
| Peripapillar retinal nerve fiber layer, µm | 96.0 (14.1) |
| Macular ganglion cell layer, µm | 33.9 (5.1) |
| Macular inner plexiform layer, µm | 37.0 (3.3) |

Values are presented as means (standard deviation) or as numbers (percentage).

The following variables had missing data: blood pressure (n = 1), blood pressure lowering medication (n = 8), body mass index (n = 0), diabetes mellitus (n = 33), total cholesterol (n = 26), smoking (n = 4), education (n = 30), and axial length (n = 202).

**Figure 3.** Association of retinal layer thickness with volumetric and microstructural brain measures.

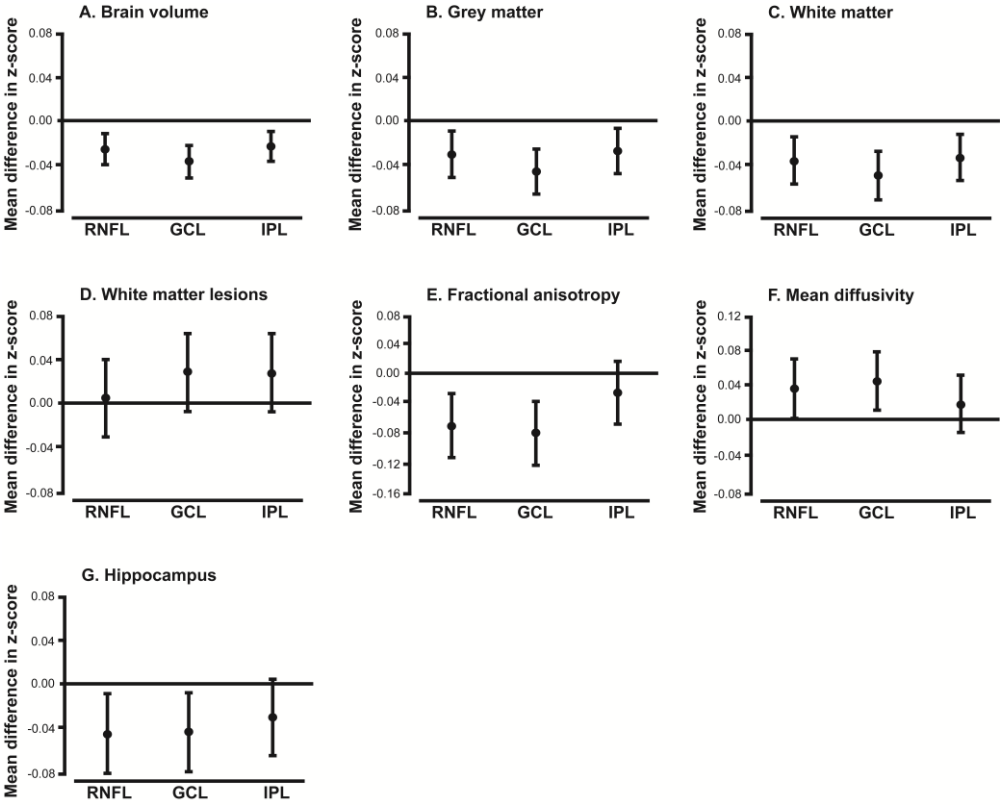


A. Brain volume; B. Grey matter; C. Total white matter; D. White matter lesion; E. Fractional anisotropy; F. Mean diffusivity. G. Hippocampus. Total white matter volume is the sum of normal white matter and white matter lesion volume. White matter lesion volumes are further natural log-transformed. Dots represent adjusted mean differences in z-score per standard deviation decrease in retinal layer thickness. Values are adjusted for age, sex, subcohort, education, axial length of the eye, intracranial volume, mean arterial blood pressure, blood pressure lowering medication, body mass index, total cholesterol, diabetes mellitus, and smoking. Analyses with grey matter, white matter lesion volumes, fractional anisotropy and mean diffusivity were also adjusted for white matter volume, whereas the analysis with white matter were adjusted for grey matter volume. Furthermore, analysis with white matter lesion volumes were adjusted for cerebral microbleeds and lacunar infarcts. Lines represent 95% confidence interval.

**Table 2. Association of retinal layer thicknesses with grey matter and white matter volume in different lobes.**

| | Retinal nerve fiber layer | P-value | Ganglion cell layer | P-value | Inner plexiform layer | P-value |
|---|---|---|---|---|---|---|
| Grey matter volume | | | | | | |
| Total volume | -0.031 (-0.052; -0.010) | 0.004 | -0.046 (-0.067; -0.026) | <0.001 | -0.027 (-0.048; -0.007) | 0.010 |
| Temporal lobe | -0.026 (-0.049; -0.003) | 0.025 | -0.045 (-0.067; -0.022) | <0.001 | -0.029 (-0.051; -0.007) | 0.011 |
| Parietal lobe | -0.007 (-0.034; 0.020) | 0.604 | -0.047 (-0.073; -0.020) | <0.001 | -0.032 (-0.059; -0.006) | 0.014 |
| Occipital lobe | -0.043 (-0.071; -0.015) | 0.003 | -0.081 (-0.108; -0.053) | <0.001 | -0.044 (-0.071; -0.017) | 0.002 |
| Frontal lobe | -0.024 (-0.048; -0.001) | 0.040 | -0.014 (-0.037; 0.009) | 0.237 | -0.006 (-0.029; 0.016) | 0.599 |
| White matter volume | | | | | | |
| Total volume | -0.034 (-0.056; -0.012) | 0.002 | -0.049 (-0.071; -0.027) | <0.001 | -0.033 (-0.054; -0.011) | 0.003 |
| Temporal lobe | -0.043 (-0.067; -0.019) | <0.001 | -0.061 (-0.084; -0.037) | <0.001 | -0.038 (-0.062; -0.015) | 0.001 |
| Parietal lobe | -0.022 (-0.047; 0.003) | 0.078 | -0.056 (-0.080; -0.031) | <0.001 | -0.045 (-0.069; -0.021) | <0.001 |
| Occipital lobe | -0.039 (-0.067; -0.011) | 0.006 | -0.080 (-0.107; -0.052) | <0.001 | -0.057 (-0.084; -0.030) | <0.001 |
| Frontal lobe | -0.035 (-0.059; -0.010) | 0.005 | -0.027 (-0.051; -0.002) | 0.031 | -0.016 (-0.040; 0.008) | 0.183 |

Values represent mean difference in z-score of grey or white matter volume (95% confidence interval) per standard deviation decrease in retinal layer thickness. Values are adjusted for age, sex, subcohort, education, axial length of the eye, intracranial volume, grey matter or white matter volume (if applicable), mean arterial blood pressure, blood pressure lowering medication, body mass index, total cholesterol, diabetes mellitus, and smoking.

**Table 3. Association of retinal layer thicknesses with focal measures.**

| | Cerebral microbleeds, n = 351 | P-value | Lacunar infarcts, n = 145 | P-value |
|---|---|---|---|---|
| Retinal nerve fiber layer | 1.02 (0.90-1.15) | 0.745 | 1.11 (0.94-1.31) | 0.212 |
| Ganglion cell layer | 0.95 (0.84-1.07) | 0.426 | 1.16 (0.98-1.38) | 0.089 |
| Inner plexiform layer | 0.90 (0.80-1.02) | 0.095 | 1.17 (0.98-1.42) | 0.095 |

Values represent odds ratio (95% confidence interval) per standard deviation decrease in retinal layer thickness adjusted for age, sex, subcohort, education, axial length of the eye, intracranial volume, white matter lesion volume, cerebral microbleeds and lacunar infarcts (if applicable).

**Supplemental Table 1. Age-stratified associations of retinal sublayer thicknesses with volumetric and microstructural brain measures.**

| Age in tertiles | Retinal nerve fiber layer | P-value | Ganglion cell layer | P-value | Inner plexiform layer | P-value |
|---|---|---|---|---|---|---|
| 1st tertile, n = 718 | | | | | | |
| Brain volume | -0.030 (-0.059; -0.001) | 0.046 | -0.017 (-0.043; 0.008) | 0.173 | -0.007 (-0.031; 0.017) | 0.561 |
| Grey Matter | -0.053 (-0.097; -0.008) | 0.020 | -0.016 (-0.055; 0.022) | 0.403 | -0.004 (-0.040; 0.032) | 0.838 |
| White matter | -0.028 (-0.071; 0.016) | 0.210 | -0.027 (-0.065; 0.010) | 0.152 | -0.013 (-0.048; 0.022) | 0.467 |
| FA | -0.065 (-0.151; 0.020) | 0.132 | -0.052 (-0.125; 0.021) | 0.161 | -0.025 (-0.095; 0.045) | 0.490 |
| MD | 0.032 (-0.026; 0.090) | 0.273 | 0.023 (-0.027; 0.073) | 0.363 | 0.005 (-0.043; 0.053) | 0.847 |
| Hippocampus | -0.049 (-0.121; 0.022) | 0.176 | -0.046 (-0.107; 0.016) | 0.144 | -0.044 (-0.102; 0.013) | 0.133 |
| 2nd tertile, n = 737 | | | | | | |
| Brain volume | -0.004 (-0.028; 0.021) | 0.765 | -0.038 (-0.062; -0.013) | 0.002 | -0.025 (-0.049; -0.002) | 0.034 |
| Grey Matter | -0.023 (-0.058; 0.011) | 0.187 | -0.055 (-0.089; -0.021) | 0.002 | -0.021 (-0.055; 0.012) | 0.208 |
| White matter | 0.006 (-0.032; 0.044) | 0.753 | -0.046 (-0.084; -0.008) | 0.017 | -0.040 (-0.076; -0.004) | 0.031 |
| FA | -0.037 (-0.110; 0.037) | 0.324 | -0.109 (-0.180; -0.036) | 0.003 | -0.008 (-0.078; 0.061) | 0.816 |
| MD | 0.012 (-0.046; 0.070) | 0.693 | 0.055 (0.002; 0.113) | 0.058 | -0.001 (-0.055; 0.054) | 0.983 |
| Hippocampus | -0.016 (-0.076; 0.045) | 0.610 | -0.055 (-0.115; 0.005) | 0.071 | -0.050 (-0.107; 0.008) | 0.091 |
| 3rd tertile, n = 669 | | | | | | |
| Brain volume | -0.025 (-0.048; -0.003) | 0.027 | -0.035 (-0.058; -0.011) | 0.004 | -0.029 (-0.054; -0.005) | 0.020 |
| Grey Matter | -0.022 (-0.056; 0.012) | 0.207 | -0.048 (-0.083; -0.012) | 0.008 | -0.045 (-0.082; -0.007) | 0.019 |
| White matter | -0.042 (-0.077; -0.007) | 0.017 | -0.047 (-0.084; -0.011) | 0.011 | -0.037 (-0.075; 0.001) | 0.058 |
| FA | -0.087 (-0.163; -0.011) | 0.025 | -0.057 (-0.138; 0.023) | 0.161 | -0.049 (-0.131; 0.034) | 0.245 |
| MD | 0.035 (-0.027; 0.097) | 0.266 | 0.033 (-0.032; 0.097) | 0.315 | 0.055 (-0.012; 0.121) | 0.109 |
| Hippocampus | -0.014 (-0.073; 0.044) | 0.624 | -0.003 (-0.064; 0.057) | 0.910 | -0.011 (-0.053; 0.007) | 0.736 |

Abbreviations: FA, fractional anisotropy; MD, mean diffusivity.

Values are adjusted mean difference in z-score per standard deviation decrease in retinal sublayer thickness. Minimum to maximum (mean) age was 47 to 61 years (55.4) for the first tertile, 62 to 72 years (68.6) for the second tertile, 73 to 96 years (77.7) for the third tertile. P-value for interaction between age and the retinal sublayer thicknesses was not significant ($p > 0.05$).

## DISCUSSION

In this population-based cohort study, we found that markers of retinal neurodegeneration assessed on OCT were associated with smaller brain volumes including hippocampal volume, and with worse white matter microstructure, whereas no association was found with white matter lesion volume, cerebral microbleeds and lacunar infarcts. As both neurodegeneration and vascular pathology in the brain often occur simultaneously, our current findings suggest that retinal OCT may provide information specifically on neurodegeneration in the brain.

Initial studies by Hinton et al.[12] and Blanks et al.[28] using postmortem specimen showed that patients with Alzheimer's disease had substantial loss of retinal ganglion cells and reduction in RNFL thickness compared to controls. However, inferences from these initial studies were difficult to draw due to small sample sizes and inclusion of highly selected individuals on whom postmortem tissues were obtained. Others have since then established this putative link in clinical settings by using in vivo optical imaging techniques. Findings from those patient-based studies have repeatedly shown that patients with Alzheimer's disease or cognitive impairment have reduced RNFL and GC-IPL complex thickness compared to controls.[10, 11, 29]

Given that cerebral atrophy is a crucial substrate for cognitive impairment in dementia, we have now shown in a population-based setting that thinner RNFL, GCL and IPL are associated with smaller grey matter, white matter and hippocampal volume. Our findings suggest that neuronal damage may occur simultaneously in the retina and throughout the brain. In addition, this neuronal damage in the retina and brain may already be present in a subclinical period, during which there are no symptoms. In line with our findings, one study (n = 164) found that thinner RNFL was associated with smaller grey matter volume only in the temporal lobe, whereas thinner GC-IPL complex was associated with smaller grey matter and white matter volumes in the temporal lobe, and with smaller grey matter volume in the occipital lobe.[14] More recently, another study (n = 79) found thinner RNFL and GCL to be related to medial temporal lobe atrophy, demonstrating the concurrent relation of the retina with Alzheimer's disease related brain structures.[30]

By extension, we have further shown that thinner RNFL and GCL were associated with worse white matter microstructure. Measures of DT-MRI provide additional information about the white matter microstructure beyond macrostructural assessment of white matter on MRI. Given that in patients with Alzheimer's disease, structural abnormalities of the white matter is present throughout the entire brain, our findings suggest that thinner RNFL and GCL may even reflect subtle changes in the white matter that are visually not detectable.

Interestingly, in our study, we have also found that thinner RNFL and GCL were associated with smaller hippocampal volume. Given that hippocampus atrophy is one of the characteristic features of Alzheimer's disease, these findings emphasize the involvement of

the retina in the pathogenesis of Alzheimer's disease. Moreover, together with our findings that thinner RNFL and GCL were associated with occipital lobe atrophy, these findings may also provide a basis for mechanisms underlying specific visual symptoms in patients with Alzheimer's disease such as reduced performance on vision, motion perception, or visual memory. Finally, we did not find a relation between retinal layer thickness and white matter lesion volume, cerebral microbleeds and lacunar infarcts, suggesting that thinner retinal layers reflect more neurodegenerative processes in the brain than vascular processes. Although white matter has been widely recognized for its susceptibility for vascular damage, it should be noted that the white matter, but more importantly the white matter microstructure, is very sensitive to other factors as well. For instance, inflammation, healthy aging, and neurodegeneration might also affect the white matter. In our study, adjusting for cardiovascular vascular risk factors and grey matter volume attenuated the associations indicating that cardiovascular risk factors and grey matter volume indeed have an effect on the association between retinal layer thickness and white matter volume. Yet, the associations remained significant indicating that other processes such as healthy aging or neurodegeneration are more likely to play a role. With regard to healthy aging, although we observed that increased age was associated with thinner retinal layers, the association of these layers with brain MRI markers remained after adjusting for and stratifying by age. Within strata of age, we did not find strong evidence for an aging effect in the association of retinal layer thickness with brain MRI markers. Although the associations were in general stronger in elderly people, indicating some aging effect, the interaction terms were not significant. Moreover, for some associations, the magnitude of the effect estimates varied across the strata, with stronger associations among younger people. These findings suggest that aging plays an important, but limited role in the association of retinal layer thickness with brain MRI markers.

With regard to the pathophysiology of our findings, it is possible that region-specific or global brain atrophy leads to retinal neurodegeneration. For instance, damage to brain regions involved in visual processing may result in damage to or disruption of connections within the visual tract and thereby causing retrograde degeneration of the optic nerve.[31] Indeed, subjective visual complaints and symptoms have repeatedly been reported in persons with traumatic brain injury, implicating structural changes in retinal structures and the presence of axonal damage along the visual pathways.[32-35] In addition, findings from a recent mouse study showed thinner inner retina in mice with traumatic brain injury compared to control mice.[36] At the same time, existing evidence showed that in patients with Alzheimer's disease, the neuritic plaque density was the highest in the occipital lobes, and that these plaques were associated with the earliest symptoms of Alzheimer's disease, including vision problems.[37, 38] Altogether, findings from those studies suggest that certain abnormalities in the brain may manifest in the retina as thinner RNFL, GCL or IPL. On the other hand, it is also possible that ganglion cell apoptosis may cause anterograde degeneration, leading to thinner RNFL, and eventually resulting in smaller white matter and

grey matter volume particularly in brain regions covering the visual tract.[39] However, there is little evidence supporting this hypothesis.

As a final explanatory mechanism, a neurodegenerative process with common pathogenesis may cause structural loss of neurons both in the retina and brain. While aging has been recognized as the greatest risk factor for neurodegeneration, other important processes that may contribute concomitantly to neurodegeneration in the retina and brain include oxidative stress and protein misfolding.[40] Yet, whether damage to retinal and cerebral structures occur simultaneously from the same systemic disease or occur after damage to the other, needs to be further explored in future studies. Given that the GCL is composed of neuronal cell bodies, and the RNFL of axons, it has been thought that the retinal layers may reflect the condition of their cerebral counterpart (e.g. GCL reflects the grey matter, and RNFL reflects the white matter). However, the fact that RNFL and GCL were associated with both the grey and white matter volumes, implicates that that notion is less likely to be the case. Of note, given that our study included relatively healthy persons, inferences about the underlying neurodegenerative disease should be drawn carefully.

The results of our study should be interpreted in light of several limitations. First, the cross-sectional design of our study limits us to draw conclusions about temporality and causality. Second, persons excluded from our study had an eye or brain disease, resulting in selection of relatively healthy persons in our analysis, which might have caused underestimation of the effect sizes. Finally, we did not use other retinal layer thickness, because the reliability of the segmentation for deeper layers were poor and their thickness measurements were not comparable across the two OCT devices. Strengths of our study include the population-based setting, large sample size, and the quantitative assessment of retinal layer thickness on OCT and different brain structures on (DT-)MRI.

In conclusion, we found that in a community-dwelling elderly population free of dementia and mild cognitive impairment, markers of retinal neurodegeneration were associated with smaller brain volumes, and with worse white matter microstructure. Our findings suggest that retinal OCT may provide information on atrophy in the brain, and that neuronal damage may occur simultaneously in the retina and throughout the brain.

## REFERENCES


1. Prince M, Bryce R, Albanese E, Wimo A, Ribeiro W, Ferri CP. The global prevalence of dementia: A systematic review and metaanalysis. Alzheimers Dement. 2013;9:63-75 e62
2. Shaw LM, Korecka M, Clark CM, Lee VM, Trojanowski JQ. Biomarkers of neurodegeneration for diagnosis and monitoring therapeutics. Nat Rev Drug Discov. 2007;6:295-303
3. Vemuri P, Jack CR, Jr. Role of structural mri in alzheimer's disease. Alzheimers Res Ther. 2010;2:23
4. Sluimer JD, van der Flier WM, Karas GB, Fox NC, Scheltens P, Barkhof F, et al. Whole-brain atrophy rate and cognitive decline: Longitudinal mr study of memory clinic patients. Radiology. 2008;248:590-598
5. Whitwell JL, Shiung MM, Przybelski SA, Weigand SD, Knopman DS, Boeve BF, et al. Mri patterns of atrophy associated with progression to ad in amnestic mild cognitive impairment. Neurology. 2008;70:512-520
6. Frisoni GB, Fox NC, Jack CR, Jr., Scheltens P, Thompson PM. The clinical use of structural mri in alzheimer disease. Nat Rev Neurol. 2010;6:67-77
7. Vernooij MW, Ikram MA, Vrooman HA, Wielopolski PA, Krestin GP, Hofman A, et al. White matter microstructural integrity and cognitive function in a general elderly population. Arch Gen Psychiatry. 2009;66:545-553
8. London A, Benhar I, Schwartz M. The retina as a window to the brain-from eye research to cns disorders. Nat Rev Neurol. 2013;9:44-53
9. Chang LY, Lowe J, Ardiles A, Lim J, Grey AC, Robertson K, et al. Alzheimer's disease in the human eye. Clinical tests that identify ocular and visual information processing deficit as biomarkers. Alzheimers Dement. 2014;10:251-261
10. Thomson KL, Yeo JM, Waddell B, Cameron JR, Pal S. A systematic review and meta-analysis of retinal nerve fiber layer change in dementia, using optical coherence tomography. Alzheimers Dement (Amst). 2015;1:136-143
11. Coppola G, Di Renzo A, Ziccardi L, Martelli F, Fadda A, Manni G, et al. Optical coherence tomography in alzheimer's disease: A meta-analysis. PLoS One. 2015;10:e0134750
12. Hinton DR, Sadun AA, Blanks JC, Miller CA. Optic-nerve degeneration in alzheimer's disease. N Engl J Med. 1986;315:485-487
13. Chiu K, Chan TF, Wu A, Leung IY, So KF, Chang RC. Neurodegeneration of the retina in mouse models of alzheimer's disease: What can we learn from the retina? Age (Dordr). 2012;34:633-649
14. Ong YT, Hilal S, Cheung CY, Venketasubramanian N, Niessen WJ, Vrooman H, et al. Retinal neurodegeneration on optical coherence tomography and cerebral atrophy. Neurosci Lett. 2015;584:12-16
15. Hofman A, Brusselle GG, Darwish Murad S, van Duijn CM, Franco OH, Goedegebure A, et al. The rotterdam study: 2016 objectives and design update. Eur J Epidemiol. 2015;30:661-708
16. Bos MJ, Koudstaal PJ, Hofman A, Ikram MA. Modifiable etiological factors and the burden of stroke from the rotterdam study: A population-based cohort study. PLoS Med. 2014;11:e1001634
17. Lee K, Buitendijk GH, Bogunovic H, Springelkamp H, Hofman A, Wahle A, et al. Automated segmentability index for layer segmentation of macular sd-oct images. Transl Vis Sci Technol. 2016;5:14
18. Keane PA, Grossi CM, Foster PJ, Yang Q, Reisman CA, Chan K, et al. Optical coherence tomography in the uk biobank study - rapid automated analysis of retinal thickness for large population-based studies. PLoS One. 2016;11:e0164095
19. Ikram MA, van der Lugt A, Niessen WJ, Koudstaal PJ, Krestin GP, Hofman A, et al. The rotterdam scan study: Design update 2016 and main findings. Eur J Epidemiol. 2015;30:1299-1315
20. Vrooman HA, Cocosco CA, van der Lijn F, Stokking R, Ikram MA, Vernooij MW, et al. Multi-spectral brain tissue segmentation using automatically trained k-nearest-neighbor classification. Neuroimage. 2007;37:71-81

21. Ikram MA, Vrooman HA, Vernooij MW, den Heijer T, Hofman A, Niessen WJ, et al. Brain tissue volumes in relation to cognitive function and risk of dementia. Neurobiol Aging. 2010;31:378-386
22. Bokde AL, Teipel SJ, Schwarz R, Leinsinger G, Buerger K, Moeller T, et al. Reliable manual segmentation of the frontal, parietal, temporal, and occipital lobes on magnetic resonance images of healthy subjects. Brain Res Brain Res Protoc. 2005;14:135-145
23. van der Lijn F, den Heijer T, Breteler MM, Niessen WJ. Hippocampus segmentation in mr images using atlas registration, voxel classification, and graph cuts. Neuroimage. 2008;43:708-720
24. de Groot M, Ikram MA, Akoudad S, Krestin GP, Hofman A, van der Lugt A, et al. Tract-specific white matter degeneration in aging: The rotterdam study. Alzheimers Dement. 2015;11:321-330
25. Vernooij MW, Ikram MA, Wielopolski PA, Krestin GP, Breteler MM, van der Lugt A. Cerebral microbleeds: Accelerated 3d t2*-weighted gre mr imaging versus conventional 2d t2*-weighted gre mr imaging for detection. Radiology. 2008;248:272-277
26. Hoogendam YY, Hofman A, van der Geest JN, van der Lugt A, Ikram MA. Patterns of cognitive function in aging: The rotterdam study. Eur J Epidemiol. 2014;29:133-140
27. de Bruijn RF, Akoudad S, Cremers LG, Hofman A, Niessen WJ, van der Lugt A, et al. Determinants, mri correlates, and prognosis of mild cognitive impairment: The rotterdam study. J Alzheimers Dis. 2014;42 Suppl 3:S239-249
28. Blanks JC, Hinton DR, Sadun AA, Miller CA. Retinal ganglion cell degeneration in alzheimer's disease. Brain Res. 1989;501:364-372
29. Cheung CY, Ong YT, Hilal S, Ikram MK, Low S, Ong YL, et al. Retinal ganglion cell analysis using high-definition optical coherence tomography in patients with mild cognitive impairment and alzheimer's disease. J Alzheimers Dis. 2015;45:45-56
30. Casaletto KB, Ward ME, Baker NS, Bettcher BM, Gelfand JM, Li Y, et al. Retinal thinning is uniquely associated with medial temporal lobe atrophy in neurologically normal older adults. Neurobiol Aging. 2017;51:141-147
31. Jindahra P, Petrie A, Plant GT. Retrograde trans-synaptic retinal ganglion cell loss identified by optical coherence tomography. Brain. 2009;132:628-634
32. Atkins EJ, Newman NJ, Biousse V. Post-traumatic visual loss. Rev Neurol Dis. 2008;5:73-81
33. Greenwald BD, Kapoor N, Singh AD. Visual impairments in the first year after traumatic brain injury. Brain Inj. 2012;26:1338-1359
34. Miyahara T, Kurimoto Y, Kurokawa T, Kuroda T, Yoshimura N. Alterations in retinal nerve fiber layer thickness following indirect traumatic optic neuropathy detected by nerve fiber analyzer, gdx-n. Am J Ophthalmol. 2003;136:361-364
35. Singman EL, Daphalapurkar N, White H, Nguyen TD, Panghat L, Chang J, et al. Indirect traumatic optic neuropathy. Mil Med Res. 2016;3:2
36. Tzekov R, Quezada A, Gautier M, Biggins D, Frances C, Mouzon B, et al. Repetitive mild traumatic brain injury causes optic nerve and retinal damage in a mouse model. J Neuropathol Exp Neurol. 2014;73:345-361
37. Tiraboschi P, Hansen LA, Thal LJ, Corey-Bloom J. The importance of neuritic plaques and tangles to the development and evolution of ad. Neurology. 2004;62:1984-1989
38. Arnold SE, Hyman BT, Flory J, Damasio AR, Van Hoesen GW. The topographical and neuroanatomical distribution of neurofibrillary tangles and neuritic plaques in the cerebral cortex of patients with alzheimer's disease. Cereb Cortex. 1991;1:103-116
39. Ohno-Matsui K. Parallel findings in age-related macular degeneration and alzheimer's disease. Prog Retin Eye Res. 2011;30:217-238
40. Wyss-Coray T. Ageing, neurodegeneration and brain rejuvenation. Nature. 2016;539:180-186

# Chapter 4.4
# Retinal Layer Thickness and Voxel-Based Morphometry of the Brain: the Rotterdam Study

Unal Mutlu, M. Kamran Ikram, Gennady V. Roshchupkin, Pieter W.M. Bonnemaijer, Johanna M. Colijn, Johannes R. Vingerling, Wiro J. Niessen, M. Arfan Ikram, Caroline C.W. Klaver, Meike W. Vernooij

**ABSTRACT**

**Background:** There is growing evidence that markers of retinal neurodegeneration such as thinner retinal nerve fiber layer (RNFL) and ganglion cell layer (GCL), assessed on optical coherence tomography (OCT), are reflective of global brain atrophy. Yet, little is known on the relation of these layers with specific brain regions. Using voxel-based analyses (VBA) of both cerebral grey matter density and white matter microstructure, we aimed to unravel which specific brain regions are associated with these retinal layers.
**Methods:** We included 2,235 persons (mean age: 67.3 years, 55% women) from the Rotterdam Study (2007–2012), who had gradable retinal OCT images and brain magnetic resonance imaging (MRI) scans, including diffusion tensor imaging. Thickness of peripapillary RNFL and perimacular GCL were measured on OCT images using an automated segmentation algorithm. Voxel-based morphometry protocols were applied to process MRI data. We investigated the association of thickness of retinal layers with voxel-wise grey matter density and white matter microstructure by performing linear regression models adjusting for age, sex, education, axial length of the eye, intracranial volume, and cardiovascular risk factors.
**Results:** We found that thinner RNFL and GCL were associated with lower grey matter density in the visual cortex, and with lower fractional anisotropy and higher mean diffusivity in white matter tracts of the optic radiation and of tracts coursing adjacent to the optic radiation. Furthermore, thinner GCL was associated with lower grey matter density of the thalamus, close to the presumed location of the lateral geniculate nucleus.
**Conclusions:** Thinner RNFL and GCL are associated with grey and white matter changes in the visual pathway suggesting that retinal thinning on OCT may be specifically associated with changes in the visual pathway rather than with global changes in the brain.

## INTRODUCTION

In search of identifying novel biomarkers for Alzheimer's disease, markers of retinal neurodegeneration are increasingly being recognized as potential candidates.[1-3] Markers of retinal neurodegeneration such as thinner retinal nerve fiber layer (RNFL) and ganglion cell layer (GCL) assessed on optical coherence tomography (OCT) have repeatedly been observed in Alzheimer's disease patients indicating that atrophy in the brain and the retina may occur concomitantly.[4, 5] Indeed, studies have shown that thinner RNFL and GCL were associated with global cerebral grey matter and white matter atrophy, even in non-demented individuals.[6-8] It has been suggested that the retina and the brain suffer from a shared underlying pathology such as a vascular disease or the accumulation of misfolded proteins, leading to concomitant atrophy. Yet, another possibility is that retinal thinning may be directly linked to changes in specific brain areas, most likely those that are anatomically connected and involved in visual processing. As previous studies have exclusively focused on global brain changes, we aim to unravel whether retinal thinning in non-diseased individuals reflects changes in specific brain regions. Voxel-based analysis (VBA) enables studying the relation between retinal layer thicknesses and brain tissues on the voxel level. Within a large population of non-demented aging people, we conducted a VBA to identify whether RNFL and GCL thickness are associated with local cerebral grey matter and white matter density.

## METHODS

### Study setting and population

This study was part of the Rotterdam Study (RS): a prospective population-based cohort study that investigates causes and consequences of chronic diseases in residents of the Ommoord district in the city Rotterdam, the Netherlands, aged 45 years or older.[9] The original cohort started in 1990 (n = 7,983), and was extended in 2000 (n = 3,011) and 2006 (n = 3,932). Follow-up examinations take place every three to four years. Participants were interviewed at home and examined at the research center. In 2007, spectral-domain OCT scanning was added to the protocol, and thus was performed in the fifth visit of the first cohort (RS-I-5), the third visit of the second cohort (RS-II-3), and at the baseline visit in about half of the third cohort (RS-III-1), see Figure 1. Since the introduction of OCT in the Rotterdam Study, a total of 5,065 persons were eligible for OCT-scanning, but 664 persons did not undergo OCT-scanning due to logistic reasons (e.g. lack of personnel, device maintenance or replacement) or personal reasons (e.g. sickness or unable to attend). A further 803 persons were excluded because OCT scans were ungradable due to motion artefacts, segmentation failures, missing data, or poor signal strength. We also excluded persons with dementia (n = 43), persons that did not undergo dementia screening (n = 21), and persons with a history of clinical stroke (n = 137). From the remaining 3,397 persons, 907 persons had no brain MRI scans (n = 799) or the scans were unusable (n = 108) for the following reasons: non-respondent or not visited the research center, refused or physical/mentally unable to attend, had MRI contra-indications, could not complete MRI scan, or poorly segmented scans. Subsequently, we only included persons if they had data on GCL thicknesses measured at the macular region, and RNFL thickness measured at the peripapillary region on the same eye (n = 2,340). Finally, we excluded persons with age-related macular degeneration (n = 10), glaucoma (n = 45), and hypertensive or diabetic retinopathy (n = 50), that could affect retinal thickness measurement. This resulted in 2,235 persons from which primarily the right eye (94%) was chosen for further analysis.
The Rotterdam Study has been approved by the Medical Ethics Committee of the Erasmus MC and by the Ministry of Health, Welfare and Sport of the Netherlands, implementing the Wet Bevolkingsonderzoek: ERGO (Population Studies Act: Rotterdam Study). All participants provided written informed consent to participate in the study and to obtain information from their treating physicians.

**Figure 1.** Flow diagram of the study population.

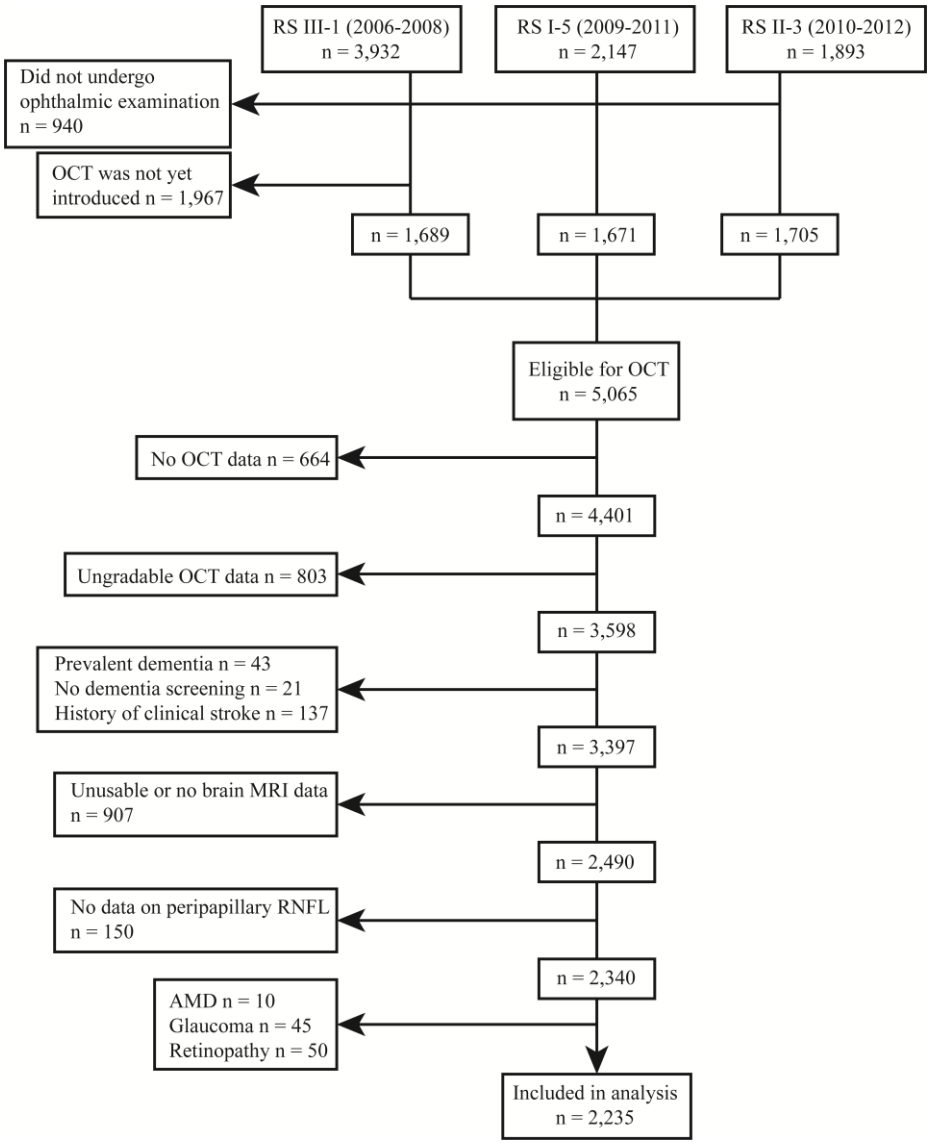


Abbreviations: RS, Rotterdam Study; OCT, optical coherence tomography; MRI, magnetic resonance imaging; RNFL, retinal nerve fiber layer; AMD, age-related macular degeneration.

**Spectral domain optical coherence tomography**

From September 2007 to June 2011 participants underwent a standard ophthalmic examination after pharmacological mydriasis, including fundus photography and OCT scanning of the macula and optic nerve. Initially, participants' eyes were scanned with the Topcon 3D OCT-1000 (n = 1,805; Topcon Optical Company, Tokyo, Japan). From August 2011 onwards, due to an update during the study, this device was replaced with the Topcon 3D OCT-2000 (n = 430). The macula and optic nerve head were scanned in the horizontal direction in an area of 6 × 6 × 1.68 mm with 512 × 512 × 480 voxels for OCT-1000 and in an area of 6 × 6 × 2.30 mm with 512 × 512 × 885 voxels for OCT-2000, enabling us to detect structures with a resolution of five µm (Figure 2). We measured the RNFL at the peripapillary region, and the GCL at the perimacular region as these layers are the thickest in those regions. Thickness of the peripapillary RNFL was measured automatically by Topcon's built-in segmentation algorithm. This was done in twelve peripapillary segments of $30^{o}$ each, and the average RNFL thickness was derived from the calculation circle. For the macula, volumes were segmented using Iowa Reference Algorithms 3.6, which has been validated for most widely available commercial OCT scanners (available from https://www.iibi.uiowa.edu/content/shared-software-download).[10] Thickness of the GCL was measured in nine regions of the Early Treatment Diabetic Retinopathy Study Grid. The average retinal layer thickness were calculated and used in further statistical analyses. Indices of quality control were used to preserve good quality images (high signal, low noise) and to exclude scans with segmentation errors. Scans included in our study had a segmentability index of more than 30%, an undefined region of less than 20%, and a quality factor of more than 30, as explained previously.[7, 11-13]

**Brain image acquisition and processing**

Brain MRI scanning was performed on a 1.5 Tesla MRI scanner (GE Healthcare, Milwaukee, Wisconsin).[14] Scan protocol consisted of four high-resolution axial sequences: a 3D T1-weighted spoiled-gradient echo (slice thickness 1.6 mm, voxel size 1 $mm^3$, zero-padded to 0.8), a proton-density-weighted (slice thickness 1.6 mm), a fluid-attenuated inversion recovery (slice thickness 2.5 mm) and a 3D T2-weighted gradient-recalled echo sequence. For the diffusion tensor imaging (DTI) sequence, we performed a single-shot, diffusion-weighted, spin-echo, echo-planar imaging sequence with maximum b-value of 1,000 $s/mm^2$ in 25 non-collinear directions (slice thickness 3.5 mm). Using a k-nearest-neighbor classifier algorithm trained on manually segmented data acquired on the same scanner, we classified supratentorial voxels on T1 images into grey matter, white matter, and cerebrospinal fluid.[15] After quality control, persons with insufficient registration quality were excluded. Of the 2,235 persons with successfully segmented tissues, 39 did not have DTI sequences.

**Figure 2.** Output of the Topcon OCT-2000 device focusing on the macula (A) and optic nerve (B) with corresponding cross-sectional view of the retina (C and D, respectively) .

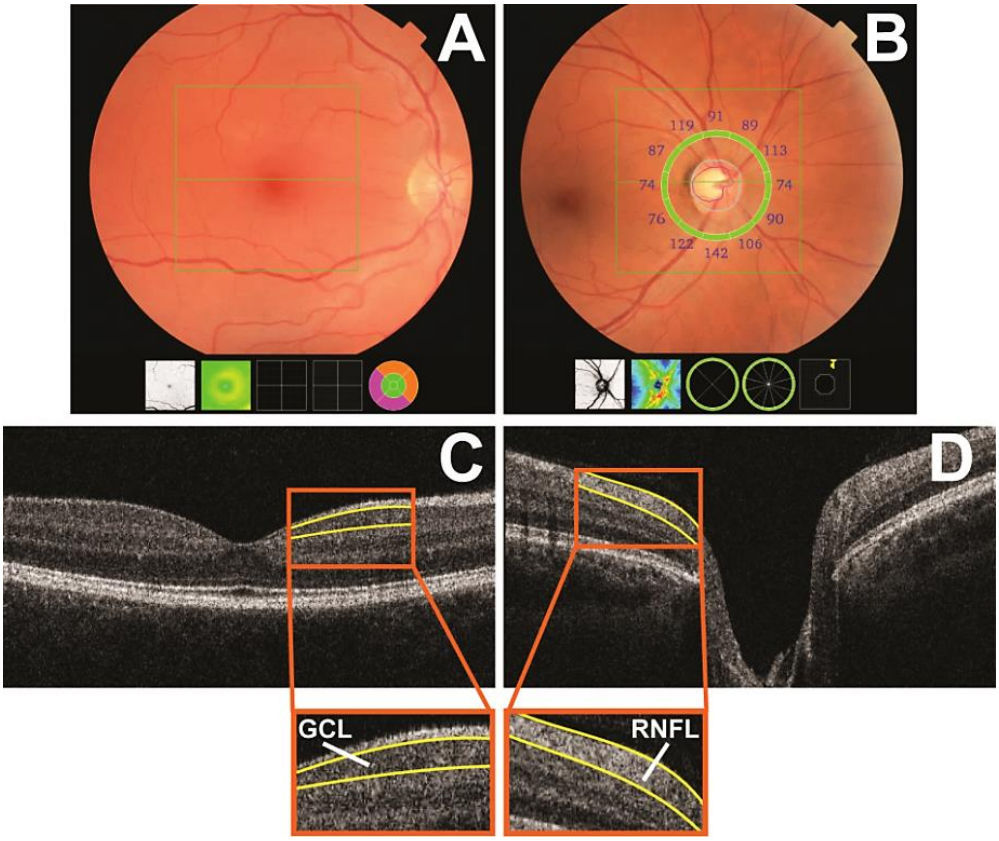


**Voxel-based analysis of grey matter**

Voxel-based analysis of the grey matter was performed with an optimized protocol using the FSL software,[16, 17] and as previously described.[18] Briefly, grey matter density maps derived from T1-weighted images were non-linearly registered to the International Consortium of Brain Mapping Montreal Neurological Institute 152 template. To preserve the grey matter volume, a spatial modulation procedure was applied, and voxel densities were multiplied by the Jacobian determinants of transformation field. Finally, images were smoothed using an isotropic Gaussian kernel of 3 mm (full width at half maximum 8 mm). Brain regions were segmented using atlas-based segmentation method based on the Hammer atlas.[19] The modulation step in the voxel-based morphometry pipeline preserves the volume of a particular tissue within a voxel. The multiplication of the voxel values in the segmented images by the Jacobian determinants derived from the spatial normalization step allows us to calculate volumes by aggregating voxels.

Given that the lateral geniculate nucleus is part of the visual pathway, we used the Oxford thalamic connectivity atlas to identify probability of anatomical connections from subthalamic regions.[20]

**Voxel-based analysis of white matter tracts**

We performed a VBA of DTI data according to the voxel-based morphometry method.[21] FSL software[16] was used for VBA data processing. All fractional anisotropy (FA) and mean diffusivity (MD) maps were non-linearly registered to the standard FA template from the FSL package with a $1 \times 1 \times 1$ $mm^3$ voxel resolution. Additionally, to assess location of associations and to compare VBA results with global DTI measures, the Rotterdam Study tract template that was used for analyzing the DTI measures per tract, was mapped to the Montreal Neurological Institute space. Participants' specific tract segmentation masks were registered to Montreal Neurological Institute template in the same way as FA and MD maps and then merged to one tract probability atlas image.[22] We used a 10% probability cutoff to define tract boundaries. In general, FA is lower and MD is higher in older and damaged brains, which is thought to reflect worse white matter microstructure. Because the Rotterdam Study tract atlas did not contain segmentation of the optic radiation, we used the Jülich histological atlas to assess changes in the optic radiation.[23] A representative tractogram of the visual pathway has been shown previously.[24]

**Covariates**

The axial length of eyes was measured using Lenstar LS900 (Haag-Streit AG, Köniz, Switzerland). Blood pressure was measured twice in sitting position at the right brachial artery with a random-zero sphygmomanometer, and the average of two readings was used for analysis. Body mass index was computed as weight (kg) divided by height squared ($m^2$). Fasting serum total and high-density lipoprotein cholesterol concentrations were determined by an automated enzymatic procedure. Diabetes mellitus was considered present if fasting serum glucose level was equal to or greater than 7.0 mmol/L, or when persons reported use of antidiabetic medication. Information on smoking (non, former, or current), and blood pressure lowering medication use was obtained during the home interview by a computerized questionnaire.

**Statistical analysis**

As eyes were scanned with two different devices and in order to standardize the measurements, we calculated z-scores for the OCT measurements of each device. We investigated the association of retinal layer thickness (per SD increase) with neuroimaging outcomes using linear regression models adjusted for age, sex, education, subcohort, axial length of the eyes, intracranial volume, and for the following cardiovascular risk factors: systolic blood pressure, diastolic blood pressure, use of blood pressure lowering medication, body mass index, total cholesterol, high-density lipoprotein cholesterol,

diabetes mellitus, and smoking. Missing data on covariates were handled using fivefold multiple imputations based on determinant, outcome, and included covariates. Since the voxels are correlated, the actual number of independent tests was calculated using 10,000 permutations. For $\alpha = 0.05$ and corrected by number of tested models, this yielded a p-value threshold for statistical significance of $9.97*10^{-8}$ for the VBA of grey matter, $1.97*10^{-8}$ for the VBA of fractional anisotropy, and $2.16*10^{-8}$ for the VBA of mean diffusivity.

**RESULTS**

Table 1 shows the characteristics of the study population. Mean age at time of OCT scanning was 67.3 years (SD: 9.7), and 55% of the participants were women.
Figures 3 and 4 show the projection of voxel-based grey matter areas and white matter tracts on axial coupes associated with RNFL and GCL, respectively. We found that mainly thinner RNFL and to a lesser extent thinner GCL was associated with lower grey matter density of the occipital lobe, in the area of the calcarine sulcus. In addition, thinner GCL was associated with lower grey matter density of the thalamus. Furthermore, we found that both thinner RNFL and GCL were associated with lower fractional anisotropy and higher mean diffusivity in white-matter tracts that are part of the optic radiation as well as in major neighboring tracts such as the inferior longitudinal fasciculus and inferior fronto-occipital fasciculus.
Table 2 shows the grey matter regions from voxel-based analysis that were significantly associated with RNFL and GCL. All grey matter regions associated with thinner RNFL and GCL belong to the visual cortex, except for the lingual gyrus and thalamus. Furthermore, comparing RNFL with GCL, the number of significant voxels were higher and the lowest p-values were smaller for associations with RNFL. All significant voxels showed a positive association, i.e. with an increase in retinal layer thickness, the voxel-wise grey matter density was also increasing. We used the Oxford thalamic connectivity atlas to identify probability of anatomical connections from subthalamic regions that were associated with the retinal layers. This showed that the associated thalamic structures had their connections to the posterior parietal cortex and occipital cortex with probabilities up to 0.84.
Tables 3 and 4 show for fractional anisotropy and mean diffusivity, respectively, the white matter tract voxels that were significantly associated with RNFL and GCL. In general, comparing RNFL with GCL, the number of significant voxels was lower and the lowest p-values were larger for associations with RNFL. All significant voxels for the fractional anisotropy showed a positive association, whereas the significant voxels for the mean diffusivity showed a negative association, as expected. These tables together with the figures show us that even within specific tracts, certain parts are more strongly associated. For instance, the inferior fronto-occipital fasciculus passes along the frontal lobe, but the figures show us that only the posterior part is associated with RNFL and GCL. Finally, we found that particularly the GCL was associated with the corpus callosum.

**Table 1. Characteristics of the study population.**

| Characteristic | Descriptive |
|---|---|
| N | 2,235 |
| Age, years | 67.3 (9.7) |
| Female sex | 1,235 (55) |
| Systolic blood pressure, mmHg | 144.2 (21.7) |
| Diastolic blood pressure, mmHg | 84.7 (10.8) |
| Blood pressure lowering medication | 881 (39) |
| Body mass index, kg/m$^2$ | 27.3 (3.9) |
| Diabetes mellitus | 231 (10) |
| Total cholesterol, mmol/L | 5.5 (1.1) |
| High-density lipoprotein cholesterol, mmol/L | 1.5 (0.4) |
| Smoking status | |
| Never smoker | 715 (32) |
| Past smoker | 1,171 (52) |
| Current smoker | 349 (16) |
| Education | |
| Lower education | 632 (28) |
| Intermediate education | 1,088 (49) |
| Higher education | 515 (23) |
| Right eyes | 2,100 (94) |
| Axial length, mm | 23.5 (1.1) |
| Retinal nerve fiber layer optic nerve, µm | 96.1 (14.3) |
| Ganglion cell layer macula, µm | 33.9 (5.2) |
| Inner plexiform layer macula, µm | 37.0 (3.3) |

Values are presented as means (standard deviation) or as numbers (percentage).

**Figure 3.** Areas of grey matter (GM) density and white matter microstructure from voxel-based analysis that were significantly associated with retinal nerve fiber layer thickness. Colors correspond to t-values and reflect the direction of the associations from regression models: red for a positive association (increase of GM, fractional anisotropy (FA), or mean diffusivity (MD)), blue for a negative association (decrease of GM, FA, or MD) per SD increase of retinal nerve fiber layer thickness.

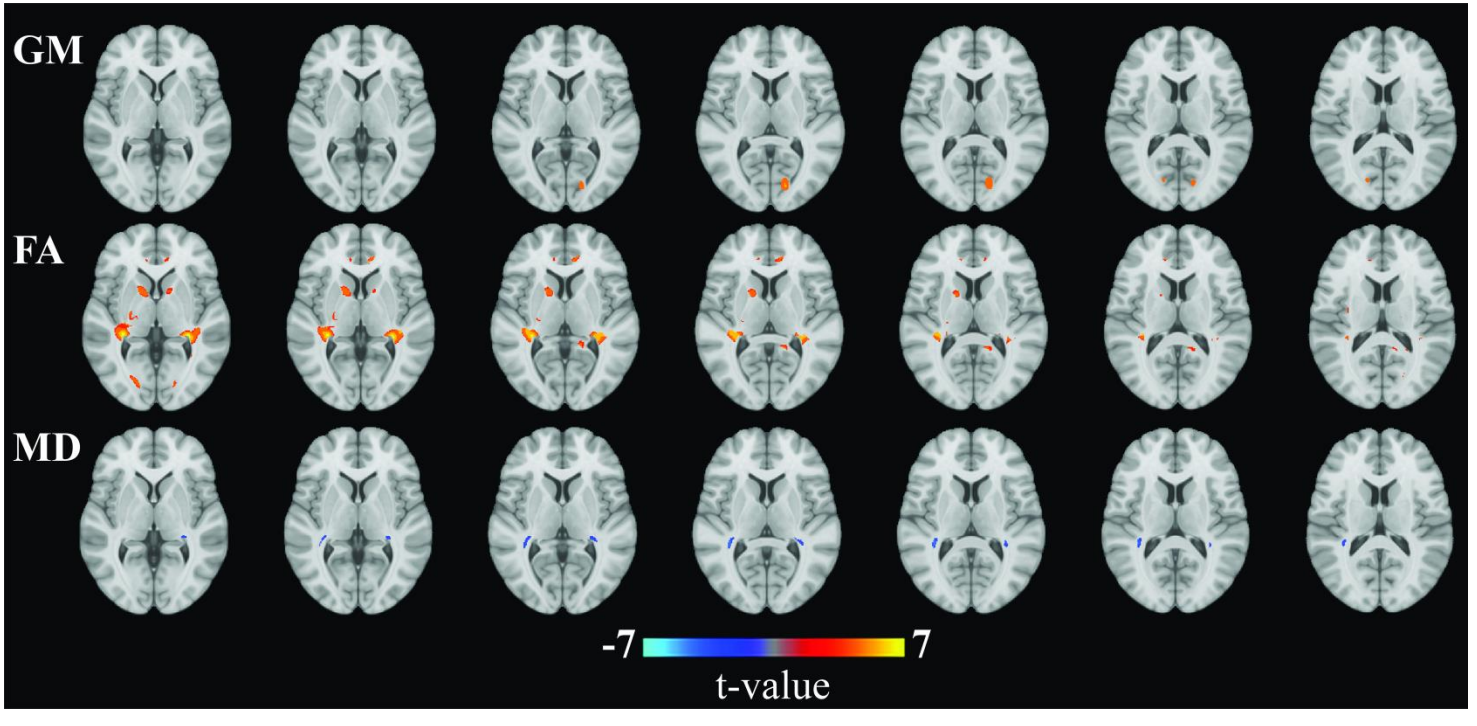

**Figure 4.** Areas of grey matter (GM) density and white matter microstructure from voxel-based analysis that were significantly associated with ganglion cell layer thickness. Colors correspond to t-values and reflect the direction of the associations from regression models: red for a positive association (increase of GM, fractional anisotropy (FA), or mean diffusivity (MD)), blue for a negative association (decrease of GM, FA, or MD) per SD increase of ganglion cell layer thickness.

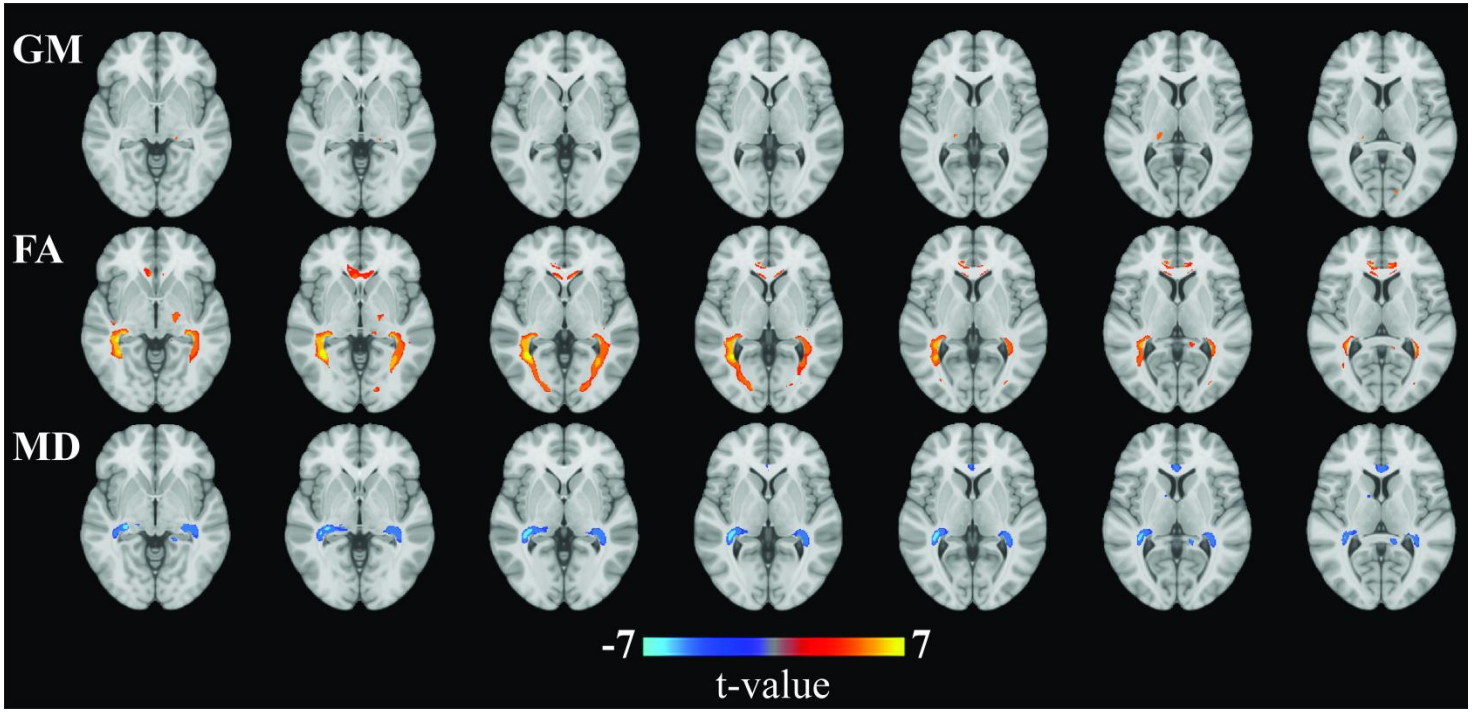

**Table 2. Retinal layer thickness associated with voxel-based grey matter areas.**

| | Retinal nerve fiber layer | | | Ganglion cell layer | |
|---|---|---|---|---|---|
| | **Number of voxels** | **Lowest p-value** | **Number of significant voxels** | **Lowest p-value** | **Number of significant voxels** |
| Cuneus left | 14454 | $1.2*10^{-10}$ | 307 | $9.2*10^{-9}$ | 84 |
| Cuneus right | 13755 | $4.3*10^{-9}$ | 131 | $9.4*10^{-7}$ | 0 |
| LROOL left | 64895 | $1.7*10^{-10}$ | 189 | $2.1*10^{-8}$ | 18 |
| LROOL right | 66957 | $5.8*10^{-8}$ | 9 | $5.3*10^{-6}$ | 0 |
| Lingual gyrus left | 18132 | $1.3*10^{-10}$ | 143 | $1.6*10^{-8}$ | 31 |
| Lingual gyrus right | 18495 | $1.3*10^{-8}$ | 33 | $6.3*10^{-7}$ | 0 |
| Thalamus left | 10524 | $7.9*10^{-8}$ | 2 | $8.5*10^{-9}$ | 101 |
| Thalamus right | 10429 | $3.5*10^{-7}$ | 0 | $3.2*10^{-9}$ | 249 |

Table shows the grey matter regions from voxel-based analysis that were significantly associated with retinal nerve fiber layer and ganglion cell layer.
Numbers indicate total number of voxels within a region, the lowest p-value observed in that region, and the number of voxels that had a p-value lower than the p-value threshold for significance: $9.97*10^{-8}$.
Abbreviation: LROOL, lateral remainder of occipital lobe.

**Table 3. Fractional anisotropy of white matter tracts from voxel-based analysis.**

| | | Retinal nerve fiber layer | | Ganglion cell layer | |
|---|---|---|---|---|---|
| | **Number of voxels** | **Lowest p-value** | **Number of significant voxels** | **Lowest p-value** | **Number of significant voxels** |
| ATR left | 14618 | $4.2*10^{-16}$ | 628 | $3.1*10^{-10}$ | 17 |
| ATR right | 15241 | $1.7*10^{-12}$ | 808 | $1.0*10^{-09}$ | 12 |
| CGC left | 4183 | $6.6*10^{-11}$ | 204 | $3.7*10^{-13}$ | 789 |
| CGC right | 3903 | $1.2*10^{-10}$ | 67 | $4.3*10^{-12}$ | 692 |
| CGH left | 2485 | $2.2*10^{-11}$ | 56 | $3.9*10^{-09}$ | 5 |
| CGH right | 2336 | $2.2*10^{-09}$ | 46 | $5.8*10^{-08}$ | 0 |
| CST left | 18423 | $1.4*10^{-20}$ | 260 | $2.7*10^{-21}$ | 597 |
| CST right | 18322 | $6.0*10^{-23}$ | 1249 | $1.9*10^{-21}$ | 278 |
| FMA | 19451 | $1.3*10^{-12}$ | 300 | $6.5*10^{-11}$ | 254 |
| FMI | 11974 | $6.4*10^{-11}$ | 80 | $6.4*10^{-12}$ | 1197 |
| Fornix right | 2870 | $7.6*10^{-06}$ | 0 | $2.4*10^{-09}$ | 4 |
| IFO left | 15152 | $1.4*10^{-15}$ | 1687 | $1.7*10^{-15}$ | 2324 |
| IFO right | 15706 | $3.6*10^{-14}$ | 2002 | $2.2*10^{-19}$ | 3218 |
| ILF left | 16422 | $1.4*10^{-15}$ | 2047 | $1.7*10^{-15}$ | 2462 |
| ILF right | 17938 | $7.1*10^{-15}$ | 2869 | $2.2*10^{-19}$ | 3655 |
| ML left | 4846 | $1.5*10^{-09}$ | 17 | $3.0*10^{-12}$ | 85 |
| ML right | 4552 | $3.4*10^{-10}$ | 32 | $2.1*10^{-10}$ | 10 |
| *Optic radiation, left | 51440 | $4.7*10^{-17}$ | 2509 | $5.9*10^{-17}$ | 2953 |
| *Optic radiation, right | 48435 | $5.7*10^{-18}$ | 3186 | $3.2*10^{-19}$ | 3485 |
| PTR left | 13000 | $4.7*10^{-17}$ | 2045 | $5.9*10^{-17}$ | 2818 |
| PTR right | 13943 | $4.3*10^{-18}$ | 2768 | $2.2*10^{-19}$ | 3736 |
| SLF left | 23378 | $6.1*10^{-10}$ | 114 | $6.1*10^{-09}$ | 21 |
| SLF right | 24206 | $7.8*10^{-11}$ | 204 | $4.9*10^{-09}$ | 6 |
| STR left | 14096 | $9.3*10^{-09}$ | 8 | $6.2*10^{-09}$ | 2 |
| STR right | 14096 | $1.5*10^{-11}$ | 159 | $4.0*10^{-08}$ | 0 |
| Uncinatus left | 5443 | $2.0*10^{-10}$ | 33 | $1.5*10^{-06}$ | 0 |
| ‡Corpus callosum | 30572 | $2.1*10^{-10}$ | 288 | $6.6*10^{-12}$ | 4583 |

Table shows the white matter tracts from voxel-based analysis that were significantly associated with retinal nerve fiber layer and ganglion cell layer.

Numbers indicate total number of voxels within a tract, the lowest p-value observed in that tract, and the number of voxels that had a p-value lower than the p-value threshold for significance: $1.97*10^{-8}$.

Abbreviations: ATR, anterior thalamic radiation; CGC, cingulate gyrus part of cingulum; CGH, parahippocampal part of cingulum; CST, corticospinal tract; FMA, forceps major; FMI, forceps minor; IFO, inferior fronto-occipital fasciculus; ILF, inferior longitudinal fasciculus; ML, medial lemniscus; PTR, posterior thalamic radiation; SLF, superior longitudinal fasciculus; STR, superior thalamic radiation.

*based on Jülich histological atlas.

‡based on Hammer atlas.

**Table 4. Mean diffusivity of white matter tracts from voxel-based analysis.**

| | | Retinal nerve fiber layer | | Ganglion cell layer | |
|---|---|---|---|---|---|
| | Number of voxels | Lowest p-value | Number of significant voxels | Lowest p-value | Number of significant voxels |
| ATR right | 15241 | $4.0*10^{-07}$ | 0 | $6.9*10^{-9}$ | 37 |
| CGC left | 4183 | $5.4*10^{-07}$ | 0 | $4.1*10^{-09}$ | 11 |
| CGH left | 2485 | $1.2*10^{-06}$ | 0 | $4.5*10^{-11}$ | 275 |
| CST left | 18423 | $7.9*10^{-09}$ | 37 | $2.2*10^{-10}$ | 55 |
| CST right | 18322 | $2.6*10^{-08}$ | 0 | $1.5*10^{-12}$ | 60 |
| FMA | 19451 | $3.4*10^{-06}$ | 0 | $4.3*10^{-11}$ | 288 |
| FMI | 11974 | $2.4*10^{-05}$ | 0 | $5.2*10^{-12}$ | 631 |
| IFO left | 15152 | $1.6*10^{-09}$ | 256 | $1.4*10^{-11}$ | 981 |
| IFO right | 15706 | $7.1*10^{-10}$ | 158 | $2.6*10^{-14}$ | 810 |
| ILF left | 16422 | $1.6*10^{-09}$ | 233 | $1.4*10^{-11}$ | 899 |
| ILF right | 17938 | $7.1*10^{-10}$ | 281 | $2.6*10^{-14}$ | 903 |
| ML right | 4552 | $2.3*10^{-05}$ | 0 | $2.3*10^{-09}$ | 19 |
| *Optic radiation, left | 51440 | $1.7*10^{-10}$ | 666 | $4.3*10^{-15}$ | 1854 |
| *Optic radiation, right | 48435 | $7.1*10^{-10}$ | 287 | $5.2*10^{-15}$ | 1387 |
| PTR left | 13000 | $1.7*10^{-10}$ | 688 | $4.3*10^{-15}$ | 2012 |
| PTR right | 13943 | $7.1*10^{-10}$ | 273 | $5.2*10^{-15}$ | 2209 |
| SLF left | 23378 | $1.6*10^{-05}$ | 0 | $9.9*10^{-10}$ | 44 |
| ‡Corpus callosum | 30572 | $2.0*10^{-06}$ | 0 | $5.2*10^{-12}$ | 1614 |

Table shows the white matter tracts from voxel-based analysis that were significantly associated with retinal nerve fiber layer and ganglion cell layer.
Numbers indicate total number of voxels within a tract, the lowest p-value observed in that tract, and the number of voxels that had a p-value lower than the p-value threshold for significance: $2.16*10^{-8}$.
Abbreviations: ATR, anterior thalamic radiation; CGC, cingulate gyrus part of cingulum; CGH, parahippocampal part of cingulum; CST, corticospinal tract; FMA, forceps major; FMI, forceps minor; IFO, inferior fronto-occipital fasciculus; ILF, inferior longitudinal fasciculus; ML, medial lemniscus; PTR, posterior thalamic radiation; SLF, superior longitudinal fasciculus.
*based on Jülich histological atlas.
‡based on Hammer atlas.

## DISCUSSION

In this large population-based study of non-demented persons, we found that thinner retinal layers, i.e. RNFL and GCL, were significantly associated with lower grey matter density of the visual cortex and with worse white matter microstructure of the optic radiation and of the tracts coursing adjacent to the optic radiation.
Previous studies investigating the association of retinal thickness with brain MRI markers in non-demented individuals found that thinner RNFL and GCL were associated with cerebral grey matter and white matter atrophy.[6-8] In addition, we have previously demonstrated that both thinner RNFL and GCL were associated with worse brain white matter microstructure (lower fractional anisotropy and higher mean diffusivity) suggesting

that RNFL and GCL may even reflect subtle changes in the white matter that are visually not detectable.[7]

Extending upon findings from previous studies, we have now shown that thinner RNFL and GCL are associated with the grey matter density of the visual cortex, and with the microstructural integrity of white matter tracts of the optic radiation and of tracts coursing adjacent to the optic radiation. Furthermore, we found that the GCL is associated with the grey matter density of the thalamus, close to the presumed location of the lateral geniculate nucleus, a relay center for the visual pathway.[25] Also, we have shown that the RNFL and GCL are associated with the lingual gyrus, and the GCL with the corpus callosum. While these structures are not directly recognized as being part of the visual pathway, they are connected to the visual cortex and are involved in visual information processing.[26-29] Similarly, most white matter tracts that were found to be associated with RNFL and GCL are not directly recognized as being part of the optic radiation, but in fact, are shown to be neighboring tracts to the optic radiation with their projections to the visual cortex.[24] That these associations were more widespread for fractional anisotropy than mean diffusivity may demonstrate that there are fewer crossing fibers in those tracts, i.e. that these tracts are rather homogenous with a single fiber population.[30]

Our findings show that in relatively healthy persons, normal variations in structure of the retina and brain are linked, but more importantly these findings may provide new insights into mechanisms underlying aging.

A possible mechanism that may link the retina to the brain is that damage to the visual cortex may lead to retrograde degeneration down to the optic nerve and retinal layers. Our voxel-based analyses between retinal layers and brain tissue exclusively showed associations along the visual pathway, including the optic radiation, and the visual cortex. Although it may be that associations in other brain regions did not survive the threshold for statistical significance, these results do indicate that the relation seems more region-specific than widespread. Indeed, a growing body of evidence suggests that damage to the visual cortex by means of an infarction, atrophy, or lobectomy may lead to retinal neurodegeneration by causing degeneration of the axons and their accompanying myelin sheaths.[31-37] For instance, a study showed that a decrease of 1 mL in visual cortex volume relates to a reduction of 0.6 μm in RNFL thickness after 1 year.[31] Similarly, another study demonstrated a 9 μm reduction in RNFL thickness per log year following occipital lobe damage due to stroke.[32]

Conversely, ganglion cell apoptosis in the retina may lead to anterograde degeneration along the visual pathway, leading to thinner RNFL, and eventually resulting in atrophy of the visual cortex. As support of this, clinical studies have shown that optic nerve axotomy, or optic neuropathy due to intraocular hypertension, glaucoma or Leber's disease, may lead to changes in the lateral geniculate nucleus and visual cortex.[38-44] It should be noted that inferences from previous studies investigating retrograde or anterograde degeneration are difficult to draw due to inclusion of animals or diseased individuals (i.e. selection bias).

Moreover, those studies consisted of small sample sizes and adjustment for potential confounders was not always done. We have now investigated the retina-brain connection in a large sample of relatively healthy persons being able to take potential confounders into account. Nonetheless, findings from previous studies together with our findings indicate the existence of a direct association between thinning of retinal layers and structural changes in the visual pathway.

Yet, our findings also support another hypothesis, which is that the presence of a common underlying process may affect both the retina and the brain simultaneously. Findings from previous studies demonstrating an association between retinal layer thickness and global brain structures were suggestive of a more widespread underlying process, and would support this hypothesis.[7] For instance, in Alzheimer's disease pathology, vascular processes and the accumulation of misfolded proteins such as amyloid-beta and tau are well-known causes of Alzheimer's disease.[45] These processes could affect both the retina and the brain, and thus could be considered as shared factors. Although we lacked information on cerebral amyloid pathology, we tried to control for potential cardiovascular risk factors, which did not change the associations. This indicates that other processes may play a role between the association of thinner RNFL and GCL with lower grey and white matter densities.

Some limitations of our study merit attention. First, the cross-sectional design of our study limits us to draw conclusions about temporality and causality. Second, persons excluded from our study had an eye or brain disease, or had unusable OCT or MRI scans, resulting in a selection of relatively healthy persons in our analysis, which may have caused underestimation of the effect sizes. Strengths of our study include the population-based setting, large sample size, the assessment of retinal layers on OCT, the assessment of brain structures on MRI, and the extensive data on covariates.

In conclusion, in a population-based setting of non-demented individuals, we found that thinner RNFL and GCL were significantly associated with grey and white matter changes along the visual pathway, including the optic radiation and the visual cortex. Our findings suggest that thinner RNFL and GCL may reflect areas with lesser cell densities in the visual pathway rather than reflecting lesser cell densities throughout the global brain. Longitudinal research is needed to assess temporality and direction of this association.

## REFERENCES


1. Lim JK, Li QX, He Z, Vingrys AJ, Wong VH, Currier N, et al. The eye as a biomarker for alzheimer's disease. Front Neurosci. 2016;10:536
2. Javaid FZ, Brenton J, Guo L, Cordeiro MF. Visual and ocular manifestations of alzheimer's disease and their use as biomarkers for diagnosis and progression. Front Neurol. 2016;7:55
3. Frost S, Martins RN, Kanagasingam Y. Ocular biomarkers for early detection of alzheimer's disease. J Alzheimers Dis. 2010;22:1-16
4. Thomson KL, Yeo JM, Waddell B, Cameron JR, Pal S. A systematic review and meta-analysis of retinal nerve fiber layer change in dementia, using optical coherence tomography. Alzheimers Dement (Amst). 2015;1:136-143
5. Coppola G, Di Renzo A, Ziccardi L, Martelli F, Fadda A, Manni G, et al. Optical coherence tomography in alzheimer's disease: A meta-analysis. PLoS One. 2015;10:e0134750
6. Ong YT, Hilal S, Cheung CY, Venketasubramanian N, Niessen WJ, Vrooman H, et al. Retinal neurodegeneration on optical coherence tomography and cerebral atrophy. Neurosci Lett. 2015;584:12-16
7. Mutlu U, Bonnemaijer PWM, Ikram MA, Colijn JM, Cremers LGM, Buitendijk GHS, et al. Retinal neurodegeneration and brain mri markers: The rotterdam study. Neurobiol Aging. 2017;60:183-191
8. Casaletto KB, Ward ME, Baker NS, Bettcher BM, Gelfand JM, Li Y, et al. Retinal thinning is uniquely associated with medial temporal lobe atrophy in neurologically normal older adults. Neurobiol Aging. 2017;51:141-147
9. Hofman A, Brusselle GG, Darwish Murad S, van Duijn CM, Franco OH, Goedegebure A, et al. The rotterdam study: 2016 objectives and design update. Eur J Epidemiol. 2015;30:661-708
10. Terry L, Cassels N, Lu K, Acton JH, Margrain TH, North RV, et al. Automated retinal layer segmentation using spectral domain optical coherence tomography: Evaluation of inter-session repeatability and agreement between devices. PLoS One. 2016;11:e0162001
11. Keane PA, Grossi CM, Foster PJ, Yang Q, Reisman CA, Chan K, et al. Optical coherence tomography in the uk biobank study - rapid automated analysis of retinal thickness for large population-based studies. PLoS One. 2016;11:e0164095
12. Lee K, Buitendijk GH, Bogunovic H, Springelkamp H, Hofman A, Wahle A, et al. Automated segmentability index for layer segmentation of macular sd-oct images. Transl Vis Sci Technol. 2016;5:14
13. Patel PJ, Foster PJ, Grossi CM, Keane PA, Ko F, Lotery A, et al. Spectral-domain optical coherence tomography imaging in 67 321 adults: Associations with macular thickness in the uk biobank study. Ophthalmology. 2016;123:829-840
14. Ikram MA, van der Lugt A, Niessen WJ, Koudstaal PJ, Krestin GP, Hofman A, et al. The rotterdam scan study: Design update 2016 and main findings. Eur J Epidemiol. 2015;30:1299-1315
15. Vrooman HA, Cocosco CA, van der Lijn F, Stokking R, Ikram MA, Vernooij MW, et al. Multi-spectral brain tissue segmentation using automatically trained k-nearest-neighbor classification. Neuroimage. 2007;37:71-81
16. Smith SM, Jenkinson M, Woolrich MW, Beckmann CF, Behrens TE, Johansen-Berg H, et al. Advances in functional and structural mr image analysis and implementation as fsl. Neuroimage. 2004;23 Suppl 1:S208-219
17. Good CD, Johnsrude IS, Ashburner J, Henson RN, Friston KJ, Frackowiak RS. A voxel-based morphometric study of ageing in 465 normal adult human brains. Neuroimage. 2001;14:21-36
18. Roshchupkin GV, Adams HH, van der Lee SJ, Vernooij MW, van Duijn CM, Uitterlinden AG, et al. Fine-mapping the effects of alzheimer's disease risk loci on brain morphology. Neurobiol Aging. 2016;48:204-211
19. Hammers A, Allom R, Koepp MJ, Free SL, Myers R, Lemieux L, et al. Three-dimensional maximum probability atlas of the human brain, with particular reference to the temporal lobe. Hum Brain Mapp. 2003;19:224-247

20. Behrens TE, Johansen-Berg H, Woolrich MW, Smith SM, Wheeler-Kingshott CA, Boulby PA, et al. Non-invasive mapping of connections between human thalamus and cortex using diffusion imaging. Nat Neurosci. 2003;6:750-757
21. Ashburner J, Friston KJ. Voxel-based morphometry--the methods. Neuroimage. 2000;11:805-821
22. de Groot M, Ikram MA, Akoudad S, Krestin GP, Hofman A, van der Lugt A, et al. Tract-specific white matter degeneration in aging: The rotterdam study. Alzheimers Dement. 2015;11:321-330
23. Eickhoff SB, Paus T, Caspers S, Grosbras MH, Evans AC, Zilles K, et al. Assignment of functional activations to probabilistic cytoarchitectonic areas revisited. Neuroimage. 2007;36:511-521
24. Kamali A, Hasan KM, Adapa P, Razmandi A, Keser Z, Lincoln J, et al. Distinguishing and quantification of the human visual pathways using high-spatial-resolution diffusion tensor tractography. Magn Reson Imaging. 2014;32:796-803
25. Fujita N, Tanaka H, Takanashi M, Hirabuki N, Abe K, Yoshimura H, et al. Lateral geniculate nucleus: Anatomic and functional identification by use of mr imaging. AJNR Am J Neuroradiol. 2001;22:1719-1726
26. Kitada R, Johnsrude IS, Kochiyama T, Lederman SJ. Brain networks involved in haptic and visual identification of facial expressions of emotion: An fmri study. Neuroimage. 2010;49:1677-1689
27. Takahashi N, Kawamura M. Pure topographical disorientation--the anatomical basis of landmark agnosia. Cortex. 2002;38:717-725
28. Bocci T, Pietrasanta M, Cerri C, Restani L, Caleo M, Sartucci F. Visual callosal connections: Role in visual processing in health and disease. Rev Neurosci. 2014;25:113-127
29. Berlucchi G. Visual interhemispheric communication and callosal connections of the occipital lobes. Cortex. 2014;56:1-13
30. Alexander AL, Lee JE, Lazar M, Field AS. Diffusion tensor imaging of the brain. Neurotherapeutics. 2007;4:316-329
31. Gabilondo I, Martinez-Lapiscina EH, Martinez-Heras E, Fraga-Pumar E, Llufriu S, Ortiz S, et al. Trans-synaptic axonal degeneration in the visual pathway in multiple sclerosis. Ann Neurol. 2014;75:98-107
32. Jindahra P, Petrie A, Plant GT. The time course of retrograde trans-synaptic degeneration following occipital lobe damage in humans. Brain. 2012;135:534-541
33. Jindahra P, Petrie A, Plant GT. Retrograde trans-synaptic retinal ganglion cell loss identified by optical coherence tomography. Brain. 2009;132:628-634
34. Cowey A, Alexander I, Stoerig P. Transneuronal retrograde degeneration of retinal ganglion cells and optic tract in hemianopic monkeys and humans. Brain. 2011;134:2149-2157
35. Herro AM, Lam BL. Retrograde degeneration of retinal ganglion cells in homonymous hemianopsia. Clin Ophthalmol. 2015;9:1057-1064
36. Park HY, Park YG, Cho AH, Park CK. Transneuronal retrograde degeneration of the retinal ganglion cells in patients with cerebral infarction. Ophthalmology. 2013;120:1292-1299
37. Bridge H, Jindahra P, Barbur J, Plant GT. Imaging reveals optic tract degeneration in hemianopia. Invest Ophthalmol Vis Sci. 2011;52:382-388
38. Zhang S, Wang H, Lu Q, Qing G, Wang N, Wang Y, et al. Detection of early neuron degeneration and accompanying glial responses in the visual pathway in a rat model of acute intraocular hypertension. Brain Res. 2009;1303:131-143
39. Ito Y, Shimazawa M, Chen YN, Tsuruma K, Yamashima T, Araie M, et al. Morphological changes in the visual pathway induced by experimental glaucoma in japanese monkeys. Exp Eye Res. 2009;89:246-255
40. Gupta N, Ang LC, Noel de Tilly L, Bidaisee L, Yucel YH. Human glaucoma and neural degeneration in intracranial optic nerve, lateral geniculate nucleus, and visual cortex. Br J Ophthalmol. 2006;90:674-678
41. Dai H, Mu KT, Qi JP, Wang CY, Zhu WZ, Xia LM, et al. Assessment of lateral geniculate nucleus atrophy with 3t mr imaging and correlation with clinical stage of glaucoma. AJNR Am J Neuroradiol. 2011;32:1347-1353

42. Lee JY, Jeong HJ, Lee JH, Kim YJ, Kim EY, Kim YY, et al. An investigation of lateral geniculate nucleus volume in patients with primary open-angle glaucoma using 7 tesla magnetic resonance imaging. Invest Ophthalmol Vis Sci. 2014;55:3468-3476
43. You Y, Gupta VK, Graham SL, Klistorner A. Anterograde degeneration along the visual pathway after optic nerve injury. PLoS One. 2012;7:e52061
44. Barcella V, Rocca MA, Bianchi-Marzoli S, Milesi J, Melzi L, Falini A, et al. Evidence for retrochiasmatic tissue loss in leber's hereditary optic neuropathy. Hum Brain Mapp. 2010;31:1900-1906
45. Serrano-Pozo A, Frosch MP, Masliah E, Hyman BT. Neuropathological alterations in alzheimer disease. Cold Spring Harb Perspect Med. 2011;1:a006189

# Chapter 5
# Clinical Outcomes

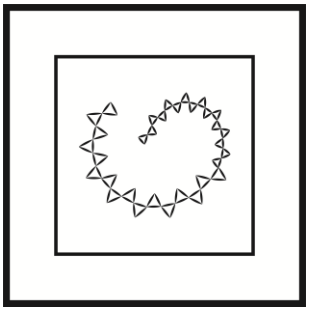

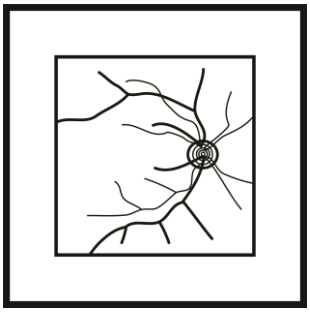

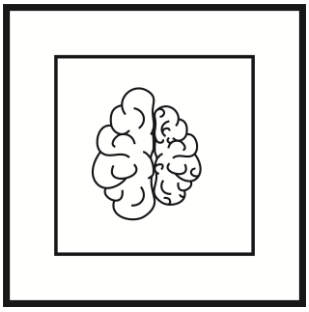

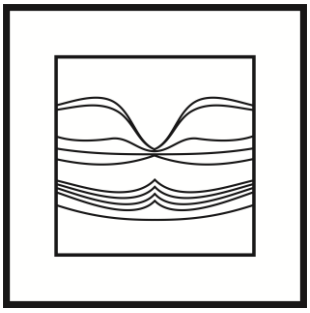

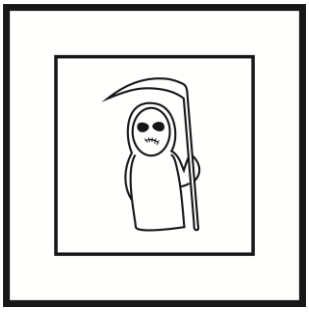

# Chapter 5.1
# The Retinal Microcirculation in Migraine: the Rotterdam Study

Ke-xin Wen, Unal Mutlu, M. Kamran Ikram, Maryam Kavousi, Caroline C.W. Klaver, Henning Tiemeier, Oscar H. Franco, M. Arfan Ikram

**ABSTRACT**

**Background:** To explore the role of microvascular pathology in migraine, we investigated the association between migraine and retinal microvascular damage.
**Methods:** We included 3270 participants (aged ≥ 45 years, 63% women) from the population-based Rotterdam Study (2006-2009). Participants with migraine were identified using a validated questionnaire based on ICHD-II criteria (n = 562). Retinopathy signs were graded on fundus photographs. Retinal arteriolar and venular caliber were measured by semi-automatic assessment of fundus photographs. Associations of migraine with retinopathy and retinal microvascular calibers were examined using logistic and linear regression models, respectively, adjusting for age, sex, and cardiovascular risk factors.
**Results:** Migraine was not associated with the presence of retinopathy (odds ratio (OR): 1.09, 95% confidence interval (CI) 0.62; 1.92). In the fully adjusted model adjusting for the companion vessel, persons with migraine did not differ in retinal arteriolar or venular caliber compared to persons without migraine (mean difference in standardized arteriolar caliber -0.05 (95% CI -0.13; 0.03); in standardized venular caliber -0.00 (95% CI -0.09; 0.08)). Migraine subtypes, including migraine with aura, were also not associated with retinal microvascular damage.
**Conclusions:** Our findings suggest that migraine is not associated with retinopathy or difference in retinal microvascular caliber. Further studies are needed to confirm these results.

## INTRODUCTION

Migraine is a chronically recurring headache disorder that affects up to 14% of adults in Europe.[1] Despite the high individual and societal burden of migraine, the exact pathogenesis remains elusive. Migraine has been shown to have a substantial vascular component. It is associated with an increased risk of cerebrovascular disease such as stroke[2-4] and markers of cerebrovascular damage such as white matter lesions.[5] It has also been identified as a risk factor for coronary heart disease.[2] Large vessel disease biomarkers such as atherosclerosis are linked to cerebrovascular disease[6, 7] and have been extensively studied in migraine,[8-10] but have not yet elucidated common mechanisms. Increasing evidence shows that microvascular pathology also contributes to stroke and coronary heart disease.[11, 12] In parallel, microvascular damage has also been implicated in the development of migraine[13] and may provide an important insight into mechanisms of migraine. Microvascular damage visible on retinal vascular imaging, including retinal vessel diameter and retinopathy signs, has been demonstrated as a useful marker for studying the microcirculation in cerebrovascular diseases.[14] However, only a few studies have examined the link between migraine and retinal markers of microvascular damage[15, 16] and the nature of the association remains uncertain. Therefore, in a large population-based cohort study, we investigated the status of the retinal microvascular circulation, as represented by retinopathy signs and retinal vessel diameter, in persons with migraine.

## METHODS

### Study setting and population

This study was based in the Rotterdam Study, a prospective population-based cohort among the middle-aged and elderly inhabitants of the district Ommoord in Rotterdam, the Netherlands.[17] We included participants from the third cohort initiated in 2006 (n = 3892). Participants were assessed by home interview and physical examination at the research facility from 2006 to 2009. Time between migraine assessment and retinal imaging averaged 6.4 weeks (standard deviation 9.6). All participants who provided information on migraine in the questionnaire (n = 3892) and had data from retinal imaging were included in the current study. Exclusion criteria were: persons classified as "probable migraine" (fulfilling all but one of the migraine criteria (n = 177)); persons missing data on retinopathy (n = 445); persons missing data on retinal vessel diameter (n = 326). The population for analysis included participants with data on migraine and retinopathy (n = 3270, age range 45-89 years) and data on migraine and retinal vessel diameter (n = 2944, age range 45-89 years), see Supplementary Figure 1.

The Rotterdam Study has been approved by the Medical Ethics Committee of the Erasmus MC according to the Population Studies Act: Rotterdam Study. All participants provided written informed consent.

**Supplementary Figure 1.** Flowchart of study participants.

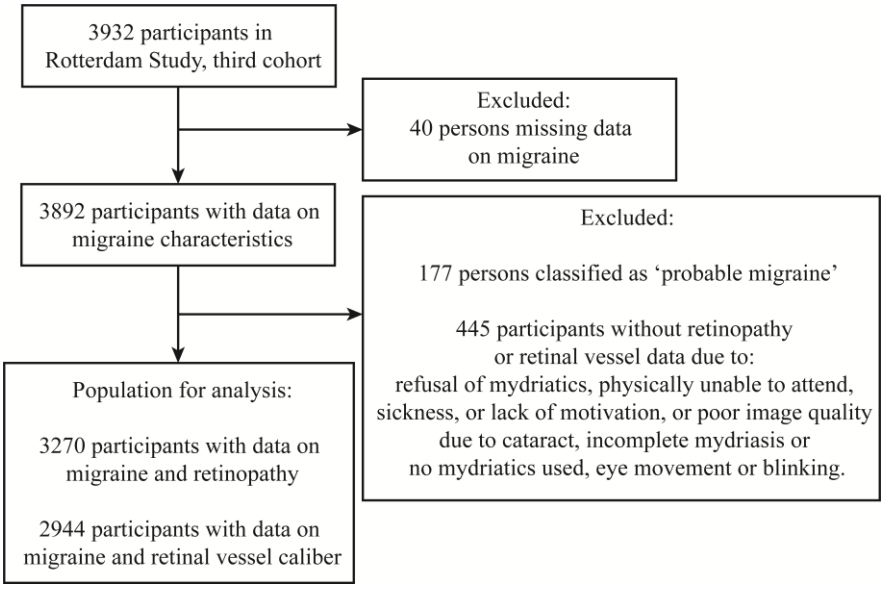

**Assessment of migraine**

Migraine was assessed at the home interview through administration of the migraine questionnaire by trained interviewers; 634 participants completed the questionnaire by phone interview. The migraine questionnaire was based on the migraine headache criteria from the International Classification of Headache Disorders, second edition (ICHD-II)[18] and was modified from the questionnaire validated for use in the Genetic Epidemiology of Migraine (GEM) study in Leiden.[19] This questionnaire had a specificity of 0.93 and a sensitivity of 0.36. The migraine questionnaire assessed lifetime occurrence of headache attacks that fulfilled the diagnostic criteria of more than five headache attacks, with a duration of 4-72 hours (when untreated), with typical migraine headache characteristics, and accompanying symptoms of photophobia or nausea.

As described previously,[20] the migraine headache criteria in our questionnaire differed moderately from the ICHD-II criteria: we asked participants if they had ever experienced headache with severe pain, affecting their activities, instead of moderate to severe pain intensity. In addition, migraine with aura was classified as at least five (instead of two) headaches fulfilling all migraine headache criteria in combination with headache accompanied by aura symptoms lasting between five to 60 minutes.[20] All individuals who met the criteria[20] for any lifetime history of migraine, including migraine with and without aura, were classified as persons with migraine. Persons with migraine were also dichotomized into active migraine (< 1 year since last attack) or non-active migraine ( > 1 year since last attack).

**Assessment of retinopathy signs and retinal microvascular calibers**

Retinopathy and retinal microvascular calibers were assessed as part of a full eye examination in the research center, including self-reported ophthalmic history and fundus color photography of the optic disc with a 35° visual field camera (TRC-50EX, Topcon Optical Company, Tokyo, Japan) after pharmacological mydriasis.[21]

Retinopathy signs were graded on fundus photographs of both eyes by two trained research physicians. Retinopathy was defined as the presence of soft or hard exudates, microaneurysms, macular edema, cotton wool spots, dot, blot or flame shaped hemorrhages, artery or vein branch occlusion, and laser coagulation scars.[21] For intrarater and interrater agreement (n = 113), fundus photographs were checked for quality and the presence of retinopathy signs by two experienced graders. These graders, each having twenty years of experience, divided their work and graded all fundus photographs particularly focusing on retinopathy signs. Consensus sessions and between-grader comparisons were performed regularly, and weighted κ coefficients ranged from 0.52 to 0.96 for various retinopathy signs.

For retinal microvascular calibers, per participant the fundus photograph of one eye with the best quality was analyzed using a retinal vessel measurement system (IVAN, University of Wisconsin-Madison, Madison, Wisconsin)[22] and a separate summary value was

calculated for the arteriolar and venular calibers (in µm) after correction for differences in magnification due to refractive status of the eye.[23-25] We verified in a random subsample of 100 participants that individual measurements in the left and right eye were similar. Measurements were performed by two raters blinded to participant characteristics. For interrater and intrarater agreement (n = 100) the Pearson correlation coefficients were 0.85 and 0.86 for arteriolar calibers, and 0.87 and 0.87 for venular calibers, respectively.[26] Persons who did not undergo ophthalmic examination, or had fundus images on both eyes that could not be graded, were excluded.

**Covariates**

Covariates were selected as cardiovascular and lifestyle factors that may confound the association between migraine and retinal microvascular damage. Education was assessed at study entry and categorized into low (primary education only), intermediate (secondary education) and high (higher vocational education or university) education level. Assessment of cardiovascular risk factors (systolic blood pressure, diastolic blood pressure, total cholesterol, high-density lipoprotein cholesterol, use of antihypertensive medication indicated for hypertension, use of lipid-lowering medication, diabetes mellitus and smoking) has been described previously.[27] C-reactive protein was measured in frozen serum samples using a near-infrared particle immunoassay method (Immage, Beckman Coulter, Fullerton, California). The presence of carotid plaques was assessed by ultrasound at the carotid artery bifurcation, common carotid artery, and internal carotid artery on both sides. Missing values for all covariates were imputed using multiple imputation based on all variables in the full regression model. All missing values were less than 5%. The percentage of missing values for each covariate are described in Supplementary Table 1.

**Supplementary Table 1. Number of missing values for each covariate.**

| | No migraine (n = 2708) | Definite migraine (n = 562) |
|---|---|---|
| Education level | 20 (0.74) | 2 (0.36) |
| Smoking | 2 (0.07) | 0 |
| Systolic blood pressure, mmHg | 13 (0.48) | 0 |
| Diastolic blood pressure, mmHg | 13 (0.48) | 0 |
| C-reactive protein, mg/L (log-transformed) | 92 (3.40) | 27 (4.80) |
| Total cholesterol, mmol/L | 33 (1.22) | 11 (1.95) |
| High-density lipoprotein cholesterol, mmol/L | 33 (1.22) | 11 (1.95) |
| Serum lipid reducing medication use | 25 (0.92) | 1 (0.18) |
| Antihypertensive use | 25 (0.92) | 2 (0.36) |
| Presence of carotid plaque | 13 (0.48) | 2 (0.36) |
| Diabetes mellitus | 41 (1.51) | 12 (2.14) |

Values are given as counts with corresponding percentage.

**Statistical analysis**

Differences in characteristics between groups were tested by ANCOVA for continuous outcomes and logistic regression for categorical outcomes, adjusted for age and sex. Associations of migraine with retinopathy and retinal microvascular calibers were modeled using logistic and linear regression models, respectively, with persons without migraine as reference group. The covariate C-reactive protein was log-transformed because of its skewed distribution. For analyses on retinopathy, two models were constructed. The first model adjusted for age and sex, and the second model additionally adjusted for education level, smoking, systolic and diastolic blood pressure, C-reactive protein, total cholesterol, high-density lipoprotein cholesterol, lipid-lowering or antihypertensive medication use, the presence of carotid plaque and diabetes mellitus. For analyses on retinal microvascular caliber, values for retinal microvascular caliber were standardized by calculating z-scores and three models were constructed. The first model adjusted for age and sex, and the second model additionally adjusting for the caliber of the other vessel; the third model additionally adjusted for education level, smoking, systolic and diastolic blood pressure, C-reactive protein, total cholesterol, high-density lipoprotein cholesterol, lipid-lowering or antihypertensive medication use, the presence of carotid plaque and diabetes mellitus. Arterial and venular calibers are highly correlated and are associated with clinical outcomes in opposite directions.[28] This may lead to confounding when the calibers are modeled alone. Therefore, adjusting the model for the caliber of the accompanying (other) vessel allows for correction of this potential confounder. We also investigated retinopathy and retinal microvascular caliber in migraine subtypes, including migraine with aura and active migraine. The potential interaction of migraine with age and sex on retinopathy or microvascular caliber was assessed by inclusion of interaction terms in the regression models and by stratified analyses. Results for retinopathy are presented as odds ratios (OR) with 95% confidence interval (CI). Results for retinal microvascular calibers are presented as betas that correspond to mean difference in standardized arteriolar or venular caliber with 95% CI. Statistical significance was considered to be two-sided p-values $< 0.05$. No adjustment was made for multiple testing due to the exploratory nature of the study. All statistical analyses were performed using the statistical software package SPSS (IBM Corporation, Armonk, New York) version 21.0 for Windows.

**RESULTS**

Table 1 presents the descriptive of the study population. In all, 562 persons were classified as persons with definite migraine, of which 126 participants had migraine with aura and 307 had active migraine. Persons with migraine were younger than those without migraine and a higher percentage were women (Table 1). After adjusting for age and sex, a lower percentage of persons with migraine were current smokers, while a higher percentage were former smokers and used lipid-lowering medication.

Amongst persons without migraine, 3.3% had retinopathy while amongst persons with migraine 2.8% had retinopathy (Table 1). After multivariable adjustment, persons with migraine were not more likely to have retinopathy (OR 1.09, 95% CI 0.62; 1.92) compared to persons without migraine (Table 2). Migraine subtypes, including migraine with aura, were not associated with a higher prevalence of retinopathy (Table 2).
The presence of migraine was associated with a lower arteriolar caliber in the age and sex adjusted model (-0.10, 95% CI -0.20; -0.01); the difference in venular caliber was in the same direction, but not significant (-0.06, 95% CI -0.16; 0.04) (Table 3). However, these differences were attenuated in both arteriolar and venular caliber after adjustment for the other vessel and further adjustment for cardiovascular risk factors. Analyses of migraine subtypes did not demonstrate any difference in the estimates (Table 3).
When investigating interaction effects, no significant interaction of migraine with age or sex on the association of migraine with retinopathy was found (Table 4). There was also no interaction of migraine with age in the association with the arteriolar or venular calibers. However, there was interaction between migraine and sex on arteriolar caliber (p-value for interaction = 0.005). Specifically, mean arteriolar caliber was narrower in women with migraine compared to women without migraine (-0.11, 95% CI -0.20; -0.02), whereas in men with migraine the mean difference in arteriolar caliber compared to men without migraine was in the opposite direction (0.15, 95% CI -0.10; 0.31). No migraine-sex interaction was found on venular caliber (p-value for interaction = 0.58).

**Table 1. Descriptive of the study population (n = 3270).**

| | | No migraine (n = 2708) | Definite migraine (n = 562) | p-value |
|---|---|---|---|---|
| Age, years | | 57.0 (6.8) | 56.1 (6.3) | 0.006* |
| Female | | 1383 (51.1%) | 449 (79.9%) | <0.001* |
| Education level | Low | 737 (27.2%) | 158 (28.1%) | 0.38 |
| | Intermediate | 1240 (45.8%) | 253 (45.0%) | 0.66 |
| | High | 731 (27.0%) | 151 (26.9%) | 0.13 |
| Smoking | Never | 789 (29.1%) | 186 (33.1%) | 0.91 |
| | Current | 765 (28.2%) | 116 (20.6%) | 0.003* |
| | Former | 1154 (42.6%) | 260 (46.3%) | 0.012* |
| Systolic blood pressure.mmHg | | 133.0 (19.3) | 131.1 (18.9) | 0.80 |
| Diastolic blood pressure, mmHg | | 82.5 (11.1) | 82.8 (10.9) | 0.14 |
| C-reactive protein, mg/L (log-transformed) | | 0.12 (0.5) | 0.13 (0.5) | 0.64 |
| Total cholesterol, mmol/L | | 5.5 (1.1) | 5.7 (1.1) | 0.52 |
| High-density lipoprotein cholesterol, mmol/L | | 1.4 (0.4) | 1.5 (0.4) | 0.17 |
| Lipid-lowering medication use | | 600 (22.2%) | 135 (24.0%) | 0.010* |
| Antihypertensive use | | 627 (23.2%) | 139 (24.7%) | 0.07 |
| Carotid plaque | | 979 (36.2%) | 178 (31.7%) | 0.65 |
| Diabetes mellitus | | 275 (10.2%) | 48 (8.5%) | 0.94 |
| Retinopathy | | 90 (3.3%) | 16 (2.8%) | |
| Mean arteriolar caliber, µm | | 158.5 (15.6) | 157.3 (15.6) | |
| Mean venular caliber, µm | | 239.7 (23.0) | 238.0 (22.9) | |
| Migraine with aura | | NA | 126 (22.4%) | |

Values are presented as mean (standard deviation) or as count (percentage).
Reported values are obtained from the imputed dataset. Percentage of missing values imputed for each covariate are described in Supplementary Table 1. Differences in characteristics between groups were tested by ANCOVA for continuous outcomes and logistic regression for categorical outcomes, adjusted for age and sex. *Significantly different compared to persons without migraine ($p < 0.05$). Abbreviation: NA, not applicable.

**Table 2. Retinopathy in persons with migraine compared to persons without migraine.**

| | n/N | Model 1 | p-value | Model 2 | p-value |
|---|---|---|---|---|---|
| No migraine | 90/2618 | 1.00 (reference) | | 1.00 (reference) | |
| Migraine | 16/546 | 0.99 (0.57; 1.73) | 0.98 | 1.09 (0.62; 1.92) | 0.77 |
| Migraine with aura | 5/121 | 1.40 (0.55; 3.56) | 0.48 | 1.65 (0.63; 4.30) | 0.31 |
| Migraine without aura | 11/425 | 0.87 (0.46; 1.67) | 0.68 | 0.96 (0.50; 1.85) | 0.90 |
| Active migraine | 9/298 | 1.11 (0.54; 2.27) | 0.78 | 1.31 (0.63; 2.72) | 0.47 |
| Non-active migraine | 7/248 | 0.86 (0.39; 1.90) | 0.71 | 0.90 (0.40; 2.01) | 0.79 |

Values given for retinopathy are odds ratios and 95% CI (from logistic regression) in persons with migraine and migraine subtypes compared to persons without migraine. Abbreviations: n, number of persons with retinopathy; N, number of persons without retinopathy. Model 1: adjusted for age and sex. Model 2: additionally adjusted for education level, smoking, systolic and diastolic blood pressure, C-reactive protein, total cholesterol, high-density lipoprotein cholesterol, lipid-lowering or antihypertensive medication use, presence of carotid plaque and diabetes mellitus. *Significantly different compared to persons without migraine ($p < 0.05$).

**Table 3. Adjusted mean difference in retinal microvascular caliber between persons with and without migraine.**

| | N | Model 1 | p-value | Model 2 | p-value | Model 3 | p-value |
|---|---|---|---|---|---|---|---|
| **Arterioles** | | | | | | | |
| No migraine | 2439 | 0.00 (reference) | | 0.00 (reference) | | 0.00 (reference) | |
| Migraine | 505 | -0.10 (-0.20; -0.01) | 0.039* | -0.07 (-0.15; 0.01) | 0.10 | -0.05 (-0.13; 0.03) | 0.20 |
| Migraine with aura | 112 | -0.15 (-0.34; 0.03) | 0.11 | -0.10 (-0.26; 0.06) | 0.21 | -0.10 (-0.25; 0.05) | 0.18 |
| Migraine without aura | 393 | -0.09 (-0.20; 0.02) | 0.09 | -0.06 (-0.16; 0.03) | 0.16 | -0.04 (-0.12; 0.05) | 0.40 |
| Active migraine | 277 | -0.08 (-0.20; 0.05) | 0.23 | -0.04 (-0.14; 0.07) | 0.51 | -0.05 (-0.15; 0.05) | 0.34 |
| Non-active migraine | 228 | -0.14 (-0.27; -0.01) | 0.040* | -0.12 (-0.23; -0.01) | 0.039* | -0.06 (-0.17; 0.05) | 0.29 |
| **Venules** | | | | | | | |
| No migraine | 2439 | 0.00 (reference) | | 0.00 (reference) | | 0.00 (reference) | |
| Migraine | 505 | -0.06 (-0.16; 0.04) | 0.22 | -0.01 (-0.09; 0.08) | 0.85 | -0.00 (-0.09; 0.08) | 0.92 |
| Migraine with aura | 112 | -0.10 (-0.29; 0.09) | 0.30 | -0.02 (-0.18; 0.14) | 0.80 | -0.01 (-0.17; 0.15) | 0.92 |
| Migraine without aura | 393 | -0.05 (-0.16; 0.06) | 0.34 | -0.00 (-0.10; 0.09) | 0.92 | -0.00 (-0.09; 0.09) | 0.92 |
| Active migraine | 277 | -0.08 (-0.21; 0.05) | 0.21 | -0.04 (-0.15; 0.07) | 0.46 | -0.02 (-0.12; 0.09) | 0.76 |
| Non-active migraine | 228 | -0.04 (-0.18; 0.10) | 0.57 | 0.04 (-0.08; 0.15) | 0.56 | 0.01 (-0.10; 0.12) | 0.85 |

Values given are mean difference and 95% confidence intervals (from linear regression) in standardized arteriolar and venular calibers of persons with migraine compared to persons without migraine. Model 1: age and sex adjusted. Model 2: additionally adjusted for the other retinal vessel. Model 3: additionally adjusted for education level, smoking, systolic and diastolic blood pressure, C-reactive protein, total cholesterol, high-density lipoprotein cholesterol, lipid-lowering or antihypertensive medication use, presence of carotid plaque and diabetes mellitus. *Significantly different compared to persons without migraine ($p < 0.05$).

**Table 4. Retinopathy and retinal microvascular caliber in persons with migraine compared to persons without migraine, stratified on age and sex.**

| | Retinopathy | | | Arteriolar caliber | | | Venular caliber | |
|---|---|---|---|---|---|---|---|---|
| | **n/N** | **OR (95% CI)** | **p-value** | **n/N** | **Mean difference (95% CI)** | **p-value** | **Mean difference (95% CI)** | **p-value** |
| Age ≤ 65 | 529/2487 | 0.91 (0.50; 1.68) | 0.77 | 478/2259 | -0.03 (-0.11; 0.05) | 0.41 | -0.00 (-0.09; 0.08) | 0.09 |
| Age > 65 | 33/221 | 0.59 (0.11; 3.31) | 0.55 | 27/180 | -0.29 (-0.59; 0.02) | 0.07 | -0.06 (-0.38; 0.26) | 0.72 |
| p-interaction | | 0.99 | | | 0.59 | | 0.23 | |
| | | | | | | | | |
| Men | 113/1325 | 0.79 (0.30; 2.09) | 0.64 | 98/1168 | 0.15 (-0.10; 0.31) | 0.07 | -0.04 (-0.21; 0.13) | 0.64 |
| Women | 449/1383 | 1.00 (0.49; 2.01) | 0.99 | 407/1271 | -0.11(-0.20; -0.02) | 0.015* | -0.00 (-0.10; 0.09) | 0.96 |
| p-interaction | | 0.78 | | | 0.005 | | 0.58 | |

Values given for retinopathy are odds ratios and 95% confidence intervals (from logistic regression) in persons with migraine for retinopathy compared to persons without migraine. Values given for arterioles and venules are mean difference and 95% confidence intervals (from linear regression) of standardized arteriolar and venular calibers of persons with migraine compared to persons without migraine. Abbreviations: n, number of persons with migraine, N, number of persons without migraine. All estimates were obtained from the model adjusted for age, sex, education level, smoking, systolic and diastolic blood pressure, C-reactive protein, total cholesterol, high-density lipoprotein cholesterol, lipid-lowering or antihypertensive medication use, presence of carotid plaque and diabetes mellitus; the model for arteriolar and venular caliber was additionally adjusted for the other vessel caliber. *Significantly different compared to persons without migraine ($p < 0.05$).

## DISCUSSION

In this population-based cohort study, we found that lifetime migraine was not associated with markers of retinal microvascular damage. Importantly, migraine was not associated with either subclinical or clinical retinal microvascular damage, as shown by retinal vessel caliber and retinopathy, respectively. Findings from previous studies on these associations have been equivocal. One previous study, reporting increased presence of retinopathy in persons with migraine,[16] had a higher prevalence of retinopathy of around 7.7% for persons with migraine without aura compared to 2.8% for all persons with migraine in our study population, despite a comparable age range. Retinopathy could be underestimated in our study population as the use of only fundus photographs centered on the macula excludes damage visible in other retinal fields. This may partially underlie the different findings. Additionally, persons with migraine or other headaches were found to have smaller mean arteriolar caliber[15, 16] and venular caliber than those without migraine.[16] These studies had mixed results for migraine subtypes: persons with migraine with aura were found to have smaller arteriolar and venular caliber[16] while the other study found only persons with migraine without aura to have smaller arteriolar caliber.[15] Notably, we found similar estimates to previous studies when modeling the retinal vessel calibers separately, whereas the differences became non-significant after modeling the arteriolar and venular caliber simultaneously. The retinal vessel calibers are highly correlated but are associated in opposite directions with cardiovascular disease.[28] Therefore, simultaneous modeling of both retinal vessels ensured adjustment for confounding by this correlation, which could have influenced the previous findings.

The reported associations between microvascular damage and increased risk of hypertension, coronary atherosclerosis and coronary heart disease[12, 29-32] may provide further indications regarding the mechanisms of a potential association between migraine and cardiovascular disease.[2, 3] Migraine has also been associated with microvascular pathology in the brain in the form of cerebral microbleeds.[13] However, we were unable to identify a link between migraine and extracerebral microvascular damage. One explanation may be that our study population was much younger than the population investigated for microbleeds and thus may have a lower load of microvascular damage. Furthermore, migraine may not be unequivocally associated with vascular pathology traditionally linked to cardiovascular disease. Persons with migraine in our study had a comparable cardiovascular risk profile to persons without migraine, supporting this theory. Persons with migraine have a shared genetic risk of stroke[4] and stroke has been strongly linked to changes in retinal microvasculature.[33] However, persons with migraine have a lower genetic risk of coronary artery disease,[34] and in these persons cerebral perfusion may be increased interictally.[20] The fact that we did not find an association between migraine and retinal microvascular damage indicates that the shared etiology of migraine and stroke may not be explained by well-established pathways such as atherosclerosis.

Alternatively, persons with severe migraine may be non-participants in our study and therefore the effects of chronic migraine could be underestimated. Analysis of migraine subgroups indicated that persons with active migraine were at a greater (non-significant) risk of retinopathy than those with non-active migraine, suggesting that any risk of retinopathy due to migraine may only be present in the active period. Similarly, the association of migraine and stroke is strongest in young women.[35] However, our analysis of migraine subgroups may have been insufficiently powered to draw conclusions from. Finally, when we explored the effects of age and sex on the association between migraine and microvascular markers, women with migraine appeared to have narrower arterioles than women without migraine. However, as the estimate amongst men was considerably in the opposite direction (although non-significant), effect modification by sex may be a spurious finding.

Our study has a number of limitations. Firstly, the migraine questionnaire used an adapted ICHD-II migraine criteria,[20] which could have misclassified persons with moderate migraine headache but not severe headache into the control group. Those with migraine with aura could have been misclassified as persons with migraine without aura due to limited information on aura symptoms. This misclassification may have led to an underestimation of our effects. Furthermore, retinopathy may be underestimated as previously explained. Due to limited information, we were unable to adjust for potential confounding effects of pain medication use in our study. Additionally, in subgroup analyses, the numbers in each group may have been too small to obtain adequate estimates. Finally, the cross-sectional design of the study precludes causal interpretation of our findings. Strengths of this study include the large population-based sample and use of both preclinical and clinical markers of retinal microvascular damage. Furthermore, adjustment of retinal microvascular caliber by the other vessel caliber allowed for correction of confounding from the positive correlation of the arteriolar and venular calibers.[28]

In conclusion, we did not find persons with migraine or migraine with aura to be more likely to have retinopathy than persons without migraine, and there was no difference in retinal arteriolar or venular caliber between the two groups. More studies are needed to corroborate the findings and understand the role of microvascular pathology in migraine.

## REFERENCES


1. Stovner LJ, Andree C. Prevalence of headache in europe: A review for the eurolight project. J Headache Pain. 2010;11:289-299
2. Kurth T, Winter AC, Eliassen AH, Dushkes R, Mukamal KJ, Rimm EB, et al. Migraine and risk of cardiovascular disease in women: Prospective cohort study. BMJ. 2016;353:i2610
3. Guidetti D, Rota E, Morelli N, Immovilli P. Migraine and stroke: "Vascular" comorbidity. Front Neurol. 2014;5:193
4. Malik R, Freilinger T, Winsvold BS, Anttila V, Vander Heiden J, Traylor M, et al. Shared genetic basis for migraine and ischemic stroke: A genome-wide analysis of common variants. Neurology. 2015;84:2132-2145
5. Kruit MC, van Buchem MA, Launer LJ, Terwindt GM, Ferrari MD. Migraine is associated with an increased risk of deep white matter lesions, subclinical posterior circulation infarcts and brain iron accumulation: The population-based mri camera study. Cephalalgia. 2010;30:129-136
6. Gronewold J, Bauer M, Lehmann N, Mahabadi AA, Kalsch H, Weimar C, et al. Coronary artery calcification, intima-media thickness, and ankle-brachial index are complementary stroke predictors. Stroke. 2014;45:2702-2709
7. Bos D, Ikram MA, Elias-Smale SE, Krestin GP, Hofman A, Witteman JC, et al. Calcification in major vessel beds relates to vascular brain disease. Arterioscler Thromb Vasc Biol. 2011;31:2331-2337
8. Goulart AC, Santos IS, Bittencourt MS, Lotufo PA, Bensenor IM. Migraine and subclinical atherosclerosis in the brazilian longitudinal study of adult health (elsa-brasil). Cephalalgia. 2016;36:840-848
9. Hamed SA, Hamed EA, Ezz Eldin AM, Mahmoud NM. Vascular risk factors, endothelial function, and carotid thickness in patients with migraine: Relationship to atherosclerosis. J Stroke Cerebrovasc Dis. 2010;19:92-103
10. Stam AH, Weller CM, Janssens AC, Aulchenko YS, Oostra BA, Frants RR, et al. Migraine is not associated with enhanced atherosclerosis. Cephalalgia. 2013;33:228-235
11. Wong TY, Klein R, Couper DJ, Cooper LS, Shahar E, Hubbard LD, et al. Retinal microvascular abnormalities and incident stroke: The atherosclerosis risk in communities study. Lancet. 2001;358:1134-1140
12. Wong TY, Klein R, Klein BE, Tielsch JM, Hubbard L, Nieto FJ. Retinal microvascular abnormalities and their relationship with hypertension, cardiovascular disease, and mortality. Surv Ophthalmol. 2001;46:59-80
13. Arkink EB, Terwindt GM, de Craen AJ, Konishi J, van der Grond J, van Buchem MA, et al. Infratentorial microbleeds: Another sign of microangiopathy in migraine. Stroke. 2015;46:1987-1989
14. Patton N, Aslam T, Macgillivray T, Pattie A, Deary IJ, Dhillon B. Retinal vascular image analysis as a potential screening tool for cerebrovascular disease: A rationale based on homology between cerebral and retinal microvasculatures. J Anat. 2005;206:319-348
15. Liew G, Mitchell P, Wong TY, Wang JJ. Retinal vascular caliber and migraine: The blue mountains eye study. Headache. 2006;46:997-1004
16. Rose KM, Wong TY, Carson AP, Couper DJ, Klein R, Sharrett AR. Migraine and retinal microvascular a bnormalities: The atherosclerosis risk in communities study. Neurology. 2007;68:1694-1700
17. Hofman A, Brusselle GG, Darwish Murad S, van Duijn CM, Franco OH, Goedegebure A, et al. The rotterdam study: 2016 objectives and design update. Eur J Epidemiol. 2015;30:661-708
18. Olesen J, Steiner TJ. The international classification of headache disorders, 2nd edn (icdh-ii). J Neurol Neurosurg Psychiatry. 2004;75:808-811
19. Launer LJ, Terwindt GM, Ferrari MD. The prevalence and characteristics of migraine in a population-based cohort: The gem study. Neurology. 1999;53:537-542

20. Loehrer E, Vernooij MW, van der Lugt A, Hofman A, Ikram MA. Migraine and cerebral blood flow in the general population. Cephalalgia. 2015;35:190-198
21. Mutlu U, Ikram MA, Hofman A, de Jong PT, Klaver CC, Ikram MK. N-terminal pro-b-type natriuretic peptide is related to retinal microvascular damage: The rotterdam study. Arterioscler Thromb Vasc Biol. 2016;36:1698-1702
22. Hubbard LD, Brothers RJ, King WN, Clegg LX, Klein R, Cooper LS, et al. Methods for evaluation of retinal microvascular abnormalities associated with hypertension/sclerosis in the atherosclerosis risk in communities study. Ophthalmology. 1999;106:2269-2280
23. Parr JC, Spears GF. Mathematic relationships between the width of a retinal artery and the widths of its branches. Am J Ophthalmol. 1974;77:478-483
24. Knudtson MD, Lee KE, Hubbard LD, Wong TY, Klein R, Klein BE. Revised formulas for summarizing retinal vessel diameters. Curr Eye Res. 2003;27:143-149
25. Littmann H. [determining the true size of an object on the fundus of the living eye] zur bestimmung der wahren grosse eines objektes auf dem hintergrund eines lebenden auges. Klin Monbl Augenheilkd. 1988;192:66-67
26. Mutlu U, Ikram MK, Wolters FJ, Hofman A, Klaver CC, Ikram MA. Retinal microvasculature is associated with long-term survival in the general adult dutch population. Hypertension. 2016;67:281-287
27. Kavousi M, Elias-Smale S, Rutten JH, Leening MJ, Vliegenthart R, Verwoert GC, et al. Evaluation of newer risk markers for coronary heart disease risk classification: A cohort study. Ann Intern Med. 2012;156:438-444
28. Liew G, Sharrett AR, Kronmal R, Klein R, Wong TY, Mitchell P, et al. Measurement of retinal vascular c aliber: Issues and alternatives to using the arteriole to venule ratio. Invest Ophthalmol Vis Sci. 2007;48:52-57
29. Wong TY, Klein R, Sharrett AR, Duncan BB, Couper DJ, Tielsch JM, et al. Retinal arteriolar narrowing and risk of coronary heart disease in men and women. The atherosclerosis risk in communities study. JAMA. 2002;287:1153-1159
30. McGeechan K, Liew G, Macaskill P, Irwig L, Klein R, Klein BE, et al. Meta-analysis: Retinal vessel caliber and risk for coronary heart disease. Ann Intern Med. 2009;151:404-413
31. Cheung N, Wang JJ, Klein R, Couper DJ, Sharrett AR, Wong TY. Diabetic retinopathy and the risk of coronary heart disease: The atherosclerosis risk in communities study. Diabetes Care. 2007;30:1742-1746
32. Rong J, Yu CQ, Yang P, Chen J. Association of retinopathy with coronary atherosclerosis determined by coronary 64-slice multidetector computed tomography angiography in type 2 diabetes. Diab Vasc Dis Res. 2013;10:161-168
33. Ong YT, De Silva DA, Cheung CY, Chang HM, Chen CP, Wong MC, et al. Microvascular structure and network in the retina of patients with ischemic stroke. Stroke. 2013;44:2121-2127
34. Winsvold BS, Nelson CP, Malik R, Gormley P, Anttila V, Vander Heiden J, et al. Genetic analysis for a shared biological basis between migraine and coronary artery disease. Neurol Genet. 2015;1:e10
35. Schurks M, Rist PM, Bigal ME, Buring JE, Lipton RB, Kurth T. Migraine and cardiovascular disease: Systematic review and meta-analysis. BMJ. 2009;339:b3914

# Chapter 5.2
# Retinal Neurodegeneration on Optical Coherence Tomography and the Risk of Dementia

Unal Mutlu, Johanna M. Colijn, M. Arfan Ikram, Pieter W.M. Bonnemaijer, Silvan Licher, Frank J. Wolters, Henning Tiemeier, Peter J. Koudstaal, Caroline C.W. Klaver, M. Kamran Ikram

**ABSTRACT**

**Background:** Retinal structures may serve as a biomarker for dementia, but longitudinal studies examining this link are lacking. We aimed to investigate the association of retinal layer thickness with prevalent and incident dementia in a general population of Dutch adults.

**Methods:** Our study was part of the Rotterdam Study, a prospective population-based cohort study in the Ommoord district in Rotterdam. From 2007 to 2012, we included individuals aged ≥ 45 years who had gradable retinal optical coherence tomography (OCT) images and who at baseline were free from stroke, glaucoma, macular degeneration, and retinopathy. Retinal nerve fiber layer (RNFL), ganglion cell layer (GCL), and inner plexiform layer (IPL) thicknesses were measured on OCT images. Individuals were followed up until January 1, 2015, for the onset of dementia. Associations of retinal layer thickness with prevalent and incident dementia were examined using logistic and Cox regression models adjusting for age, sex, axial length of the eye, education, and cardiovascular risk factors.

**Results:** Of 3532 individuals (mean age 68.6 years,57% women), 45 individuals had dementia. Thinner GCL was associated with prevalent dementia (odds ratio per standard deviation decrease in GCL: 1.51 (95% confidence interval (CI)): 1.11-2.06). No association was found of RNFL and IPL thickness with prevalent dementia. During 15845 person-years of follow-up (mean: 4.5 years), 90 individuals developed dementia of whom 70 had Alzheimer's disease. Thinner RNFL at baseline was associated with an increased risk of developing dementia (hazard ratio per standard deviation decrease in RNFL: 1.45 (1.20-1.75)), which was similar for Alzheimer's disease (1.44 (1.16-1.79)). No association was found of GCL and IPL thickness with incident dementia.

**Conclusions:** Thinner RNFL is associated with an increased risk of dementia, including Alzheimer's disease, suggesting that retinal neurodegeneration may serve as a preclinical biomarker for dementia.

## INTRODUCTION

Dementia is a major cause of morbidity and mortality among elderly populations worldwide.[1] Alzheimer's disease (AD) is the most common type of dementia, characterized by the accumulation of abnormally folded amyloid-beta and tau protein in the brain over a long preclinical period.[2] Studies have shown that the accumulation of amyloid-beta deposits also occurs in the retina of patients with AD and in the retina of transgenic mouse models of AD.[3, 4] Hence, these findings not only underpin the involvement of the retina and the visual pathway in AD-pathology, but also show the potential to use retinal structures as biomarkers for AD.[5-7]

In recent years, noninvasive optical imaging techniques have increasingly been used to study neurodegenerative disorders of the eye, such as macular degeneration and glaucoma, as well as neurodegeneration of the brain. In particular, optical coherence tomography (OCT) provides an excellent opportunity to visualize retinal nerve tissue in vivo with biopsy-like precision (spatial resolution < 10 μm) and to detect neuroaxonal degeneration. Several cross-sectional studies using OCT have shown that patients with AD have thinner retinal nerve fiber layer (RNFL) and ganglion cell layer (GCL) compared to controls.[8-12] Additionally, recent studies have shown that thinner RNFL and GCL were associated with structural MRI markers of brain atrophy, suggesting that neuronal damage indeed occurs simultaneously in the retina and throughout the brain.[13, 14] Although cross-sectional studies have suggested that thinning of retinal layers may serve as a biomarker for various dementias, including AD, it remains unclear whether retinal changes precede the occurrence of dementia, or only occur once the disease has become clinically manifest. Longitudinal studies examining the link between the retinal layers and incident dementia are lacking, and are crucial to disentangle the temporal relation. Therefore, in order to bridge this gap in the current literature, we investigated the association of retinal layer thickness on OCT (i.e. RNFL, GCL, and inner plexiform layer (IPL)), with prevalent and incident dementia in the general adult Dutch population. Given that thinning of these retinal layers may reflect ongoing cerebral neurodegeneration, we hypothesize that thinner RNFL, GCL and IPL are associated with both prevalent and incident dementia.

## METHODS

### Study setting and population

This study was embedded within the Rotterdam Study (RS): a prospective population-based cohort study among individuals aged 45 years and older, residing in Ommoord, a district in the city Rotterdam, the Netherlands.[15] The Rotterdam Study has been approved by the medical ethics committee according to the Population Study Act: Rotterdam Study, executed by the Ministry of Health, Welfare and Sports of the Netherlands. All individuals gave written informed consent.

The original cohort started in 1990 (n = 7983), and was extended in 2000 (n = 3011) and in 2006 (n = 3932). Follow-up examinations take place every three to four years. In 2007, spectral-domain OCT scanning was added to the protocol, and was performed in the fifth visit of the first cohort (RS-I-5), the third visit of the second cohort (RS-II-3), and in about half of the individuals at the first visit of the third cohort (RS-III-1), Figure 1.

Since the introduction of OCT in the Rotterdam Study, a total of 5065 individuals were eligible for OCT scanning. Individuals were excluded if they did not undergo OCT scanning, or had ungradable OCT scans due to poor quality scans (e.g. motion artifacts, segmentation failures). We also excluded individuals with age-related macular degeneration, glaucoma, and hypertensive or diabetic retinopathy that could affect retinal thickness measurements. For the exact definitions of these eye diseases, we refer to previous publications from our study. Briefly, for age-related macular degeneration and retinopathy, both eyes of individuals were graded on retinal photographs by experienced graders or physicians. For glaucoma, diagnosis was made based on the presence of visual field loss with either high intraocular pressure or high cup-disk ratio. Next, we excluded individuals with a history of clinical stroke, individuals who underwent insufficient dementia screening, and individuals who did not provide informed consent to access medical records and hospital discharge letters. Individuals with insufficient dementia screening were those who did not undergo the Mini-Mental State Examination or Geriatric Mental Schedule during the interview, which was required for dementia assessment (see ‘assessment of dementia’). These exclusions resulted in 3532 individuals for analysis with the RNFL measured at the peripapillary region (sample I), and in 3222 individuals for analysis with the GCL and IPL measured at the macular region (sample II), from which primarily the right eye (95% for the RNFL and 94% for the GCL and IPL measurements) was chosen for further analysis. From the macula towards the optic nerve, the RNFL becomes thicker, whereas the GCL and IPL becomes thinner. For this reason, we have measured the RNFL at the peripapillary region, and the GCL and IPL at the perimacular region as these layers are the thickest in those regions.

**Figure 1.** Flow diagram of the study population.

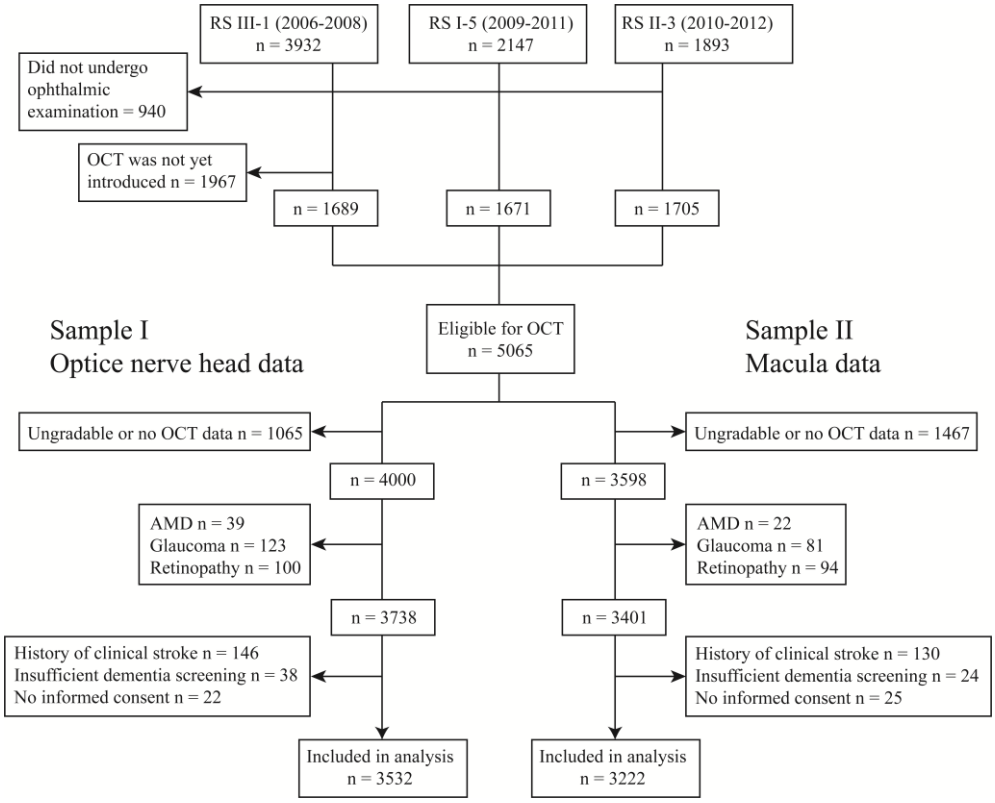


Abbreviations: RS, Rotterdam Study; OCT, optical coherence tomography; AMD, age-related macular degeneration.

**Assessment of retinal layer thickness**

From September 2007 to June 2011, both eyes of each participant were scanned after pharmacological mydriasis with the Topcon 3D spectral domain OCT-1000 (Topcon Optical Company, Tokyo, Japan), n = 2886 (sample I) and n = 2575 (sample II). From August 2011 onwards, this device was replaced with the Topcon 3D spectral domain OCT-2000 due to an update following the start of the study, n = 646 (sample I) and n = 647 (sample II). The macula and optic nerve head were scanned in the horizontal direction in an area of 6 × 6 × 1.68 mm with 512 × 512 × 480 voxels for OCT-1000 and in an area of 6 × 6 × 2.30 mm with 512 × 512 × 885 voxels for OCT-2000, enabling us to detect structures with a resolution of 5µm (Figure 2). Thickness of the peripapillary RNFL was measured automatically by Topcon's built-in segmentation algorithm. This was done in 12 peripapillary segments of 30$^{o}$ each, and the average RNFL thickness was derived from the calculation circle. For the macula, volumes were segmented using Iowa Reference

Algorithms 3.6 (available at https://www.iibi.uiowa.edu/content/shared-software-download). The inter-session repeatability of segmentations and agreement between OCT devices of this algorithm has been previously validated.[16, 17] Thicknesses of the GCL and IPL were measured in nine regions of the Early Treatment Diabetic Retinopathy Study Grid. The average of the retinal layer thicknesses was calculated and used in further statistical analyses.

Indices of quality control were used to preserve good quality images (high signal, low noise) and to exclude scans with segmentation errors. Scans included in our study had a segmentability index of more than 30%, an undefined region of less than 20%, and a quality factor of more than 30. These quality metrics have been described previously.[17-19] At the beginning of the study, only the right eyes were scanned due to time constraints. This was the case for 883 individuals. To maintain consistency, we chose primarily the right eye.

**Figure 2.** Output of the retinal optical coherence tomography (Topcon OCT-2000) focusing on the macula (A) and optic nerve (B) with corresponding cross-sectional view of the retina (C and D, respectively).

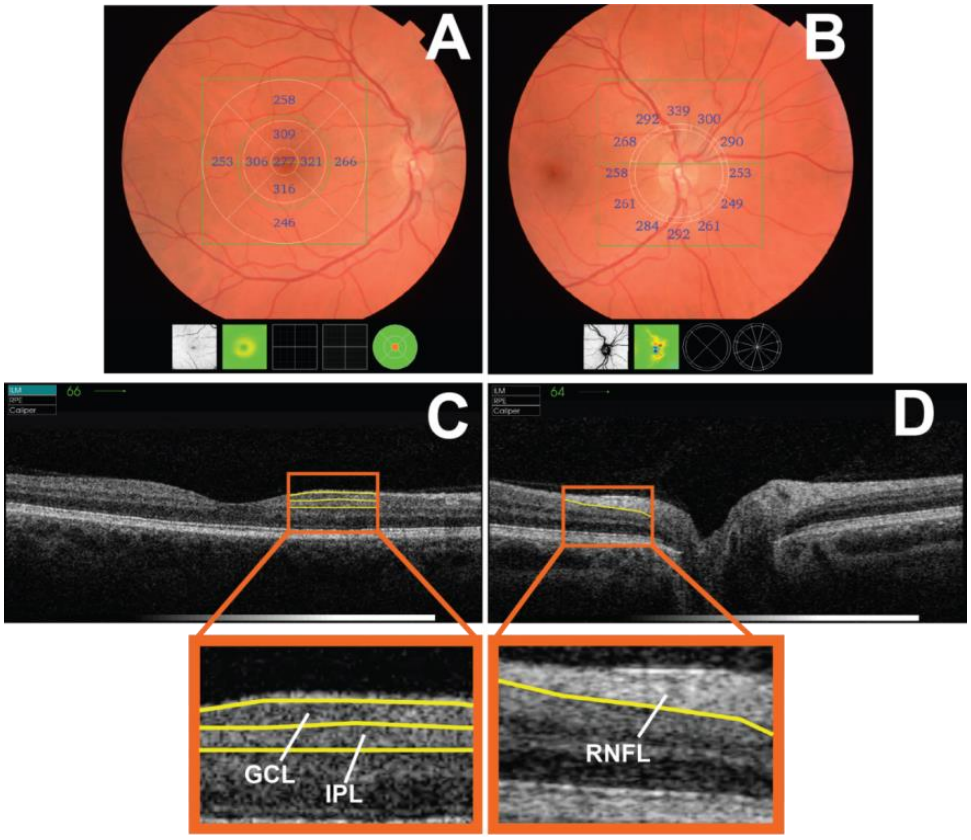

**Assessment of dementia**

Participants were screened for dementia at baseline and at subsequent visits to the study center, using the Mini-Mental State Examination and the Geriatric Mental Schedule organic level. Those with a Mini-Mental State Examination score < 26 or Geriatric Mental Schedule score > 0 underwent further investigation and informant interview, including the Cambridge Examination for Mental Disorders of the Elderly. In addition, the entire cohort was continuously being monitored for dementia through electronic linkage of the study center with medical records from general practitioners and the regional institute for outpatient mental health care. Available information on cognitive testing and clinical neuroimaging was used when required for diagnosis of dementia subtype. A consensus panel led by a consultant neurologist established the final diagnosis according to a standard criteria for dementia (Diagnostic and Statistical Manual of Mental Disorders, version III, Revised), AD (National Institute of Neurological and Communicative Disorders and Stroke-Alzheimer's Disease and Related Disorders Association), and vascular dementia (National Institute of Neurological Disorders and Stroke and Association Internationale pour la Recherché et l'Enseignement en Neurosciences).[20, 21] Follow-up until January 1, 2015, was virtually complete (95% of potential person-years). Within this period, participants were censored at date of dementia diagnosis, death, loss to follow-up, or January 1, 2015, whichever came first.

**Assessment of covariates**

Blood pressure was measured twice in sitting position at the right brachial artery with a random-zero sphygmomanometer, and the average of two readings was used for the analysis. Body mass index was computed as weight (kg) divided by height squared ($m^2$). Fasting serum total and high-density lipoprotein cholesterol concentrations (mmol/L) were determined by an automated enzymatic procedure. Diabetes mellitus was considered present if fasting serum glucose level was equal to or greater than 7.0 mmol/L, or when use of antidiabetic medication was reported. Information on smoking (non, former, or current), education (low, intermediate, or high) and blood pressure lowering medication use was obtained during the home interview by a questionnaire. The axial length of the eyes was measured using Lenstar LS900 (Haag-Streit AG, Köniz, Switzerland).

**Statistical analysis**

Analysis included all individuals who underwent OCT scanning at the research center. We used analysis of covariance, adjusted for age and sex, to assess differences in baseline characteristics between individuals included and excluded from the analysis.

Because the retinal layer thickness is a continuous measure, we first categorized this by taking the median. Subsequently, given an overall cumulative incidence of 3% in our sample and an $\alpha$ of 5%, we calculated a sample size of n = 3023 in order to achieve a power of 80%. In view of this calculation our current sample size is sufficient to examine the

longitudinal associations.[22] As two different generations of OCT devices were used during the course of the study, we standardized the retinal thickness measurements for each device by calculating z-scores. Missing data for the covariates were imputed using fivefold multiple imputation based on determinant, outcome and included covariates. Covariates in the imputed dataset had a similar distribution compared to covariates in the non-imputed dataset. In cross-sectional analysis, we assessed the association of retinal layer thicknesses with prevalent dementia using logistic regression. Using analysis of covariance, adjusted for covariates as in Model 1, we assessed mean differences in retinal layer thickness between individuals with and without dementia. In a subsample where both left and right eyes were scanned, we assessed differences in retinal layer thickness between eyes using a paired t-test. In longitudinal analysis, we excluded individuals with prevalent dementia, and assessed the association of retinal layer thicknesses with the risk of developing dementia and AD using Cox proportional hazards regression. We adjusted for covariates that are generally considered to be important confounders for dementia. In Model 1, we adjusted for age, sex, subcohort, OCT signal strength, axial length of the eye, and education. In Model 2, we additionally adjusted for systolic blood pressure, diastolic blood pressure, use of blood pressure lowering medication, body mass index, total cholesterol, high-density lipoprotein cholesterol, diabetes mellitus, and smoking. The proportionality assumption in the Cox regression models was tested by plotting the Schoenfeld residuals against follow-up time, which showed no deviation from a horizontal line. To avoid overfitting of Model 2, we also adjusted in longitudinal associations for the covariates by means of propensity scores. We used exactly the same covariates as in Model 2 to make the propensity scores. Furthermore, in longitudinal analysis, we studied the association of retinal layer thickness with dementia and AD by making quartiles of the retinal layers and taking the highest quartile as reference and adjusting for covariates as in Model 1. We determined Pearson correlation coefficients between the retinal layers, and investigated the association of retinal layers with prevalent and incident dementia by adjusting the retinal layers for each other. Next, retinal layer thicknesses were combined to assess their combined effect. Finally, we repeated abovementioned analysis for retinal layer thickness and dementia after censoring for stroke, and excluding individuals who developed stroke prior to dementia. All analyses were performed at the 0.05 level of significance (two-tailed) using SPSS version 21.0 (IBM Corporation, Armonk, New York) for Windows.

## RESULTS

Table 1 shows the baseline characteristics of the study population. Compared to individuals included in the analysis, those who were excluded were significantly older, and had a worse cardiovascular risk profile. Moreover, the prevalence of dementia cases in the excluded individuals was nearly 2.5 times higher than those who were included in the analysis. Among the included individuals, prevalent dementia was diagnosed in 45 (1.3%)

individuals in sample I and in 38 (1.2%) individuals in sample II. Among the excluded individuals, these numbers were 50 (3.3%) for sample I and 57 (3.1%) for sample II.
Table 2 shows the association of retinal layer thickness with prevalent dementia. This revealed that thinner GCL was significantly associated with prevalent dementia (Model 1: odds ratio (95% CI) per SD decrease in GCL: 1.53 (1.13-2.08)). For RNFL and IPL, the odds ratios were 1.09 (0.82-1.45) and 1.10 (0.78-1.56), respectively. Mean thickness (μm) with adjusted mean difference (95% CI) in individuals with and without dementia was: 91.48 vs 95.13; -3.65 (-8.17; 0.87) for RNFL, 30.94 vs 33.59; -2.65 (-4.38; -0.92) for GCL; 36.86 vs 36.76; 0.10 (-1.12; 1.32) for IPL. Furthermore, we did not find significant differences in retinal layer thicknesses between the left and right eyes.
In longitudinal analysis, for sample I, total and mean person-time was 15845 years and 4.5 years, respectively (94.9% of potential person-years if there was no loss to follow-up). Of the 3487 individuals at risk for dementia, 90 individuals developed dementia of whom 70 were diagnosed with AD, 4 with vascular dementia, 2 with Parkinson's dementia, 6 with another type of dementia, and 2 remained undetermined. For sample II, total and mean person-time was 14573 years and 4.6 years (94.8% of potential person-years if there was no loss to follow-up). In this sample, of the 3184 individuals at risk for dementia, 64 individuals developed dementia of whom 52 were diagnosed with AD, 3 with vascular dementia, 2 with Parkinson's dementia, 4 with another type of dementia, and 3 remained undetermined.
Table 3 shows the association of retinal layer thicknesses with incident dementia. Thinner RNFL at baseline was significantly associated with a higher risk of developing dementia (hazard ratio (HR) per SD decrease in RNFL: 1.51 (95% CI: 1.26-1.82)). After adjustment for cardiovascular risk factors, this association attenuated slightly, but remained statistically significant (HR: 1.45, 95% CI: 1.20-1.75). Similar associations were observed for AD (adjusted HR: 1.44 (95% CI: 1.16-1.79). We found no significant association for the association of GCL and IPL thickness with incident dementia. In order to avoid overfitting of Model 2, adjustment for the covariates was undertaken by means of propensity scores. Yet, all our effect associations remained similar to the effect estimates obtained by adjusting for the covariates in Model 2.
Supplemental Table 1 shows the association of retinal layer thicknesses in quartiles with incident dementia. We found that individuals in the lowest quartile of RNFL thickness had a higher risk of developing dementia compared to individuals in the highest quartile, HR: 2.68 (1.44-5.00). For incident AD, the magnitude of the effect estimates across the quartiles remained similar with particularly higher HRs for GCL.
Supplemental Table 2 shows the association of retinal layer thickness with prevalent and incident dementia after adjusting the retinal layers for each other. Pearson correlation was 0.380 between RNFL and GCL; 0.099 between RNFL and IPL; 0.273 between GCL and IPL. When combining the retinal layers, the associations were primarily driven by the association of GCL (cross-sectional) and RNFL (longitudinal) with dementia

(Supplemental Table 3).

Of all dementia cases, 7 (sample I) and 5 (sample II) cases were preceded by a stroke, for both samples, a median 2.5 year before diagnosis of dementia. After censoring for stroke, the associations of RNFL thickness with all dementia and AD, if anything, became stronger, adjusted HR for dementia and AD: 1.58 (1.31-1.91) and 1.58 (1.28-1.95), respectively. After excluding these individuals, the adjusted HRs (95% CI) for RNFL, GCL, and IPL were: 1.51 (1.21-1.89), 1.11 (0.84-1.46), and 1.08 (0.83-1.39), respectively.

**Table 1. Baseline characteristics of the study population.**

| | Descriptive | | | |
|---|---|---|---|---|
| | Sample I | | Sample II | |
| **Characteristic** | **Included** | **Excluded‡** | **Included** | **Excluded‡** |
| N | 3532 | 1533 | 3222 | 1843 |
| Age, years | 68.8 (10.0) | 72.6 (11.0)* | 68.0 (9.9) | 73.3 (10.5)* |
| Female sex | 2006 (57) | 907 (59) | 1835 (57) | 1078 (59) |
| Systolic blood pressure, mmHg | 145.7 (22.3) | 147.4 (24.1) | 145.5 (22.4) | 147.5 (23.5)* |
| Diastolic blood pressure, mmHg | 84.6 (11.1) | 83.9 (11.7)* | 84.9 (11.2) | 83.5 (11.4)* |
| Blood pressure lowering medication | 1540 (44) | 848 (55)* | 1365 (42) | 1025 (56)* |
| Body mass index, kg/m$^2$ | 27.5 (4.3) | 27.8 (4.5)* | 27.5 (4.2) | 27.6 (4.5) |
| Diabetes mellitus | 399 (11) | 227 (15)* | 357 (11) | 269 (15)* |
| Total cholesterol, mmol/L | 5.5 (1.1) | 5.3 (1.1)* | 5.5 (1.1) | 5.3 (1.1)* |
| HDL cholesterol, mmol/L | 1.5 (0.4) | 1.4 (0.4)* | 1.5 (0.4) | 1.4 (0.4)* |
| Smoking status | | | | |
| Non-smoker | 1112 (32) | 489 (32) | 1024 (32) | 579 (31) |
| Former smoker | 1853 (52) | 764 (50)* | 1674 (52) | 939 (51)* |
| Current smoker | 567 (16) | 271 (18)* | 524 (16) | 314 (17)* |
| Education | | | | |
| Lower education | 1081 (31) | 573 (37)* | 966 (30) | 692 (38)* |
| Intermediate education | 1706 (48) | 683 (45) | 1549 (48) | 835 (45) |
| Higher education | 745 (21) | 249 (16) | 707 (22) | 285 (16)* |
| Right eyes | 3356 (95) | - | 3029 (94) | - |
| Axial length of the eye, mm | 23.5 (1.1) | - | 23.5 (1.1) | - |
| Peripapillary retinal nerve fiber layer, µm | 95.1 (15.8) | - | - | - |
| Macular ganglion cell layer, µm | - | - | 33.6 (5.5) | - |
| Macular inner plexiform layer, µm | - | - | 36.8 (3.9) | - |
| Prevalent dementia | 45 (1.3) | 50 (3.3)* | 38 (1.2) | 57 (3.1)* |

Values are presented as means (standard deviation) or as numbers (percentage).

Abbreviation: HDL, high-density lipoprotein.

‡ Missing values are not imputed.

*Age-and sex adjusted mean differences ($p < 0.05$).

Percentage of missing values for all variables was less than 2%, except for axial length it was less than 12%.

**Table 2. Association of retinal layer thickness with prevalent dementia.**

| | All dementia | | |
|---|---|---|---|
| | | Odds ratio (95% CI) | |
| **Per SD decrease in** | **n/N** | **Model 1** | **Model 2** |
| Retinal nerve fiber layer | 45/3532 | 1.09 (0.82-1.45) | 1.06 (0.80-1.42) |
| Ganglion cell layer | 38/3222 | 1.53 (1.13-2.08) | 1.51 (1.11-2.06) |
| Inner plexiform layer | 38/3222 | 1.10 (0.78-1.56) | 1.12 (0.80-1.56) |

Abbreviations: SD, standard deviation; n/N, number of individuals with dementia/total number of individuals.
Model 1: adjusted for age, sex, subcohort, signal strength, axial length of the eye, and education.
Model 2: as in Model 1 and additionally adjusted for systolic blood pressure, diastolic blood pressure, blood pressure lowering medication, body mass index, total cholesterol, high-density lipoprotein cholesterol, diabetes mellitus, and smoking.

**Table 3. Association of retinal layer thickness with incident dementia.**

| | All dementia | | | Alzheimer's disease | | |
|---|---|---|---|---|---|---|
| | | Hazard ratio (95% CI) | | | Hazard ratio (95% CI) | |
| **Per SD decrease in** | **n/N** | **Model 1** | **Model 2** | **n/N** | **Model 1** | **Model 2** |
| Retinal nerve fiber layer | 90/3487 | 1.51 (1.26-1.82) | 1.45 (1.20-1.75) | 70/3487 | 1.51 (1.22-1.85) | 1.44 (1.16-1.79) |
| Ganglion cell layer | 64/3184 | 1.11 (0.87-1.41) | 1.10 (0.86-1.41) | 52/3273 | 1.14 (0.87-1.48) | 1.13 (0.86-1.48) |
| Inner plexiform layer | 64/3184 | 1.09 (0.86-1.38) | 1.10 (0.88-1.39) | 52/3273 | 1.08 (0.83-1.40) | 1.11 (0.86-1.42) |

Abbreviations: SD, standard deviation; n/N, number of individuals with dementia/total number of individuals.
Model 1: adjusted for age, sex, subcohort, signal strength, axial length of the eye, and education.
Model 2: as in Model 1 and additionally adjusted for systolic blood pressure, diastolic blood pressure, blood pressure lowering medication, body mass index, total cholesterol, high-density lipoprotein cholesterol, diabetes mellitus, and smoking.

**Supplemental Table 1. Association of retinal layer thickness in quartiles with risk of dementia and Alzheimer's disease.**

| | All dementia | | | | | |
|---|---|---|---|---|---|---|
| | | Hazard ratio (95% CI) | | | | |
| Quartiles | n/N | Retinal nerve fiber layer | n/N | Ganglion cell layer | n/N | Inner plexiform layer |
| 4th quartile | 14/872 | 1.00 (reference) | 12/796 | 1.00 (reference) | 7/796 | 1.00 (reference) |
| 3rd quartile | 17/872 | 1.19 (0.58-2.43) | 8/796 | 1.44 (0.57-3.64) | 13/797 | 0.54 (0.22-1.33) |
| 2nd quartile | 14/872 | 1.10 (0.52-2.34) | 22/796 | 1.95 (0.82-4.64) | 20/795 | 1.40 (0.69-2.86) |
| 1st quartile | 45/871 | 2.68 (1.44-5.00) | 22/796 | 1.73 (0.73-4.10) | 24/796 | 1.22 (0.59-2.52) |
| P-value for trend | | 0.001 | | 0.194 | | 0.173 |
| | **Alzheimer's disease** | | | | | |
| | | **Hazard ratio (95% CI)** | | | | |
| Quartiles | n/N | Retinal nerve fiber layer | n/N | Ganglion cell layer | n/N | Inner plexiform layer |
| 4th quartile | 11/872 | 1.00 (reference) | 4/796 | 1.00 (reference) | 10/796 | 1.00 (reference) |
| 3rd quartile | 13/872 | 1.13 (0.50-2.54) | 12/796 | 2.15 (0.69-6.76) | 6/796 | 0.48 (0.17-1.34) |
| 2nd quartile | 11/872 | 1.09 (0.47-2.52) | 16/796 | 2.61 (0.87-7.85) | 19/796 | 1.45 (0.67-3.15) |
| 1st quartile | 35/871 | 2.57 (1.27-5.19) | 20/796 | 2.27 (0.76-6.78) | 17/796 | 1.09 (0.49-2.45) |
| P-value for trend | | 0.003 | | 0.211 | | 0.297 |

Abbreviations: CI, confidence interval; n/N, number of individuals with Alzheimer's disease/total number of individuals.
Values are adjusted for age, sex, subcohort, signal strength, axial length of the eye, and education.
Minimum to maximum (mean) retinal nerve fiber layer thickness for each quartile was: 32.87-86.01 (74.9) µm for the first quartile, 86.04-96.00 (91.2) µm for the second quartile, 96.00-105.35 (100.7) µm for the third quartile, and 105.35-210.10 (113.7) µm for the fourth quartile. Minimum to maximum (mean) ganglion cell layer thickness for each quartile was: 6.52-30.64 (26.8) µm for the first quartile, 30.64-33.77 (32.2) µm for the second quartile, 33.77-36.97 (35.3) µm for the third quartile, and 36.98-73.93 (40.1) µm for the fourth quartile.

**Supplemental Table 2. Association of retinal layer thickness with prevalent and incident dementia adjusting the retinal layers for each other.**

| | Odds ratio (95% CI), n/N: 34/3032 | | Hazard ratio (95% CI), n/N: 63/2998 | |
|---|---|---|---|---|
| **Per SD decrease in** | **Model 1** | **Model 2** | **Model 1** | **Model 2** |
| Retinal nerve fiber layer | 1.06 (0.76-1.48) | 0.81 (0.57-1.17) | 1.52 (1.20-1.93) | 1.51 (1.18-1.94) |
| Ganglion cell layer | 1.58 (1.15-2.17) | 1.76 (1.22-2.54) | 1.14 (0.89-1.46) | 0.99 (0.75-1.31) |
| Inner plexiform layer | 1.08 (0.76-1.53) | 0.91 (0.68-1.22) | 1.11 (0.87-1.42) | 1.09 (0.80-1.49) |

Abbreviations: CI, confidence interval; SD, standard deviation; n/N, number of individuals with dementia/total number of individuals.
Model 1: adjusted for age, sex, subcohort, signal strength, axial length of the eye, and education.
Model 2: as in Model 1 and additionally adjusted the retinal layers for each other.

**Supplemental Table 3. Association of composite retinal layer thickness with prevalent and incident dementia.**

| **Per SD decrease in** | **Odds ratio (95% CI), n/N: 34/3032** | **Hazard ratio (95% CI), n/N: 63/2998** |
|---|---|---|
| RNFL-GCL-IPL complex | 1.12 (0.80-1.57) | 1.46 (1.17-1.82) |
| RNFL-GCL complex | 1.13 (0.81-1.57) | 1.46 (1.17-1.83) |
| RNFL-IPL complex | 0.97 (0.69-1.37) | 1.48 (1.19-1.85) |
| GCL-IPL complex | 1.41 (1.03-1.95) | 1.16 (0.91-1.47) |

Abbreviations: CI, confidence interval; SD, standard deviation; n/N, number of individuals with dementia/total number of individuals; RNFL, retinal nerve fiber layer; GCL, ganglion cell layer; IPL, inner plexiform layer.
Values are adjusted for age, sex, subcohort, signal strength, axial length of the eye, and education.

## DISCUSSION

In this prospective population-based cohort study in the general adult Dutch population, we found that thinner GCL at baseline was associated with prevalent dementia and that thinner RNFL was associated with a higher risk of developing dementia, including AD, independent of cardiovascular risk factors.

Thus far, evidence for retinal involvement in AD pathology comes primarily from histopathological studies, in which postmortem specimens were examined. Those early studies have shown that people with AD had substantial loss of retinal ganglion cells and thinner RNFL compared to controls.[23, 24] Subsequently, several clinical-based studies have consistently observed thinning of the RNFL among people with AD using optical imaging techniques in vivo.[8, 9] Advances in OCT technology allowed us to observe the retina in greater detail and enabled automated segmentation of other retinal layers as well. Hence, apart from the RNFL, studies have shown that people with AD had thinner RNFL, GCL and GCL–IPL complex compared to cognitively healthy controls, suggesting that thinner GC–IPL complex is accompanied by thinner peripapillary RNFL.[10-12] Despite methodological differences between previous studies, these studies have successfully demonstrated that OCT imaging provides a great opportunity to assess neurodegeneration in individuals with and without AD. However, due to the cross-sectional nature of those studies, the temporal relation remained unclear, that is, whether retinal thinning preceded the clinical manifestation of AD or was only seen after a diagnosis had been made. In line with findings from these previous studies, we also found that particularly thinner GCL was associated with prevalent dementia. More importantly, our study is the first that shows an association between thinner RNFL and the risk of dementia, including AD.

In the pathophysiology of dementia, damage to brain regions covering the visual tract may cause retrograde degeneration of the optic nerve (i.e. Wallerian degeneration) by affecting the neuronal connections of the visual tract. Subsequently, this cerebral neurodegenerative process may manifest itself in the retina initially as thinning of the RNFL, after which thinning of the GCL follows. With the improved resolution of the OCT enabling to measure the GCL thickness, recent studies have repeatedly and consistently observed not only thinner RNFL but also thinner GCL in people with AD.[10-12] Moreover, a recent study has shown that a reduction in GCL–IPL complex at baseline was associated with the progression of AD as measured by Clinical Dementia Rating Scale.[11] Hence, given our findings, it is possible that thinning of the GCL is reflecting more advanced stages of AD-pathology. However, if this hypothesis holds, an important question remains why thinner RNFL was not associated with prevalent dementia. We acknowledge that this finding is difficult to explain, but we speculate that the time course when dementia occurs might play a role. For instance, animal studies showed that damage to the optic nerve causes swelling and gliosis formation of the axons.[25-27] In fact, there appears to be a time delay between optic nerve degeneration and retinal ganglion cell loss, during which swelling or gliosis

formation of structures can occur, and after which structural losses become more evident. Furthermore, apart from loss of power due to smaller number of prevalent dementia cases available, another possibility might be that differences between those included and excluded may have introduced selection bias in our cross-sectional analyses, and thus may underlie the lack of an association between RNFL and prevalent dementia. In contrast, in the longitudinal analyses, selection bias was not an issue, because our follow-up for incident dementia was virtually complete.

Another complementary explanation for our findings might be that a common pathogenesis may underlie the association between retinal layer thickness and dementia. Studies have observed the accumulation of amyloid-beta deposits both in the retina and brain of transgenic mouse models, and corroborated those findings in postmortem studies in people with AD.[3, 4, 28, 29] Although the exact mechanisms that underlie the forming of amyloid plaques are unknown, factors associated with the formation of these plaques such as inflammatory markers and genetic variants, may partly explain our findings. However, we were not able to control for such confounding factors.

Several methodological aspects of our study need to be discussed. First, individuals excluded from our study may have had a poor health, resulting in selection of relatively healthy individuals in our analysis. Second, the segmentation algorithms may have misclassified the retinal layers e.g. the GCL as the IPL and vice versa. Third, participants in the Rotterdam Study were mainly middle-class white individuals, which limits the generalizability of our findings. Another limitation might be that we performed OCT in the right eyes. Previous studies have suggested that there might be structural and functional differences between the eyes.[30] However, in a subsample we did not find significant differences in retinal layer thickness between left and right eyes at a population level. Hence, we do not think that local ocular differences will have influences the associations we found with dementia. Finally, we did not use other retinal layer thickness, because the reliability of the segmentation for outer layers were poor and the thickness measurements were not comparable across the two OCT devices. Strengths of our study include the population-based setting, the longitudinal design and thorough collection of events.

In conclusion, we found that thinner GCL at baseline was associated with prevalent dementia and that thinner RNFL was associated with an increased risk of developing dementia, including AD. These findings suggest that thinner RNFL may be a novel biomarker for dementia, specifically for AD. Moreover, there is an opportunity to use OCT in clinical or research settings as an accessible and noninvasive tool to help clinicians or researchers in eligibility determination for clinical trials, in monitoring disease progression or in evaluating treatment response.

## REFERENCES


1. Prince M, Bryce R, Albanese E, Wimo A, Ribeiro W, Ferri CP. The global prevalence of dementia: A systematic review and metaanalysis. Alzheimers Dement. 2013;9:63-75 e62
2. Sperling RA, Aisen PS, Beckett LA, Bennett DA, Craft S, Fagan AM, et al. Toward defining the preclinical stages of alzheimer's disease: Recommendations from the national institute on aging-alzheimer's association workgroups on diagnostic guidelines for alzheimer's disease. Alzheimers Dement. 2011;7:280-292
3. Koronyo-Hamaoui M, Koronyo Y, Ljubimov AV, Miller CA, Ko MK, Black KL, et al. Identification of amyloid plaques in retinas from alzheimer's patients and noninvasive in vivo optical imaging of retinal plaques in a mouse model. Neuroimage. 2011;54 Suppl 1:S204-217
4. Koronyo Y, Biggs D, Barron E, Boyer DS, Pearlman JA, Au WJ, et al. Retinal amyloid pathology and proof-of-concept imaging trial in alzheimer's disease. JCI Insight. 2017;2
5. McGrory S, Cameron JR, Pellegrini E, Warren C, Doubal FN, Deary IJ, et al. The application of retinal fundus camera imaging in dementia: A systematic review. Alzheimers Dement (Amst). 2017;6:91-107
6. Hart NJ, Koronyo Y, Black KL, Koronyo-Hamaoui M. Ocular indicators of alzheimer's: Exploring disease in the retina. Acta Neuropathol. 2016;132:767-787
7. Javaid FZ, Brenton J, Guo L, Cordeiro MF. Visual and ocular manifestations of alzheimer's disease and their use as biomarkers for diagnosis and progression. Front Neurol. 2016;7:55
8. Coppola G, Di Renzo A, Ziccardi L, Martelli F, Fadda A, Manni G, et al. Optical coherence tomography in alzheimer's disease: A meta-analysis. PLoS One. 2015;10:e0134750
9. den Haan J, Verbraak FD, Visser PJ, Bouwman FH. Retinal thickness in alzheimer's disease: A systematic review and meta-analysis. Alzheimers Dement (Amst). 2017;6:162-170
10. Cheung CY, Ong YT, Hilal S, Ikram MK, Low S, Ong YL, et al. Retinal ganglion cell analysis using high-definition optical coherence tomography in patients with mild cognitive impairment and alzheimer's disease. J Alzheimers Dis. 2015;45:45-56
11. Choi SH, Park SJ, Kim NR. Macular ganglion cell -inner plexiform layer thickness is associated with clinical progression in mild cognitive impairment and alzheimers disease. PLoS One. 2016;11:e0162202
12. Marziani E, Pomati S, Ramolfo P, Cigada M, Giani A, Mariani C, et al. Evaluation of retinal nerve fiber layer and ganglion cell layer thickness in alzheimer's disease using spectral-domain optical coherence tomography. Invest Ophthalmol Vis Sci. 2013;54:5953-5958
13. Ong YT, Hilal S, Cheung CY, Venketasubramanian N, Niessen WJ, Vrooman H, et al. Retinal neurodegeneration on optical coherence tomography and cerebral atrophy. Neurosci Lett. 2015;584:12-16
14. Mutlu U, Bonnemaijer PWM, Ikram MA, Colijn JM, Cremers LGM, Buitendijk GHS, et al. Retinal neurodegeneration and brain mri markers: The rotterdam study. Neurobiol Aging. 2017
15. Hofman A, Brusselle GG, Darwish Murad S, van Duijn CM, Franco OH, Goedegebure A, et al. The rotterdam study: 2016 objectives and design update. Eur J Epidemiol. 2015;30:661-708
16. Terry L, Cassels N, Lu K, Acton JH, Margrain TH, North RV, et al. Automated retinal layer segmentation using spectral domain optical coherence tomography: Evaluation of inter-session repeatability and agreement between devices. PLoS One. 2016;11:e0162001
17. Lee K, Buitendijk GH, Bogunovic H, Springelkamp H, Hofman A, Wahle A, et al. Automated segmentability index for layer segmentation of macular sd-oct images. Transl Vis Sci Technol. 2016;5:14
18. Patel PJ, Foster PJ, Grossi CM, Keane PA, Ko F, Lotery A, et al. Spectral-domain optical coherence tomography imaging in 67 321 adults: Associations with macular thickness in the uk biobank study. Ophthalmology. 2016;123:829-840
19. Keane PA, Grossi CM, Foster PJ, Yang Q, Reisman CA, Chan K, et al. Optical coherence tomography in the uk biobank study - rapid automated analysis of retinal thickness for large population-based studies. PLoS One. 2016;11:e0164095

20. McKhann G, Drachman D, Folstein M, Katzman R, Price D, Stadlan EM. Clinical diagnosis of alzheimer's disease: Report of the nincds-adrda work group under the auspices of department of health and human services task force on alzheimer's disease. Neurology. 1984;34:939-944
21. Roman GC, Tatemichi TK, Erkinjuntti T, Cummings JL, Masdeu JC, Garcia JH, et al. Vascular dementia: Diagnostic criteria for research studies. Report of the ninds-airen international workshop. Neurology. 1993;43:250-260
22. Chow S; Shao J; Wang H; Lokhnygina Y. Sample size calculations in clinical research. Chapman & Hall/CRC 2017.
23. Hinton DR, Sadun AA, Blanks JC, Miller CA. Optic-nerve degeneration in alzheimer's disease. N Engl J Med. 1986;315:485-487
24. Blanks JC, Hinton DR, Sadun AA, Miller CA. Retinal ganglion cell degeneration in alzheimer's disease. Brain Res. 1989;501:364-372
25. Rovere G, Nadal-Nicolas FM, Agudo-Barriuso M, Sobrado-Calvo P, Nieto-Lopez L, Nucci C, et al. Comparison of retinal nerve fiber layer thinning and retinal ganglion cell loss after optic nerve transection in adult albino rats. Invest Ophthalmol Vis Sci. 2015;56:4487-4498
26. Abbott CJ, Choe TE, Lusardi TA, Burgoyne CF, Wang L, Fortune B. Evaluation of retinal nerve fiber layer thickness and axonal transport 1 and 2 weeks after 8 hours of acute intraocular pressure elevation in rats. Invest Ophthalmol Vis Sci. 2014;55:674-687
27. Vidal-Sanz M, Galindo-Romero C, Valiente-Soriano FJ, Nadal-Nicolas FM, Ortin-Martinez A, Rovere G, et al. Shared and differential retinal responses against optic nerve injury and ocular hypertension. Front Neurosci. 2017;11:235
28. Koronyo Y, Salumbides BC, Black KL, Koronyo-Hamaoui M. Alzheimer's disease in the retina: Imaging retinal abeta plaques for early diagnosis and therapy assessment. Neurodegener Dis. 2012;10:285-293
29. Ning A, Cui J, To E, Ashe KH, Matsubara J. Amyloid-beta deposits lead to retinal degeneration in a mouse model of alzheimer disease. Invest Ophthalmol Vis Sci. 2008;49:5136-5143
30. Cameron JR, Megaw RD, Tatham AJ, McGrory S, MacGillivray TJ, Doubal FN, et al. Lateral thinking - interocular symmetry and asymmetry in neurovascular patterning, in health and disease. Prog Retin Eye Res. 2017;59:131-157

# Chapter 5.3
# Retinal Microvasculature is Associated with Long-Term Survival in the General Adult Dutch Population

Unal Mutlu, M. Kamran Ikram, Frank J. Wolters, Albert Hofman, Caroline C.W. Klaver, M. Arfan Ikram

**ABSTRACT**

**Background:** Retinal vascular diameters are associated with (sub)clinical cardiovascular disease and short-term cardiovascular mortality, but their association with long-term mortality is uncertain. We studied the association of retinal vascular diameters with cause-specific mortality in the general adult Dutch population during 25 years of follow-up.
**Methods:** From 1990 to1993, arteriolar and venular diameters were measured semi-automatically on digitized images in 5674 persons (mean age 68.0 years, 59% women) from the population-based Rotterdam Study. Follow-up for mortality was complete till March 2015. Associations between vascular diameters and mortality were examined using Cox proportional hazards models, adjusting for age, sex, cardiovascular risk factors, and the fellow vessel diameter.
**Results:** During 85770 person-years (mean ± standard deviation: 15.1 ± 6.67), 3794 (66.8%) persons died, of whom 1034 due to cardiovascular causes. We found that narrower arterioles and wider venules were associated with higher risk of mortality (adjusted hazard ratio (95% confidence interval) per standard deviation decrease in arterioles 1.04 (1.00-1.08) and increase in venules 1.07 (1.03-1.12)). For arterioles, these associations were strongest for cardiovascular mortality, whereas venules showed consistent associations for cardiovascular and non-cardiovascular mortality. Importantly, these associations remained unchanged after excluding the first 10 years of follow-up as immortal person-time. We found evidence for effect modification with stronger associations in persons < 70 years (venules only) and smokers (p-value for interaction terms < 0.01). We replicated our findings in another independent cohort from the Rotterdam Study of 3106 persons with 19880 person-years of follow-up and 144 deaths (hazard ratio for venules 1.22 (1.00-1.49)).
**Conclusions:** Markers of retinal microvasculature are associated with long-term mortality in the general adult Dutch population.

## INTRODUCTION

Cardiovascular diseases remain the most common cause of death worldwide, accounting for up to 23.1% of all deaths.[1] In addition, cardiovascular risk factors and subclinical cardiovascular pathology contribute to deaths that might not be formally classified as cardiovascular, such as due to chronic obstructive pulmonary disease, diabetes mellitus, dementia, or even cancer.[2, 3] An important cornerstone in cardiovascular research has been the identification of early biomarkers that relate to subclinical and clinical disease as well as subsequent mortality. Such markers are not only important for understanding pathogenesis or disease monitoring, but – if feasible in community-dwelling individuals – can also serve as potential intervention targets for prevention or even used as risk predictors. For instance, coronary calcification and carotid plaques are strong predictors of myocardial infarction and stroke, and also associate with subsequent mortality.[4, 5] However, most population-based research on cardiovascular biomarkers has revolved around noninvasive imaging of the large or medium-sized vessels, for example, aorta, carotid arteries, and coronary arteries.[6] Yet, it is increasingly recognized that the microvasculature is important for cardiovascular health as well.[7, 8] Retinal imaging provides a unique opportunity to visualize the microvasculature in vivo and indeed, there is now abundant literature demonstrating strong associations of retinal markers with cardiovascular diseases.[9-11] By extension, several studies have shown an association of retinal microvasculature with cardiovascular mortality, but these studies usually had a short follow-up.[12-14] To really play a role as long-term biomarker, it is important to establish a link between retinal microvasculature with long-term mortality. This entails not only extending the follow-up time but also investigating long-term associations after accounting for the short-term increased risk. Moreover, it is interesting to study the role of the microvasculature in non-cardiovascular mortality, especially given the established link between microvessels and diseases such as diabetes mellitus, dementia, and chronic obstructive pulmonary disease. Therefore, we studied the association between retinal microvasculature and long-term cause-specific mortality in the general adult Dutch population.

## METHODS

### Study setting and population

This study was performed as part of the Rotterdam Study (RS), a prospective population-based cohort study, details of which have been described previously.[15] In brief, the initial cohort (RS-I) started in 1990 and there have been two expansion waves: in 2000 (RS-II) and 2005 (RS-III). Retinal vessel diameters were systematically quantified in RS-I and RS-III. For the this study, the main analyses were carried out in RS-I, which was the largest sample with longest follow-up, whereas RS-III served as a replication sample. For RS-I, all inhabitants of the Ommoord district in the city of Rotterdam, the Netherlands, aged ≥ 55 years were invited to the study, of whom 7983 participated (overall response 78%). Because the ophthalmic part became only operational after the study had started, a total of 6780 participants underwent ophthalmic examination in RS-I. Baseline home interviews and examinations were performed from 1990 to 1993. For RS-III, we invited all inhabitants who reached the age of 45 years, or migrated into the study district since the start of RS-I, but who were not part of RS-II. A total of 3932 people enrolled (overall response 64.9%), and baseline data were collected from 2005 to 2009. The Rotterdam Study has been approved by the medical ethics committee according to the Population Study Act Rotterdam Study, executed by the Ministry of Health, Welfare and Sports of the Netherlands. A written informed consent was obtained from all participants. This study adhered to the principles of the declaration of Helsinki.

### Assessment of retinal vessels

In both RS-I and RS-III, participants underwent a full eye examination at baseline including fundus color photography of the optic disc after pharmacological mydriasis (20° visual field TRC-SS2 (RS-I) and 35° visual field TRC-50EX (RS-III), Topcon Optical Company, Tokyo, Japan). For each participant, the image of one eye with the best quality was analyzed with a retinal vessel measurement system (IVAN, University of Wisconsin-Madison, Madison, Wisconsin).[16] For each participant, one summary value was calculated for the arteriolar diameters (in μm) and one for the venular diameters (in μm) of the blood column after correction for differences in magnification due to refractive status of the eye, enabling us to use the separate arteriolar and venular diameter sum values.[17-19] We verified in a random subsample of 100 participants in RS-I that individual measurements in the left and right eye were similar. Measurements were performed by four (RS-I) and one (RS-III) trained raters, masked for participant characteristics, masked for the endpoints, and blinded to each other's measurements. Pearson correlation coefficients for interrater agreement in RS-I (n = 40) and RS-III (n = 100) were for arteriolar diameters 0.67 to 0.80 and 0.85, and for venular diameters 0.91 to 0.94 and 0.87, respectively. For intrarater agreement, the correlation coefficients were 0.69 to 0.88 and 0.86 for arteriolar diameters, and 0.90 to 0.95 and 0.87 for venular diameters, respectively.

**Assessment of cause-specific and all-cause mortality**

For the entire cohort from baseline onwards, information on vital status was obtained for cause-specific mortality and all-cause mortality from the municipal health services in Rotterdam on a biweekly basis. Also, the general practitioners in the study area reported deaths on a continuous basis. Specially trained study personnel verified reported deaths by checking the medical records. Research physicians reviewed all available information and independently coded the events according to the International Classification of Diseases, Tenth Revision (ICD-10). Cases on which they disagreed were discussed to reach consensus in a separate session. If the cause of death was coded as I20–25, I46, I50, I61, I63, I64, I66, I68–70, or R96, the cause of death was labelled as cardiovascular. The following codes (label) were all labelled as non-cardiovascular mortality: A32-B99 (infectious disease), C00-C97 (cancer), F00-F03 (dementia), J15-J19 (pneumonia), J30-J98 (chronic respiratory disease), S12.1, S32-72 or T90.2 (fracture), and the remaining codes (other). A consensus panel of medical specialists in cardiovascular disease and internal medicine, adjudicated the final cause of death according to ICD-10 codes using standardized definitions, as described in detail previously.[20] This panel consisted of a cardiologist, two geriatricians, and a general practitioner experienced in cardiac disease, and their judgement was considered decisive.

All participants were followed up from date of study entry until date of death, 15 March 2015 (for all-cause mortality) or 1 January 2013 (for cause-specific mortality). A flow diagram of the study population is depicted in Supplemental Figure 1. Data on vital status was complete.

**Supplemental Figure 1.** Flow diagram of the study population.

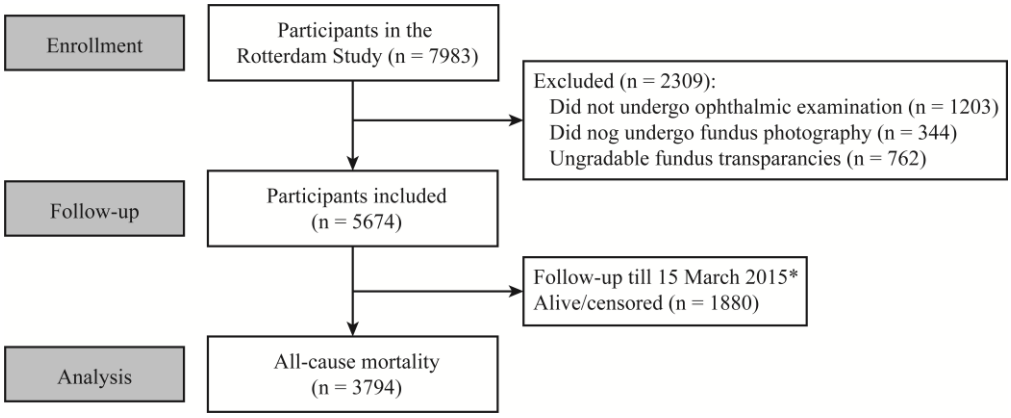


*Follow-up for cause-specific mortality was till 1 January 2013 (alive/censored n = 2216).

**Assessment of covariates**

In both cohorts, baseline blood pressure was measured twice in sitting position at the right brachial artery with a random-zero sphygmomanometer. We used the average of two readings for analysis. Body mass index was computed as weight (kg) divided by height squared ($m^2$). Serum total and high-density lipoprotein cholesterol concentrations were determined by an automated enzymatic procedure.[21] Diabetes mellitus was considered present if participants reported use of antidiabetic medication or when non-fasting serum glucose level was equal to or greater than 11.1 mmol/L, or when fasting serum glucose level was equal to or greater than 7.0 mmol/L. Serum levels of C-reactive protein were determined by a near-infrared particle immunoassay method (Immage, Beckman Coulter, Fullerton, California). Carotid plaques were assessed by ultrasound at the carotid artery bifurcation, common carotid artery, and internal carotid artery on both sides. Plaques were defined as focal thickening of the vessel wall of at least 1.5 times the average intima-media thickness for RS-I, or at least 2 mm thickening of the intima-media thickness for RS-III, relative to adjacent segments with or without calcified components.[22] The carotid artery plaque score (range: 0-6) reflected the number of these locations with plaques. Information on smoking (categorized as current, former or never) and antihypertensive medication use was obtained during the home interview by a computerized questionnaire.

**Statistical analysis**

Analysis included all participants who underwent ophthalmological examination at the study center. We used analysis of covariance, adjusted for age and sex, to assess differences in baseline characteristics between participants and non-participants from the eligibility cohort. We determined associations between baseline retinal vessel diameter (arteriolar and venular) and all-cause and cause-specific mortality, using Cox proportional hazards models. Hazard ratios (HRs) with corresponding 95% confidence intervals (CIs) for mortality were calculated per standard deviation (SD) decrease in arterioles or increase in venules, and per quartile of retinal vessel diameter, adjusted for age, sex, the other vessel diameter, and additionally for systolic and diastolic blood pressure, antihypertensive medication, body mass index, serum total and high-density lipoprotein cholesterol, diabetes mellitus, C-reactive protein, carotid artery plaque score, and baseline history of smoking. We subsequently determined HRs after excluding 10-year immortal person-time to investigate whether retinal vessel diameters were specifically associated with mortality in the long term. We also explored effect modification by stratifying for sex, age, diabetes mellitus, hypertension, smoking status and carotid artery plaque score and by constructing interaction terms in the statistical models.

In RS-III, similar models were constructed, but we only considered all-cause mortality, since the numbers of cause-specific mortality were too small. We explored the possibility of collinearity, given the Pearson correlation coefficient between arteriolar and venular diameter ($r = 0.59$), using the variance inflation factor, but no indication of high collinearity

was identified (variance inflation factor < 1.1). Analyses were performed using SPSS version 21.0 (IBM Corporation, Armonk, New York) for Windows.

**RESULTS**

Of 6780 participants undergoing ophthalmic examination in RS-I, 6436 persons underwent optic disc photography. From these, fundus transparencies of 762 (11.2%) persons could not be rated on either eye, leaving 5674 participants for analysis. Compared to participants, non-participants were significantly older, and more often had diabetes mellitus and hypertension, a lower body mass index, higher diastolic blood pressure and higher serum levels of C-reactive protein (Table 1).

During a total follow-up of 85,770 person-years (mean ± SD: 15.1 ± 6.67), 3794 (66.8%) participants died. Cause of death was cardiovascular in 1079 participants (19.0%) predominantly due to cardiac arrest (n = 183), heart failure (n = 230), stroke (n = 264) and myocardial infarction (n = 183). Non-cardiovascular cause of death in 2379 participants (41.9%) was due to infectious disease (n = 56), cancer (n = 910), dementia (n = 348), pneumonia (n = 103), chronic respiratory disease (n = 123), fracture (n = 65), and other remaining causes (n = 774).

Figure 1 shows the hazard of all-cause mortality associated with retinal vessel diameters, both continuously and in quartiles. Both narrower arterioles and wider venules were associated with an increased risk of mortality (HR (95% CI) for arterioles per SD decrease 1.05 (1.01-1.09), and HR for venules per SD increase 1.11 (1.07-1.16)). Adjustment for cardiovascular risk factors had no effect on arterioles (HR per SD decrease 1.04 (1.00-1.08)), but attenuated the effect size for venules, although it remained statistically significant (HR per SD increase 1.07 (1.03-1.12)).

Table 2 shows the hazard of cause-specific mortality in relation to retinal vessel diameters. We found that the increased risk of mortality associated with arterioles was primarily driven by the association of arterioles with cardiovascular mortality. In contrast, the effect sizes of cardiovascular and non-cardiovascular mortality were similar for venules (HR per SD increase 1.07 (0.99-1.15) and 1.08 (1.02-1.13), respectively). Further investigating specific causes, we found large effect sizes of wider venules on infectious diseases, dementia, pneumonia, and chronic obstructive pulmonary disease. Interestingly, arteriolar narrowing was only associated with pneumonia.

When excluding the first 10 years of follow-up as immortal person-time, the association of arterioles with cardiovascular mortality, and venules with both cardiovascular and non-cardiovascular mortality remained significant, even after adjusting for cardiovascular risk factors (Table 3).

In stratified analyses (Figure 2), we found that the associations of arterioles with mortality was modified by hypertension, whereas the associations of venules with mortality were modified by age and smoking. Baseline characteristics for RS-III are shown in

Supplemental Table 1. Over a mean follow-up of 6.4 years, 144 persons died. Wider venules were strongly associated with mortality (unadjusted HR per SD increase 1.26 (1.03-1.53) and adjusted 1.24 (1.01-1.52)). In contrast, the association with narrower arterioles was non-significant (unadjusted HR per SD decrease 1.05 (0.86-1.28) and adjusted 0.99 (0.80-1.22)), although the effect size of the unadjusted model was the same as in RS-I: 1.05 (1.01-109).

**Table 1. Baseline characteristics.**

| Characteristic | Participants | Non-participants | Mean difference (95% CI)* |
|---|---|---|---|
| Number | 5674 | 2309 | |
| Age, years | 68.0 (8.2) | 77.1 (10.3) | -8.90 (-9.3; -8.5)† |
| Female | 59 | 67 | -2.4 (-5.0; 0.2) |
| Systolic blood pressure, mmHg | 138.6 (22.0) | 143.2 (23.2) | 0.56 (-0.79; 1.91) |
| Diastolic blood pressure, mmHg | 73.7 (11.3) | 73.7 (12.8) | -1.19 (-1.91; -0.47)† |
| Body mass index, kg/m$^2$ | 26.3 (3.7) | 26.1 (3.9) | 0.31 (0.07; 0.54)† |
| Serum total cholesterol, mmol/L | 6.64 (1.21) | 6.46 (1.28) | 0.05 (-0.03; 0.12) |
| Serum HDL cholesterol, mmol/L | 1.35 (0.37) | 1.32 (0.39) | 0.02 (-0.01; 0.04) |
| Diabetes mellitus | 7 | 17 | -7.0 (-8.9; -5.2)† |
| C-reactive protein, mg/L | 3.20 (6.02) | 4.32 (9.18) | -0.57 (-1.00; -0.14)† |
| Number of carotid artery plaques ≥ 4 | 11 | 21 | -5.3 (-7.7; -3.0)† |
| Current smoker | 23 | 17 | -1.1 (-3.2; 1.1) |
| Arteriolar diameter, µm | 146.9 (14.4) | NA | NA |
| Venular diameter, µm | 222.0 (20.9) | NA | NA |

Values are presented as means (standard deviation) or as percentages.
*Age and gender adjusted if applicable.
†Significantly different from non-participants ($p < 0.05$).
Abbreviations: CI, confidence interval; HDL, high-density lipoprotein; NA, not applicable.

**Table 2. Hazard ratios (95% confidence interval) of cause-specific mortality per standard deviation difference in baseline retinal vessel diameters.**

| Cause of death | Arteriolar diameter | Venular diameter |
|---|---|---|
| All-cause mortality (n = 3794 deaths) | 1.04 (1.00; 1.08) | 1.07 (1.03; 1.12) |
| CVD mortality (n = 1079 deaths) | 1.07 (0.99; 1.15) | 1.07 (0.99; 1.15) |
| Non-CVD mortality (n = 2379 deaths) | 1.03 (0.98; 1.08) | 1.08 (1.02; 1.13) |
| Infectious disease (n = 56 deaths) | 0.95 (0.68; 1.32) | 1.31 (0.95; 1.81) |
| Cancer (n = 910 deaths) | 1.02 (0.94; 1.11) | 1.00 (0.92; 1.09) |
| Dementia (n = 348 deaths) | 0.99 (0.86; 1.14) | 1.08 (0.94; 1.23) |
| Pneumonia (n = 103 deaths) | 1.54 (1.19; 1.99) | 1.64 (1.30; 2.06) |
| Chronic respiratory disease (n = 123 deaths) | 0.92 (0.74; 1.14) | 1.18 (0.95; 1.47) |
| Fracture (n = 65 deaths) | 0.98 (0.71; 1.34) | 0.83 (0.60; 1.14) |
| Other (n = 774 deaths) | 1.03 (0.94; 1.13) | 1.09 (1.00; 1.19) |

Values are hazard ratios (95% confidence interval) per standard deviation decrease (for arterioles) or increase (for venules), adjusted for age, sex, other retinal vessel, systolic and diastolic pressure, antihypertensive medication, body mass index, total cholesterol, High-density lipoprotein cholesterol, diabetes mellitus, C-reactive protein, carotid artery plaque score, and smoking.

**Table 3. Hazard ratios (95% confidence interval) per standard deviation difference in baseline retinal vessel diameters, excluding 10-year as immortal person-time.**

| | Arteriolar diameter | | Venular diameter | |
|---|---|---|---|---|
| **Cause of death** | **Model 1*** | **Model 2†** | **Model 1** | **Model 2** |
| All-cause mortality (n = 2212 deaths) | 1.04 (0.98; 1.09) | 1.02 (0.97; 1.08) | 1.13 (1.07; 1.19) | 1.09 (1.04; 1.15) |
| CVD mortality (n = 560 deaths) | 1.15 (1.02; 1.28) | 1.13 (1.01; 1.26) | 1.19 (1.07; 1.33) | 1.11 (1.00; 1.24) |
| Non-CVD mortality (n = 1435 deaths) | 1.00 (0.93; 1.08) | 0.98 (0.92; 1.05) | 1.14 (1.07; 1.22) | 1.09 (1.02; 1.17) |

Values are hazard ratios (95% confidence interval) per standard deviation decrease in arterioles or increase in venules.
*Model 1, adjusted for age, gender and for the fellow vessel diameter.
†Model 2, adjusted for covariates in Model 1 plus systolic and diastolic pressure, antihypertensive medication, body mass index, total cholesterol, high-density lipoprotein cholesterol, diabetes mellitus, C-reactive protein, carotid artery plaque score, and smoking.

**Figure 1.** Hazard ratios (95% confidence interval) of all-cause mortality per standard deviation difference and per quartile in baseline retinal (A) arteriolar and (B) venular diameters (n = 5674) adjusted for age, gender and the fellow vessel diameter.

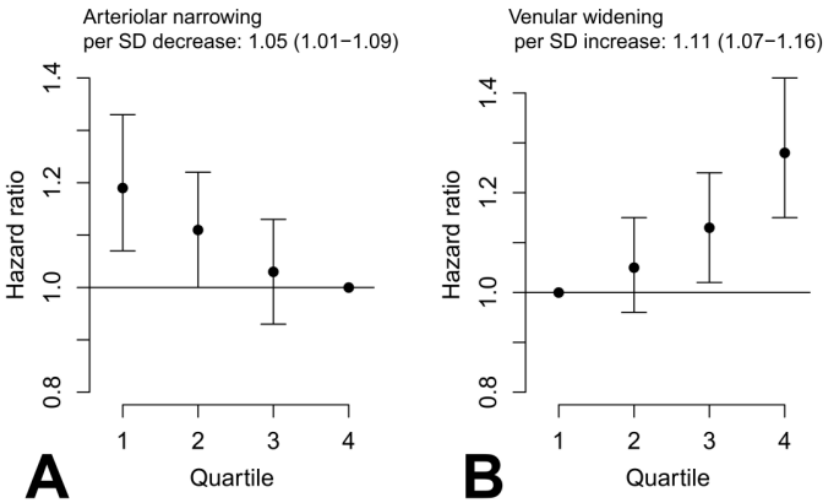

**Figure 2.** Effect measure modification with interaction terms for (A) arterioles and (B) venules.

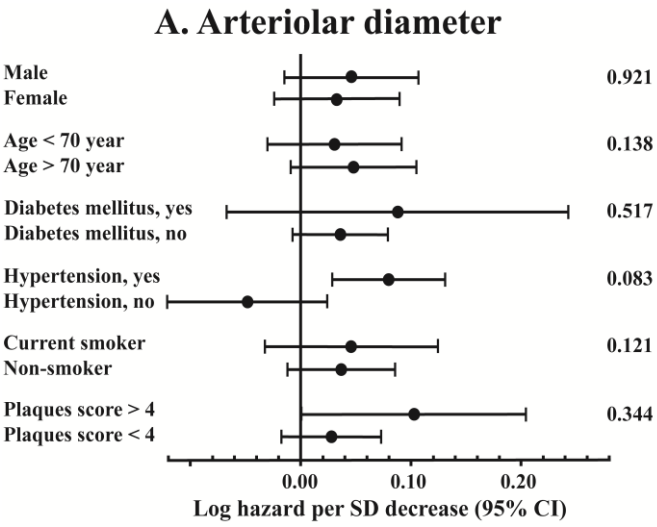


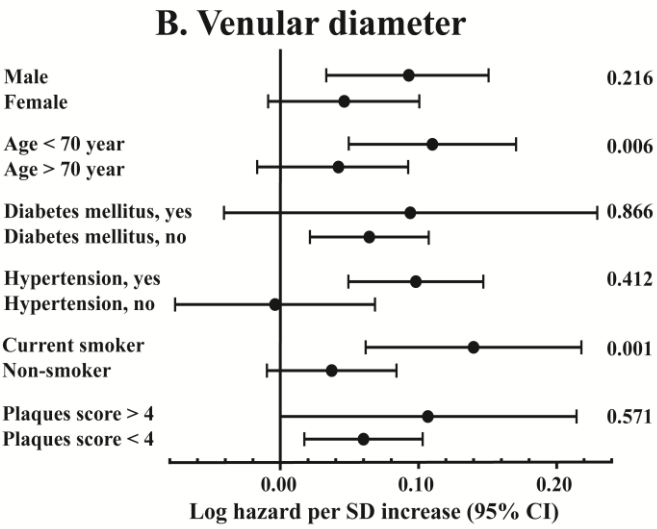

| Supplemental Table 1. Baseline characteristics of the replication cohort (RS-III). | | | |
|---|---|---|---|
| **Characteristic** | **Participants** | **Non-participants** | **Mean difference (95% CI)*** |
| Number | 3106 | 826 | |
| Age, years | 56.8 (6.5) | 58.5 (9.3) | -1.77 (-2.3; -1.2)† |
| Female | 57 | 57 | 1.1 (-2.8; 4.9) |
| Systolic blood pressure, mmHg | 132.4 (19.0) | 134.3 (17.2) | -0.75 (-2.13; 0.63) |
| Diastolic blood pressure, mmHg | 82.5 (11.0) | 82.9 (9.6) | -0.49 (-1.31; 0.34) |
| Body mass index, kg/m$^2$ | 27.7 (4.6) | 28.3 (4.0) | 0.51 (-0.86; -0.17)† |
| Serum total cholesterol, mmol/L | 5.56 (1.07) | 5.57 (0.88) | -0.01 (-0.09; 0.07) |
| Serum HDL cholesterol, mmol/L | 1.43 (0.44) | 1.41 (0.37) | 0.02 (-0.01; 0.05) |
| Diabetes mellitus | 8 | 8 | 2.0 (-0.3; 3.8) |
| C-reactive protein, mg/L | 2.65 (4.45) | 4.00 (4.87) | -1.25 (-1.60; -0.90)† |
| Intima media thickness > 2 mm | 35 | 36 | 3.3 (-1.0; 6.8) |
| Current smoker | 23 | 29 | -7.4 (-10.6; -4.1)† |
| Arteriolar diameter, µm | 158.4 (15.5) | NA | NA |
| Venular diameter, µm | 239.6 (22.8) | NA | NA |

Values are presented as means (standard deviation) or as percentages.
*Age and gender adjusted if applicable.
†Significantly different from non-participants ($p < 0.05$).
Abbreviations: RS, Rotterdam Study; CI, confidence interval; HDL, high-density lipoprotein; NA, not applicable.

## DISCUSSION

In this prospective population-based cohort study with more than 23 years of follow-up, we found that narrower arteriolar and wider venular diameters are associated with all-cause mortality. While for arterioles this was driven by an association with cardiovascular mortality, venules were equally associated with cardiovascular and non-cardiovascular mortality. These associations remained statistically significant even after excluding the first 10 years of follow-up, and were stronger in persons aged under 70 (venules only) and in smokers. Cardiovascular diseases remain the most important cause of death worldwide and studies have repeatedly shown that markers of large vessel disease are strong predictors of mortality.[23] Increasing evidence now suggests that small vessels, that is, arterioles, play also an important role in determining risk of cardiovascular morbidity and mortality.[13] Our study adds important corroboration to those findings by showing narrower arterioles to be associated with cardiovascular mortality during long-term follow-up. Importantly, we further expanded on the role of small vessels by also investigating venular diameters. We found that wider venules were associated with cardiovascular, as well as non-cardiovascular mortality. The finding that wider venules are detrimental to health is in line with previous studies, but the underlying mechanism remains uncertain. Wider venules have been shown to reflect microvascular damage due to smoking, inflammation, hypoxia and metabolic disturbances.[8, 24] In our study, adjusting for markers of these mechanisms did

attenuate the associations of venules with mortality, indeed pointing toward some effect of these mechanisms. Still, the associations remained statistically significant, indicating that other processes probably also play a role. Similarly, the associations remained significant in persons without diabetes or low carotid artery plaque score, again pointing to other contributing factors. The notion that wider venules reflect more diverse pathways than merely arteriolosclerotic or atherosclerotic disease also fits the observation that venules are associated with non-cardiovascular disease. At the same time, we note that some of the diseases that drive the association with non-cardiovascular disease, that is, chronic obstructive pulmonary disease and dementia, have been shown to have a partly vascular pathogenesis. It is therefore also possible that cardiovascular damage contributed to deaths due to those diseases, which formally get classified as non-cardiovascular. Taken together, we suspect that our findings are explained by both wider venules reflecting more diverse pathways and cardiovascular damage contributing to deaths formally classified as non-cardiovascular.

A major novelty of our study is that excluding the first 10 years of follow-up did not alter the associations; if anything, these became stronger. Many biomarkers for cardiovascular disease and subsequent mortality have been identified, but usually these associate with outcome only in the short term.[25] Examples include NT-proBNP and troponin T in clinical and non-clinical populations. There is a dearth of markers that indicate an increased risk in the long term. This is on the one hand caused by single measurements of the biomarker that can vary considerably over time, leading to measurement error and noise. On the other hand, reverse causality, that is, biomarker changes due to accumulation of preclinical damage, can restrict significant associations with clinical outcomes in the short term. Apart from a few genetic factors, such as APOE, that remain stable throughout life, not many long-term predictors of mortality have been identified.[26] Our findings that microvascular damage, both arteriolar and venular, associate with mortality beyond a 10-year horizon might open the way for further risk prediction and for prognostic research incorporating these markers. Given the semi-automated and noninvasive nature of measuring retinal vessels, there might thus be an opportunity for translation to clinical practice and public health. Future studies should focus on the clinical applications of retinal vascular imaging in patients with cardiovascular risk factors. It may help to noninvasively stratify cardiovascular risk of patients with consequent optimization of treatment. For instance, patients with wide venular calibers might benefit from aggressive management of cardiovascular risk factors.

Strengths of this study include the population-based setting, more than 23 years of follow-up, replication of the findings in an independent sample, and the adjustment for arterioles and venules for each other, which otherwise due to their positive correlation might obscure significant effects. Instead using the arteriole-to-venule ratio as in previous studies, which has become an obsolete marker, we modeled arteriolar and venular diameters simultaneously as independent predictors, because this provides unbiased and biologically

plausible results.[27] For further discussion on the utility of retinal imaging, we refer the reader to the study by Rizzoni and Muiesan.[28]

Limitations of this study are the limited sample for further categorization of causes of death, as well as the use of a static measure of vascular diameter. Future studies should investigate more dynamic measurements of small vessels, including flowmetry and dynamic vessel assessments. Finally, the population of the Rotterdam Study is fairly homogeneous consisting of middle-class white persons. Therefore, the generalizability of our findings to other populations needs to be determined.

This study provides evidence that retinal microvascular abnormalities are predictive of cardiovascular and non-cardiovascular mortality for 23-years and beyond in the general adult Dutch population. Wider venules in relatively young individuals and smokers are associated with higher risk of mortality compared to relatively old individuals and non-smokers.

There is an opportunity to use retinal vascular imaging in clinical settings as a noninvasive tool to help clinicians in identifying high-risk patients of future cardiovascular events. Given our findings, further study is warranted to understand the different pathogeneses of arterioles and venules in cardiovascular diseases, and in non-cardiovascular diseases with vascular origins.

## REFERENCES


1. World Health Organization. Global status report on noncommunicable diseases 2014. 2014
2. Mannino DM, Thorn D, Swensen A, Holguin F. Prevalence and outcomes of diabetes, hypertension and cardiovascular disease in copd. Eur Respir J. 2008;32:962-969
3. Bos D, Vernooij MW, de Bruijn RF, Koudstaal PJ, Hofman A, Franco OH, et al. Atherosclerotic calcification is related to a higher risk of dementia and cognitive decline. Alzheimers Dement. 2015;11:639-647 e631
4. Arad Y, Goodman KJ, Roth M, Newstein D, Guerci AD. Coronary calcification, coronary disease risk factors, c-reactive protein, and atherosclerotic cardiovascular disease events: The st. Francis heart study. J Am Coll Cardiol. 2005;46:158-165
5. Cao JJ, Arnold AM, Manolio TA, Polak JF, Psaty BM, Hirsch CH, et al. Association of carotid artery intima-media thickness, plaques, and c-reactive protein with future cardiovascular disease and all-cause mortality: The cardiovascular health study. Circulation. 2007;116:32-38
6. Kavousi M, Elias-Smale S, Rutten JH, Leening MJ, Vliegenthart R, Verwoert GC, et al. Evaluation of newer risk markers for coronary heart disease risk classification: A cohort study. Ann Intern Med. 2012;156:438-444
7. Wong TY, Klein R, Sharrett AR, Manolio TA, Hubbard LD, Marino EK, et al. The prevalence and risk factors of retinal microvascular abnormalities in older persons: The cardiovascular health study. Ophthalmology. 2003;110:658-666
8. Ikram MK, de Jong FJ, Vingerling JR, Witteman JC, Hofman A, Breteler MM, et al. Are retinal arteriolar or venular diameters associated with markers for cardiovascular disorders? The rotterdam study. Invest Ophthalmol Vis Sci. 2004;45:2129-2134
9. Wong TY, Klein R, Klein BE, Tielsch JM, Hubbard L, Nieto FJ. Retinal microvascular abnormalities and their relationship with hypertension, cardiovascular disease, and mortality. Surv Ophthalmol. 2001;46:59-80
10. Wong TY, Klein R, Sharrett AR, Duncan BB, Couper DJ, Tielsch JM, et al. Retinal arteriolar narrowing and risk of coronary heart disease in men and women. The atherosclerosis risk in communities study. JAMA. 2002;287:1153-1159
11. Ikram MK, de Jong FJ, Bos MJ, Vingerling JR, Hofman A, Koudstaal PJ, et al. Retinal vessel diameters and risk of stroke: The rotterdam study. Neurology. 2006;66:1339-1343
12. Wong TY, Klein R, Nieto FJ, Klein BE, Sharrett AR, Meuer SM, et al. Retinal microvascular abnormalities and 10-year cardiovascular mortality: A population-based case-control study. Ophthalmology. 2003;110:933-940
13. Wang JJ, Liew G, Klein R, Rochtchina E, Knudtson MD, Klein BE, et al. Retinal vessel diameter and cardiovascular mortality: Pooled data analysis from two older populations. Eur Heart J. 2007;28:1984-1992
14. Witt N, Wong TY, Hughes AD, Chaturvedi N, Klein BE, Evans R, et al. Abnormalities of retinal microvascular structure and risk of mortality from schemic heart disease and stroke. Hypertension. 2006;47:975-981
15. Hofman A, Darwish Murad S, van Duijn CM, Franco OH, Goedegebure A, Ikram MA, et al. The rotterdam study: 2014 objectives and design update. Eur J Epidemiol. 2013;28:889-926
16. Hubbard LD, Brothers RJ, King WN, Clegg LX, Klein R, Cooper LS, et al. Methods for evaluation of retinal microvascular abnormalities associated with hypertension/sclerosis in the atherosclerosis risk in communities study. Ophthalmology. 1999;106:2269-2280
17. Parr JC, Spears GF. Mathematic relationships between the width of a retinal artery and the widths of its branches. Am J Ophthalmol. 1974;77:478-483
18. Knudtson MD, Lee KE, Hubbard LD, Wong TY, Klein R, Klein BE. Revised formulas for summarizing retinal vessel diameters. Curr Eye Res. 2003;27:143-149

19. Littmann H. [determining the true size of an object on the fundus of the living eye] zur bestimmung der wahren grosse eines objektes auf dem hintergrund eines lebenden auges. Klin Monbl Augenheilkd. 1988;192:66-67
20. Leening MJ, Kavousi M, Heeringa J, van Rooij FJ, Verkroost-van Heemst J, Deckers JW, et al. Methods of data collection and definitions of cardiac outcomes in the rotterdam study. Eur J Epidemiol. 2012;27:173-185
21. van Gent CM, van der Voort HA, de Bruyn AM, Klein F. Cholesterol determinations. A comparative study of methods with special reference to enzymatic procedures. Clin Chim Acta. 1977;75:243-251
22. van der Meer IM, Bots ML, Hofman A, del Sol AI, van der Kuip DA, Witteman JC. Predictive value of noninvasive measures of atherosclerosis for incident myocardial infarction: The rotterdam study. Circulation. 2004;109:1089-1094
23. Lernfelt B, Forsberg M, Blomstrand C, Mellstrom D, Volkmann R. Cerebral atherosclerosis as predictor of stroke and mortality in representative elderly population. Stroke. 2002;33:224-229
24. Liew G, Sharrett AR, Wang JJ, Klein R, Klein BE, Mitchell P, et al. Relative importance of systemic determinants of retinal arteriolar and venular caliber: The atherosclerosis risk in communities study. Arch Ophthalmol. 2008;126:1404-1410
25. James SK, Lindahl B, Siegbahn A, Stridsberg M, Venge P, Armstrong P, et al. N-terminal pro-brain natriuretic peptide and other risk markers for the separate prediction of mortality and subsequent myocardial infarction in patients with unstable coronary artery disease: A global utilization of strategies to open occluded arteries (gusto)-iv substudy. Circulation. 2003;108:275-281
26. Walter S, Mackenbach J, Voko Z, Lhachimi S, Ikram MA, Uitterlinden AG, et al. Genetic, physiological, and lifestyle predictors of mortality in the general population. Am J Public Health. 2012;102:e3-10
27. Liew G, Sharrett AR, Kronmal R, Klein R, Wong TY, Mitchell P, et al. Measurement of retinal vascular caliber: Issues and alternatives to using the arteriole to venule ratio. Invest Ophthalmol Vis Sci. 2007;48:52-57
28. Rizzoni D, Muiesan ML. Retinal vascular caliber and the development of hypertension: A meta-analysis of individual participant data. J Hypertens. 2014;32:225-227

# Chapter 6
# General Discussion

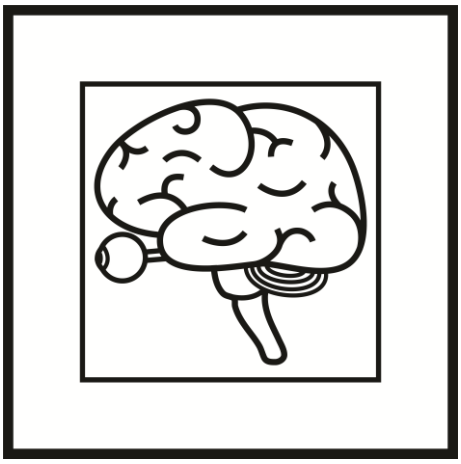

# General Discussion

In this thesis, my goal was to expand our current knowledge on retinal microvascular damage and retinal neurodegeneration as biomarker of vascular and neurodegenerative brain diseases. In this chapter, I will review the main findings, discuss general methodological issues, and consider implications of the findings with respect to the future. The Figure gives an overview of the studies that I have conducted in this thesis.

**Figure.** An overview of the studies described in this thesis. The role of retinal microvascular damage and retinal neurodegeneration in vascular and neurodegenerative brain diseases.

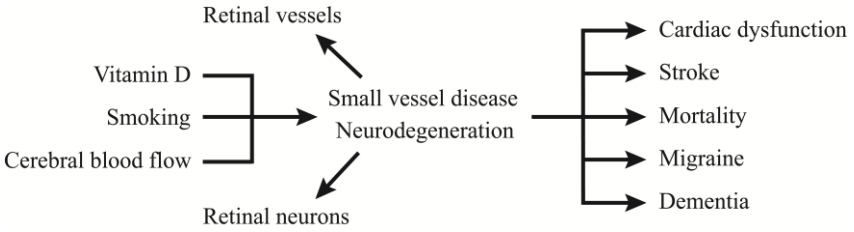


## MAIN FINDINGS

### Mediation and interaction

Epidemiologic research on the etiology of a disease can be perceived as a search for causal associations which either can be hypothesis-driven or hypothesis-free.[1] Traditionally, questions pertaining to one-on-one associations are tackled by regressing the outcome on the exposure. In stroke research, many modifiable risk factors have been identified by performing regression analysis, but a better understanding of their role in the pathophysiology of stroke is still needed.[2-4] Interaction and mediation analyses have been widely recognized as suitable tools to provide further insight into the pathophysiology of a disease. Given that persons with stroke often have vascular damage at multiple locations in the vascular system from heart to brain, it is conceivable that the presence of multiple damaged vessels may amplify their effect on stroke.[5] Interaction between known risk factors may thus provide new insight into the pathophysiology of stroke. Two potential risk factors that may interact in causing ischemic stroke are the presence of large vessel disease and small vessel disease.[6-8] In chapter 2.1, I showed that persons with a combination of impaired cerebral blood flow and wider retinal venules had an increased risk of developing stroke and transient ischemic attack. Interestingly, a low perfusion by itself seemed not sufficient to increase the risk of stroke, but only in the presence of wider venules. I hypothesized that a good cerebral autoregulation may compensate for a diminished perfusion, and a high perfusion for a diminished cerebral autoregulation. However, if both

fail, this may lead to an increased risk of stroke and transient ischemic attack. Along with these findings, existing evidence shows that among patients with carotid stenosis or occlusion, those with hypoperfusion have a fourfold increase in developing stroke than patients without hypoperfusion.[9] Those patients likely face stroke risk from hypoperfusion in vascular territories where vasodilatory capacity is maximally exhausted. Taken together, these findings suggest that research should also focus on interaction between exposures and not merely on one exposure.

Recent advances in the conceptual framework of causal mediation even allow estimating the effect of two exposures on an outcome where there is both interaction and mediation. Causal mediation analysis provides insight into relevant processes in the pathways under study, and enables researchers to better understand biological mechanisms. Therefore, I investigated in chapter 2.2 to what extent the effect of smoking on ischemic stroke is possibly mediated by the venules via the recently developed causal mediation analysis.[10, 11] This approach allows to decompose the exposure's effect on the outcome into components related to mediation only, interaction only, both, or neither. I showed that in the pathophysiology of ischemic stroke, the effect of smoking on ischemic stroke may partly be explained by changes in the venules, where there is both pure mediation and mediated interaction. Hence, apart from interaction between two risk exposures, both interaction and mediation can also take place. When decomposing the exposure's total effect into four components, the interpretation of the estimated effect sizes of each component will be hard when some components are of opposite sign. Particularly, a negative mediated interaction might be intuitively difficult to conceptualize. In chapter 2.3, I focused on negative mediated interaction, and proposed an interpretation using biological examples. I showed that negative mediated interaction might actually reflect relevant processes in the mechanism under study, and suggest investigators using causal mediation analysis to interpret components with opposite sign carefully.

**Blood markers**

In chapter 3, I aimed to further elucidate whether novel cardiovascular risk factors are linked to cardiovascular disease possibly through the presence of a microvascular component. In the past decades, investigators identified several potential markers of stroke such as vitamin D and NT-proBNP, and sought to understand the role of these markers in the pathophysiology of stroke.[12-15] Existing evidence shows a strong link between vitamin D and indices of large vessel disease which themselves contribute to the development of stroke.[16, 17] However, whether vitamin D could be linked to stroke through the presence of small vessel disease remained unclear. In chapter 3.1, I focused on the association of vitamin D with retinal microvascular damage, and found indeed that lower vitamin D serum levels were associated with the presence of retinal microvascular damage. These findings suggest that the association of vitamin D with stroke may partly run through changes in the microvasculature. As aforementioned, another emerging marker of stroke is NT-proBNP,

which is a marker of cardiac dysfunction.[18] Given that coronary heart disease has a substantial component due to small vessel disease,[19] it is conceivable that NT-proBNP also relates to indices of small vessel disease. In chapter 3.2, I focused on the association of NT-proBNP with retinal microvascular damage, and found that higher levels of NT-proBNP were associated with retinal microvascular damage. Although I have used the retinal vasculature as a marker for small vessel disease of the heart, previous studies have already established a link between retinal microvascular damage and coronary heart disease.[20-23] In agreement with findings from those studies, our findings suggest a potential role for NT-proBNP as marker for small vessel disease.

**Subclinical brain damage**

In chapter 4, I investigated whether global brain damage due to small vessel disease or atrophy may be reflected in the retina. Small vessel disease in the brain has been recognized as a crucial substrate for mechanisms underlying dementia and stroke.[24] Although the small vessels in the brain are not easily detected by MRI, the term small vessel disease is often used to describe brain tissue lesions detected on MRI, which are thought to be caused by small vessel disease. These lesions of small vessel disease on MRI include white matter lesions, lacunar infarcts, and microbleeds.[25] Although these lesions are often encountered before onset of vascular brain disease such as clinical stroke or vascular dementia, they are still a late manifestation of damage within the brain.[26] It remains unknown whether small vessel disease already leads to changes in the white matter before they are detectable on MRI as lesions. In chapter 4.1, I investigated the small vessels as reflected by retinal vascular calibers in relation to microstructural integrity of normal-appearing white matter. I showed that both narrower arterioles and wider venules were associated with worse white matter microstructure, suggesting that small vessel disease in the white matter is more widespread than visually detectable on MRI. Interestingly, the joint effect of narrower arterioles and wider venules on white matter microstructure appeared to be much stronger than their individual effect. In addition, the effect of narrower arterioles and wider venules were modified by sex and diabetes mellitus. Apart from conventional lesions of small vessel disease on MRI, a substantial body of literature is emerging indicating that enlarged perivascular spaces in the brain are also consequences of small vessel disease.[27-30]

In chapter 4.2, I have confirmed this putative link between retinal microvascular damage and enlarged perivascular spaces, suggesting enlarged perivascular spaces to be a marker of small vessel disease. How exactly small vessel disease contributes to enlarged perivascular spaces needs to be demonstrated in future studies.

While the vessels in the retina might reflect the condition of the vessels in the brain, it has also been thought that global brain damage due to small vessel disease or atrophy, may manifest in the retina as thinner retinal layers.[31] Given that the retina is formed embryonically from neuronal tissue, and is connected to the brain by the optic nerve, it is possible that the retina may reflect global brain damage. I explored this hypothesis in

chapter 4.3 and demonstrated that thinner retinal layers were associated with smaller brain volumes, and with worse white matter microstructure. These findings suggest that retinal optical coherence tomography may provide information on global brain atrophy. In addition, I also found that thinner retinal layers were associated with hippocampus atrophy suggesting a role for the retina as potential novel biomarker for Alzheimer's disease. As both neurodegeneration and vascular pathology in the brain often occur simultaneously, these findings suggest that retinal optical coherence tomography may provide information specifically on neurodegeneration in the brain. To further elucidate which exact brain regions were reflected by thinner retinal layers, I performed a voxel-based analysis in chapter 4.4 to acquire information on the smallest regional level, the voxel level. I found that thinner retinal nerve fiber layer and ganglion cell layer were associated with grey matter and white matter changes in the visual pathway, including the optic radiation and visual cortex. While retinal nerve fiber layer was mainly associated with grey matter densities in the visual cortex, ganglion cell layer was mainly associated with grey matter densities in the thalamus. These findings suggest that thinner retinal layers may be reflecting atrophy in the visual pathway rather than reflecting global brain atrophy. Three possible mechanisms have been proposed for these findings. First, a common disease process such as a vascular process or accumulation of misfolded proteins may play a role. Second, brain atrophy may lead to degeneration of the retina causing retrograde degeneration.[32-35] Although these two mechanisms likely occur simultaneously, these results do indicate that the relation seems to be more region-specific than widespread. Yet, it may be that associations in other brain regions from the voxel-based analysis did not survive the threshold for statistical significance. Another possibility for our findings might be that retinal damage may lead to degeneration of the brain causing anterograde degeneration, but evidence for this notion is not strong.[36, 37] Perhaps, both anterograde and retrograde degeneration occur simultaneously till the lateral nucleus geniculate, particularly were the trans-synaptic regions is.

**Clinical outcomes**

Given the potential of the retinal vasculature and the retinal layers as marker for brain damage on MRI, I further explored in chapter 5 whether these markers were also associated with clinical outcomes. In chapter 5.1, I investigated the role of small vessel disease in migraine. It has been thought that migraine has a substantial vascular component.[38, 39] While large vessel disease has been extensively studied in migraine,[40, 41] evidence regarding small vessel disease was lacking. I found that lifetime migraine was not associated with retinal microvascular damage. Notably, women with migraine had narrower retinal arterioles than men with migraine, which supports the notion that small vessel disease plays a more prominent role in women. Apart from migraine, in chapter 5.2, I investigated the association of retinal layer thickness with prevalent and incident dementia. Previous studies have repeatedly observed thinner retinal nerve fiber layer and ganglion cell layer in patients

with Alzheimer's disease compared to controls,[42-44] but longitudinal studies examining the link between retinal layer thickness and incident dementia were lacking. While I confirmed the findings from those studies, I have additionally shown that thinner retinal nerve fiber layer was associated with a higher risk of developing dementia, including Alzheimer's disease, independent of cardiovascular risk factors. These findings suggest that thinner retinal nerve fiber layer may be a novel biomarker for dementia, specifically for Alzheimer's disease. Moreover, there is an opportunity to use optical coherence tomography in clinical or research settings as an accessible and noninvasive tool to help clinicians or researchers in eligibility determination for clinical trials, in monitoring disease progression or in evaluating treatment response.
Finally, in chapter 5.3, I investigated the association of retinal vascular calibers with all-cause and cause-specific mortality. I found that narrower arterioles and wider venules were associated with all-cause mortality for more than 20 years. While for arterioles this association was driven by an association with cardiovascular mortality, venules were equally associated with cardiovascular and non-cardiovascular mortality. For venules, the associations were stronger in persons aged under 70 years and in smokers.

## METHODOLOGICAL CONSIDERATIONS

### Study design, setting and population

In the previous chapters, the strengths and limitations of each study have been discussed. Here, I would like to discuss methodological issues from a more general perspective. Studies in this thesis were all conducted within the framework of the Rotterdam Study: a prospective population-based cohort study designed to investigate causes and consequences of diseases.[45, 46] All inhabitants of the district Ommoord of the city Rotterdam aged 55 years or over were invited to participate to the study in 1990 and 2000. In 2006 a further extension of the cohort was initiated and inhabitants aged 45 years or over were invited. Follow-up examinations for participants take place every three to four years, and the total cohort is continuously monitored for morbidity, mortality and medication use through automated linkage of the study base with databases from general practitioners, the pharmacies, and the municipality. The implementation of MRI in 2005 and of optical coherence tomography in 2007 made the Rotterdam Study one of the few large studies able to investigate brain damage and retinal damage on a population level.
Before moving on discussing internal validity (i.e. selection, information and confounding bias), it should be noted that the large number of participants in the Rotterdam Study allows us to obtain precise effect estimates (i.e. small confidence interval). Furthermore, the generalizability of our findings to other populations needs to be determined by other studies among different populations.

**Selection bias**

Although the design of the Rotterdam Study limits the possibility for selection bias, some form of selection bias may have affected my findings. The main characteristic of selection bias is that the association between exposure and outcome among those selected for analysis differs from the association among those eligible.[47] Using causal diagrams, selection bias can be viewed as conditioning on a variable, which is a common effect of (a cause of) the exposure and (a cause of) the outcome. A possibility for selection bias starts already at the stage of participation to the Rotterdam study. Volunteer or self-selection bias may have occurred because those who did and did not participate to the Rotterdam Study may have had different health conditions. Although we are not able to test this, it is conceivable that older and physically handicapped persons were not able to participate and visit the research center. Persons included in the analysis of the studies covered by this thesis had good quality retinal photographs, optical coherence tomography scans, or MRI scans, whereas those who were eligible but not included in the analysis were often persons with physical or mental disabilities, or lens opacities that contributed to the poor quality of the retinal images. I have shown that, in general, persons not included in the analyses had a worse cardiovascular risk profile than persons included in the analyses, suggesting a role for selection bias. Taken together, if anything, those forms of selection bias likely resulted in inclusion of relatively healthy persons, and thus an underestimation of the effect estimates. With respect to longitudinal analysis, it is less likely that a form of selection bias affected our findings on stroke, dementia, or mortality, because the ascertainment of follow-up information through medical records continued also in participants who terminated their visit to the study center. The design and the continuous follow-up through linkage of databases avoids selection bias including differential loss to follow-up.

**Information bias**

This form of bias pertains misclassification or measurement error of the exposure, outcome, or confounders. Misclassification is said to be random or non-differential if the measured exposure is independent of the true outcome conditional on the true exposure, or if the measured outcome is independent of the true exposure conditional on the true outcome; otherwise it is said to be non-random or differential.[48] In the studies that I have conducted, it is unlikely that differential misclassification of the exposure or the outcome might have occurred for two reasons. First, measurement of the exposures and the outcomes were performed independently from each other, which is a way of blinding. Although a common factor still may have influenced the measurement of both the exposure and the outcome, if the true exposure does not affect the measured outcome, the misclassification is still non-differential.[48] Second, in longitudinal analysis, it is unlikely that the occurrence of the outcome may have affected the measurement of the exposure at baseline, which happens before onset of disease. Therefore, measurement of the exposure or the outcome are likely to be non-differential, and if anything, this may have resulted in dilution of the effects.

**Confounding**

This form of bias pertains common causes of the exposure and the outcome that mixes up the effect of the exposure on the outcome.[49] One can take this confounding effect into account using various methods such as restriction, stratification, or regression analysis. Although I have adjusted for potential confounders, there is still a role for residual confounding due to insufficient measurement of the confounders. For instance, in a case of left-sided stroke, blood pressure measured on the right arm may not fully reflect the pressure in the carotid arteries of the left side. Perhaps more importantly, we measured blood pressure at one point in time, whereas blood pressure fluctuates throughout the day. Similarly, the confounders I adjusted for were measured once at baseline, and thus might not cover life-long exposure. Besides residual confounding, there might be unmeasured confounders that I did not take into account. While adjustment for confounders may show us the true effect of the exposure on the outcome, one should be careful not to adjust for too many confounders. If the potential confounders, of which we think are confounders, in fact, are intermediates, adjusting for (proxies of) intermediates may increase bias.[50] To overcome this issue, I always presented, if necessary, more than one model. Another issue worth mentioning is the bias-variance trade-off that lies at the heart of all analyses. While adding confounders to regression models may provide an unbiased effect estimate, it may also result in a larger variance. Hence, model misspecification may have happened regardless of the interpretation of the findings.

## IMPLICATIONS FOR FUTURE RESEARCH

Studies investigating retinal structures as biomarkers for brain diseases have increased in the last decade, and contributed to our knowledge on the etiology of vascular and neurodegenerative brain diseases. Here, I would like to point out some knowledge gaps that future studies still have to fill in.

**Mediation and interaction**

In population-based studies, the identification of novel biomarkers for diseases has been mainly done by searching for associations between exposure and outcome. In several studies that I have described in this thesis, such analyses were also conducted. While this way of doing research is valid, and should be continued, there is an increasing need to study the exposure of interest together with other potential exposures in order to gain more insight into a disease process. For that reason I have focused on interaction and mediation analysis, and believe that this way of doing research should be more encouraged. Not only in neuro-ophthalmology research, but also in other fields of epidemiologic research, these approaches can move the field forward. Future work may build upon the studies described in this thesis, and may investigate, for instance, whether cardiac dysfunction is an intermediate in the association between small vessel disease and stroke, or interacts with small vessel disease.

**Longitudinal studies**

At the same time, the cross-sectional analyses in this thesis should be replicated in a longitudinal setting to assess temporality and likely, but not necessarily, causality. I have repeatedly pointed out that brain damage may lead to retrograde degeneration causing thinner retinal layers. Yet, such a notion can only be established by investigating the association between brain damage and retinal layer thickness over time. Another consideration is to investigate the notion that retinal neurodegeneration leads to brain damage. While this hypothesis can be studied longitudinally, one can also consider to study the relation of glaucoma, as a form of advanced retinal neurodegeneration, with brain damage on MRI or dementia. Accordingly, one can make claims on shared etiology or anterograde degeneration. Perhaps, it might even be that glaucoma is a local disease process that does not affect the brain at all. Further, I have demonstrated that apart from global brain atrophy, retinal layer thicknesses are specifically reflecting degeneration of the visual pathway. However, I did not find evidence for an association between retinal layer thickness and white matter lesion, lacunar infarcts, or cerebral microbleeds. It should be noted that I considered the presence of these lesions throughout the brain and not specifically whether these lesions were affecting the visual pathway. As such, future research may investigate the association of retinal layer thicknesses with brain lesions affecting the visual pathway.

**Imaging methods**

Beside voxel-based analysis, future studies can build upon the work presented in this thesis by extending the scope of retinal imaging to assess retinal structures in relation to other brain imaging markers (e.g. cortical infarcts) or techniques (e.g. functional connectivity assessed by functional MRI). In turn, there is a wide range of retinal imaging methods and algorithms which can be applied to gain more information on the structure and function of the retinal vasculature and the retinal layers. For instance, apart from the retinal vascular calibers, there are other morphologic parameters of the retinal vessels such as tortuosity, branching angle, and fractal dimensions, which have been linked to selected cardiovascular risk factors and diseases.[51-53] However, this has only been investigated in few studies, and thus there is an opportunity to further extend this field of research. At the same time, newer retinal imaging methods such as hyperspectral imaging may enable us to detect retinal amyloid-beta depositions in humans.[54] Studies have visualized fluorescent ligand of curcumin bound to amyloid-beta in donor retinas of Alzheimer's disease patients, whereas such staining was not seen in healthy controls.[55, 56] Although promising, these studies are mainly conducted in mice or post-mortem retinas from Alzheimer's disease patients, and thus, there utility in living humans needs yet to be determined.

**Clinical research**

While the use of retinal imaging to study brain diseases has increased over the past decades, the implementation of retinal imaging in clinical practice has not. Using retinal imaging in clinical practice depends mainly on to what extent the retinal structures contribute to disease prediction beyond known risk factors. For this purpose, further research should consider studying the retinal structures with respect to disease prediction, and thereby focusing on specific subpopulations. The contribution of small vessel disease in cardiovascular diseases has shown to be more prominent in women and persons with diabetes mellitus.[57, 58] Hence, targeted application of retinal imaging may be more effective. Also, it is noteworthy to mention that before retinal imaging can be translated into clinical practice, the cost-effectiveness should also be considered, particularly when the assessment of traditional risk factors are relatively inexpensive and widely available. With regard to MRI scanning, this technique may not be available in routine clinical care of frail persons. Moreover, undergoing MRI scanning is time-consuming, costly and some patients may have contraindication. In such circumstances, optical coherence tomography might be a good alternative given its accessibility, availability, and affordability.

## CONCLUDING REMARKS

The scientific discoveries described in my thesis provide new insights into the role of small vessel disease and retinal neurodegeneration in vascular and neurodegenerative brain diseases. Furthermore, they emphasize the importance of applying interaction and mediation analysis in epidemiologic research on disease etiology. In this chapter, I gave an overview of the main findings, discussed methodological issues, and gave implications of the findings for future research. The findings described in this thesis may serve as a groundwork for future research and will hopefully inspire new research.

## REFERENCES


1. Greenland S, Gago-Dominguez M, Castelao JE. The value of risk-factor ("black-box") epidemiology. Epidemiology. 2004;15:529-535
2. O'Donnell MJ, Chin SL, Rangarajan S, Xavier D, Liu L, Zhang H, et al. Global and regional effects of potentially modifiable risk factors associated with acute stroke in 32 countries (interstroke): A case-control study. Lancet. 2016;388:761-775
3. Bos MJ, Koudstaal PJ, Hofman A, Ikram MA. Modifiable etiological factors and the burden of stroke from the rotterdam study: A population-based cohort study. PLoS Med. 2014;11:e1001634
4. Feigin VL, Roth GA, Naghavi M, Parmar P, Krishnamurthi R, Chugh S, et al. Global burden of stroke and risk factors in 188 countries, during 1990-2013: A systematic analysis for the global burden of disease study 2013. Lancet Neurol. 2016;15:913-924
5. Bos D, Ikram MA, Elias-Smale SE, Krestin GP, Hofman A, Witteman JC, et al. Calcification in major vessel beds relates to vascular brain disease. Arterioscler Thromb Vasc Biol. 2011;31:2331-2337
6. Ikram MK, de Jong FJ, Bos MJ, Vingerling JR, Hofman A, Koudstaal PJ, et al. Retinal vessel diameters and risk of stroke: The rotterdam study. Neurology. 2006;66:1339-1343
7. Dubow JS, Salamon E, Greenberg E, Patsalides A. Mechanism of acute ischemic stroke in patients with severe middle cerebral artery atherosclerotic disease. J Stroke Cerebrovasc Dis. 2014;23:1191-1194
8. van der Veen PH, Muller M, Vincken KL, Hendrikse J, Mali WP, van der Graaf Y, et al. Longitudinal relationship between cerebral small-vessel disease and cerebral blood flow: The second manifestations of arterial disease-magnetic resonance study. Stroke. 2015;46:1233-1238
9. Gupta A, Chazen JL, Hartman M, Delgado D, Anumula N, Shao H, et al. Cerebrovascular reserve and stroke risk in patients with carotid stenosis or occlusion: A systematic review and meta-analysis. Stroke. 2012;43:2884-2891
10. VanderWeele TJ. A unification of mediation and interaction: A 4-way decomposition. Epidemiology. 2014;25:749-761
11. Valeri L, Vanderweele TJ. Mediation analysis allowing for exposure-mediator interactions and causal interpretation: Theoretical assumptions and implementation with sas and spss macros. Psychol Methods. 2013;18:137-150
12. Sun Q, Pan A, Hu FB, Manson JE, Rexrode KM. 25-hydroxyvitamin d levels and the risk of stroke: A prospective study and meta-analysis. Stroke. 2012;43:1470-1477
13. Brondum-Jacobsen P, Nordestgaard BG, Schnohr P, Benn M. 25-hydroxyvitamin d and symptomatic ischemic stroke: An original study and meta-analysis. Ann Neurol. 2013;73:38-47
14. Zonneveld HI, Ikram MA, Hofman A, Niessen WJ, van der Lugt A, Krestin GP, et al. N-terminal pro-b-type natriuretic peptide and subclinical brain damage in the general population. Radiology. 2017;283:205-214
15. Michos ED, Carson KA, Schneider AL, Lutsey PL, Xing L, Sharrett AR, et al. Vitamin d and subclinical cerebrovascular disease: The atherosclerosis risk in communities brain magnetic resonance imaging study. JAMA Neurol. 2014;71:863-871
16. de Boer IH, Kestenbaum B, Shoben AB, Michos ED, Sarnak MJ, Siscovick DS. 25-hydroxyvitamin d levels inversely associate with risk for developing coronary artery calcification. J Am Soc Nephrol. 2009;20:1805-1812
17. Ng YM, Lim SK, Kang PS, Kadir KA, Tai MS. Association between serum 25-hydroxyvitamin d levels and carotid atherosclerosis in chronic kidney disease patients. BMC Nephrol. 2016;17:151
18. Weber M, Hamm C. Role of b-type natriuretic peptide (bnp) and nt-probnp in clinical routine. Heart. 2006;92:843-849
19. Marinescu MA, Loffler AI, Ouellette M, Smith L, Kramer CM, Bourque JM. Coronary microvascular dysfunction, microvascular angina, and treatment strategies. JACC Cardiovasc Imaging. 2015;8:210-220

20. Wong TY, Klein R, Sharrett AR, Duncan BB, Couper DJ, Tielsch JM, et al. Retinal arteriolar narrowing and risk of coronary heart disease in men and women. The atherosclerosis risk in communities study. JAMA. 2002;287:1153-1159
21. McGeechan K, Liew G, Macaskill P, Irwig L, Klein R, Klein BE, et al. Meta-analysis: Retinal vessel caliber and risk for coronary heart disease. Ann Intern Med. 2009;151:404-413
22. Liew G, Wong TY, Mitchell P, Cheung N, Wang JJ. Retinopathy predicts coronary heart disease mortality. Heart. 2009;95:391-394
23. Cheung N, Wang JJ, Klein R, Couper DJ, Sharrett AR, Wong TY. Diabetic retinopathy and the risk of coronary heart disease: The atherosclerosis risk in communities study. Diabetes Care. 2007;30:1742-1746
24. Pantoni L. Cerebral small vessel disease: From pathogenesis and clinical characteristics to therapeutic challenges. Lancet Neurol. 2010;9:689-701
25. Wardlaw JM, Smith C, Dichgans M. Mechanisms of sporadic cerebral small vessel disease: Insights from neuroimaging. Lancet Neurol. 2013;12:483-497
26. de Groot M, Verhaaren BF, de Boer R, Klein S, Hofman A, van der Lugt A, et al. Changes in normal-appearing white matter precede development of white matter lesions. Stroke. 2013;44:1037-1042
27. Hurford R, Charidimou A, Fox Z, Cipolotti L, Jager R, Werring DJ. Mri-visible perivascular spaces: Relationship to cognition and small vessel disease mri markers in ischaemic stroke and tia. J Neurol Neurosurg Psychiatry. 2014;85:522-525
28. Wardlaw JM, Smith EE, Biessels GJ, Cordonnier C, Fazekas F, Frayne R, et al. Neuroimaging standards for research into small vessel disease and its contribution to ageing and neurodegeneration. Lancet Neurol. 2013;12:822-838
29. van Veluw SJ, Biessels GJ, Bouvy WH, Spliet WG, Zwanenburg JJ, Luijten PR, et al. Cerebral amyloid angiopathy severity is linked to dilation of juxtacortical perivascular spaces. J Cereb Blood Flow Metab. 2016;36:576-580
30. Doubal FN, MacLullich AM, Ferguson KJ, Dennis MS, Wardlaw JM. Enlarged perivascular spaces on mri are a feature of cerebral small vessel disease. Stroke. 2010;41:450-454
31. Ong YT, Hilal S, Cheung CY, Venketasubramanian N, Niessen WJ, Vrooman H, et al. Retinal neurodegeneration on optical coherence tomography and cerebral atrophy. Neurosci Lett. 2015;584:12-16
32. Cowey A, Alexander I, Stoerig P. Transneuronal retrograde degeneration of retinal ganglion cells and optic tract in hemianopic monkeys and humans. Brain. 2011;134:2149-2157
33. Park HY, Park YG, Cho AH, Park CK. Transneuronal retrograde degeneration of the retinal ganglion cells in patients with cerebral infarction. Ophthalmology. 2013;120:1292-1299
34. Jindahra P, Petrie A, Plant GT. Retrograde trans-synaptic retinal ganglion cell loss identified by optical coherence tomography. Brain. 2009;132:628-634
35. Dinkin M. Trans-synaptic retrograde degeneration in the human visual system: Slow, silent, and real. Curr Neurol Neurosci Rep. 2017;17:16
36. You Y, Gupta VK, Graham SL, Klistorner A. Anterograde degeneration along the visual pathway after optic nerve injury. PLoS One. 2012;7:e52061
37. Kanamori A, Catrinescu MM, Belisle JM, Costantino S, Levin LA. Retrograde and wallerian axonal degeneration occur synchronously after retinal ganglion cell axotomy. Am J Pathol. 2012;181:62-73
38. Kurth T, Winter AC, Eliassen AH, Dushkes R, Mukamal KJ, Rimm EB, et al. Migraine and risk of cardiovascular disease in women: Prospective cohort study. BMJ. 2016;353:i2610
39. Dalkara T, Nozari A, Moskowitz MA. Migraine aura pathophysiology: The role of blood vessels and microembolisation. Lancet Neurol. 2010;9:309-317
40. Goulart AC, Santos IS, Bittencourt MS, Lotufo PA, Bensenor IM. Migraine and subclinical atherosclerosis in the brazilian longitudinal study of adult health (elsa-brasil). Cephalalgia. 2016;36:840-848
41. Stam AH, Weller CM, Janssens AC, Aulchenko YS, Oostra BA, Frants RR, et al. Migraine is not associated with enhanced atherosclerosis. Cephalalgia. 2013;33:228-235

42. Thomson KL, Yeo JM, Waddell B, Cameron JR, Pal S. A systematic review and meta-analysis of retinal nerve fiber layer change in dementia, using optical coherence tomography. Alzheimers Dement (Amst). 2015;1:136-143
43. den Haan J, Verbraak FD, Visser PJ, Bouwman FH. Retinal thickness in alzheimer's disease: A systematic review and meta-analysis. Alzheimers Dement (Amst). 2017;6:162-170
44. Coppola G, Di Renzo A, Ziccardi L, Martelli F, Fadda A, Manni G, et al. Optical coherence tomography in alzheimer's disease: A meta-analysis. PLoS One. 2015;10:e0134750
45. Hofman A, Brusselle GG, Darwish Murad S, van Duijn CM, Franco OH, Goedegebure A, et al. The rotterdam study: 2016 objectives and design update. Eur J Epidemiol. 2015;30:661-708
46. Ikram MA, van der Lugt A, Niessen WJ, Koudstaal PJ, Krestin GP, Hofman A, et al. The rotterdam scan study: Design update 2016 and main findings. Eur J Epidemiol. 2015;30:1299-1315
47. Hernan MA, Hernandez-Diaz S, Robins JM. A structural approach to selection bias. Epidemiology. 2004;15:615-625
48. VanderWeele TJ, Hernan MA. Results on differential and dependent measurement error of the exposure and the outcome using signed directed acyclic graphs. Am J Epidemiol. 2012;175:1303-1310
49. VanderWeele TJ, Shpitser I. On the definition of a confounder. Ann Stat. 2013;41:196-220
50. Schisterman EF, Cole SR, Platt RW. Overadjustment bias and unnecessary adjustment in epidemiologic studies. Epidemiology. 2009;20:488-495
51. Cheung CY, Zheng Y, Hsu W, Lee ML, Lau QP, Mitchell P, et al. Retinal vascular tortuosity, blood pressure, and cardiovascular risk factors. Ophthalmology. 2011;118:812-818
52. Ong YT, Hilal S, Cheung CY, Xu X, Chen C, Venketasubramanian N, et al. Retinal vascular fractals and cognitive impairment. Dement Geriatr Cogn Dis Extra. 2014;4:305-313
53. Li LJ, Cheung CY, Ikram MK, Gluckman P, Meaney MJ, Chong YS, et al. Blood pressure and retinal microvascular characteristics during pregnancy: Growing up in singapore towards healthy outcomes (gusto) study. Hypertension. 2012;60:223-230
54. More SS, Beach JM, Vince R. Early detection of amyloidopathy in alzheimer's mice by hyperspectral endoscopy. Invest Ophthalmol Vis Sci. 2016;57:3231-3238
55. Koronyo-Hamaoui M, Koronyo Y, Ljubimov AV, Miller CA, Ko MK, Black KL, et al. Identification of amyloid plaques in retinas from alzheimer's patients and noninvasive in vivo optical imaging of retinal plaques in a mouse model. Neuroimage. 2011;54 Suppl 1:S204-217
56. Koronyo Y, Biggs D, Barron E, Boyer DS, Pearlman JA, Au WJ, et al. Retinal amyloid pathology and proof-of-concept imaging trial in alzheimer's disease. JCI Insight. 2017;2
57. McClintic BR, McClintic JI, Bisognano JD, Block RC. The relationship between retinal microvascular abnormalities and coronary heart disease: A review. Am J Med. 2010;123:374 e371-377
58. Ikram MK, Cheung CY, Lorenzi M, Klein R, Jones TL, Wong TY, et al. Retinal vascular caliber as a biomarker for diabetes microvascular complications. Diabetes Care. 2013;36:750-759

# Chapter 7
# Summary/Samenvatting

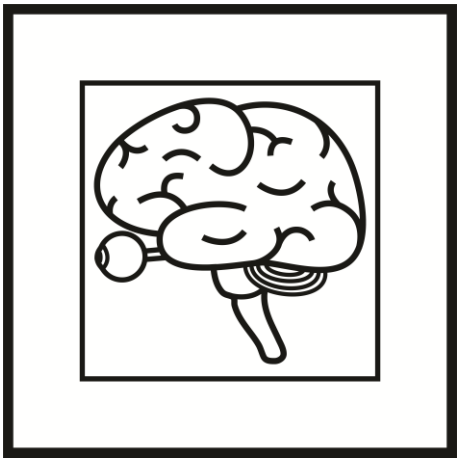

# Summary

Over the last decade, retinal imaging has truly emerged as a complementary technique to neuroimaging to probe microvascular and neurodegenerative processes within the brain. Given that the vessels in the retina and the brain share similarities in anatomy and physiology, the vessels in the retina may reflect similar changes in the vessels in the brain. Besides, the small vessels of the brain cannot be visualized easily with current neuroimaging modalities, and retinal imaging offers a unique opportunity to study the small vessels non-invasively. Various studies have shown that traditional cardiovascular risk factors such as high blood pressure, diabetes mellitus, and smoking can lead to microvascular damage. This microvascular damage, as reflected in the retina, has even been related to incident stroke and dementia. Despite these discoveries, mechanisms underlying the relation between retinal microvascular damage and vascular brain diseases are poorly understood.

Apart from the retinal vasculature as marker for vascular brain diseases, it has been thought that the retinal layers (consisting of neurons) can serve as marker for neurodegenerative brain diseases. Given that the retina is embryonically formed from the neural tissue and connected to the brain by the optic nerve, it is possible that global brain damage due to small vessel disease or atrophy may manifest in the retina as thinning of the retinal layers. In recent years, advances in medical imaging technology allowed the quantification of structures of the retina and the brain more easily and accurately. These advances enable us to study the relation of the retinal layers with brain structures on imaging.

The main objective of this thesis was to expand our current knowledge on retinal microvascular damage and retinal neurodegeneration as markers of vascular and neurodegenerative brain diseases. The studies in this thesis were embedded within the Rotterdam Study: a large prospective population-based cohort study.

**Chapter 1** gives a general introduction of the thesis by highlighting some historical moments that played an important role in our understanding about the eye-brain connection, and by describing the current knowledge on the use of retinal imaging to study brain diseases.

**Chapter 2** provides further insight into the pathophysiology of stroke by applying interaction and mediation analysis. In the pathophysiology of stroke, damage to small and large vessels are considered to be associated with different types of stroke such as cortical infarcts and lacunar infarcts. In chapter 2.1, I investigated whether lower brain perfusion and retinal microvascular damage interact in their effect on stroke and transient ischemic attack. I found that the risk of stroke and transient ischemic attack was increased in persons with a combination of impaired brain perfusion and retinal microvascular damage. Apart from interaction analysis, to further elucidate mechanisms underlying stroke, I investigated in chapter 2.2 to what extent the effect of smoking on ischemic stroke is possibly mediated

by the venules via the recently developed causal mediation analysis.
I found that the effect of smoking on the risk of ischemic stroke may partly be explained by changes in the venules, where there is both pure mediation and mediated interaction between smoking and venules. Subsequently, I observed that in caual mediation analysis, the interpretation of the estimated effect of the four components will be hard when the effect of some components are of opposite sign. In chapter 2.3, I focused on negative mediated interaction, and showed that this may actually reflect relevant processes in the mechanism under study e.g. allosteric effect within molecules and antagonistic interaction between drugs. I also suggested investigators using causal mediation analysis to interpret effects of components with opposite sign carefully.
**Chapter 3** addresses the relation of small vessel disease with potential markers of stroke. In chapter 3.1, I showed that lower vitamin D levels were associated with the presence of retinal microvascular damage, suggesting that the association of vitamin D with stroke may partly run through changes in the microvasculature. Next, in chapter 3.2, I showed that higher levels of NT-proBNP were associated with retinal microvascular damage, suggesting a potential role for NT-proBNP as marker for small vessel disease.
**Chapter 4** is dedicated to the relation of retinal vascular calibers and retinal layer thicknesses with structural brain imaging markers. In chapter 4.1, I found that narrower arterioles and wider venules were related to a worse white matter microstructure of the brain. The joint effect of narrower arterioles and wider venules on white matter microstructure appeared to be stronger than their individual effect. These findings suggest that small vessel disease in the white matter is more widespread than visually detectable on MRI. Next, in chapter 4.2, I investigated the relation between retinal vascular calibers and enlarged perivascular spaces on MRI, and found that narrower arterioles and wider venules were related to the amount of enlarged perivascular spaces. These findings confirm the putative link between microvascular damage and enlarged perivascular spaces. The study in chapter 4.3 focuses on the hypothesis that global brain damage may manifest in the retina as thinning of the layers. I found that thinning of the retinal nerve fiber layer and ganglion cell layer were associated with global grey matter and white matter atrophy of the brain, and with worse white matter microstructure, whereas no association was found with markers of cerebral small vessel disease. As both neurodegeneration and vascular pathology in the brain often occur simultaneously, our current findings suggest that retinal OCT may provide information specifically on neurodegeneration in the brain. To shed light into mechanisms underlying these associations, and to study findings from the previous study more in-depth, I refined the study by investigating the association of retinal layer thicknesses with brain structures by looking at the voxel level in chapter 4.4. I found that thinner retinal nerve fiber layer and ganglion cell layer were associated with grey and white matter changes in the visual pathway, suggesting that thinner retinal layers may be reflecting atrophy in the visual pathway rather than global brain atrophy.

**Chapter 5** explores the association of the retinal vasculature and the retinal layers with clinical outcomes. In chapter 5.1, I investigated the role of microvascular damage in migraine, and found that retinal microvascular damage was not associated with migraine. Next, in chapter 5.2, I investigated the association of thickness of retinal layers with prevalent and incident dementia. I found that thinner retinal nerve fiber layer was associated with an increased risk of developing dementia, including Alzheimer's disease. These findings suggest that thinner retinal nerve fiber layer may be a novel marker for dementia, specifically for Alzheimer's disease. In chapter 5.3, I studied the association between retinal microvasculature and long-term cause-specific mortality, and found that retinal microvascular abnormalities were associated with cardiovascular and non-cardiovascular mortality for more than 20 years. Particularly, wider venules in relatively young persons, and smoker were associated with higher risk of mortality.
**Chapter 6** reviews the main findings, discusses general methodological issues, and considers implications of the findings with respect to the future.

# Samenvatting

In het afgelopen decennium heeft medische beeldvorming van het netvlies (retina) in toenemende mate een belangrijke rol gespeeld in het bestuderen van vasculaire en neurodegenerative hersenaandoeningen als aanvulling op beeldvorming van de hersenen. De bloedvaten in de retina en de hersenen bezitten namelijk vergelijkbare anatomische en fysiologische eigenschappen, waardoor vaatschade in de retina een goede afspiegeling is van vaatschade in de hersenen. Aangezien de kleine bloedvaten van de hersenen niet eenvoudig kunnen worden afgebeeld met de huidige beeldvormingstechnieken, biedt beeldvorming van de retina een unieke kans om op non-invasieve wijze de kleine bloedvaten te bestuderen. Verschillende studies hebben aangetoond dat traditionele risicofactoren voor hart- en vaatziekten zoals hoge bloeddruk, suikerziekte, en roken kunnen leiden tot schade aan de kleine vaten. Deze schade, zoals weerspiegeld in de retina, is gerelateerd aan schade aan de bloedvaten in de hersenen, wat zich kan uiten in een hoger risico op het krijgen van een beroerte en dementie. Ondanks deze belangrijke bevindingen blijft het onderliggend mechanisme van de relatie tussen retinale vaatafwijkingen en hersenafwijkingen onduidelijk.
Naast de retinale vaten als marker voor vasculaire hersenaandoeningen, bestaat ook de gedachte dat de retinale zenuwlagen (bestaand uit zenuwcellen) kunnen dienen als marker voor neurodegeneratieve hersenaandoeningen. Aangezien de retina zich ontwikkelt uit embryonale zenuwcellen en verbonden is met de hersenen via de oogzenuw, kunnen hersenafwijkingen ten gevolge van vaatschade of verschrompeling (atrofie) van weefesel zich uiten in de retina als verdunning van de zenuwlagen. De laatste jaren hebben technologische ontwikkelingen in medische beeldvorming ervoor gezorgd dat structuren van de retina en de hersenen eenvoudiger en nauwkeuriger gekwantificeerd kunnen worden. Deze ontwikkelingen stellen ons in staat om de relatie tussen de retinale zenuwlagen en hersenstructuren op beeldvorming te onderzoeken.
Het doel van dit proefschrift was het onderzoeken of schade in de retina (waaronder schade aan de bloedvaten en aan de zenuwlagen) gebruikt kan worden als marker voor vasculaire en neurodegeneratieve hersenaandoeningen. Alle studies in dit proefschrift waren onderdeel van een groot prospectief bevolkingsonderzoek, genaamd de Rotterdam Studie.

**Hoofdstuk 1** betreft een algemene introductie waarin kort de historische momenten benoemd worden die een belangrijke rol hebben gespeeld in het begrijpen van de nauwe samenwerking tussen ogen en hersenen. Daarnaast wordt de huidige stand van zaken betreffende de rol van retinale beeldvorming in het bestuderen van hersenaandoeningen beschreven.
**Hoofdstuk 2** belicht de pathofysiologie van beroerte door statistische interactie en mediatie analyses toe te passen. Er is sterk bewijs dat schade aan de kleine en grote bloedvaten in de hersenen gerelateerd is aan het type herseninfarct (corticaal of lacunair) en dat er mogelijk

verschillende mechanismen aan ten grondslag liggen. In hoofdstuk 2.1 heb ik gekeken of een combinatie van verminderde doorbloeding van de hersenen en retinale vaatschade elkaars effect versterken in het ontwikkelen van beroerte en transient ischemic attack (TIA). Ik heb gevonden dat het risico op het ontwikkelen van een beroerte en TIA hoger was in personen met een combinatie van verminderde hersendoorbloeding en retinale vaatschade. In hoofdstuk 2.2 onderzocht ik in hoeverre het effect van roken op een herseninfarct gemedieerd wordt door kleine aders (venulen). Ik vond dat het effect van roken op het risico van een herseninfarct deels verklaard werd door veranderingen in de venulen daar waar sprake was van pure mediatie en gemedieerde interactie tussen roken en venulen. Verder merkte ik op dat in causale mediatie analyse, de interpretatie van de effecten van de vier componenten lastig kan zijn wanneer het effect van bepaalde componenten in tegengestelde richting is. In hoofdstuk 2.3 focuste ik op negatief gemedieerde interactie, en liet zien dat negatief gemedieerde interactie relevante processen weerspiegelt in het mechanisme dat bestudeerd wordt zoals allosterische regulatie van moleculen en antagonisme tussen antibiotica. Ik suggereerde ook dat onderzoekers die causale mediatie analyse gebruiken, effecten van componenten in tegengestelde richting voorzichtig moeten interpreteren.

**Hoofdstuk 3** is gericht op de relatie tussen schade aan de kleine vaten en potentiële markers van beroerte. In hoofdstuk 3.1 toonde ik dat lage bloedwaarden van vitamine D geassocieerd waren met de aanwezigheid van retinale vaatschade. Deze bevinding suggereert dat de associatie tussen lage bloedwaarden van vitamine D en beroerte deels kan verlopen via schade aan de kleine vaten. Vervolgens liet ik in hoofdstuk 3.2 zien dat hoge bloedwaarden van NT-proBNP geassocieerd waren met de aanwezigheid van retinale vaatschade, wat een potentiële rol voor NT-proBNP als marker voor de beschadiging van de kleine vaten suggereert.

**Hoofdstuk 4** is toegewijd aan de relatie van retinale vaatdiameters en retinale zenuwlagen met hersenstructuren op beeldvorming. In hoofdstuk 4.1 vond ik dat nauwere arteriolen en wijdere venulen gerelateerd waren aan een slechte microstructuur van de witte stof van de hersenen. Het gezamenlijk effect van nauwere arteriolen en wijdere venulen op de microstructuur van de witte stof bleek sterker te zijn dan het individuele effect van deze vaten. Deze bevindingen suggereren dat schade aan de kleine vaten in de witte stof mogelijk meer diffuus is dan dat we met het blote oog kunnen zien op beeldvorming. Vervolgens in hoofdstuk 4.2 heb ik onderzocht of de diameter van de retinale vaten gerelateerd is aan het aantal vergrote perivasculaire ruimten, en vond dat nauwere arteriolen en wijdere venulen gerelateerd waren aan het aantal vergrote perivasculaire ruimten. Deze bevindingen bevestigen de vermeende link tussen beschadiging van de kleine vaten en vergrote perivasculaire ruimten.

De studie in hoofdstuk 4.3 richt zich op de hypothese dat globale hersenschade zich mogelijk manifesteert in de retina als verdunning van de zenuwlagen. Ik vond dat een verdunning van de retinale zenuwvezellaag en ganglion cellaag geassocieerd was met

globale atrofie van de grijze en witte stof van de hersenen en met een slechte microstructuur van de witte stof. Ik vond geen associatie met vasculaire hersenafwijkingen op beeldvorming zoals wittestofafwijkingen, lacunes en microbloedingen. Alhoewel atrofie en vaatschade in de hersenen vaak tegelijkertijd optreden, laten mijn bevindingen zien dat retinale beeldvorming specifiek informatie kan geven over atrofie van de hersenen. Om meer inzicht te krijgen in mechanismen die mogelijk ten grondslag liggen aan deze associaties, en om de bevindingen van de vorige studie verder te bestuderen, heb ik in hoofdstuk 4.4 de studie verfijnd door de associatie tussen retinale zenuwlagen en hersenstructuren op voxel niveau te bekijken. Ik vond dat een dunnere retinale zenuwvezellaag en ganglion cellaag geassocieerd waren met veranderingen in de grijze en witte stof van de visuele banen, wat suggereert dat dunnere retinale zenuwlagen eerder atrofie van de visuele banen reflecteren dan globale hersenatrofie.

**Hoofdstuk 5** verkent de associatie van de retinale vaten en zenuwlagen met klinische uitkomstmaten. In hoofdstuk 5.1 heb ik de rol van beschadiging van de kleine vaten in migraine onderzocht, en vond dat retinale vaatschade niet geassocieerd was met migraine. Vervolgens in hoofdstuk 5.2 heb ik onderzocht of de dikte van de retinale zenuwlagen geassocieerd is met het hebben of het ontwikkelen van dementie. Ik vond dat een dunnere retinale zenuwvezellaag geassocieerd was met een verhoogde risico op het ontwikkelen van dementie. Deze bevindingen suggereren dat een dunnere retinale zenuwvezellaag een nieuwe marker kan zijn voor dementie, en in het bijzonder voor de ziekte van Alzheimer. In hoofdstuk 5.3 bestudeerde ik de associatie tussen retinale vaten en oorzaak-specifieke sterfte op de lange termijn, en vond dat veranderingen in de retinale vaten geassocieerd waren met een hoger risico op cardiovasculaire en niet-cardiovasculaire sterfte over meer dan 20 jaar. Uit deze studie bleek dat wijdere venulen in relatief jongere personen en in rokers in het bijzonder geassocieerd waren met een hoger risico op sterfte.

**Hoofdstuk 6** geeft een overzicht weer van de voornaamste bevindingen, bespreekt algemene methodologische overwegingen, en belicht de implicaties van de bevindingen met zicht op de toekomst.

# Chapter 8
# Epilogue


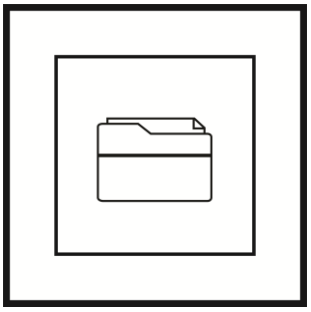

# Chapter 8.1
## Acknowledgments

More than three years have passed since I started working at the Department of Epidemiology. First as a MSc-student and later as a PhD-candidate, but as everything comes to an end one way or another, this PhD journey is no exception and successfully ends here. During my journey many people have walked alongside me who made it possible for me to write this thesis. Here, I would like to thank them all.

I would like to express my deepest gratitude to my promotors Prof.dr. Ikram and Prof.dr. Klaver, and to my co-promotor dr. Ikram. Dear Arfan, my supervisor whose attention to detail drove me to identify double spaces and different fonts in texts. Thank you for the opportunity to be part of your team, and for the pleasant years that we worked together. Your support has meant a lot to me, and I have learned much from you. Not only have you taught me how to practically conduct scientific research, but also how to think scientifically which to me is even more important. You are a true source of inspiration to every young researcher out there. Dear Caroline, my caring supervisor who always supported me in my choices. You are undoubtedly one of the most successful women I have ever known. I really admire how you manage to combine your clinical work with academic research. Thank you for the freedom you have given me to work on projects in my own way, and for your efforts to help improve my research skills. Dear Kamran, my daily supervisor whose open attitude has always made me feel comfortable to come to him with any issue. I really enjoyed our weekly meetings and particularly the ones about poems. Not only were you a great mentor, but you have been like an older brother to me.

I would also like to thank other members of my committee including Prof.dr. Jansonius and Prof.dr. Bots, who devoted their valuable time to critically review my thesis. I am happy to have the opportunity to discuss this thesis with you.
In addition, my sincere thanks to Prof.dr. Vernooij who agreed to review my thesis and to serve as secretary of the committee. Dear Meike, I have appreciated your input during our neuromeetings, and your insightful comments on my work. I am looking forward to continue working with you and learning from you in the clinic.
Dear Sonja, thank you for agreeing to serve as an expert in the committee. I have learned a lot from your knowledge on causal inference. Your feedback on my papers was always of great importance. I would further like to express my sincere gratitude to Prof.dr. Frens.
Dear Maarten, my first mentor in my academic career, I am honored to have you as part of the committee. Thank you for placing your trust in me, and your support and guidance during the Honours Class program.

This thesis has been made possible with the contribution of many other colleagues: people from the technical support, ladies at the ERGO-center, people from the eye-group, and of course the secretary. I would like to mention a couple of people by name: Ada, Anneke, Corina, Frank, Gabriëlle, Jolande, Jeroen, Magda, Nano and Nicole, thank you all for being so approachable, friendly, and helpful!

My life at the department was extremely facilitated by the enjoyable work atmosphere created by many great people. Alis, Annemarie, Daniel, Eline, Frank, Gena, Hazel, Hieab, Hoyan, Jan Roelof, Jeremy, Kimberly, Lana, Lotte, Maria, Mahmoud, Milly, Nina, Noor, Pauline, Pieter, Pınar, Rens, Ryan, Saima, Saira, Saloua, Sanaz, Sander, Sirwan, Silvan, Tavia, Thom, Timo, and Virginie, thank you all! We have shared many moments together, and I wish you all the best. Daniel, thanks a lot for being my paranimph. During my PhD, I have spent some of the greatest time with you on playing FIFA, football, foosball, or eating kapsalon. Thanks for the good moments! It is now time to go on a motorcycle road trip!

On this place I would like to show my deepest gratitude and appreciation to my family. My brother Atilla, you have always meant a lot to me, probably more than you can suspect. I have lived my best stories with you. Thank you for standing by me, and making me laugh. My dear brother Hacı Süleyman, the moments I have spent with you brought me always a lot of joy. The time we spent on playing FIFA and football, or just going out for a ride were moments of relaxing and distraction from my work. Thank you for being always ready, always there for me. My lovely sister, I could not have wished for a better sister. You always showed great attention and interest in my research and its progression. I regret not spending more time with you, but I surely will compensate this! My beautiful cousins: Seha, Berivan, Müfit, and Elif. Having a glance at the world through your eyes made me always realize how beautiful life can be, and how free we can be. Thank you for that. My lovely wife, thank you for standing beside me throughout my career. Your quiet patience and tolerance are a testament itself on your unyielding devotion and love. Finally, my beloved parents: dear mom and dad, if it was not your effort, support and especially your unconditional love, I would not be standing here. This thesis is dedicated to you. I hope I have made you proud.

**Ünal Mutlu**
Rotterdam 2018

# Chapter 8.2
## PhD portfolio

| | |
|---|---|
| **Name PhD student:** | **Ünal Mutlu** |
| **Research School:** | **Netherlands Institute for Health Sciences** |
| **Erasmus MC Departments:** | **Epidemiology and Ophthalmology** |
| **PhD period:** | **September 2016 – February 2018** |
| **Promotors:** | **Prof.dr. M.A. Ikram and Prof.dr. C.C.W. Klaver** |
| **Copromotor:** | **Dr. M.K. Ikram** |

| | Year | ECTS |
|---|---|---|
| **1. PhD training** | | |
| **General courses** | | |
| Master of Science in Health Sciences (NIHES) | 2014-2016 | 120 |
| Research Integrity | 2017 | 0.3 |
| **Conferences** | | |
| European Congress of Radiology, Vienna, Austria. Oral presentation. | 2018 | 1.5 |
| Consortium meeting 'SENSE-Cog', Rotterdam, The Netherlands. | 2017 | 0.7 |
| Alzheimer's Association International Conference, London, UK. Poster presentation. | 2017 | 1.2 |
| Consortium meeting 'SENSE-Cog', Bordeaux, France. | 2016 | 0.5 |
| European Congress of Radiology, Vienna, Austria. Oral presentation. | 2017 | 1.5 |
| International Society of Vascular Behavioral and Cognitive Disorders, Amsterdam, The Netherlands. Poster presentation. | 2016 | 1.2 |
| European Stroke Organisation Conference, Barcelona, Spain. Poster presentation. | 2016 | 1.2 |
| European Society of Retinal Specialists, Rotterdam, The Netherlands. Attendance. | 2016 | 0.3 |
| European Congress of Epidemiology, Maastricht, The Netherlands. Poster presentation. | 2015 | 1.2 |
| Dutch Ophthalmology PhD Students Conference, Nijmegen, The Netherlands. Oral presentation. | 2015 | 0.8 |
| **2. Teaching activities** | | |
| Supervisor Junior Med School students | 2016 | 1.5 |
| Supervisor master student | 2017 | 1.5 |
| Teaching assistant, Biostatistical Methods - CC02 | 2016 | 0.2 |
| Teaching assistant, Erasmus Summer Program - ESP01 | 2017 | 0.4 |
| Teaching assistant, Erasmus Summer Program - ESP65 | 2017 | 0.2 |
| Teaching assistant, Clinical trials - Ma1A3 | 2017 | 0.2 |
| Teaching assistant, Diagnostic tests - Ma1A1 | 2017 | 0.2 |
| **3. Other activities** | | |
| Peer review | 2016-2018 | 0.6 |

1 ECTS (European Credit Transfer System) is equal to a workload of 28 hours

# Chapter 8.3
## About the author

Ünal Mutlu was born on November 10th 1989 in Rotterdam, the Netherlands.
After graduating in 2008 at the City College St. Franciscus in Rotterdam, he went on to study Medicine at the Erasmus University Rotterdam. During his medical school, he participated in the Honours Class program, and then founded the Erasmus MC Honours Class Alumni Vereniging (EHAV). He also participated in the Research Master program in Health Sciences with specialization in Clinical Epidemiology provided by the Netherlands Institute of Health Sciences (NIHES). During this program he spent part of his training at the Harvard School of Public Health in Boston, USA, and at the Cambridge Institute of Public Health in Cambridge, UK. In 2016, he obtained his MSc degrees in Health Sciences and Medicine. Subsequently, he continued his research project as a PhD research at the department of Epidemiology (head: Prof.dr. MA Ikram). As of June 2018, Ünal will start his residency in Radiology and Nuclear Medicine at the Erasmus MC (head: Prof.dr. GP Krestin).